

IMKE M. WILLERS

**Molecular mechanisms controlling  
the translation of the mRNA encoding  
the human catalytic  $\beta$ -subunit of  
mitochondrial H<sup>+</sup>-ATP synthase in  
cancer and development**

TESIS DOCTORAL



Universidad Autónoma de Madrid  
Facultad de Ciencias  
Departamento de Biología Molecular  
Centro de Biología Molecular "Severo Ochoa" (CSIC-UAM)

**MOLECULAR MECHANISMS CONTROLLING THE  
TRANSLATION OF THE mRNA ENCODING THE HUMAN  
CATALYTIC  $\beta$ -SUBUNIT OF MITOCHONDRIAL  
 $H^+$ -ATP SYNTHASE IN CANCER AND DEVELOPMENT**

Memoria presentada por la licenciada  
**IMKE MARIA WILLERS**  
para optar al grado de  
Doctora en Biología Molecular  
por la Universidad Autónoma de Madrid

Director de Tesis: **Dr. José Manuel Cuezva Marcos**  
Co-Director de Tesis: **Dr. Álvaro D. Ortega Moreno**

Madrid, 2011



Este trabajo ha sido realizado en el laboratorio del Doctor José Manuel Cuezva Marcos, Catedrático del Departamento de Biología Molecular del Centro de Biología Molecular “Severo Ochoa” (CSIC-UAM), de la Facultad de Ciencias de la Universidad Autónoma de Madrid (Septiembre 2007 - Abril 2011). Durante este periodo, la licenciada Imke Maria Willers ha disfrutado de una beca lanzadera CIBER de enfermedades raras (Septiembre 2007 - Agosto 2008) y de una beca (Septiembre 2008 - Agosto 2010) / contrato (Septiembre 2010 - fecha de hoy) predoctoral del Programa Nacional de Formación de Profesorado Universitario del MEC.



## Departamento de Biología Molecular

**José Manuel Cuezva Marcos**, Catedrático de Bioquímica y Biología Molecular del Departamento de Biología Molecular de la Universidad Autónoma de Madrid,

### INFORMA:

Que **D<sup>a</sup>. IMKE MARIA WILLERS** ha realizado bajo mi dirección en el Departamento de Biología Molecular el trabajo original de investigación titulado "*Molecular mechanisms controlling the translation of the mRNA encoding the human catalytic  $\beta$ -subunit of mitochondrial  $H^+$ -ATP synthase in cancer and development*", que presenta para optar al grado de Doctor en Biología Molecular por la Universidad Autónoma de Madrid. Este trabajo ha sido co-dirigido por el **Dr. D. Álvaro D. Ortega**, específicamente en el apartado 4.2., correspondiente a la caracterización molecular y funcional de las proteínas de unión al mRNA.

La subunidad catalítica de la  $H^+$ -ATP sintasa ( $\beta$ -F1-ATPasa) es cuello de botella para la provisión mitocondrial de energía metabólica. Nuestro grupo ha puesto de manifiesto que la disminución de la expresión de esta proteína es un rasgo característico de la mayoría de los tumores y constituye, además, una herramienta para el pronóstico de pacientes oncológicos. Los resultados obtenidos por Imke Willers aportan nuevos datos de gran interés sobre la regulación de la actividad bioenergética de la mitocondria en tumores humanos así como sobre los mecanismos moleculares que controlan la expresión de la subunidad  $\beta$ -F1-ATPasa en cáncer y en desarrollo. En este contexto, en una primera parte de la tesis demuestra que en carcinomas de mama, colon y pulmón la pérdida de la expresión relativa de  $\beta$ -F1-ATPasa se ejerce por control post-transcripcional y, en colaboración con D. Antonio Isidoro, demuestran la relevancia de la represión selectiva de la traducción del mRNA en carcinomas de mama, pulmón y esófago. Con el fin de contribuir al conocimiento de los mecanismos moleculares que promueven este fenotipo, Imke ha caracterizado molecular y funcionalmente parte de los factores que se unen al mRNA de  $\beta$ -F1-ATPasa y controlan su traducción. En este sentido, Imke Willers ha demostrado que la proteína G3BP1 se une en el contexto celular al 3'UTR del mRNA de  $\beta$ -F1-ATPasa y ha descartado la unión de otras RNABPs (IMP1 y NPM1) a dicho transcrito. G3BP1 inhibe específicamente, tanto *in vitro* como *in vivo*, la síntesis de  $\beta$ -F1-ATPasa. Por datos *in vitro*, Imke ha puesto de manifiesto que G3BP1 interfiere con la fase de iniciación de la traducción. Con objeto de resaltar la relevancia clínica de estos estudios, Imke ha estudiado la expresión de G3BP1 en una cohorte de noventa adenocarcinomas de mama. En este estudio demuestra que la mayor expresión de G3BP1 en el carcinoma es un factor de mala prognosis para las pacientes y, más concretamente que una expresión elevada de G3BP1 en los carcinomas está significativamente asociada con una mayor probabilidad de desarrollar enfermedad metastásica en pacientes que por otros marcadores se adscriben a un grupo de buena prognosis. Es decir, aporta un nuevo marcador molecular de progresión en cáncer de mama que puede ser de gran utilidad en clínica. En conjunto, estos resultados apoyan fuertemente que G3BP1 puede jugar un papel determinante en el control del cambio metabólico que ocurre durante la transformación de las células cancerígenas y sugieren en última instancia que G3BP1 puede ser una nueva diana para el tratamiento de cáncer de mama. Por último, Imke Willers se planteó caracterizar el papel que los microRNAs pueden ejercer sobre el



## Departamento de Biología Molecular

control de la traducción del mRNA de  $\beta$ -F1-ATPasa. Para ello, y tras un análisis *in silico* de los miRNA que teóricamente podrían interactuar con el 3'UTR de  $\beta$ -mRNA, ha generado líneas celulares estables de BT549 y HCT116 que expresan RNA quiméricos de GFP que contienen el 3'UTR de los mRNAs de las subunidades  $\beta$  y  $\alpha$  de la  $H^+$ -ATP sintasa. Ha demostrado de un conjunto de potenciales miRNAs, que miRNA-127-5p reprime específicamente la expresión de la  $\beta$ -F1-ATPasa humana por inhibición de la traducción. Desde el punto de vista del desarrollo, Imke aporta las primeras evidencias de que en hígado humano también se produce la diferenciación postnatal de la mitocondria y que, al igual que ocurre en hígado de rata, el control de la expresión de  $\beta$ -F1-ATPasa también se ejerce en este momento del desarrollo por control la traducción del mRNA, estando muy probablemente este proceso regulado por miRNA-127-5p, ya que su expresión en hígado fetal humano es muy elevada.

Quiero resaltar que estos resultados son pioneros en este campo de investigación y que han contribuido y contribuirán al desarrollo de nuevas vías de actuación relacionadas con el papel de la mitocondria en progresión tumoral y, eventualmente, haciendo de este orgánulo una diana terapéutica para atajar la enfermedad. Parte de los resultados obtenidos ya han sido objeto de publicación en artículos y revisiones: *Biochem. J.* 426: 319-26 (2010); *J. Cell. Sci.* 23: 2685-2696 (2010); *Cancer Lett.* 276: 125-135 (2009); *Biochim. Biophys. Acta* 792:1145-58. (2009) y *Biochim. Biophys. Acta* (2010) (en prensa), y en diversas contribuciones a congresos nacionales e internacionales. Además, a fecha de hoy, se tiene en preparación otros dos artículos sobre el papel de G3BP1 en cáncer de mama y sobre la regulación de la expresión de  $\beta$ -F1-ATPasa por microRNA en los que Imke es primer autor.

Por todo lo anterior, y dadas las aportaciones originales de este trabajo y la madurez científica que a mi juicio acredita Imke Maria Willers, considero que puede procederse a la presentación y defensa de esta Memoria.

Lo que hago constar a los efectos oportunos en Madrid, a 27 de Abril de 2011.

José Manuel Cuezva Marcos



Für meine Eltern





## **AGRADECIMIENTOS**

En primer lugar quisiera dar las gracias de corazón a mi director de tesis, Pepe Cuezva, por haberme dado la oportunidad de realizar mi tesis doctoral en su laboratorio. Muchas gracias por tu ayuda, consejos y confianza.

También quiero dar mil gracias a mi co-director de tesis, Álvaro Ortega, por su gran apoyo durante el primer periodo de esta tesis doctoral. Muchas gracias por tu entusiasmo motivador para la ciencia, tu conocimiento profundo, tu ayuda constante y sobre todo por ser un amigo.

Para llevar a cabo esta tesis, ha sido indispensable la colaboración y el trabajo de muchas personas. Muchas gracias al Dr. Manuel González Barón y al equipo que dirige en el Hospital La Paz, por la colección de muestras de pacientes de carcinoma de mama y por los datos clínicos y de seguimiento de los pacientes. Quiero agradecer al Dr. Pedro Fernández, del IDIBAPS en el Hospital Clinic, por suministrarnos las muestras de carcinomas de pulmón y de tejido normal del mismo paciente. También quiero agradecer al Dr. Stefan Hüttelmeier de la Martin-Luther-University Halle-Wittenberg en Alemania, por habernos suministrado los plásmidos de la proteína YFP<sub>CT</sub>MS2CP y YFP<sub>NT</sub>ZBP1.

Estoy muy agradecida a todo el personal de los servicios del CBM que han facilitado y contribuido en la elaboración de esta tesis. Especialmente gracias a Maite Rejas por su ayuda en microscopía electrónica, a Fernando Carraso y Sandra Gonzalo del Servicio de Genómica y a Teresa Villalba, María Ángeles Muñoz y Verónica Labrador del Servicio de Microscopía confocal.

Quiero dar mil gracias a Ignacio por haberme ayudado con la traducción al castellano, por haberse metido en foros y buscado en internet para saber cómo se traduce “splicing” o qué es un “cap”. Muchas gracias por todas tus horas libres que has invertido en esto. Gracias también a Álvaro por haber hecho la revisión del castellano incluso estando enfermo.

Muchas gracias a todos los compañeros y ex-compañeros del laboratorio 326: a Laura, la compañera del doctorado de la primera hora, por su alegría y amistad, a la “jefa” María por su empatía, a Formentini por sus historias, a Marcos por sus gracias y críticas, a Inma por su buen carácter y a Cris, Fulvio y Javi por su alegría. Muchas gracias por vuestra ayuda, por la costumbre de las cañas del viernes y sobre todo por las risas y el buen ambiente en el laboratorio que me han hecho el tiempo del doctorado muy divertido y especial. Por último, muchas gracias a Margarita por sus historias, su amor a todos nosotros, su alegría del día a día, por el belén y por ser el duende de la navidad. También quiero dar las gracias a los vecinos del 321, por su ayuda, préstamos, alegría y por las charlas en los cultivos y pasillos. Gracias a Enrique por sus visitas diarias al laboratorio 326.

Quiero dar también las gracias a Rocío, Iván, Robert, Noe, las chicas de Colonia y Sirona. Gracias por muchos momentos y excursiones juntos, fuese para pasar las tardes en El Retiro o en los bares de Madrid o para andar, escalar o esquiar por el monte. Me alegra saber que siempre puedo confiar en todos vosotros.

## *Agradecimientos*

---

Muchas gracias a ti, por tus ánimos, por mostrarme hacer las cosas con calma y sobre todo por hacerme reír, feliz y llenar mi vida con alegría.

Vielen Dank an meine Freunde aus Wuppertal und vor allem an meinen Bruder Thomas. Auch wenn wir alle weit verstreut voneinander leben, tut es jedesmal gut euch zu sehen und es ist als ob keine Zeit vergangen wäre. Vielen Dank für die feucht, fröhlichen, verrückten und lustigen Treffen in Madrid oder Barcelona. Ich hoffe, dass wir diese Gewohnheit noch viele Jahre aufrecht erhalten werden.

Tausen Dank an meine Geschwister für ihre Besuche und Aufmunterung und an meine Eltern für ihre unerbittbare Liebe, Zuneigung und Unterstützung.



## ABBREVIATIONS

Akt/PKB	Protein kinase B
AMP/ADP/ATP	Adenosine mono/di/triphosphate
$\alpha$ -KG	$\alpha$ -Ketoglutarate
ARF	ADP Ribosylation Factors
Asp	Aspartate
a.u.	Arbitrary units
$\beta$ Gal	$\beta$ -galactosidase
$\beta$ -mRNA	mRNA of $\beta$ -F1-ATPase subunit
$\beta$ -RNP	Ribonucleoprotein particle of the mRNA of $\beta$ -F1-ATPase
BSA	Bovine serum albumin
CI	Confidence interval
COX	Cytochrome c oxidase
cpm	counts per minutes
CytC	Cytochrome C
DFS	Disease-free survival
ETC	Electron transport chain
DMEM	Dulbecco's Modified Eagle Medium
FAD <sup>+</sup> /FADH	Flavin adenine dinucleotide
FISH	Fluorescence in situ hybridization
GAPDH	Glyceraldehyde 3-phosphate dehydrogenase
G3BP1	Ras-GAP SH3 binding protein 1
GFP	Green fluorescent protein
GW182	Glycine-tryptophan protein of 182 kDa
HA	Hemagglutinin
HIF1 $\alpha$	Hypoxia inducible factor 1 alpha
HK	Hexokinase
HR	Hazard ratio
Hsp60	Heat shock protein 60
IF1	ATPase inhibitory factor 1
IP	Immunoprecipitate or Immunoprecipitation
IF	Immunofluorescence
LDH-A	Lactate dehydrogenase A
mtDNA	mitochondrial DNA
MEF	Murine embryonic fibroblast
miRNA	microRNA
MS2CP/CP	Coat protein of the bacteriophage MS2
mRNA	messenger RNA
NAD <sup>+</sup> /NADP	Nicotinamide adenine dinucleotide
NCI	National cancer institute
n.e.	non-essential
nls	Nuclear localization signal
Nt	N-terminal
NTP	Nucleoside triphosphate
MS2	MS2-RNA-hairpins, recognized by MS2CP
OAA	Oxaloacetate

OCR	Oxygen consumption rate
Oligo	Oligonucleotide
ORF	Open reading frame
OS	Overall survival
OXPPOS	Oxidative phosphorylation
PABP	Poly A binding protein
PBS	Phosphate buffered saline
PCR	Polymerase chain reaction
PDH	Pyruvate dehydrogenase
PDK-1	Pyruvate dehydrogenase kinase 1
PET	Positron emission tomography
PFA	Paraformaldehyde
p $\beta$ /pre $\beta$	pre-sequence of $\beta$ -F1-ATPase
PK	Pyruvate kinase
PPP	Pentose phosphate pathway
Q	biquinone
RPMI	Roswell Park Memorial Institute medium
PI3K	Phosphoinositol-3-kinase
PTEN	Phosphatase and tensin homolog
PVDF	Polyvinylidene fluoride
qPCR	Real time quantitative polymerase chain reaction
RNP	Ribonucleoprotein particle
RT	Reverse transcription
SDS	Sodium dodecyl sulfate
SDH-B	Subunit b succinate dehydrogenase B
SG	Stress granule
RAS-GAP	p120-Ras GTPase activating protein
RNABP	RNA binding protein
RNA-IP	RNA immunoprecipitation
ROS	Reactive oxygen species
SCO2	Protein SCO2 homolog, mitochondrial
SEM	Standard error of the mean
TCA	Tricarboxylic acid cycl
TIGAR	TP53-induced glycolysis and apoptosis regulator
mTOR	Mammalian target of rapamycin
UTR	Untranslated region
YFP	Yellow fluorescent protein
ZBP1	Zipcode binding protein



# INDEX

<b>Summary</b>	<b>1</b>
<b>1 Introduction</b>	<b>5</b>
<b>1.1 An introduction to mitochondria</b>	<b>5</b>
<b>1.2 The altered energetic metabolism of tumors</b>	<b>7</b>
1.2.1 The aerobic glycolytic phenotype of cancer	7
1.2.2 Mitochondria and the bioenergetic signature of cancer	9
1.2.3 Molecular mechanisms defining the glycolytic phenotype of cancer cells	10
1.2.4 Aerobic glycolysis: the phenotype of proliferating cells	12
1.2.5 Energetic metabolism and cancer progression	13
<b>1.3 The biology of <math>\beta</math>-F1-ATPase</b>	<b>15</b>
1.3.1 Overview of post-transcriptional regulation of gene expression	15
1.3.2 Mitochondrial biogenesis and post-transcriptional regulation of $\beta$ -F1-ATPase	17
1.3.3 Repression of $\beta$ -F1-ATPase expression in development and in cancer	19
1.3.4 Mechanisms and <i>trans</i> -acting factors that affect the expression/activity of the H <sup>+</sup> -ATP synthase in cancer	20
<b>1 Introducción</b>	<b>25</b>
<b>1.1 Una introducción a la mitocondria</b>	<b>25</b>
<b>1.2 El metabolismo energético alterado de los tumores</b>	<b>27</b>
1.2.1 El fenotipo aeróbico glicolítico del cáncer	27
1.2.2 La mitocondria y la huella bioenergética del cáncer	29
1.2.3 Mecanismos moleculares que definen el fenotipo glicolítico de las células cancerígenas	30
1.2.4 Glicólisis aeróbica: el fenotipo de células proliferativas	32
1.2.5 Metabolismo energético y progresión del cáncer	34
<b>1.3 La biología de <math>\beta</math>-F1-ATPasa</b>	<b>35</b>
1.3.1 Visión general de la regulación post-transcripcional de la expresión génica	35
1.3.2 Biogénesis mitocondrial y regulación post-transcripcional de $\beta$ -F1-ATPasa	38
1.3.3 Represión de la expresión de $\beta$ -F1-ATPasa en el desarrollo y en cáncer	41
1.3.4 Mecanismos y factores <i>trans</i> que afectan la expresión/actividad de H <sup>+</sup> -ATP sintasa en cáncer	41
<b>2 Objectives</b>	<b>47</b>
<b>3 Material and Methods</b>	<b>51</b>
<b>3.1 Material</b>	<b>51</b>
3.1.1 Tumor biopsies	51
3.1.2 Human cell lines	51
3.1.3 Bacterial strains	51
3.1.4 Plasmids	52



---

3.1.5	Antibodies	53
3.1.6	Oligonucleotides	53
3.1.7	Radioisotopes	53
3.1.8	Human Protein and RNA Liver extracts	56
3.1.9	siRNAs and miRNAs	56
<b>3.2</b>	<b>Molecular Biology Methods</b>	<b>56</b>
3.2.1	DNA purification from bacterial strain	56
3.2.2	DNA restriction by endonucleases	56
3.2.3	Separation of DNA fragments by gel electrophoresis	56
3.2.4	Purification of DNA fragments from agarose gels	57
3.2.5	Ligation of DNA fragments	57
3.2.6	Transformation of competent <i>E. coli</i> cells	57
3.2.7	PCR amplification for cloning	57
3.2.8	PCR to identify recombinant clones	57
3.2.9	RT-PCR	58
3.2.10	Quantification of RNA by real-time PCR (qPCR)	58
3.2.10.1	Quantification of $\beta$ -mRNA in human tissues	58
3.2.10.2	Quantification of immunoprecipitated mRNA	59
3.2.10.3	Quantification of mature miR-127-5p in human cells and during human and rat liver development	59
3.2.11	Cloning	59
3.2.11.1	pIW21: p $\beta$ GFP / pIW22: p $\beta$ GFP-3' $\beta$ / pIW23: p $\beta$ GFP-3' $\alpha$	59
3.2.11.2	pIW24: YFP <sub>Nt</sub> -Flag-IMP1 / pIW25: YFP <sub>Nt</sub> -Flag-G3BP1 / pIW26: YFP <sub>Nt</sub> -Flag-NPM1	60
3.2.11.3	Cloning of pre $\beta$ GFP-3' $\beta$ MUT (pIW29) by PCR-site directed mutagenesis	60
<b>3.3</b>	<b>Biochemical Methods</b>	<b>61</b>
3.3.1	Extraction of RNA and miRNA from cells and tissue samples	61
3.3.3	SDS-polyacrylamide gel electrophoresis, western blotting and fluography	61
3.3.4	Determination of G3BP1 expression in human breast tumor biopsies	62
3.3.5	Distribution of $\beta$ -mRNA in polysomes	62
3.3.6	Immunoprecipitation of RNA (RNA-IP) from Flag-RNABP transfected cells	63
3.3.7	<i>In vitro</i> transcription	63
3.3.8	<i>In vitro</i> translation	64
3.3.9	Eukaryotic cell-free transcription and translation assays	64
<b>3.4</b>	<b>Cell biology Methods</b>	<b>65</b>
3.4.1	Cell culture	65
3.4.2	Transient plasmid transfections	65
3.4.3	siRNA and miRNA transfection	65
3.4.4	Generation of stable transfected cell lines	65

3.4.5	Flow cytometry	66
3.4.6	<i>In vivo</i> RNA imaging by trimolecular fluorescence complementation (TriFC) assay	66
3.4.7	Indirect immunofluorescence microscopy	66
3.4.8	Preparation of riboprobes for fluorescence in situ hybridization (FISH)	67
3.4.9	Combined immunofluorescence and FISH	67
3.4.10	High-resolution immunoelectron microscopy	67
3.4.11	Screening for miRNA that affect $\beta$ -F1-ATPase expression using a fluorescence plate reader	68
3.4.12	Measurement of oxygen consumption rates in adherent cells	68
<b>4</b>	<b>Results</b>	<b>73</b>
<b>4.1</b>	<b>Post-transcriptional control of <math>\beta</math>-F1-ATPase expression</b>	<b>73</b>
4.1.1	Evidence of post-transcriptional regulation of $\beta$ -F1-ATPase expression in human colon, lung and breast cancer	73
4.1.2	The 3'UTR of human $\beta$ -mRNA is a <i>cis</i> -acting element involved in the control of its translation	74
4.1.3	Human tumor extracts promote the specific repression of $\beta$ -mRNA translation	75
<b>4.2</b>	<b>Molecular and functional characterization of <math>\beta</math>-mRNA Binding proteins</b>	<b>78</b>
4.2.1	G3BP1 interacts <i>in vivo</i> with $\beta$ -mRNA	79
4.2.1.1	$\beta$ -mRNA pull-down assays	79
4.2.1.2	Fluorescence in situ hybridization	80
4.2.2	Visualizing RNA-protein interactions <i>in vivo</i> (TriFC)	81
4.2.2.1	G3BP1 binds $\beta$ -mRNA in vivo in small fluorescence foci	81
4.2.2.2	No evidence that IMP1 and NPM1 associate with $\beta$ -mRNA	83
4.2.2.3	G3BP1 binds in vivo the 3'UTR of $\beta$ -mRNA	83
4.2.3	$\beta$ -mRNA is sorted to the vicinity of mitochondria	84
4.2.4	G3BP1 inhibits the synthesis of $\beta$ -F1-ATPase	86
4.2.5	G3BP1 inhibits translation initiation of $\beta$ -mRNA	87
<b>4.3</b>	<b>The relevance of G3BP1 in human breast cancer</b>	<b>88</b>
4.3.1	G3BP1 is a marker of breast cancer progression	88
<b>4.4</b>	<b>The role of miRNAs as post-transcriptional regulators of <math>\beta</math>-F1-ATPase expression</b>	<b>93</b>
4.4.1	<i>In silico</i> approach to identify miRNA candidates that might be involved in $\beta$ -F1-ATPase expression	93
4.4.2	Generation of stable cell lines expressing p $\beta$ GFP-3' $\alpha$ and p $\beta$ GFP-3' $\beta$	95
4.4.3	miR-127-5p is identified as a potential regulator of $\beta$ -F1-ATPase expression in a screening for miRNAs in BT549 cells	97

4.4.4	miR-127-5p binds to the 3'UTR of $\beta$ -mRNA and inhibits its translation	99
4.4.5	miR-127-5p might be involved in controlling $\beta$ -F1-ATPase expression during liver development in humans	101
4.4.5.1	No expression of miR-127-5p in human cancer cell lines	101
4.4.5.2	Potential role of mir127-5p as a regulator of $\beta$ -F1-ATPase expression during human liver development	102
4.4.5.3	miR-127-5p does not control rat $\beta$ -F1-ATPase expression	104
<b>5</b>	<b>Discussion</b>	<b>109</b>
<b>5.1</b>	<b>Translation of <math>\beta</math>-mRNA is selectively down-regulated in human cancer</b>	<b>109</b>
<b>5.2</b>	<b>G3BP1, a regulator of <math>\beta</math>-mRNA translation</b>	<b>111</b>
<b>5.3</b>	<b>G3BP1, a <math>\beta</math>-mRNABP involved in breast cancer progression</b>	<b>115</b>
<b>5.4</b>	<b>The role of miR-127-5p in controlling <math>\beta</math>-F1-ATPase expression: The biogenesis of mitochondria during human liver development</b>	<b>117</b>
<b>5.5</b>	<b>Why is the bioenergetic function of mitochondria repressed in cancer?</b>	<b>120</b>
<b>6</b>	<b>Conclusions</b>	<b>127</b>
<b>6</b>	<b>Conclusiones</b>	<b>131</b>
	<b>Bibliography</b>	<b>135</b>
	<b>APPENDIX</b>	<b>171</b>
	<b>Publications</b>	<b>179</b>

---

## INDEX OF TABLES

<b>Table 1:</b> Plasmids.	52
<b>Table 2:</b> Antibodies.	53
<b>Table 3:</b> Oligonucleotides.	55
<b>Table 4:</b> Univariate overall survival analysis of patients stratified by tumor expression of G3BP1.	90
<b>Table 5:</b> Univariate disease-free survival analysis of patients stratified by tumor expression of G3BP1.	90
<b>Table 6:</b> Multivariate disease-free survival analysis.	92
<b>Table A1:</b> Summary of clinicopathological characteristics of the patients studied for analysis of post-transcriptional mechanism(s) controlling $\beta$ -F1-ATPase expression.	173
<b>Table A2:</b> Summary of clinicopathological characteristics and G3BP1 expression level in the cohort of breast cancer patients studied.	174
<b>Table A3:</b> Univariate Cox regression analysis of breast cancer patients.	175
<b>Table A4:</b> G3BP1 expression and clinicopathological characteristics of breast tumors.	176
<b>Table A5:</b> Univariate disease-free survival analysis of breast cancer patients.	177

## INDEX OF FIGURES

<b>Figure 1.1:</b> Glycolytic and mitochondrial metabolic pathways.	6
<b>Figure 1.2:</b> Schematic illustration of the structure of the mitochondrial H <sup>+</sup> -ATP synthase.	7
<b>Figure 1.3:</b> The Hallmarks of cancer.	8
<b>Figure 1.4:</b> Cellular processes controlling the expression of genes involved the biogenesis of mitochondria.	19
<b>Figura 1.1:</b> Metabolismo glucolítico y mitocondrial.	26
<b>Figura 1.2.:</b> Ilustración esquemática de la estructura de la H <sup>+</sup> -ATP sintasa mitocondrial.	27
<b>Figura 1.3:</b> Los marcadores del cáncer.	28
<b>Figura 1.4.</b> Procesos celulares que controlan la expresión de los genes implicados en la biogénesis mitocondrial.	40
<b>Figure 3.1:</b> Site directed mutagenesis by PCR mutagenesis for cloning of pβGFP-3'βMUT (pIW29).	60
<b>Figure 4.1:</b> Expression of β-mRNA in human breast, colon and lung tumors.	74
<b>Figure 4.2:</b> The 3'UTR of the β-mRNA is required for efficient translation.	75
<b>Figure 4.3:</b> Human breast tumor extracts specifically repress β-mRNA translation.	76
<b>Figure 4.4:</b> Human lung tumor extracts specifically repress β-mRNA translation.	77
<b>Figure 4.5:</b> Human esophageal tumor extracts specifically repress β-mRNA translation.	78
<b>Figure 4.6:</b> Co-immunoprecipitation of β-mRNA with G3BP1.	79
<b>Figure 4.7:</b> Fluorescence <i>in situ</i> hybridization of β-mRNA.	80
<b>Figure 4.8:</b> G3BP1 interacts with β-mRNA.	81
<b>Figure 4.9:</b> G3BP1 is localized both in TIA1 positive (SGs) and negative cytoplasmic granules.	82
<b>Figure 4.10:</b> Analysis of IMP1 and NPM1 interaction with β-mRNA by TriFC.	83
<b>Figure 4.11:</b> G3BP1 interacts with 3'UTR of β-mRNA.	84
<b>Figure 4.13:</b> β-mRNA is sorted to the vicinity of mitochondria.	85
<b>Figure 4.12:</b> β-mRNA granules co-localize with mitochondria.	85
<b>Figure 4.14:</b> G3BP1 inhibits the translation of β-mRNA <i>in vivo</i> .	86
<b>Figure 4.15:</b> G3BB1 inhibits translation of β-mRNA <i>in vitro</i> .	87
<b>Figure 4.16:</b> G3BB1 inhibits translation initiation of β-mRNA.	87
<b>Figure 4.17:</b> G3BP1 is over-expressed in human breast cancer.	88
<b>Figure 4.18:</b> A high expression of G3BP1 predicts a worse prognosis in human breast cancer patients.	89
<b>Figure 4.19:</b> Expression of G3BP1 in good prognosis patients defines a group of patients with higher probability of developing metastasis.	91
<b>Figure 4.20:</b> miRNAs that are predicted to bind to the 3'UTR of human β-F1-ATPase.	94
<b>Figure 4.21:</b> Analysis of stable BT549:pβGFP-3'β and BT549:pβGFP-3'α cell lines.	95

---

<b>Figure 4.22:</b> Analysis of stable HCT116:pβGFP-3'β and HCT116:pβGFP-3'α cell lines.	96
<b>Figure 4.23:</b> Expression level of GFP in BT549 and HCT116 clones.	
<b>Figure 4.24:</b> Screening for miRNAs that affect expression of pβGFP-3'β in BT549 cells.	97
<b>Figure 4.25:</b> Analysis of the oxygen consumption rate after over-expression and silencing of miRNAs.	98
<b>Figure 4.26:</b> miR-127-5p down-regulates endogenous β-F1-ATPase expression.	99
<b>Figure 4.27:</b> miR-127-5p inhibits translation of β-F1-ATPase.	100
<b>Figure 4.28:</b> miR-127-5p is expressed in human and rat fetal liver.	101
<b>Figure 4.29:</b> OXPHOS during human liver development.	103
<b>Figure 4.30:</b> miR-127-5p has no effect on rat β-mRNA.	104
<b>Figure 5.1:</b> Mechanisms that regulate β-mRNA translation in humans.	122



# **SUMMARY**

---

---





## SUMMARY

Mitochondria are essential organelles in cell physiology, playing key roles in bioenergetics, the execution of the cell death and intracellular signaling by  $\text{Ca}^{2+}$  and reactive oxygen species (ROS). Mitochondrial dysfunction is associated with a large number of human pathologies, which include cancer, diabetes and neurodegeneration. It is nowadays accepted that a phenotypic trait of most human carcinomas is the reprogramming of their cellular energetic metabolism from mitochondrial oxidative phosphorylation to an enhanced aerobic glycolysis, the so-called Warburg Effect. In this scenario, the mitochondrial  $\text{H}^+$ -ATP synthase is an essential component both in the transduction of biological energy as well as in the execution of cell death. In fact, the down-regulation of the catalytic subunit of the  $\text{H}^+$ -ATP synthase ( $\beta$ -F1-ATPase) is a hallmark of many human carcinomas affording a marker of prognosis and of the response to therapy. Moreover, cancer cells and tumors over-express IF1, an inhibitor of the  $\text{H}^+$ -ATP synthase. In the present PhD Thesis we have investigated the molecular mechanisms that control at post-transcriptional levels the expression of human  $\beta$ -F1-ATPase. We illustrate that down-regulation of  $\beta$ -F1-ATPase in human breast, lung, esophageal and colon cancer originates from a specific translation repression event that can be recapitulated in *in vitro* translation assays. We demonstrate that the human 3'UTR of  $\beta$ -F1-ATPase mRNA ( $\beta$ -mRNA) is an important *cis*-acting element necessary for efficient translation. However, and at variance with previous findings with the rat transcript, recapitulation of translational repression requires the participation of additional *cis*-acting elements of the human transcript. In order to characterize the molecular mechanisms that underlie the masking of  $\beta$ -mRNA we have undertaken studies aimed at the identification of the RNA binding proteins and miRNAs that target the human transcript. Herein, we demonstrate that Ras-GAP SH3 binding protein 1 (G3BP1) interacts within the cellular context with the 3'UTR of  $\beta$ -mRNA and is part of the cytoplasmic RNA granules that contain  $\beta$ -mRNA. Furthermore, we show that G3BP1 promotes the repression of  $\beta$ -mRNA translation both *in vivo* and *in vitro*. Specifically, we demonstrate that G3BP1 hampers the initiation step of  $\beta$ -mRNA translation, strongly supporting that the regulated binding of G3BP1 to the transcript might be involved in masking the translation of  $\beta$ -mRNA in human cancer. Moreover, we demonstrate in a cohort of 93 breast cancer patients that a high expression of G3BP1 affords a marker of cancer progression, specially providing a reliable indicator of developing metastatic disease within the group of breast cancer patients with a good prognosis as assessed by their metabolic phenotype. In contrast to these findings, we show that the RNABPs IMP1 and NPM1 do not interact with  $\beta$ -mRNA playing no relevant role in  $\beta$ -F1-ATPase biology. Finally, we have developed cellular systems to analyze the role of miRNAs in  $\beta$ -F1-ATPase expression. Using these systems we show that  $\beta$ -mRNA is targeted and translationally silenced by miR-127-5p, whereas miR-101, miR-103, miR-186, miR-200b, miR-423-5p and miR-581 have no apparent functional role. miR-127-5p is not expressed in human cancer cell lines. However, we observed its expression in human fetal liver strongly suggesting that it might play a relevant role controlling the translation of  $\beta$ -mRNA during development of the human liver.



# **INTRODUCTION**

---

**A translation of this chapter into spanish can be found on page 25.**



## INTRODUCTION

### 1.1 AN INTRODUCTION TO MITOCHONDRIA

Mitochondria are membrane-enclosed organelles found in most eukaryotes. From a structural point of view mitochondria are exceptional as they are composed of two membranes forming four distinct compartments, the outer membrane, the inter membrane space, the inner membrane and the matrix. Mitochondria have conserved their own genetic system. However, the vast majority of the mitochondrial proteins is encoded by the nuclear genome while only ~1% are encoded by the circular mitochondrial DNA (mtDNA) and synthesized in the matrix. Mitochondria are often called the power house of the cell, since most of the cellular energy (ATP) is produced by oxidative phosphorylation (OXPHOS).

Complete oxidation of glucose and fatty acids, yields acetyl coenzyme A (acetyl-CoA) that is further degraded to CO<sub>2</sub> in the tricarboxylic-cycle (TCA-cycle) producing a large amount of electrons in redox coenzymes (Fig. 1.1). The electrons trapped in the reduced co-enzymes NADH and FADH<sub>2</sub> are transferred to the multiprotein complexes that form the electron-transport chain (ETC) down to molecular oxygen, which is the final electron acceptor. This electronic transfer through the ETC complexes produces free energy that is used to transport protons out of the matrix into the inter membrane space. The resulting proton electrochemical gradient across the inner mitochondrial membrane is used by the mitochondrial H<sup>+</sup>-ATP synthase to generate ATP out of ADP and Pi (Fig. 1.1). Mitochondria are also the principal source of cellular reactive oxygen species (ROS) that are produced as byproducts during oxidative metabolism mainly at the level of complex I and complex III as a result of electron transfer to oxygen forming superoxide anion (O<sub>2</sub><sup>-</sup>) (Fig. 1.1).

The mitochondrial H<sup>+</sup>-ATP synthase is a multiprotein complex that can be divided into the hydrophobic membrane bound FO-ATPase complex, which builds the proton channel, and the hydrophilic F1-ATPase complex containing the catalytic core (Boyer, 1997; Karrasch and Walker, 1999) (Fig. 1.2). Crystal structure analysis of the F1-ATPase showed that three catalytic β-subunits (β-F1-ATPase) and three non-catalytic α-subunits (α-F1-ATPase) are alternating arranged around a central stalk γ-subunit (Fig. 1.2) (Abrahams et al., 1994). Each of the three α-and β-subunit contain a substrate-binding site, being those on the β-subunits catalytic and those on the α-subunits regulatory. When protons pass through the membrane-spanning channel the FO complex rotates and the central γ-subunit stalk, which is tightly attached to the FO complex, rotates within the α<sub>3</sub>β<sub>3</sub>-ring forcing the catalytic β-subunits to undergo a sequence of conformational changes leading to the synthesis of ATP (Fig. 1.2) (Boyer, 1993; Capaldi and Aggeler, 2002; Yoshida et al., 2001).

The physiological role of mitochondria in the cell, however, is not limited to supplying energy. Mitochondria are also involved in other important cellular processes such as signaling both by calcium (Satrústegui et al., 2007) and ROS (Brunelle et al., 2005; Guzy and Schumacker, 2006; Hamanaka and Chandel, 2010), the metabolism of amino acids and lipids as well as the biosynthesis

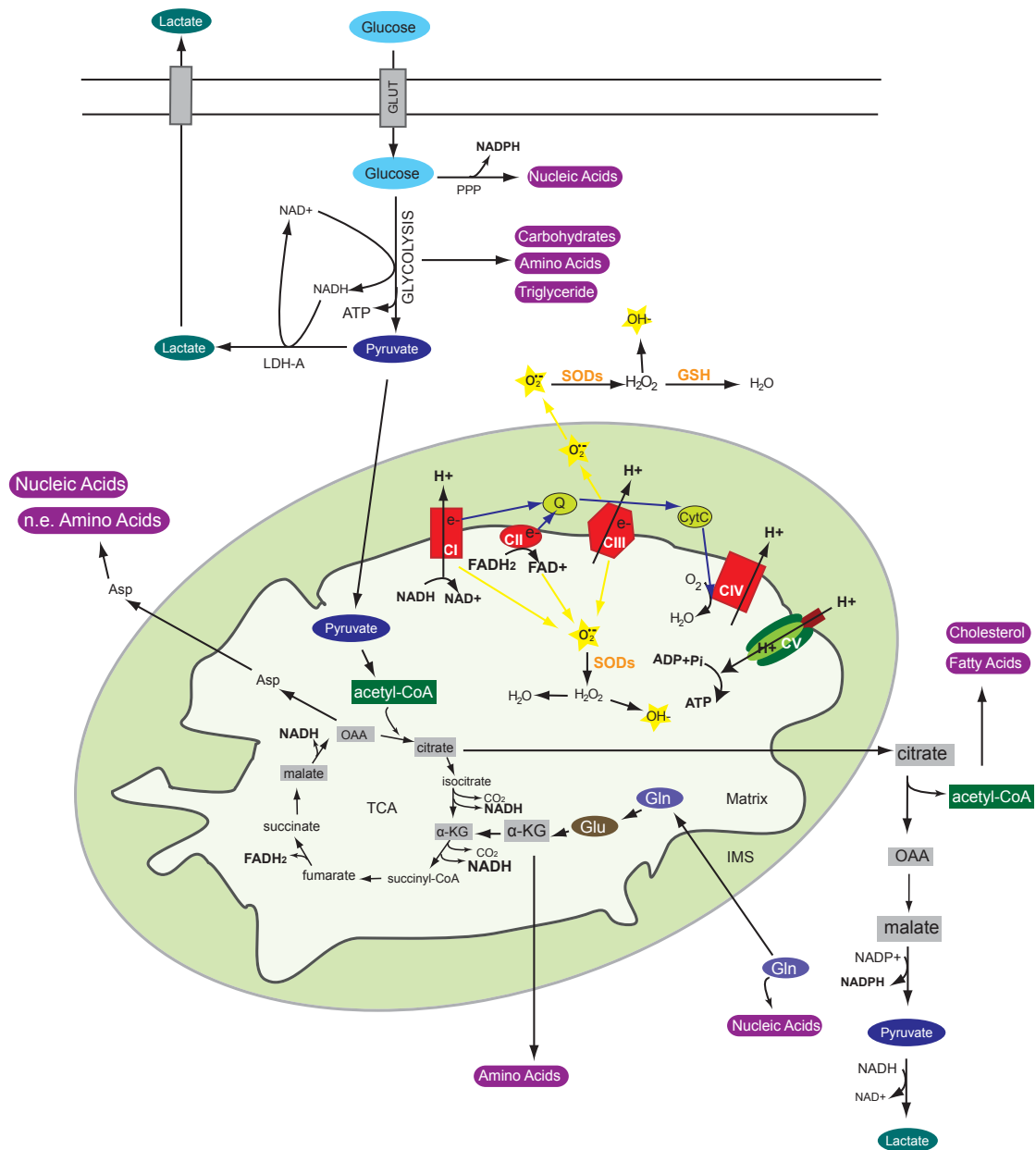


**Figure 1.1: Glycolytic and mitochondrial metabolic pathways.** After entering the cell by specific transporters (GLUT), glucose can be catabolized in the pentose phosphate pathway (PPP) generating reducing power NADPH and precursor for nucleic acid synthesis. Partial oxidation of glucose to pyruvate (glycolysis) yields ATP and NADH. Numerous intermediates of the glycolytic pathway are important precursors for the biosynthesis of other molecules: nucleic acids, carbohydrates, amino acids and triglyceride (purple box). Reduction of pyruvate to lactate by LDH-A regenerates NAD<sup>+</sup> and ensures a high glycolytic flux. Glucose-derived pyruvate can be transported into mitochondria where it is oxidized to acetyl-CoA, which enters the TCA-cycle by condensation with OAA forming citrate. The TCA-cycle produces CO<sub>2</sub> and reduced co-enzymes NADH and FADH<sub>2</sub>. Re-oxidation of NADH and FADH<sub>2</sub> by the complexes CI, CII, CIII and CIV of the respiratory chain leads to the transfer of electrons (e<sup>-</sup>) (blue arrows CI to CIV), which is reduced to H<sub>2</sub>O. The flow of e<sup>-</sup> through the respiratory complexes is coupled to a pumping of H<sup>+</sup> out of the matrix producing an electrochemical gradient across the inner membrane. Complexes I, II and III produce also ROS such as superoxide (O<sub>2</sub><sup>-</sup>) by direct transfer of e<sup>-</sup> to O<sub>2</sub> (yellow arrows). The toxic radical is converted to hydrogen peroxide (H<sub>2</sub>O<sub>2</sub>) through the action of superoxide dismutase (SOD) both within the mitochondria and in the cytosol. The H<sub>2</sub>O<sub>2</sub> can be reduced by the glutathione peroxidase (GSH) in H<sub>2</sub>O or be transformed in a metal-catalyzed oxidation into hydroxyl radical (OH<sup>-</sup>). Intermediates (α-KG, OAA) of the TCA-cycle are converted to amino acids and nucleic acids. Citrate can be exported into the cytoplasm, where it feeds membrane biogenesis by its conversion into fatty acids and cholesterol. Cytosolic OAA generated by cleavage of citrate can be transformed into malate, enter the mitochondria and replenish the TCA cycle or be transformed into pyruvate producing NADPH as a biosynthetic reducing power. Glutamine (Gln) can enter the mitochondria, be converted to glutamate (Glu) and further catabolized to α-KG. The glutamine derived α-KG can either refill the TCA-cycle or be used for the synthesis of amino acids. Q, ubiquinone; CytC, cytochrome C; Asp, aspartate; n.e., non essential.

of heme and iron sulfur clusters. In addition to their central role in various biochemical pathways, mitochondria are key regulators in the control and execution of cell death (Wang, 2001) and recent research has identified their involvement in the innate immune defense (Seth et al., 2005; Ishikawa and Barber, 2008; Zhong et al., 2008; West et al., 2011).

Mitochondria are highly dynamic organelles whose steady-state morphology is constantly regulated by fusion, fission and motility events (Suen et al., 2008). In fact, different tissues can differ in the number, function and structure of the mitochondria (Garesse and Vallejo, 2001; Pagliarini et al., 2008), and changes in the mitochondrial morphology are highly linked to their functionality and determine the cell-type specific appearance (Benard et al., 2007; Li et al., 2004; Szabadkai et al., 2004; Yu et al., 2006). Furthermore, correct functioning of the mitochondrial dynamics is essential for the maintenance of the mitochondrial tasks and inheritance (Westermann, 2010). Given the broad contribution of mitochondria to the cellular physiology, it's not surprising that changes in the mitochondria morphology and function have been linked to several human diseases such as diabetes, neurodegenerative disease and cancer.

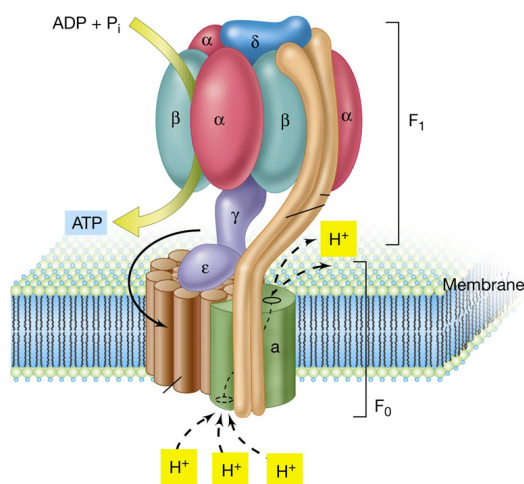


**Figure 1.2: Schematic illustration of the structure of the mitochondrial  $H^+$ -ATP synthase.** The membrane bound complex  $F_0$  that contains the proton channel is linked to the  $F_1$  complex by a peripheral stalk and by the  $\gamma$ -subunit which forms the central shaft of the rotor. The  $F_1$  domain contains three catalytic  $\beta$ -subunits and three non catalytic  $\alpha$ -subunits that are alternating arranged forming a ring. As protons ( $H^+$ ) pass through the  $F_0$  complex the ring of  $c$ -subunits (brown) rotates and as a result the central  $\gamma$ -subunit spins within the  $\alpha_3\beta_3$ -ring causing the catalytic binding sites ( $\beta$ ) to undergo conformational changes that lead to ATP synthesis.

## 1.2 THE ALTERED ENERGETIC METABOLISM OF TUMORS

### 1.2.1 The aerobic glycolytic phenotype of cancer

The term cancer is used for a set of heterogeneous diseases in which abnormal cells divide without control and are able to invade other tissues. By which normal cells become malignant is a complex and multilayer process and different types of cancer differ widely in their etiology and biology. Nevertheless, in the year 2000 in a milestone review Hanahan and Weinberg (Hanahan and Weinberg, 2000) described six essential alterations that acquire tumor cells during transformation, including self sufficiency in growth signals, insensitivity to growth inhibitory signals, evasion of programmed cell death, limitless replicative potential, inducing angiogenesis as well as invasion and metastasis (Fig. 1.3). In the last decade however, a lot of progress was done in the field of



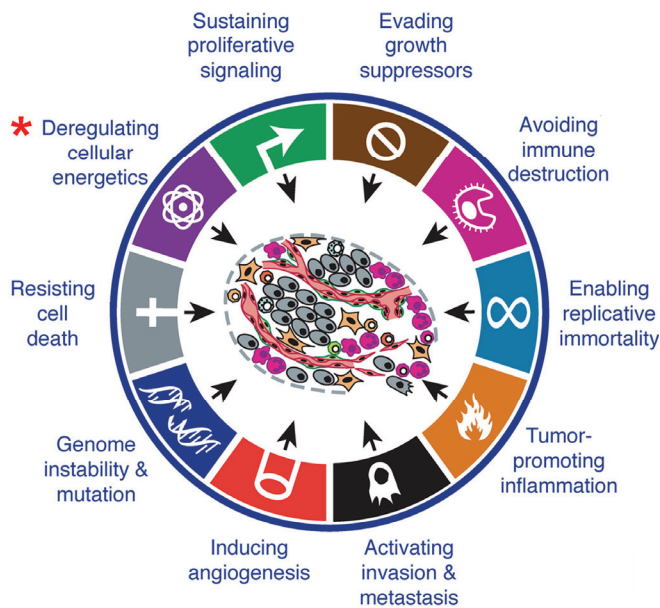


**Figure 1.3: The Hallmarks of cancer.** The illustration depicts the essential characteristics described by Hanahan and Weinberg that acquire most of the tumor cells during transformation. The red asterisk marks the metabolic reprogramming. Additionally, genome instability and mutation as well as tumor-promoting inflammation are included as proposed characteristics that facilitate the acquisition of the core hallmarks. (Adapted from Hanahan and Weinberg, 2011).

cancer research and recently, aerobic glycolysis, known as the Warburg Effect, was added as another important hallmark of most tumors (Kroemer and Pouyssegur, 2008; Cuezva et al., 2009; Ortega et al., 2009; Vander Heiden et al., 2009; Hanahan and Weinberg, 2011) (Fig. 1.3).

The aerobic glycolytic metabolism of tumor and cancer cells was first discovered by Otto Warburg many years ago (Warburg, 1956a; Warburg, 1956b). Because the activity of glycolysis is elevated independent of oxygen, and thus distinguished from the Pasteur Effect, Warburg suggested that the abnormal aerobic glycolysis in rapidly growing tumor and cancer cells was due to an impaired bioenergetic activity of mitochondria that might provoke cell transformation (Warburg, 1956a). His hypothesis was heatedly debated and mostly abandoned or considered as epiphenomena of cell transformation (Garber, 2006; Weinhouse, 1956; Weinhouse, 1976) until the last decade of the 20<sup>th</sup> century when radiologists demonstrated that 18F-2-deoxyglucose (18-FDG) positron emission tomography (PET) can detect and map many tumors. Chemically, FDG is a non-metabolizable glucose analog with the positron-emitting radioactive isotope fluorine-18 substituted at the second hydroxyl group (-OH). When 18-FDG is injected into a patient it enters the cells but cannot be metabolized, and the gamma rays emitted by the accumulated 18-FDG are detected by the PET system. As a result, the detection of 18-FDG reflects the distribution of glucose uptake by cells in the body. Nowadays, the widespread clinical application of tumor imaging by 18-FDG-PET has substantiated that most primary and metastatic human tumors have an increased glucose uptake (Plathow and Weber, 2008; Rigo et al., 1996). Furthermore, a number of transcriptomic, proteomic and functional studies have underlined Warburg’s postulate, demonstrating that most of the human tumors and cancer cells when compared to normal cells have both an increased expression and activity of glycolytic genes, a high glucose consumption rate as well as an elevated lactate production rate (Bi et al., 2006; Cuezva et al., 2002; Gullino et al., 1967; Isidoro et al., 2005; Isidoro et al., 2004; Kallinowski et al., 1988; Lu et al., 2007; Ortega et al., 2009; Sauer et al., 1982).

### 1.2.2 Mitochondria and the bioenergetic signature of cancer

The assumption that the glycolytic phenotype of cancer cells might be due to impaired mitochondrial respiration (Warburg, 1956a) is still a matter of debate (Funes et al., 2007; Zu and Guppy, 2004). Nevertheless, several studies have described that tumor mitochondria are often fewer and smaller, lack cristae, have profound ultrastructure alterations and are less active than in normal tissues (Carew and Huang, 2002; Krieg et al., 2004; Modica-Napolitano et al., 2007; Modica-Napolitano and Singh, 2002; Pedersen, 1978; Simonnet et al., 2002; Springer, 1980).

Furthermore, recent proteomic studies of our laboratory provide compelling evidence supporting Warburg's assumption. These studies determined in normal and tumor biopsies derived from the same patients the expression level of the catalytic subunit of the H<sup>+</sup>-ATP synthase ( $\beta$ -F1-ATPase) as a marker of oxidative phosphorylation. Given that either a reduction of the total mitochondrial content or a dysfunction of the OXPHOS system might provoke a decreased bioenergetic activity of the mitochondria (Cuezva et al., 2002), the expression of Hsp60 as a structural mitochondrial protein and of the glycolytic enzyme Glyceraldehyde 3-phosphate dehydrogenase (GAPDH) was also determined. This method allowed the estimation of the bioenergetic competence of the mitochondria as assessed by the  $\beta$ -F1-ATPase/Hsp60 ratio, and the overall mitochondrial potential of the cell as determined by the  $\beta$ -F1-ATPase/Hsp60/GAPDH ratio (Cuezva et al., 2002; Isidoro et al., 2005; Isidoro et al., 2004).

By this approach it was demonstrated that the normalized expression of  $\beta$ -F1-ATPase is significantly diminished in rat hepatomas (de Heredia et al., 2000) and a number of different human carcinomas, when compared to the surrounding normal tissue (Cuezva et al., 2002; Isidoro et al., 2005; Isidoro et al., 2004; Cuezva et al., 2004), indicating that the mitochondrial bioenergetic capacity of tumor cells is defective. In agreement with Warburg's hypothesis, these changes in the mitochondrial proteomic composition were accompanied by the induction of glycolytic markers. This proteomic feature was defined as the "bioenergetic signature of cancer" (Cuezva et al., 2002; Cuezva et al., 2009) (recently simplified to the  $\beta$ -F1-ATPase/GAPDH ratio, Lopez-Rios et al., 2007) and is fulfilled by more than 95% of the patients analyzed in large cohorts of lung (Cuezva et al., 2004), breast (Isidoro et al., 2005) and colon (Cuezva et al., 2002) tumors. Moreover, other studies have confirmed and extended this proteomic feature to different carcinomas, such as renal, liver, esophageal and gastric cancer (Cuezva et al., 2009; He et al., 2004; Hervouet et al., 2005; Li et al., 2010b; Lin et al., 2008; Meierhofer et al., 2004; Unwin et al., 2003; Yin et al., 2004).

Remarkably, the bioenergetic signature also affords a predictive marker of the response to chemotherapy (Hernlund et al., 2009; Lin et al., 2008; Sanchez-Arago and Cuezva, 2011; Sanchez-Arago et al., 2010; Shin et al., 2005) and an indicator of disease progression, because its degree of alteration is associated with cancer prognosis of lung (Cuezva et al., 2004; Lopez-Rios et al., 2007), colon (Cuezva et al., 2002; Lin et al., 2008) and breast (Isidoro et al., 2005) cancer patients.

The relevance of Warburg's postulate was functionally underlined by demonstrating that alteration of the bioenergetic signature observed in different tumors is associated to metabolic and biochemical transformation of the cell. In this regard, in human lung cancer the rate of glucose consumption, as assessed *in vivo* by 18-FDG-PET imaging (Lopez-Rios et al., 2007), displays a significant inverse correlation with both  $\beta$ -F1-ATPase expression and the bioenergetic signature. Moreover, by the generation of HCT116 colon cancer cell lines expressing different levels of  $\beta$ -F1-ATPase it has been demonstrated that the activity of oxidative phosphorylation defines the rate of glucose utilization by aerobic glycolysis (Lopez-Rios et al., 2007; Sanchez-Arago et al., 2010). Overall these data support that an impaired mitochondrial respiration participates in inducing the augmented glucose avidity of cancer cells (Ortega et al., 2009).

### 1.2.3 Molecular mechanism defining the glycolytic phenotype of cancer cells

In the last years, several papers have demonstrated a connection between common cancer genes and the Warburg effect. In particular, the activation of oncogenes, the inhibition of tumor-suppressor genes and the expression of hypoxia inducible factor 1 alpha (HIF1 $\alpha$ ) have been shown to trigger the glycolytic shift promoting the expression of glycolytic enzymes/transporters and attenuate mitochondrial respiration.

For instance, the oncogene *c-myc*, which is frequently over-expressed in cancer is a positive transcription factor of several glycolytic enzymes including glucose transporters and the lactate dehydrogenase-A (LDH-A) (O'Connell et al., 2003; Osthus et al., 2000; Shim et al., 1997). LDH-A is over-expressed in several tumors and remarkably its down-regulation compromises the proliferation of cancer cells (Fantin et al., 2006; Le et al., 2010). c-MYC can also activate mitochondrial biogenesis (Li et al., 2005), and recently c-MYC has been shown to enhance the expression of the mitochondrial glutaminase (Gao et al., 2009), stimulating in this way glutamine metabolism and cancer cell anaplerosis, which is discussed in further detail below (1.2.4).

Furthermore, the PTEN/Akt/mTOR signaling pathway, a key regulator of cell growth, proliferation and glucose metabolism, is often deregulated in cancer cells. Enhanced Akt signaling stimulates the metabolic reprogramming of cancer cells by regulating the expression and activity of key glycolytic enzymes, such as hexokinase (HK) and 6-phosphofructo-2-kinase (PFK2) as well as glucose and other nutrients transporters (Edinger and Thompson, 2002; Elstrom et al., 2004). Furthermore, Akt has been found to inhibit  $\beta$ -oxidation of lipids by hampering the expression of carnitine palmitoyltransferase (CPT1A) (DeBerardinis et al., 2006), supporting in this way the anabolic program of highly proliferating cells (see 1.2.4).

Intriguingly, the tumor suppressor protein p53 also influences the metabolic balance between glycolysis and OXPHOS. On the one hand, p53-responsive elements are present in the promoter of HK2 (Mathupala et al., 1997) and over-expression of a dominant negative form of p53 in MCF7 cells has been shown to trigger an increase in the HK2 activity and glucose uptake (Smith et al.,

2006). On the other hand, p53 down-regulates the glucose transporter GLUT1 and activates TIGAR and SCO2 (Bensaad et al., 2006; Matoba et al., 2006; Schwartzberg-Bar-Yoseph et al., 2004). TIGAR is a negative regulator of fructose-2,6-bisphosphatase and SCO2 is required for assembling the mitochondrial cytochrome c oxidase subunit II of complex VI of the electron transport chain (Bensaad et al., 2006; Matoba et al., 2006). Consequently, loss of function of p53 impairs mitochondrial respiration and promotes the glycolytic pathway.

It has been further suggested that adaptation to the hypoxic microenvironment where the tumor grows favors glycolysis and reduces mitochondrial glucose oxidation. Low oxygen conditions promote the stabilization of the transcription factor HIF1 $\alpha$  (Semenza, 2003), which in turn triggers the up-regulation of a number of glycolytic proteins (glucose transporter, glycolytic enzymes, LDH-A) as well as proteins involved in angiogenesis facilitating tumor neo-vascularization (Ebert et al., 1995; Semenza et al., 1994). Additionally, HIF1 $\alpha$  decreases the rate of oxidative phosphorylation and reinforces the glycolytic phenotype by bringing on the discharging of pyruvate away from mitochondria activating the expression of pyruvate dehydrogenase kinase 1 (PDK1) (Kim et al., 2006; Papandreou et al., 2006). PDK1 is a negative regulator of pyruvate dehydrogenase (PDH), which is the rate-limiting enzyme in the conversion of glucose derived pyruvate to acetyl-CoA. Furthermore, HIF1 $\alpha$  can modulate the mitochondrial structure and dynamics (Chiche et al., 2010), and inhibits mitochondrial biogenesis counteracting c-MYC (Zhang et al., 2007b). HIF1 $\alpha$  alters also the activity of cytochrome c oxidase (COX) by inducing a preferred expression of the isoform COX4-2 (instead of COX4-1) that results in a more efficient transfer of electrons to O<sub>2</sub> limiting in this way the oxidative stress derived from mitochondrial metabolism (Fukuda et al., 2007). Moreover, HIF1 $\alpha$  induces the expression of miR-210, which plays a fundamental role in the control of mitochondrial metabolism during hypoxia, as miR-210 represses the expression of the iron sulfur cluster assembly proteins (ISCU1/2) and of COX10 resulting in a decreased activity of complexes of the mitochondrial ETC (Chan et al., 2009; Chen et al., 2010).

Interestingly, mitochondria itself are involved in the stabilization of HIF1 $\alpha$ . Loss-of-function mutation of two enzymes of the TCA-cycle, succinate dehydrogenase (SDH) and fumarate hydratase (FH) causes the accumulation of their substrates, succinate and fumarate, which in turn trigger the stabilization of HIF1 $\alpha$  by interfering with prolyl-hydroxylases that are involved in the degradation of HIF1 $\alpha$  (Isaacs et al., 2005; King et al., 2006; Selak et al., 2005). Likewise, deficiencies in mitochondrial respiratory functions increases the production of ROS that in turn inhibit HIF1 $\alpha$  degradation (Brunelle et al., 2005; Guzy et al., 2005; Mansfield et al., 2005) leading ultimately to a positive feed-forward cycle of glycolytic enhancement.

Finally, several studies have demonstrated that cancer cells of various tissue origins exhibit frequently somatic mutations in their mtDNA (Carew and Huang, 2002; Carew et al., 2003; Copeland et al., 2002; Polyak et al., 1998) that also may come up along tumor progression caused by increased ROS production due to a dysfunctional oxidative respiration (Brandon et al., 2006). Some mtDNA mutations actively support the production of ROS promoting in this way tumor progression

(Brandon et al., 2006; Petros et al., 2005; Zhou et al., 2007), tumor invasion (Amuthan et al., 2001; van Waveren et al., 2006) and metastasis (Ishikawa et al., 2008), while other mtDNA mutations are thought to be important contributing factors for the malfunction of mitochondrial respiration in cancer cells (Simonnet et al., 2002; Wallace, 2005). In this regard, a decreased expression of some of the mtDNA-encoded OXPHOS complexes provokes a minor activity of mitochondrial respiration in cancers (Gallardo et al., 2006; Krieg et al., 2004; Simonnet et al., 2003, Bonora et al., 2006).

### 1.2.4 Aerobic glycolysis: the phenotype of proliferating cells

The glycolytic phenotype is not a unique feature of tumors cells, in fact aerobic glycolysis is the predominant metabolism used of highly proliferating (Brand and Hermfisse, 1997; Hume et al., 1978; Wang et al., 1976) and embryonic cells (Cuezva et al., 1997; Johnson et al., 2003; Kondoh et al., 2007). In this regard, rat thymocytes and human lymphocytes when stimulate to proliferate show an increase in the uptake of glucose, an increased activity of glycolytic enzymes and an almost complete conversion of glucose to lactate. A return of these cells to the non-proliferative state is accompanied by a decrease in the glycolytic rate and lactate production (Brand et al., 1988; Wang et al., 1976). Consistently, *S. cerevisiae* cell culture growth is bound to a cyclic oscillation in the activity of glycolysis and OXPHOS, in which the cell division cycle is strictly constraint to glycolysis and a decreased respiration (Tu et al., 2005; Tu and McKnight, 2006). Given that mitochondria, apart from their important role in the production of energy are also the primary source of ROS, aerobic glycolysis by proliferating cells has been discussed as a mean to minimize oxidative stress during the phase of the cell cycle when enhanced biosynthesis and cell division occur and the DNA is most vulnerable (Brand and Hermfisse, 1997; Chen et al., 2007).

It has been further argued that cancer cells benefit from the boost in aerobic glycolysis, because it ensures the provision of large amounts of precursors for biosynthesis of proteins, nucleotides and lipids as well as reducing power required for the biosynthetic processes of rapidly growing cells (Fig. 1.1) (DeBerardinis et al., 2008; Ortega et al., 2009). Within this context, one has to consider that the glycolytic pathway not only catabolizes glucose and provides energy, but also is crucial for anabolic processes. Intermediates of the glycolysis are important precursors for the synthesis of amino acids and lipids, and metabolization of glucose into the pentose phosphate pathway (PPP) provides ribose-5-phosphate needed for nucleic acid synthesis and NADPH as a reducing agent used in anabolic processes (Fig. 1.1) (Ortega et al., 2009).

Furthermore, cancer cells enhance their anabolic processes by a preferred expression of the fetal M2 isoform of pyruvate kinase (PKM2) (Mazurek et al., 2005), which catalyzes the conversion of phosphoenolpyruvate (PEP) to pyruvate. In contrast to other isoforms the enzyme activity of PKM2 is less active (Mazurek et al., 2005) and can be negatively regulated in response to growth factor stimulation by binding of phosphotyrosine peptides (Christofk et al., 2008b). Strikingly, it is the ability to decrease the pyruvate kinase activity that appears to be important for rapid growth in cancer cells (Christofk et al., 2008a; Christofk et al., 2008b). It is suggested that the

major advantage for the cancer cell to express PKM2 is the shunting of the glycolytic intermediates into biosynthetic processes due to the lesser activity of PKM2 (Christofk et al., 2008a; Christofk et al., 2008b). A recent study has illustrated that expression of PKM2 provides a selective growth advantage over cells expressing the PKM1 isoform (Christofk et al., 2008a) and strikingly the classical oncoprotein c-MYC promotes a preferential expression of PKM2 over PKM1 (David et al., 2010). Alternatively, it has been proposed that the decreased PKM2 activity in cancer cells might promote an unconventional glycolytic pathway, in which PEP donates its phosphate to the glycolytic enzyme phosphoglycerate mutase (PGAM1). This in turn increases the activity of PGAM1 and the production of pyruvate, promoting altogether a positive feedback loop to increase the glycolytic pathway and its anabolic branches (Vander Heiden et al., 2010).

Intermediates of the TCA-cycle are also used for the biosynthesis of different macromolecules. Oxaloacetate (OAA) and  $\alpha$ -ketoglutarate ( $\alpha$ -KG) are essential precursors of non-essential amino acids used in the synthesis of proteins and nucleotides (Fig. 1.1). Furthermore, the TCA-cycle of tumor mitochondria can be truncated between the citrate and  $\alpha$ -KG step (Parlo and Coleman, 1984). In this situation, citrate is not oxidized through the TCA-cycle, but preferentially exported from the mitochondria into the cytoplasm to furnish acetyl-CoA units for cholesterol and fatty acid synthesis, thus fueling the membrane biogenesis of proliferating cells (Fig. 1.1) (Hatzivassiliou et al., 2005; Parlo and Coleman, 1984). The cytoplasmic OAA resulting from the cleavage of citrate into acetyl-CoA is converted into malate and can either be returned into mitochondria and enter the TCA-cycle or be converted into pyruvate by malic enzyme generating NADPH as a reductive agent (Fig. 1.1) (DeBerardinis et al., 2007). In order to refill the TCA-cycle intermediates “lost” in biosynthetic reactions and guarantee a continuous flux through the cycle, pyruvate can be carboxylated generating OAA, and  $\alpha$ -KG can be replenished by glutamine intake that is converted to glutamate by glutaminase and further catabolized to  $\alpha$ -KG (Fig. 1.1) (DeBerardinis et al., 2007; Ortega et al., 2009). Glutamine is highly utilized by some cancer and proliferating cells (Baggetto, 1992; DeBerardinis et al., 2007) and on entering the TCA-cycle,  $\alpha$ -KG derived from glutamine can be metabolized to OAA for biosynthetic processes or to malate that can be converted in the cytoplasm to pyruvate and the reducing power NADPH (DeBerardinis et al., 2007). Overall, the energetic metabolism and in particular glycolysis and the TCA-cycle of a cancer cell is reorganized to increase anabolic reactions. Therefore, the glycolytic phenotype of cancer has been ascribed for the most part of it to the inevitable metabolic reprogramming experienced by the cells as a result of the onset of cellular proliferation (Cuezva et al., 2009; Ortega et al., 2009).

### **1.2.5 Energetic metabolism and cancer progression**

In order to characterize the metabolic changes that occur during cellular transformation to a cancerous state, a recent study has performed an extensive metabolic analysis in different cell lines treated with several compounds that disturb the energetic metabolism. Using this perturbation profiling approach it was demonstrated that glycolytic conversion in response to

aberrant mitochondrial respiration started early and expanded as the cells become more malignant (Ramanathan et al., 2005). Interestingly, it has been reported that transformation of human mesenchymal stem cells promotes an increase in their dependency on oxidative phosphorylation (Funes et al., 2007). However, when these transformed cells were implanted into nude mice an increase in glycolysis was observed accompanied by the down-regulation of genes of the TCA-cycle (Funes et al., 2007). Likewise, H-RasV12/E1A transformed cells show an activation of oxidative phosphorylation at an early stage of transformation (de Groof et al., 2009). However, as the tumorigenic potential of these cells increases, an enhancement of glycolysis and a diminished activity of mitochondrial respiration are observed accompanied by elevated survival chances (de Groof et al., 2009).

Generally, while solid tumors grow the microenvironment becomes more hypoxic and in fact the decreased dependence on aerobic respiration becomes advantageous for the cell (Gatenby and Gillies, 2004). Furthermore, increased glycolysis leading to an acidification of the tumor microenvironment as well as mtDNA mutations, mitochondrial membrane damage and OXPHOS dysfunction enhance tumor progression and favor a more invasive behavior of the tumor (Amuthan et al., 2001; Gatenby and Gillies, 2004; Ishikawa et al., 2008; van Waveren et al., 2006). Consistent with these findings, we have recently demonstrated that for *in vivo* tumor progression the previous selection of cancer cells with a cellular phenotype, in which the bioenergetic activity of mitochondria is repressed, is required (Sanchez-Arago et al., 2010). The acquisition of this metabolic trait is not based on a permanent genetic change; rather it represents a reversible feature that results from the metabolic adaptation of the cells to the *milieu* where tumor cells develop *in vivo* (Sanchez-Arago et al., 2010). Within this context, pharmacologic treatment of cancer cells with dichloroacetate (DCA) that triggers a switch to a mitochondrial-dependent pathway of energy provision promotes *in vivo* tumor regression (Bonnet et al., 2007; Michelakis et al., 2010; Michelakis et al., 2008; Sanchez-Arago et al., 2010). Likewise, molecular based activation of oxidative metabolism inhibits the cancer growth in mammals (Schulz et al., 2006) and prevents tumorigenicity (McFate et al., 2008; Shakya et al., 2009). On the contrary, mice with an impaired mitochondrial function and decreased oxidative phosphorylation, due to a disrupted expression of the mitochondrial Friedreich ataxia protein frataxin in the liver, exhibited reduced survival and developed hepatic tumors (Thierbach et al., 2005).

Overall, these findings highlight the role of energetic metabolism in the regulation of tumorigenesis. It further suggest that in particular *in vivo* at the stage of development of a macroscopic tumor where the microenvironment controls cellular growth, that repression of oxidative phosphorylation is a prerequisite for tumor development (Sanchez-Arago et al., 2010).

## 1.3 THE BIOLOGY OF $\beta$ -F1-ATPase

### 1.3.1 Overview of post-transcriptional regulation of gene expression

Throughout the live cycle of a cell, gene expression is constantly and dynamically modified to adapt to distinct environmental and physiological conditions. Regulation of gene expression was thought to be mainly controlled at the level of transcription. However, nowadays it is apparent that multiple levels of post-transcriptional regulation, such as mRNA processing, export, localization, degradation, silencing and translation are also essential steps involved in the control of gene expression (Hieronymus and Silver, 2004; Moore, 2005). Compared to transcriptional regulation post-transcriptional control provides a more rapid mechanism to increase the cellular concentration of the encoded proteins and thus to respond more effectively to cell physiological demands (Martin and Ephrussi, 2009).

In the nucleus, pre-mRNAs are co- and/or post-transcriptionally processed (splicing, 5'-capping, 3'-cleavage, polyadenylation) by specific proteins, and packaged into a messenger ribonucleoprotein particle (mRNP) composed of the mRNA, proteins and small non-coding RNAs. During its entire lifespan, the mRNA acts as a platform for the binding of proteins and non-coding RNAs (e.g. miRNAs). In fact, it is the unique composition of the mRNP which is the actual substrate of post-transcriptional processes and dictates the fate of mRNAs mediating their subcellular localization, decay, translation as well as interaction with exterior signals (Hieronymus and Silver, 2004; Keene and Tenenbaum, 2002; Moore, 2005). Most of the RNA binding factors target specific sequences or structures, called *cis*-regulatory elements, in the mRNA. These *cis*-regulatory elements mainly occur in 3'UTR of the mRNA (de Moor et al., 2005), but can also be found in the 5'UTR (Muckenthaler et al., 1998; Tsai et al., 2007) or in coding regions (Ricart et al., 2002).

Upon export into the cytoplasm mRNPs can be immediately translated or held in a translational quiescent state until the appropriate subcellular localization is reached and/or a signal indicates the precise time to synthesize the protein. The combination of subcellular localization and controlled translation serves to restrict protein synthesis to a specific compartment and enables the cell to organize different cellular compartments and its functions (Holt and Bullock, 2009; Lecuyer et al., 2007). Prominent examples of translation confined in time and space were studied during *Drosophila* and *Xenopus* oogenesis, in which mRNA localization and translational control play a crucial role in specifying the future embryonic body axes (Driever and Nusslein-Volhard, 1988; Ephrussi et al., 1991; Gavis and Lehmann, 1992; Rebagliati et al., 1985). For instance, localization of *bicoid* mRNA to the anterior pole of the *Drosophila* oocyte and its proper translation is essential to produce a Bicoid protein gradient that patterns the anterior-posterior axis of the embryo (Driever and Nusslein-Volhard, 1988). Likewise, transport of *oskar* mRNA to the posterior pole of *Drosophila* oocytes and its specific translation during mid to late oogenesis are essential for germline and abdomen formation (Ephrussi et al., 1991; Riechmann and Ephrussi, 2001). Asymmetric segregation



of mRNAs in subcellular locations was also observed in somatic cells (Adereth et al., 2005; Mingle et al., 2005; St Johnston, 2005). A well characterized example is the localization of  $\beta$ -actin mRNA to sites of actin polymerization, contributing thereby to the overall cell motility through the provision of new actin monomers (Lawrence and Singer, 1986; Ross, 1997; Zhang et al., 2001). The zipcode region in the 3'UTR of the  $\beta$ -actin mRNA is bound by the Zipcode binding protein (ZBP1) that in turn promotes  $\beta$ -actin mRNA localization and prevents at the same time an early translation of the transcript in the cytoplasm (Hüttelmaier et al., 2005). Several mechanisms exist to achieve an asymmetric localization of mRNA in the cell including diffusion and local entrapment (Forrest and Gavis, 2003), local protection from degradation (Ding et al., 1993) and the most commonly used active transport along the cytoskeleton (St Johnston, 2005).

Translational silencing targets all steps of translation (initiation, elongation and termination). However, translation initiation, being in most cases the rate limiting step of translation, appears to be the most frequently regulated point (Martin and Ephrussi, 2009). In this regard, shortening of the poly(A) tails has been shown to be a crucial mechanism to silence mRNAs during development (Paris et al., 1988; Vassalli et al., 1989). Furthermore, eukaryotic cap-dependent translation initiation requires the association of the translation initiation factor 4G (eIF4G) to the cap-binding protein eIF4E. This step is frequently targeted either globally by 4E binding proteins (4E-BP), which sequester eIF4E or individually by specific *trans*-acting factors targeting the eIF4G-eIF4E interface (Richter and Sonenberg, 2005). For example, cytoplasmic polyadenylation element binding protein (CPEB) binds to the polyadenylation element in the transcript and recruits Maskin, a protein that competes with eIF4G for binding to eIF4E (Sonenberg and Hinnebusch, 2009). Likewise, *oskar* mRNA is silenced by the 3'tethered and eIF4E inhibitory protein Cup (Nakamura et al., 2004; Richter and Sonenberg, 2005). Translation can equally be inhibited by blocking the recruitment of the 60S subunit to the transcript (Deng et al., 2008).

In the recent years, it has become apparent that in addition to RNABPs, miRNAs play an important role in post-transcriptional regulation of mRNA expression. miRNAs are short, approximately 22-nucleotides long RNAs expressed in metazoan, animals and plants. They cannot act alone and have to be incorporated into a miRNA-induced silencing complex (RISC). Following transcription, the RNA precursor, which is a ~70-nucleotide hairpin transcript, is exported into the cytoplasm and processed by Dicer into an approximately 20-nucleotide miRNA duplex. One strand of the duplex represents the mature miRNA (called guide strand or miRNA) and is retained in the RISC complex, whereas the other strand is released (called passenger strand or miRNA\*) (Krol et al., 2010). The retained strand generally is the thermodynamically more stable strand (Han et al., 2006; Khvorova et al., 2003). However, in the case that both miRNA strands, excised from opposite arms of the same hairpin precursor (called mir-X-3' and mir-X-5'), display similar thermodynamic stability, a co-accumulation of both strands with different seed sequences and target mRNAs can occur (Ro et al., 2007). Historically, the less abundant miRNA strand was defined as the miRNA\*. Yet recent research indicate that miRNA\* strands are not always byproducts of miRNA biogenesis and can also be loaded in the RISC complex to function as miRNAs (Czech et al., 2009; Ghildiyal et al.,

2009). Furthermore, high depth sequencing has revealed that miRNA/miRNA\* ratios as well as the steady state levels of each strand of a miRNA may vary among developmental stages and across tissues (Okamura et al., 2008; Ro et al., 2007).

Usually, animal miRNAs regulate gene expression by imperfectly base pairing to the 3'-UTR of target mRNAs inhibiting protein synthesis or inducing the degradation of the target mRNAs (Fabian et al., 2010). However, recently it has been reported that some miRNAs also induce the translation of the target mRNA (Henke et al., 2008; Orom et al., 2008; Vasudevan et al., 2007). The exact mechanisms of miRNA mediated inhibition of protein synthesis are still not well understood and controversial (Fabian et al., 2010). In contrast, miRNA induced degradation of mRNAs following deadenylation is known to be mediated by GW182, which is a core component of the RISC and recruits deadenylases to the transcript (Eulalio et al., 2009; Fabian et al., 2010).

### **1.3.2 Mitochondrial biogenesis and post-transcriptional regulation of $\beta$ -F1-ATPase**

Mitochondria have their own genome, a circular mtDNA that encodes 37 genes, which include components of the mitochondrial translation machinery and 13 subunits of respiratory complexes I, III, IV and V. However, the majority of the proteins of the respiratory apparatus and all the factors needed for mtDNA metabolism and function of the organell are nuclear encoded. It is generally accepted that mitochondrial biogenesis is mainly regulated at the level of transcription by a set of core transcription factors (NRF-1, NRF-2, PPAR $\alpha$ , ERR $\alpha$  and SP1) and co-activators (PGC-1 $\alpha$ , PGC-1 $\beta$  and PRC) (Scarpulla, 2008). In particular, the activity and differential expression of the co-activators can be modulated by a variety of extracellular signals providing a mechanism to fine-tune the cell and tissue specific bioenergetic phenotype (Scarpulla, 2008). However, and in agreement with the fundamental role that mRNA localization exerts in the regulation of gene expression (see 1.3.1), mechanisms that control the spatial localization (Corral-Debrinski et al., 2000; Lithgow, 2000) and translation (Izquierdo and Cuezva, 1997; Martinez-Diez et al., 2006) of nucleus-encoded mRNAs of mitochondria contribute to define the bioenergetic phenotype of the cell. In this regard, several genome wide studies have shown that about half of the nuclear mRNAs encoding mitochondrial proteins are sorted to the vicinity of mitochondria (Eliyahu et al., 2010; Marc et al., 2002; Saint-Georges et al., 2008). Moreover, the preferred enrichment of mitochondrial transcripts next to the mitochondria is a conserved feature of both yeast and human cells (Sylvestre et al., 2003), and affects in particular mRNAs of prokaryotic origin as well as core components of the mitochondrial complex (Garcia et al., 2007; Marc et al., 2002).

As aforementioned (see 1.3.1), localization of mRNAs to discrete subcellular sites is a multistep process and involves *cis*-acting elements within the mRNA, which are bound by *trans*-acting factors and together account for mRNA transport, anchoring, stability and localized translation (Martin and Ephrussi, 2009; Rodriguez et al., 2008). In this regard, in *S. cerevisiae* it has been described that the asymmetric localization of more than 200 nuclear encoded mitochondrial

mRNAs to mitochondria-bound polysomes depends on the association of the RNA binding protein Puf3p to its canonical sequence in the 3'UTR of the mRNAs (Gerber et al., 2004; Saint-Georges et al., 2008). Consistently, cellular strains over-expressing Puf3p exhibit respiratory dysfunction, abnormal mitochondrial morphology and motility (Garcia-Rodriguez et al., 2007; Gerber et al., 2004). Intriguingly, a second group of about 224 mitochondria-associated transcripts lack the Puf3p binding site and its expression and localization is not affected by Puf3p (Saint-Georges et al., 2008), indicating the existence of at least two independent pathways for mRNA to be transported and localized specifically to the mitochondria. Notably, the division in these two classes of mRNAs reflects also a separation in both its temporal expression and the functionality of the encoded proteins. The first group of Puf3p-dependent mRNAs encodes for basic components of mitochondrial biogenesis, such as proteins of protein import, translation machinery or assembly factors, which are transcribed early in the mitochondrial cycle (Lelandais et al., 2009). The transcripts of the second group are transcribed later in the mitochondrial cycle (Lelandais et al., 2009) and encode mainly proteins of respiration and mitochondrial morphology (Saint-Georges et al., 2008). Overall, these findings suggest that temporal and spatial localization of mitochondrial mRNAs encoded in the nucleus determine mitochondrial biogenesis.

The post-transcriptional regulation of the mRNA of the catalytic subunit of the H<sup>+</sup>-ATP synthase ( $\beta$ -F1-ATPase) is a paradigmatic case that has been largely studied both in yeast and in rat liver during development (Cuezva et al., 1997; Egea et al., 1997; Garcia et al., 2010; Izquierdo and Cuezva, 1997; Margeot et al., 2002; Margeot et al., 2005). In yeast, the 3'UTR (Margeot et al., 2002) and two *cis*-regulatory elements, located in the open reading frame (ORF) of the mRNA (Garcia et al., 2010) are required for an appropriate mitochondrial localization and translation of the transcript. Removal of the 3'UTR in the *ATP2* gene leads to deficient protein import, reduced ATP synthesis, mtDNA depletion and respiratory dysfunction (Margeot et al., 2002; Margeot et al., 2005). The sequences in the ORF are also necessary for localization of the transcript to the vicinity of mitochondria, and their deletion leads probably to a failed anchoring of the mRNA to the mitochondria (Garcia et al., 2010; Margeot et al., 2002). It has been proposed that translation of the *cis*-acting elements in the ORF of yeast  $\beta$ -mRNA is needed to maintain the transcript next to the mitochondria (Garcia et al., 2010; Komili et al., 2007).

In rat hepatocytes,  $\beta$ -F1-ATPase mRNA ( $\beta$ -mRNA) is present in large (~150 nm) ribonucleoprotein complexes ( $\beta$ -RNP) preferentially associated to the outer mitochondrial membrane (Fig. 1.4) (Egea et al., 1997; Ricart et al., 1997). Likewise to yeast, proper assembly and subcellular localization of the mammalian  $\beta$ -RNP depends on two *cis*-acting elements placed in the 3'UTR and in the ORF, and a set of proteins that interact with these mRNA elements (Ricart et al., 2002). Interestingly, the transcript of the  $\beta$ -F1-ATPase was not found as a target of the PUF family, neither in yeast (Saint-Georges et al., 2008) nor in mammalian cells (Galgano et al., 2008). It belongs to the above mentioned second group of mRNAs, which are localized to the vicinity of mitochondria independent of Puf3p (Saint-Georges et al., 2008) and for which the *trans*-acting factors remain to be identified.

### 1.3.3 Repression of $\beta$ -F1-ATPase expression in development and in cancer

Post-transcriptional control of the expression of  $\beta$ -F1-ATPase is particularly important during development of rat liver (Luis et al., 1993), rat hepatocarcinogenesis (Cuezva et al., 1997; de Heredia et al., 2000) and progression through the cell cycle (Martinez-Diez et al., 2006). In these situations, it has been shown that expression of  $\beta$ -F1-ATPase is especially regulated at the level of translation. During fetal development of the rat,  $\beta$ -mRNA is accumulated in the liver as a result of an increase in its stability (Izquierdo et al., 1995; Luis et al., 1993) and maintained in a translationally repressed state until the time of birth (Fig. 1.4) when a rapid increase in expression of the protein occurs (Luis et al., 1993; Ostronoff et al., 1996; Valcarce et al., 1988). Likewise, in rat hepatomas the amount of  $\beta$ -F1-ATPase protein is significantly diminished when compared to normal adult liver, while the level of its transcript remains unchanged (de Heredia et al., 2000). Mechanistically, in both fetal liver and hepatomas the  $\beta$ -mRNA is translationally masked by specific RNA binding proteins (RNABPs) that hinder its efficient translation (Fig. 1.4) (de Heredia et al., 2000; Izquierdo and Cuezva, 1997). Within this context, it has been shown that the 3'UTR of rat  $\beta$ -mRNA acts as a

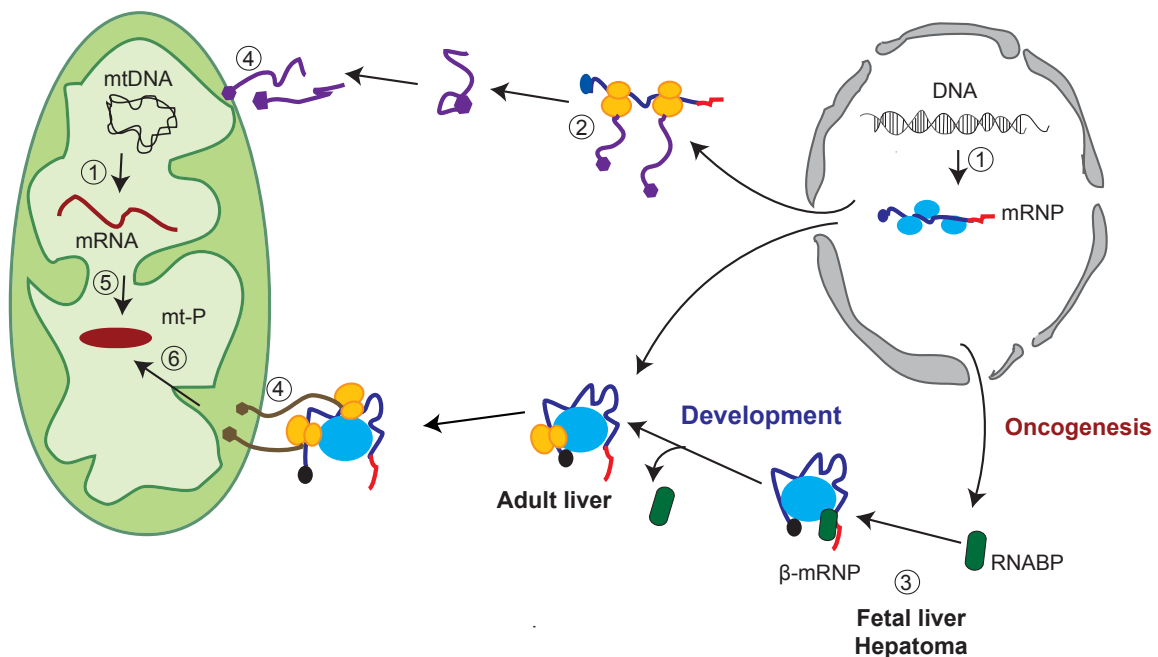


**Figure 1.4: Cellular processes controlling the expression of genes involved in the biogenesis of mitochondria.** (1) Transcription, splicing and maturation of mtDNA and mitochondrial genes encoded in the nucleus. In the nucleus, mRNAs are assembled into ribonucleoprotein particles (mRNP) and exported into the cytoplasm. (2) Some nucleus-encoded mRNAs are translated by cytoplasmic ribosome, whereas others mRNPs are sorted to the mitochondrial periphery where localized translation of the transcript takes place. (3) The transcript of the  $\beta$ -F1-ATPase ( $\beta$ -mRNA) interacts with regulatory proteins (RNABP,  $\beta$ -RNP) that define the metabolic fate of  $\beta$ -mRNA. During development of fetal rat liver and in rat hepatocarcinomas (oncogenesis) translation of  $\beta$ -mRNA is silenced by association of specific RNABPs. In these situations, the bioenergetic function of mitochondria is diminished. Following specific cellular signals the masking of  $\beta$ -mRNA by RNABPs could be relieved and translation therefore completed. (4) Precursor proteins are imported into the mitochondria by the mitochondrial import machinery. (5) Mitochondrial translation machinery synthesizes mt-encoded polypeptides (mt-P) that (6) in some case assemble with the nucleus-encoded proteins to mitochondrial complexes. ribosome, orange; 3'UTR, red; RNABP, green.

translational enhancer both *in vitro* (Izquierdo and Cuezva, 1997; Izquierdo and Cuezva, 2000) and *in vivo* (Di Liegro et al., 2000), and is essential for the translation of the transcript due to its ability to interact with the translation machinery (Izquierdo and Cuezva, 1997). It has been proposed that the binding of RNABPs to the 3'UTR inhibits the intrinsic translation enhancing activity of this element (Izquierdo and Cuezva, 2000), presumably by hindering the access of the translational machinery onto the mRNA (Di Liegro et al., 2000; Ricart et al., 2002). The conserved translation repression mechanism for regulating the expression of  $\beta$ -F1-ATPase in fetal rat liver (Izquierdo and Cuezva, 1997) and in rat hepatomas (de Heredia et al., 2000) suggests that this mechanism might also contribute to the altered bioenergetic phenotype observed in human cancer cells (see 1.2.1 and 1.2.2). This study has been one of the aims of the present PhD thesis.

### **1.3.4 Mechanisms and *trans*-acting factors that affect the expression/activity of the H<sup>+</sup>-ATP synthase in cancer**

Several independent mechanisms have been reported that can affect the bioenergetic activity of mitochondria in cancer including targeting of the H<sup>+</sup>-ATP synthase. In colorectal cancer the gene *ATP5A1*, which codes for the  $\alpha$ -subunit of the H<sup>+</sup>-ATP synthase is frequently down-regulated (Bacolod and Barany, 2010). In chronic myeloid leukemia cells  $\beta$ -F1-ATPase expression is limited by promoter hypermethylation of the encoding gene *ATP5B*, thus compromising the bioenergetic activity of mitochondria and contributing to Adriamycine resistance (Li et al., 2010a).

On the other hand, the inhibitor peptide of the mitochondrial ATPase, called ATPase Inhibitory Factor 1 or IF1 (Cabezón et al., 2000; Gledhill et al., 2007; Pullman and Monroy, 1963) is up-regulated in human breast, colon and lung carcinomas when compared to paired normal tissues (Sanchez-Cenizo et al., 2010). Originally, IF1 was described as an inhibitor of the hydrolase activity of the H<sup>+</sup>-ATP synthase, i.e., the transport of protons against the electrochemical gradient by ATP hydrolase, when mitochondrial respiration is altered. In this situation, the pH of the mitochondrial matrix becomes more acidic; IF1 is activated and binds  $\beta$ -F1-ATPase to prevent a useless waste of energy (Cabezón et al., 2000; Gledhill et al., 2007). Over-expression assays of IF1 and its pH-insensitive constitutive active H49K mutant (Cabezón et al., 2000) in cells that express low levels of IF1 (Sanchez-Cenizo et al., 2010) illustrated that IF1 triggers also a decrease in the activity of the H<sup>+</sup>-ATP synthase, the up-regulation of aerobic glycolysis and a concurrent increase in the mitochondrial membrane potential, mimicking the effects of oligomycin (Sanchez-Cenizo et al., 2010). Conversely, siRNA mediated silencing of IF1 in cells expressing high levels of IF1 triggers the down-regulation of aerobic glycolysis and an increase in the activity of the H<sup>+</sup>-ATP synthase (Sanchez-Cenizo et al., 2010). Therefore, it was suggested that inhibition of the H<sup>+</sup>-ATP synthase by IF1 depends also on the mass-action ratio and in situations of increased IF1 expression, such as in certain tumors and cancer cells (Sanchez-Cenizo et al., 2010), the protein inhibits both the synthetic and hydrolytic activities, providing the cancer cell with an additional mechanism to regulate its energetic metabolism (Sanchez-Cenizo et al., 2010).

Finally, and as mentioned previously RNABPs have been proposed to be involved in the control of rat  $\beta$ -mRNA translation during development (Izquierdo and Cuezva, 1997; Izquierdo et al., 1995) and oncogenesis (de Heredia et al., 2000) (see also 1.3.3) as well as  $\beta$ -mRNA localization (Ricart et al., 2002). Recently, it has been shown that HuR which is a central regulator of post-transcriptional gene expression (Levy et al., 1998) and whose expression is increased in most human tumors (Lopez de Silanes et al., 2003), interacts with the 3'UTR of human  $\beta$ -mRNA (Izquierdo, 2006; Ortega et al., 2008). However, silencing and over-expression experiments did not reveal a significant participation of HuR in the control of  $\beta$ -F1-ATPase expression (Ortega et al., 2008), suggesting that it might participate in other post-transcriptional events such as sorting and/or anchoring of  $\beta$ -mRNA (Ortega et al., 2008).

Although  $\beta$ -mRNA binding proteins could, analogously to their observed function in rat, play an important role in controlling the bioenergetic phenotype in human cancer, our knowledge about their molecular identity is scarce. Therefore, a main goal of our laboratory has been the identification of putative  $\beta$ -mRNA binding proteins. Using an improved RNABP purification assay based on fusion of the target mRNA with MS2 RNA hairpins of the bacteriophage MS2 followed by affinity chromatography procedure, nine putative  $\beta$ -mRNA binding proteins that interact *in vitro* with the human transcript have been identified (Ortega et al., 2010). These proteins are involved in transcription (DHX9, SFPQ, NONO, ILF3, NCL and NPM1), splicing (SFPQ and NONO), RNA export to the cytoplasm (DHX9, NCL, ILF3 and IMP1), RNA processing (SFPQ, NONO, NCL and NPM1), RNA localization (NCL, NPM1, SFPQ, NONO, G3BP1 and IMP1), RNA stability (IMP1 and G3BP1) and translation (ILF3, G3BP1, IMP and RL8) (Ortega et al., 2010). Furthermore, DHX9, NCL, NPM1, ILF3, G3BP1 and IMP1 shuttle from the nucleus to the cytoplasm depending upon environmental conditions (Gallouzi et al., 1998; Hüttelmaier et al., 2005; Parrott et al., 2005; Tourriere et al., 2001) and form part of different RNPs that are sorted throughout the cytoplasm by kinesin and dynein motor proteins (Elvira et al., 2006; Kanai et al., 2004). The analysis of the *in vivo* interaction and putative functional role of three RNABPs (IMP1, NPM1 and G3BP1) on the expression of  $\beta$ -F1-ATPase is part of the present study. A brief summary of the major cellular roles played by the three RNABPs under study is provided in the Appendix.



# **INTRODUCCIÓN**

---





# 1 INTRODUCCIÓN

## 1.1 UNA INTRODUCCIÓN A LA MITOCONDRIA

Las mitocondrias son orgánulos celulares que se encuentran en la mayoría de células eucariotas. Desde un punto de vista estructural, las mitocondrias son excepcionales debido a que están compuestas por dos membranas que forman cuatro compartimentos diferenciados: la membrana externa, el espacio inter membrana, la membrana interna y la matriz. Las mitocondrias han conservado su propio material genético. Sin embargo, la gran mayoría de sus proteínas están codificadas por el genoma nuclear mientras que sólo aproximadamente el 1% están codificadas por el DNA circular de la mitocondria (mtDNA) y son sintetizadas en la matriz. Tradicionalmente, las mitocondrias han sido conocidas como la planta energética de la célula, debido a que la mayoría de la energía celular (ATP) es producida por fosforilación oxidativa (OXPHOS).

La oxidación completa de la glucosa y de los ácidos grasos da como resultado acetil-coenzima A (acetil-CoA), el cual se degrada en  $\text{CO}_2$  en el ciclo de los ácidos tricarbónicos (ciclo TCA) produciendo la reducción de transportadores redox difusibles o coenzimas (Fig. 1.1). Los electrones atrapados en las coenzimas reducidas NADH y  $\text{FADH}_2$  son transferidos a los complejos multiproteicos que forman la cadena de transporte de electrones (ETC, electron transport chain) hasta el oxígeno molecular, que es el aceptor final de electrones. Esta transferencia electrónica entre los complejos de la ETC produce una liberación de energía que se utiliza para transportar protones fuera de la matriz hacia el espacio inter membrana. El gradiente electroquímico resultante  $\text{H}^+$  es utilizado por la  $\text{H}^+$  ATP-sintasa mitocondrial para generar ATP a partir de ADP y de Pi (Fig. 1.1). Las mitocondrias son también la fuente principal de especies reactivas de oxígeno (ROS, reactive oxygen species) las cuales son subproductos producidos durante el metabolismo oxidativo principalmente al nivel del complejo I y del complejo III como resultado de la transferencia de electrones al oxígeno, formando el anión superóxido ( $\text{O}_2^-$ ) (Fig. 1.1).

La  $\text{H}^+$ -ATP sintasa mitocondrial es un complejo multiproteico que puede ser dividido en el complejo hidrofóbico  $\text{F}_0$ -ATPasa embebido en la membrana y que constituye el canal de protones, y en el complejo  $\text{F}_1$ -ATPasa hidrofílico que contiene el núcleo catalítico (Boyer, 1997; Karrasch y Walker, 1999) (Fig. 1.2). El análisis de la estructura cristalográfica de la subunidad  $\text{F}_1$  mostró que tres subunidades  $\beta$  catalíticas ( $\beta$ - $\text{F}_1$ -ATPasa) y tres subunidades  $\alpha$  no catalíticas ( $\alpha$ - $\text{F}_1$ -ATPasa) se alternan de forma ordenada alrededor de un tallo central formado por la subunidad  $\gamma$  (Fig. 1.2) (Abrahams et al., 1994). Cada una de las tres subunidades  $\alpha$  y  $\beta$  contiene un sitio de unión de sustrato, siendo los de la subunidad  $\beta$  de naturaleza catalítica y los de la subunidad  $\alpha$  de naturaleza regulatoria. Cuando los protones pasan por el canal que atraviesa la membrana, el complejo  $\text{F}_0$  rota y el tallo de la subunidad  $\gamma$ , que está firmemente sujeto al complejo  $\text{F}_0$ , rota sobre el anillo  $\alpha_3\beta_3$ , forzando una secuencia de cambios conformacionales en las subunidades  $\beta$  catalíticas que lleva a la síntesis del ATP (Fig. 1.2) (Boyer, 1993; Capaldi y Aggeler, 2002; Yoshida et al., 2001).

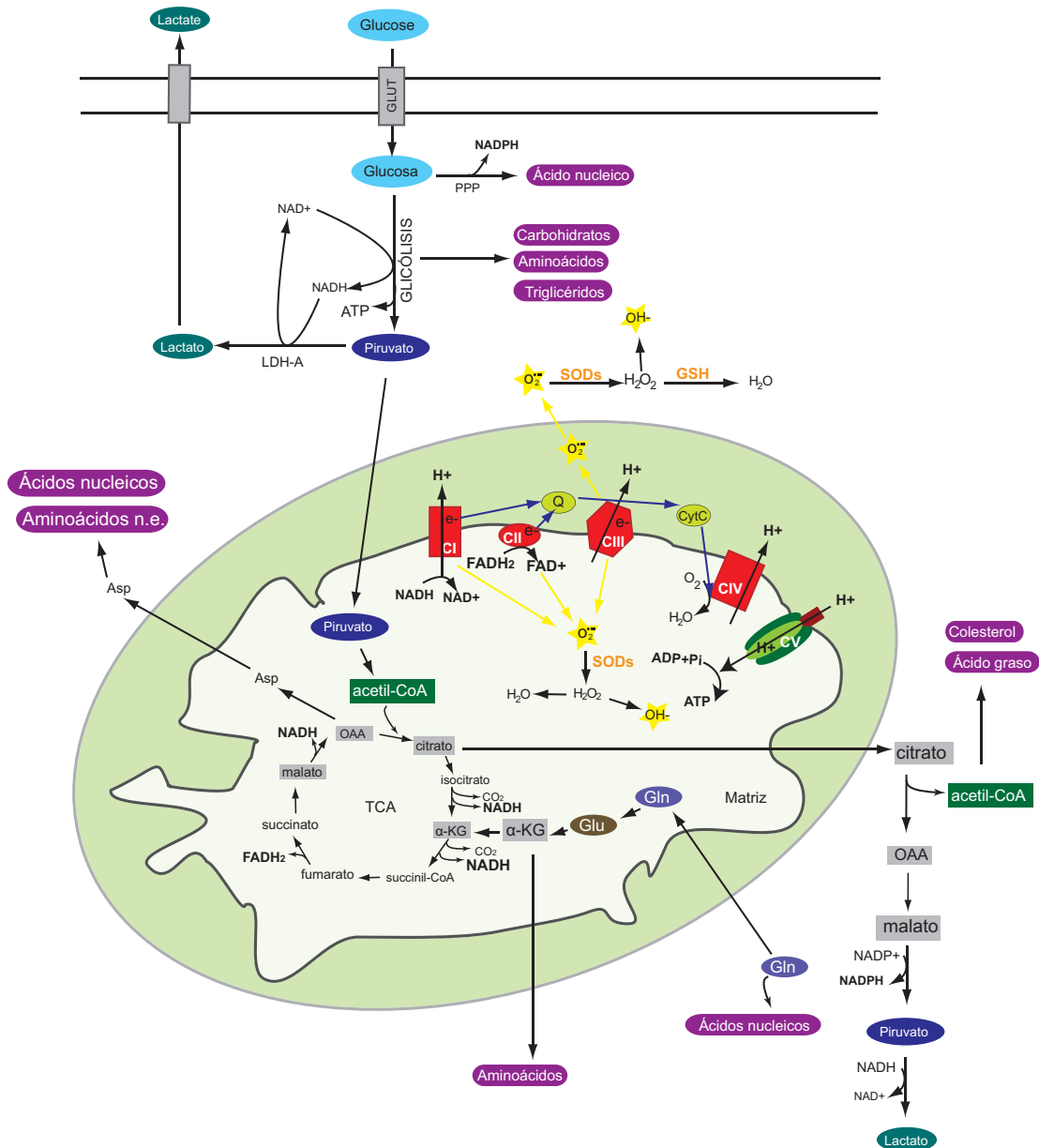


**Figura 1.1: Metabolismo glucolítico y mitocondrial.** Después de que la glucosa entre en la célula mediante transportadores específicos (GLUT), esta puede ser catabolizada en la vía de las pentosas fosfato (PPP) generando poder reductor NADPH y precursores para la síntesis de ácidos nucleicos. La oxidación parcial de la glucosa a piruvato (glicólisis) produce ATP y NADH. Numerosos intermediarios de la vía glicolítica son importantes precursores de la biosíntesis de otras moléculas: ácidos nucleicos, carbohidratos, aminoácidos y triglicéridos (caja morada). La reducción del piruvato a lactato mediante la enzima LDH-A regenera a  $\text{NAD}^+$  y asegura de esta forma un alto flujo glicolítico. El piruvato derivado de la glucosa puede ser también transportado a la mitocondria donde es oxidado a acetil-CoA, que entra en el ciclo TCA a través de la condensación con el oxalacetato (OAA) formando citrato. El ciclo TCA genera  $\text{CO}_2$  y coenzimas reducidas NADH y  $\text{FADH}_2$ . La re-oxidación de NADH y  $\text{FADH}_2$  mediante los complejos respiratorios CI, CII, CIII y CIV lleva a una transferencia de  $e^-$  (flechas azules CI a CIV) al  $\text{O}_2$ , que es reducido a  $\text{H}_2\text{O}$ . El flujo de  $e^-$  a través de la cadena respiratoria está asociado a un bombeo de  $\text{H}^+$  fuera de la matriz produciendo un gradiente electroquímico que atraviesa la membrana interna, el cual es la fuerza usada por la  $\text{H}^+$ -ATP sintasa (CV) para sintetizar ATP. Los complejos I, II y III producen también ROS, tales como el radical superóxido ( $\text{O}_2^-$ ) mediante transferencia directa de  $e^-$  al  $\text{O}_2$  (flecha amarilla). El radical tóxico es transformado en peróxido de hidrógeno ( $\text{H}_2\text{O}_2$ ) por la acción de la enzima superóxido dismutasa (SOD) tanto en la mitocondria como en el citosol. El  $\text{H}_2\text{O}_2$  puede ser reducido por la enzima glutatión peroxidasa (GSH) a  $\text{H}_2\text{O}$  o ser transformado en el radical hidroxilo ( $\text{OH}^-$ ) mediante una oxidación catalizada por metales. Los intermediarios ( $\alpha$ -KG, OAA) del ciclo TCA son convertidos en aminoácidos y en ácidos nucleicos. El citrato puede ser exportado al citosol, donde alimenta la biogénesis de la membrana mediante su conversión a ácidos grasos y colesterol. El OAA citoplásmico generado por la rotura del citrato puede ser transformado en malato, entrar en la mitocondria y reponer el ciclo TCA o bien ser transformado en piruvato, produciendo NADPH como poder reductor biosintético. La glutamina (Gln) puede entrar en la mitocondria, ser convertida en glutamato (Glu) y éste catabolizado a su vez en  $\alpha$ -KG. El  $\alpha$ -KG derivado de la glutamina puede bien reponer el ciclo TCA o ser usado para la síntesis de aminoácidos. Q, ubiquinonas; CytC, citocromo C; Asp, aspartato; n.e., no esencial.

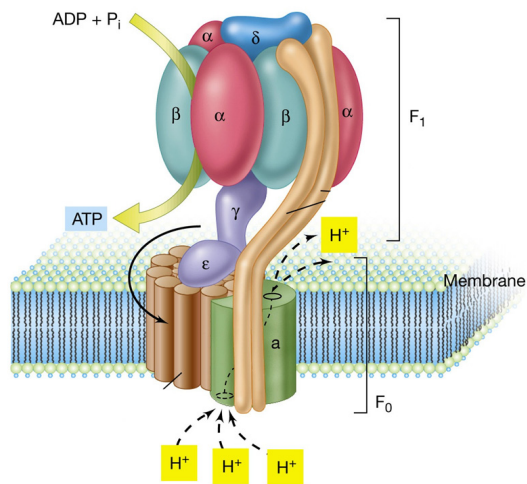


**Figura 1.2.: Ilustración esquemática de la estructura de la H<sup>+</sup>-ATP sintasa mitocondrial.** El complejo F<sub>0</sub> unido a la membrana contiene el canal de protones y está ligado al complejo F<sub>1</sub> por un tallo periférico y por la subunidad γ, la cual forma el eje central del rotor. El dominio F<sub>1</sub> contiene tres subunidades β catalíticas y tres subunidades α no catalíticas que son ordenadas alternadamente formando un anillo. Cuando los protones atraviesan el complejo F<sub>0</sub>, el anillo compuesto de subunidades c (marrón) rota y como resultado la subunidad γ central gira dentro del anillo αβ<sub>3</sub> provocando que los sitios de unión catalítica (β) sufran cambios conformacionales que llevan a la síntesis de ATP.

Sin embargo, la relevancia fisiológica de la mitocondria en la célula no está limitada al suministro de energía. Las mitocondrias están también involucradas en otros procesos celulares importantes tales como la señalización del calcio (Satrustegui et al., 2007) y de especies reactivas de oxígeno (Brunelle et al., 2005; Guzy y Schumacker, 2006; Hamanaka y Chandel, 2010), en el metabolismo de aminoácidos y lípidos y en la biosíntesis del grupo hemo y de los núcleos con hierro y azufre. Además de este papel fundamental en varias vías bioquímicas, las mitocondrias son reguladoras clave en el control y ejecución de la muerte celular (Wang, 2001) e investigaciones recientes han identificado su relación con el sistema inmunitario innato (Seth et al., 2005; Ishikawa y Barber, 2008; Zhong et al., 2008; West et al., 2011).

Las mitocondrias son orgánulos muy dinámicos cuya morfología en su estado estacionario está regulada constantemente por fusión, fisión y procesos de movilidad (Suen et al., 2008). De hecho, la cantidad, función y estructura de las mitocondrias es característico en cada tejido (Garesse y Vallejo, 2001; Pagliarini et al., 2008) y los cambios en la morfología mitocondrial están muy relacionados con su funcionalidad y determinan la apariencia específica del tipo celular (Benard et al., 2007; Li et al., 2004; Szabadkai et al., 2004; Yu et al., 2006). Más aún, el correcto funcionamiento de la dinámica mitocondrial es esencial para el mantenimiento de las tareas y la herencia de la mitocondria (Westermann, 2010). Dada la amplia contribución de la mitocondria a la fisiología celular, no sorprende que cambios en la morfología y función mitocondrial hayan sido relacionados con múltiples enfermedades humanas tales como la diabetes, enfermedades neurodegenerativas y el cáncer.

## 1.2 EL METABOLISMO ENERGÉTICO ALTERADO DE LOS TUMORES

### 1.2.1 El fenotipo aeróbico glicolítico del cáncer

El término cáncer hace referencia a un grupo heterogéneo de enfermedades que se caracteriza por la proliferación descontrolada de células anormales y que son capaces de invadir otros tejidos. El proceso a través del que las células normales se convierten en malignas es complejo y ocurre

a múltiples niveles de forma que diferentes tipos de cáncer difieren ampliamente en su etiología y biología. No obstante, en el año 2000, en un artículo de revisión que marcó un hito, Hanahan y Weinberg (Hanahan y Weinberg, 2000) propusieron la existencia de seis alteraciones esenciales que sufren las células tumorales durante su transformación incluyendo auto suficiencia en señales del crecimiento, insensibilidad a señales inhibitoras del crecimiento, evasión de la muerte celular, potencial proliferativo ilimitado, capacidad invasiva y metástasis de tejidos e inducción de angiogénesis. No obstante, en los últimos años el campo de investigación del cáncer ha avanzado mucho y recientemente la glicólisis aeróbica, conocida como el efecto Warburg, fue añadido como otra característica esencial de la mayoría de las células cancerígenas (Kroemer y Pouyssegur, 2008; Cuezva et al., 2009; Ortega et al., 2009; Vander Heiden et al., 2009; Hanahan y Weinberg, 2011) (Fig. 1.3).

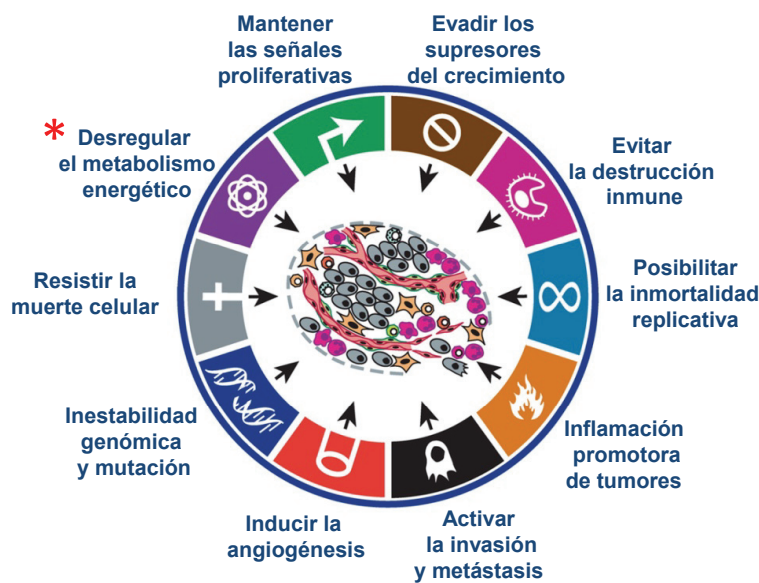


**Figura 1.3: Los marcadores del cáncer.** La ilustración muestra las características esenciales descritas por Hanahan y Weinberg que adquieren la mayoría de las células tumorales durante el desarrollo tumorigénico. El asterisco rojo marca la reprogramación metabólica. Además, la inestabilidad genómica y la mutación así como la inflamación promotora de tumores se han incluido también como características propuestas que facilitan la adquisición de los marcadores esenciales. (Modificado de Hanahan D. and Weinberg RA., Cell 2011)

El metabolismo glicolítico y aeróbico de las células cancerígenas y tumorales fue descubierto por primera vez hace muchos años por Otto Warburg (Warburg, 1956a; Warburg, 1956b). Como resultado de la observación de que la actividad de la glicólisis en las células tumorales es elevada independientemente de la presencia de oxígeno, distinguiéndose de esta manera del Efecto Pasteur, Warburg sugirió que la anormal glicólisis aeróbica en células tumorales y cancerígenas de rápido crecimiento era debida a una reducida actividad bioenergética de la mitocondria, lo que podría provocar la transformación de las células (Warburg, 1956a). Su hipótesis fue acaloradamente debatida y mayoritariamente abandonada o considerada un efecto secundario de la transformación celular (Garber, 2006; Weinhouse, 1956; Weinhouse, 1976) hasta la última década del siglo XX en la que se desarrolló la técnica radiológica de la tomografía de emisión de positrones (PET, positron emission tomography) usando 18F-2-desoxiglucosa (18-FDG) para la detección de tumores. Químicamente, FDG es un análogo no metabolizable de glucosa en que el segundo grupo hidroxilo (-OH) está sustituido por el isótopo radiactivo emisor de positrones fluor-18. Cuando se inyecta 18-FDG en un paciente, éste entra en las células pero no puede ser metabolizado y los rayos gamma

emitidos por el 18-FDG acumulado son detectados por el sistema PET. Como resultado, la detección de 18-FDG refleja la distribución del consumo de glucosa en las células corporales. Actualmente, la extendida aplicación clínica de formación de imágenes tumorales mediante 18-FDG-PET ha confirmado que la mayoría de tumores humanos primarios y metastáticos tiene un consumo de glucosa elevado (Plathow y Weber, 2008; Rigo et al., 1996). Además, una serie de estudios transcriptómicos, proteómicos y funcionales han puesto de manifiesto el postulado de Warburg, demostrando que la mayoría de tumores humanos y de células cancerígenas, comparadas con células normales, tienen una expresión y actividad aumentada de sus genes glicolíticos, una alta tasa de consumo de glucosa así como una elevada tasa de producción de lactato (Bi et al., 2006; Cuezva et al., 2002; Gullino et al., 1967; Isidoro et al., 2005; Isidoro et al., 2004; Kallinowski et al., 1988; Lu et al., 2007; Ortega et al., 2009; Sauer et al., 1982).

### **1.2.2 La mitocondria y la huella bioenergética del cáncer**

La hipótesis de que el fenotipo glicolítico de las células de cáncer era el resultado de un daño de la respiración mitocondrial (Warburg, 1956a) es aún un asunto de debate (Funes et al., 2007; Zu y Guppy, 2004). De todas formas, muchos estudios han descrito que las mitocondrias tumorales son a menudo menos numerosas y más pequeñas, carecen de crestas, poseen profundas alteraciones ultraestructurales y son menos activas que en tejidos normales (Carew y Huang, 2002; Krieg et al., 2004; Modica-Napolitano et al., 2007; Modica-Napolitano y Singh, 2002; Pedersen, 1978; Simonnet et al., 2002; Springer, 1980).

Más aún, recientes estudios proteómicos de nuestro laboratorio proporcionan evidencias convincentes que apoyan los postulados de Warburg. Estos estudios determinaron los niveles de la expresión de la subunidad catalítica de la H<sup>+</sup>-ATP sintasa ( $\beta$ -F1-ATPasa) como un marcador de la fosforilación oxidativa en biopsias de tejido normal y tumoral de los mismos pacientes. Dado que tanto una reducción del complemento total de mitocondrias como una disfunción del sistema OXPHOS pueden provocar una actividad bioenergética reducida de la mitocondria (Cuezva et al., 2002), se determinó la expresión de Hsp60 como proteína estructural de la mitocondria, así como la de la enzima de la vía glicolítica gliceraldehído-3-fosfato deshidrogenasa (GAPDH). De esta manera se realizó la estimación del potencial bioenergético de la mitocondria evaluado según el ratio  $\beta$ -F1-ATPasa/Hsp60 y de la capacidad mitocondrial global de la célula evaluado según el ratio  $\beta$ -F1-ATPasa/Hsp60/GAPDH (Cuezva et al., 2002; Isidoro et al., 2005; Isidoro et al., 2004).

Con esta aproximación se demostró que la expresión normalizada de  $\beta$ -F1-ATPasa se reduce significativamente en hepatoma de rata (de Heredia et al., 2000) y en diferentes carcinomas humanos comparado con el tejido normal que los rodea (Cuezva et al., 2002; Isidoro et al., 2005; Isidoro et al., 2004; Cuezva et al., 2004), lo que indica que la capacidad bioenergética mitocondrial de las células tumorales es defectuosa. De acuerdo con hipótesis de Warburg, estos cambios en la composición proteómica mitocondrial fueron acompañados por la inducción de marcadores

glicolíticos. Este rasgo proteómico se definió como la “huella bioenergética del cáncer” (Cuezva et al., 2002; Cuezva et al., 2009) (recientemente simplificado como el ratio  $\beta$ -F1-ATPasa/GAPDH, Lopez-Rios et al., 2007) y se ha demostrado su alteración en más del 95% de los pacientes analizados en grandes cohortes de carcinomas de pulmón (Cuezva et al., 2004), mama (Isidoro et al., 2005) y colon (Cuezva et al., 2002). Más aún, otros estudios han confirmado y extendido esta característica proteómica a diferentes carcinomas tales como cáncer renal, de hígado, de esófago y gástrico (Cuezva et al., 2009; He et al., 2004; Hervouet et al., 2005; Li et al., 2010b; Lin et al., 2008; Meierhofer et al., 2004; Unwin et al., 2003; Yin et al., 2004).

Notablemente, la huella bioenergética también proporciona un marcador predictivo de la respuesta a quimioterapia (Hernlund et al., 2009; Lin et al., 2008; Sanchez-Arago y Cuezva, 2011; Sanchez-Arago et al., 2010; Shin et al., 2005) y un indicador de la progresión de la enfermedad, dado que su grado de alteración está asociado con el pronóstico del cáncer de pacientes con carcinomas de pulmón (Cuezva et al., 2004; Lopez-Rios et al., 2007), colon (Cuezva et al., 2002; Lin et al., 2008) y mama (Isidoro et al., 2005).

La relevancia del postulado de Warburg se vio reforzada funcionalmente al demostrar que la alteración de la huella bioenergética observada en distintos tumores está asociada con la transformación metabólica y bioquímica de las células cancerígenas. Así, la tasa de consumo de glucosa estimada mediante FDG-PET es, de manera significativa, inversamente proporcional tanto a la expresión de  $\beta$ -F1-ATPasa como a su huella bioenergética en cáncer humano de pulmón (Lopez-Rios et al., 2007). Además, mediante la generación de líneas celulares de cáncer de colon HCT116 que expresan diferentes niveles de  $\beta$ -F1-ATPasa, se ha demostrado que la actividad de la fosforilación oxidativa define la tasa de utilización de glucosa por la glicólisis aeróbica (Lopez-Rios et al., 2007; Sanchez-Arago et al., 2010). En conjunto, estos datos apoyan el hecho de que una respiración mitocondrial dañada participa en la inducción de un aumento en la avidéz de glucosa de las células cancerígenas (Ortega et al., 2009).

### **1.2.3 Mecanismos moleculares que definen el fenotipo glicolítico de las células cancerígenas**

En los últimos años muchos artículos han demostrado una conexión entre genes vinculados con el cáncer y el efecto Warburg. En particular, se ha demostrado que la activación de los oncogenes, la inhibición de genes supresores de tumores y la expresión del factor inducible por hipoxia 1 alfa (HIF1 $\alpha$ ) provocan el cambio glicolítico estimulando la expresión de enzimas/transportadores glicolíticos y atenuando la respiración mitocondrial.

Por ejemplo, el oncogen *c-myc*, frecuentemente sobreexpresado en cáncer, es un factor de transcripción positivo de muchas enzimas glicolíticas, incluyendo los transportadores de glucosa y el lactato deshidrogenasa-A (LDH-A) (O’Connell et al., 2003; Osthus et al., 2000; Shim et al., 1997). LDH-A se encuentra sobreexpresado en numerosos tumores y su disminución compromete la proliferación de células cancerígenas (Fantin et al., 2006; Le et al., 2010). c-MYC puede activar

también la biogénesis mitocondrial (Li et al., 2005) y recientemente se ha demostrado que c-MYC aumenta la expresión de la glutaminasa mitocondrial, estimulando por tanto el metabolismo glutamínico y la anaplerosis de las células cancerígenas, asunto discutido con más detalle en la sección 1.2.4 (Gao et al., 2009).

La vía de señalización PTEN/Akt/mTOR, un regulador clave del crecimiento, proliferación y metabolismo de la glucosa celular, está a menudo desregulada en células tumorales. Una señalización aumentada de Akt estimula la reprogramación metabólica mediante la regulación de la expresión y actividad de enzimas glicolíticas clave tales como la hexoquinasa (HK) y 6-fosfofructo-2-quinasa (PFK2) así como también de transportadores de glucosa y de otros nutrientes (Edinger y Thompson, 2002; Elstrom et al., 2004). Más aún, se ha descubierto que Akt inhibe la  $\beta$ -oxidación de ácidos grasos al impedir la expresión de la carnitina palmitoiltransferasa (CPT1A) (DeBerardinis et al., 2006), apoyando de este modo el programa anabólico de células altamente proliferativas (ver 1.2.4).

La proteína supresora de tumores p53 también influye en el equilibrio metabólico entre la glicólisis y OXPHOS. Por un lado, el promotor HK2 dispone de sitios de unión de p53 (Mathupala et al., 1997) y se ha demostrado que una sobreexpresión de una versión dominante negativa de p53 en células de MCF7 promueve un incremento en la actividad de HK2 y en el consumo de glucosa (Smith et al., 2006). Por otro lado, p53 disminuye la expresión del transportador de glucosa GLUT1 y activa el regulador TIGAR (TP53-induced glycolysis and apoptotic regulator) y SCO2 (Bensaad et al., 2006; Matoba et al., 2006; Schwartzberg-Bar-Yoseph et al., 2004). TIGAR es un regulador negativo de fructosa-2,6-bisfosfatasa y SCO2 es necesario para el ensamblaje de citocromo c oxidasa subunidad 2 del complejo IV de la cadena de transporte de electrones (Bensaad et al., 2006; Matoba et al., 2006). En consecuencia, la pérdida de la función de p53 daña la respiración mitocondrial y fomenta la vía glicolítica.

Se ha sugerido además que la adaptación al microambiente hipóxico en el que crecen los tumores favorece la glicólisis y reduce la oxidación completa de la glucosa en la mitocondria. En condiciones de baja presión de oxígeno se estabiliza el factor de transcripción HIF1 $\alpha$  (Semenza, 2003), lo que a su vez provoca el incremento de una serie de proteínas glicolíticas (transportador de glucosa, enzimas glicolíticas, LDH-A) y de proteínas involucradas en la angiogénesis, facilitando la neovascularización tumoral (Ebert et al., 1995; Semenza et al., 1994). Además, HIF1 $\alpha$  reduce la tasa de fosforilación oxidativa y refuerza el fenotipo glicolítico al provocar la descarga de piruvato de la mitocondria mediante la inducción de la piruvato deshidrogenasa quinasa 1 (PDK1) (Kim et al., 2006; Papandreou et al., 2006). PDK1 es un regulador negativo del piruvato deshidrogenasa (PDH), que es la enzima cuello de botella en la conversión del piruvato derivado de la oxidación parcial de la glucosa en acetil-CoA. HIF1 $\alpha$  puede también modular la estructura y dinámica mitocondrial (Chiche et al., 2010) e inhibir la biogénesis mitocondrial al contrarrestar a c-MYC (Zhang et al., 2007b). Además, HIF1 $\alpha$  altera la actividad de la citocromo c oxidasa (COX) al inducir un cambio de la isoforma COX4-1 por la COX4-2, que resulta en una transferencia más eficiente de electrones a



O<sub>2</sub>, reduciendo así el estrés oxidativo derivado del metabolismo mitocondrial (Fukuda et al., 2007). Junto a esto, HIF1 $\alpha$  induce la expresión de miR-210, que tiene una participación fundamental en el control del metabolismo mitocondrial durante la hipoxia: miR-210 reprime la expresión de las proteínas de ensamblado de los núcleos de hierro y azufre 1 y 2 (ISCU1/2) y de COX10, lo que resulta en una reducción de la actividad de los complejos de la ETC (Chan et al., 2009; Chen et al., 2010).

Es interesante destacar que las propias mitocondrias están involucradas en la estabilización de HIF1 $\alpha$ . La mutación de pérdida de función de las enzimas del ciclo TCA, succinato deshidrogenasa (SDH) y fumarato hidratasa (FH) causa la acumulación de sus sustratos -succinato y fumarato-, lo que a su vez provoca la estabilización de HIF1 $\alpha$  al interferir con prolihidroxilasas que están involucradas en la degradación de HIF1 $\alpha$  (Isaacs et al., 2005; King et al., 2006; Selak et al., 2005). De forma similar, la alteración funcional de la respiración mitocondrial promueve un aumento en la producción de ROS que inhibe la degradación de HIF1 $\alpha$  (Brunelle et al., 2005; Guzy et al., 2005; Mansfield et al., 2005) lo que finalmente lleva a un ciclo de retroalimentación positiva de regulación de la actividad glicolítica.

Por último, muchos estudios han demostrado que las células de cáncer provenientes de distintos tejidos muestran frecuentemente mutaciones somáticas en el mtDNA (Carew y Huang, 2002; Carew et al., 2003; Copeland et al., 2002; Polyak et al., 1998). Estas mutaciones mitocondriales pueden surgir junto con una progresión tumoral como resultado de una producción de ROS incrementada debido a una respiración oxidativa disfuncional (Brandon et al., 2006). Algunas mutaciones del mtDNA favorecen activamente la producción de ROS, fomentando de esta forma la progresión (Brandon et al., 2006; Petros et al., 2005; Zhou et al., 2007), invasión (Amuthan et al., 2001; van Waveren et al., 2006) y metástasis (Ishikawa et al., 2008) tumoral, mientras que otras se cree que son factores importantes que contribuyen a la disfunción de la respiración mitocondrial (Simonnet et al., 2002; Wallace, 2005). En este sentido, la expresión reducida de algunas de las subunidades de los complejos OXPHOS codificadas en el mtDNA provoca una menor actividad de la respiración mitocondrial en cáncer (Gallardo et al., 2006; Krieg et al., 2004; Simonnet et al., 2003; Bonora et al., 2006).

### **1.2.4 Glicólisis aeróbica: el fenotipo de células proliferativas**

El fenotipo glicolítico no es una característica única de las células tumorales, de hecho la glicólisis aeróbica es el metabolismo predominante usado por las células altamente proliferativas (Brand y Hermfisse, 1997; Hume et al., 1978; Wang et al., 1976) y por las células embrionarias (Cuezva et al., 1997; Johnson et al., 2003; Kondoh et al., 2007). En este sentido, al ser estimulados para proliferar, los timocitos de rata y los linfocitos humanos muestran un incremento en el consumo de glucosa, una actividad aumentada de las enzimas glicolíticas y una conversión casi total de glucosa a lactato. La vuelta de estas células al estado no proliferativo está acompañada de una disminución de la tasa glicolítica y de la producción de lactato (Brand et al., 1988; Wang et al., 1976). De forma

coherente, el crecimiento de *S. cerevisiae* en cultivo está ligado a una oscilación en la actividad de la glicólisis y de la OXPHOS de tal manera que durante el ciclo de división celular se observa una actividad preferente de la glicólisis frente a una respiración mitocondrial disminuida (Tu et al., 2005; Tu y McKnight, 2006). Dado que aparte de su implicación en la producción de energía, las mitocondrias son la fuente principal de producción de ROS de la célula, se ha sugerido que la utilización preferente de la glicólisis aeróbica durante la fase proliferativa podría ser un medio desarrollado para limitar el daño oxidativo durante una etapa en la que el DNA podría ser más vulnerable (Brand y Hermfisse, 1997; Chen et al., 2007).

Se ha razonado que las células tumorales se benefician del aumento de la glicólisis aeróbica porque éste garantiza el suministro de grandes cantidades de precursores para la biosíntesis de las proteínas, nucleótidos y lípidos así como de poder reductor necesario para los procesos biosintéticos de células proliferativas (Fig. 1.1) (DeBerardinis et al., 2008; Ortega et al., 2009). En este contexto, se ha de considerar que la vía glicolítica no solamente cataboliza glucosa y proporciona energía, sino que también es crucial para los procesos anabólicos. Los intermediarios de la glicólisis son importantes precursores para la síntesis de aminoácidos y lípidos y la metabolización de glucosa en la vía de las pentosas fosfato (PPP, pentose phosphate pathway) proporciona la ribosa-5-fosfato necesaria para la síntesis de ácidos nucleicos y NADPH, el coenzima reducido fundamental utilizado para aportar poder reductor en los procesos anabólicos (Fig. 1.1) (Ortega et al., 2009).

Por otro lado, las células cancerígenas regulan sus procesos anabólicos mediante la expresión preferencial de la isoforma fetal M2 de la piruvato quinasa (PKM2) (Mazurek et al., 2005), la enzima que cataliza la conversión de fosfoenolpiruvato (PEP) en piruvato. La actividad enzimática de PKM2 es menor que la de otras isoformas (Mazurek et al., 2005) y se regula negativamente en respuesta a la estimulación por factores de crecimiento por la unión de péptidos fosfotirosina (Christofk et al., 2008b). Sorprendentemente, es la habilidad de disminuir la actividad del piruvato quinasa lo que parece ser importante para un rápido crecimiento de las células tumorales (Christofk et al., 2008a; Christofk et al., 2008b). Se cree que la principal ventaja para que las células tumorales expresen a PKM2 es que su menor actividad favorece la desviación de los intermediarios glicolíticos hacia procesos biosintéticos (Christofk et al., 2008a; Christofk et al., 2008b). Un estudio reciente ha mostrado que la expresión de PKM2 proporciona una ventaja selectiva sobre las células que expresan PKM1 (Christofk et al., 2008a) y que, sorprendentemente, la oncoproteína c-MYC estimula una expresión preferencial de PKM2 sobre PKM1 (David et al., 2010). De manera alternativa, se ha propuesto que la actividad disminuida de PKM2 en células tumorales podría también fomentar una vía glicolítica no convencional, en la cual el PEP donaría su fosfato a la enzima glicolítica fosfoglicerato mutasa (PGAM1). Esto a su vez incrementa la actividad de PGAM1 y la producción de piruvato, fomentando un ciclo de retroalimentación positivo que estimula la vía glicolítica y sus ramas anabólicas (Vander Heiden et al., 2010).

Los intermediarios del ciclo TCA son también utilizados para la biosíntesis de diferentes macromoléculas. El oxaloacetato (OAA) y el  $\alpha$ -ketoglutarato ( $\alpha$ -KG) son precursores esenciales

de aminoácidos no esenciales utilizados en la síntesis de proteínas y nucleótidos (Fig. 1.1). Más aún, se ha observado que el ciclo TCA en células tumorales puede ser interrumpido entre el citrato y  $\alpha$ -KG (Parlo y Coleman, 1984). En esta situación, el citrato no resulta oxidado, sino que es preferencialmente exportado desde la mitocondria al citoplasma para suministrar unidades de acetil-CoA para la síntesis de colesterol y ácidos grasos, avivando de esta forma la biogénesis de la membrana de células proliferativas (Fig. 1.1) (Hatzivassiliou et al., 2005; Parlo y Coleman, 1984). El OAA citoplasmático resultante de la rotura del citrato en acetil-CoA es convertido en malato y puede bien ser devuelto a la mitocondria y entrar en el ciclo TCA o ser convertido en piruvato por la enzima málica generando NADPH como un agente reductor (Fig. 1.1) (DeBerardinis et al., 2007). Para reponer los intermediarios “perdidos” en las reacciones biosintéticas del ciclo TCA y garantizar un flujo continuo en todo el ciclo, el piruvato puede ser carboxilado generando OAA, y el  $\alpha$ -KG puede ser completado mediante el consumo de glutamina que es convertida en glutamato por la glutaminasa y catabolizado a su vez en  $\alpha$ -KG (Fig. 1.1) (DeBerardinis et al., 2007; Ortega et al., 2009). La glutamina es muy utilizada por algunos cánceres y células PROLIFERATIVAS (Baggetto, 1992; DeBerardinis et al., 2007) y al entrar en el ciclo TCA, el  $\alpha$ -KG derivado de la glutamina puede ser metabolizado a OAA para procesos biosintéticos o a malato que puede ser convertido en el citoplasma en piruvato y en poder reductor NADPH (DeBerardinis et al., 2007). En general el metabolismo energético y en particular la glicólisis y el ciclo TCA de una célula de cáncer se reorganiza para aumentar las reacciones anabólicas. Por tanto, al fenotipo glicolítico del cáncer se le ha relacionado con la inevitable reprogramación metabólica experimentada por las células como resultado del comienzo de la proliferación celular (Cuezva et al., 2009; Ortega et al., 2009).

### 1.2.5 Metabolismo energético y progresión del cáncer

Con el objetivo de caracterizar los cambios metabólicos que ocurren durante la transformación a un estado cancerígeno, un trabajo reciente ha llevado a cabo un análisis multiparamétrico metabólico de varias líneas celulares tratadas con compuestos que perturban el metabolismo energético. Así, este estudio demostró que la conversión glicolítica en respuesta a una respiración mitocondrial anómala es un evento temprano que se expande a medida que las células se malignizan (Ramanathan et al., 2005). Es interesante destacar el hecho de que la transformación de células madre adultas mesenquimatosas humanas fomenta un incremento en su dependencia de la fosforilación oxidativa (Funes et al., 2007). Sin embargo, cuando estas células transformadas fueron implantadas en ratones inmunodeprimidos se observó un incremento en la glicólisis acompañado por la disminución de los genes del ciclo TCA (Funes et al., 2007). De forma similar, las células transformadas de H-RasV12/E1A muestran una activación de la fosforilación oxidativa en una etapa temprana de transformación (de Groof et al., 2009). No obstante, según se incrementa el potencial tumorigénico de estas células, se observa un aumento de la glicólisis y una disminución de la respiración mitocondrial unida a altas posibilidades de supervivencia (de Groof et al., 2009). Generalmente, a medida que crece un tumor sólido, el microambiente o núcleo del tumor se vuelve más hipóxico y de hecho una menor dependencia de la respiración aeróbica se vuelve

ventajosa para la célula (Gatenby y Gillies, 2004). Más aún, una glicólisis aumentada que resulta en la acidificación del microambiente tumoral así como en la aparición de mutaciones de mtDNA, daños a la membrana mitocondrial y disfunciones en OXPHOS que contribuyen a la progresión tumoral y favorecen un comportamiento más invasivo del tumor (Amuthan et al., 2001; Gatenby y Gillies, 2004; Ishikawa et al., 2008; van Waveren et al., 2006).

En concordancia con estas observaciones, hemos demostrado recientemente que para la progresión de tumores in vivo es necesaria la selección previa de células cancerígenas con un fenotipo celular en el que la actividad bioenergética de la mitocondria esté reprimida (Sanchez-Arago et al., 2010). La adquisición de este rasgo metabólico no está basada en un cambio genético permanente; más bien respresenta una característica reversible que resulta de la adaptación metabólica de las células al medio en el que las células tumorales se desarrollan in vivo (Sanchez-Arago et al., 2010). En este contexto, el tratamiento farmacológico de células cancerígenas con dicloroacetato (DCA) que desencadena un cambio a una vía de provisión de energía dependiente de la mitocondria fomenta in vivo la regresión tumoral (Bonnet et al., 2007; Michelakis et al., 2010; Michelakis et al., 2008; Sanchez-Arago et al., 2010) De forma similar, la activación molecular del metabolismo oxidativo inhibe el crecimiento tumoral en mamíferos (Schulz et al., 2006) y previene la tumorigenicidad (McFate et al., 2008; Shakya et al., 2009). Al contrario, un modelo animal con la función mitocondrial dañada y la fosforilación oxidativa reducida debido a la anulación de la expresión de la proteína frataxina de la ataxia de Friedreich en el hígado, muestra una supervivencia reducida y desarrolla tumores hepáticos (Thierbach et al., 2005).

En conjunto, estos hallazgos ponen de manifiesto la relevancia del metabolismo energético en la regulación de la tumorigénesis. Además, también sugieren que la represión de la fosforilación oxidativa es un requisito para el desarrollo tumoral in vivo, en el que el microambiente controla el crecimiento celular (Sanchez-Arago et al., 2010).

### **1.3 LA BIOLOGÍA DE $\beta$ -F1-ATPasa**

#### **1.3.1 Visión general de la regulación post-transcripcional de la expresión génica**

A lo largo del ciclo de vida de una célula, la expresión de sus genes se modifica de forma constante y dinámica para adaptarse a distintas condiciones ambientales y fisiológicas. Anteriormente se creía que la regulación de la expresión génica estaba controlada principalmente al nivel de la transcripción. Hoy en día se ha demostrado que múltiples niveles de regulación post-transcripcional, tales como el procesado, exportación, localización, degradación, silenciamiento y traducción de mRNA representan etapas esenciales en el control de la expresión de genes (Hieronymus y Silver, 2004; Moore, 2005). En comparación con la regulación transcripcional, el control post-transcripcional proporciona un mecanismo más rápido para incrementar la concentración celular de las proteínas

codificadas y, por tanto, para responder más efectivamente a las demandas fisiológicas de la célula (Martin y Ephrussi, 2009).

En el núcleo, los pre-mRNA son co- y/o post-transcripcionalmente procesados (proceso de corte y empalme o splicing, adición en 5' de 7-metil-guanosina o cap, procesamiento del extremo 3' y poliadenilación) mediante proteínas específicas y empaquetado en una partícula ribonucleoproteica (mRNP) compuesta por el mRNA, proteínas y RNA pequeños no codificantes. Durante todo su ciclo de vida, el mRNA actúa como una plataforma para la unión de proteínas y RNA no codificantes (por ej. miRNA). De hecho, la composición única de la mRNP representa el substrato real de los eventos de regulación post-transcripcional y, por tanto, lo que dicta el destino metabólico de los mRNA, i.e., su localización subcelular, degradación y traducción, así como con su interacción con señales exteriores (Hieronymus y Silver, 2004; Keene y Tenenbaum, 2002; Moore, 2005). La mayoría de los factores de unión del RNA se unen a secuencias o estructuras específicas, llamadas elementos reguladores *cis*, en el mRNA. Estos elementos reguladores *cis* se encuentran principalmente en el 3'UTR del mRNA (de Moor et al., 2005), aunque también aparecen en el 5'UTR (Muckenthaler et al., 1998; Tsai et al., 2007) o en regiones codificantes (Ricart et al., 2002).

Tras ser exportados al citoplasma, las mRNP pueden ser inmediatamente traducidas o mantenidas en un estado traduccional inactivo hasta que se alcanza la localización subcelular apropiada y/o una señal inicia el momento preciso en el que sintetizar la proteína. La combinación de la localización subcelular y una traducción controlada sirve para restringir la síntesis de proteínas a un compartimento específico y permite a la célula organizar los diferentes compartimentos celulares y sus funciones (Holt y Bullock, 2009; Lecuyer et al., 2007). Se han descrito numerosos e importantes ejemplos de traducción restringida en el tiempo y el espacio durante la ovogénesis de *Drosophila* y *Xenopus*, en la que la localización del mRNA y el control traduccional juegan un papel crucial en especificar los futuros ejes del cuerpo embrionario (Driever y Nusslein-Volhard, 1988; Ephrussi et al., 1991; Gavis y Lehmann, 1992; Rebagliati et al., 1985). Por ejemplo, la localización del mRNA bicoid en el polo anterior del oocito de *Drosophila* y su correcta traducción son esenciales para producir un gradiente de la proteína Bicoid que se ajuste a los ejes anterior-posterior del embrión (Driever y Nusslein-Volhard, 1988). De forma similar, el transporte del mRNA de oskar al polo posterior de los oocitos de *Drosophila* y su traducción específica entre la ovogénesis intermedia a tardía son esenciales para la formación de la línea germinal y del abdomen (Ephrussi et al., 1991; Riechmann y Ephrussi, 2001). La segregación asimétrica del mRNA en localizaciones subcelulares fue también observada en células somáticas (Adereth et al., 2005; Mingle et al., 2005; St Johnston, 2005). Un ejemplo bien caracterizado es la localización del mRNA  $\beta$ -actina a lugares de polimerización de actina, contribuyendo por tanto a la motilidad general de la célula mediante la provisión de nuevos monómeros de actina (Lawrence y Singer, 1986; Ross, 1997; Zhang et al., 2001). En el 3'UTR del mRNA  $\beta$ -actina existe un elemento en *cis* denominado región de código de barras o zipcode que es el elemento de unión de la proteína de unión a RNA ZBP1 (Zipcode-binding protein) y que fomenta la localización del mRNA  $\beta$ -actina y previene al mismo

tiempo una traducción temprana del transcrito en el citoplasma (Hüttelmaier et al., 2005). Se han descrito diversos mecanismos moleculares para asegurar una localización asimétrica del mRNA en la célula, incluyendo la difusión y el atrapamiento local (Forrest y Gavis, 2003), la protección local frente a la degradación (Ding et al., 1993) y el más comúnmente utilizado, el transporte activo a lo largo del citoesqueleto (St Johnston, 2005).

El objetivo del silenciamiento traduccional son todas las etapas de la traducción (iniciación, elongación y terminación). Sin embargo, la iniciación de la traducción, que es en la mayoría de los casos el paso que limita la tasa de traducción, es el paso que más frecuentemente está sujeto a regulación (Martin y Ephrussi, 2009). A este respecto, se ha demostrado que el acortamiento de la cola de adeninas o poli(A) es un mecanismo crucial para silenciar a los mRNA durante su desarrollo (Paris et al., 1988; Vassalli et al., 1989). Más aún, el comienzo de la traducción eucariótica dependiente de *cap* requiere la asociación del factor de iniciación de la traducción 4G (eIF4G) a la proteína de unión al *cap* eIF4E. Este paso está frecuentemente regulado bien globalmente mediante proteínas de unión 4E (4E-BP), las cuales aíslan a eIF4E, o bien de forma individual mediante la acción de factores que actúan en *trans* que intervienen en la interacción eIF4G-eIF4E (Richter y Sonenberg, 2005). Así, por ejemplo, la proteína de unión al elemento citoplasmático de poliadenilación (CPEB) se une a este elemento en el transcrito y recluta a Maskin, una proteína que compite con eIF4G por la unión a eIF4E (Sonenberg y Hinnebusch, 2009). De forma similar, el mRNA oskar es silenciado por la proteína Cup, que se ancla al 3'UTR del mRNA e inhibe eIF4E (Nakamura et al., 2004; Richter y Sonenberg, 2005). La traducción puede igualmente ser inhibida bloqueando el reclutamiento de la subunidad 60S al transcrito (Deng et al., 2008).

En los últimos años se ha demostrado que además de las RNABP, los miRNA juegan un papel muy importante en la regulación post-transcripcional de la expresión de mRNA. Los miRNA son RNA no codificantes cortos, aproximadamente de 22 nucleótidos de longitud expresados en metazoos, animales y plantas. Los miRNA no pueden actuar solos y deben ser incorporados en el complejo silenciador inducido por RNA (RISC). Después de la traducción, el precursor de miRNA, un transcrito con estructuras secundarias tipo horquilla de aproximadamente 70 nucleótidos de longitud, es exportado al citoplasma y procesado por Dicer en un dúplex de miRNA de aproximadamente 20 nucleótidos de longitud. Una hebra del dúplex representa el miRNA maduro (llamada hebra guía o miRNA) y se integra en el complejo RISC, mientras que la otra hebra es liberada (llamada hebra pasajera o miRNA\*) (Krol et al., 2010). La hebra integrada es generalmente la más estable termodinámicamente (Han et al., 2006; Khvorova et al., 2003). De todas formas, en el caso de que ambas hebras, originarias de brazos opuestos del mismo precursor de horquilla (llamados mir-X-3' y mir-X-5'), posean una estabilidad termodinámica similar, puede ocurrir una coacumulación de ambas hebras con diferentes sitios de unión o seed sequences y, por tanto, distintos mRNA diana (Ro et al., 2007). Históricamente, la menos abundante hebra miRNA fue definida como la miRNA\*, pero estudios recientes indican que las hebras de miRNA\* no siempre son subproductos de la biogénesis de los miRNA y pueden también ser cargadas en el complejo RISC y funcionar como

miRNA (Czech et al., 2009; Ghildiyal et al., 2009). Más aún, estudios de secuenciación masiva han demostrado que los ratios de miRNA/miRNA\* así como los niveles de cada hebra de un miRNA en su estado estable pueden variar durante sus fases de desarrollo y en diferentes tejidos (Okamura et al., 2008; Ro et al., 2007).

Normalmente, los miRNA en animales regulan la expresión génica mediante el apareamiento imperfecto con el 3'-UTR de los mRNA diana inhibiendo la síntesis de la proteína o induciendo la degradación del mRNA (Fabian et al., 2010). Sin embargo, recientemente se ha mostrado que algunos miRNA pueden también regular de forma positiva la traducción del mRNA diana (Henke et al., 2008; Orom et al., 2008; Vasudevan et al., 2007). Los mecanismos precisos de la inhibición de la síntesis de proteínas mediada por miRNA son, a día de hoy, controvertidos y aún no bien comprendidos (Fabian et al., 2010). En comparación, se sabe que la degradación de mRNA inducida por miRNA que ocurre tras la desadenilación está mediada por la proteína glicina-triptófano de 182 kDa (GW182), la cual es un componente principal del complejo RISC y recluta desadenilasas al transcrito (Eulalio et al., 2009; Fabian et al., 2010).

### 1.3.2 Biogénesis mitocondrial y regulación post-transcripcional de $\beta$ -F1-ATPasa

Las mitocondrias tienen su propio genoma, un mtDNA que codifica 37 genes, incluyendo componentes de la maquinaria de traducción mitocondrial y 13 subunidades de los complejos respiratorios I, III, IV y V. De todas formas, la mayoría de las proteínas de los complejos de la ETC y todos los factores necesarios para el metabolismo del mtDNA y para la función de los orgánulos están codificados en el núcleo. Se acepta que la biogénesis mitocondrial está regulada principalmente al nivel de la transcripción por un conjunto de factores de transcripción centrales (NRF-1, NRF-2, PPAR $\alpha$ , ERR $\alpha$  y SP1) y por coactivadores (PGC-1 $\alpha$ , PGC-1 $\beta$  y PRC) (Scarpulla, 2008). En concreto, la actividad y expresión diferencial de los coactivadores puede ser modulada por una variedad de señales extracelulares que proporcionan un mecanismo para ajustar finamente el fenotipo bioenergético específico de la célula y del tejido (Scarpulla, 2008). De todas formas y de acuerdo con el papel fundamental que la localización de mRNA ejerce en la regulación de la expresión génica (ver 1.3.1), los mecanismos que controlan la localización (Corral-Debrinski et al., 2000; Lithgow, 2000) y la traducción (Izquierdo y Cuezva, 1997; Martínez-Diez et al., 2006) de mRNA de proteínas mitocondriales codificados en el núcleo contribuyen a definir el fenotipo bioenergético de la célula. A este respecto, varios estudios genómicos a gran escala han mostrado que alrededor de la mitad de los mRNA nucleares que codifican proteínas mitocondriales están dispuestos en los alrededores de la mitocondria y asociados a ésta (Eliyahu et al., 2010; Marc et al., 2002; Saint-Georges et al., 2008). Más aún, la localización preferencial de los transcritos en la periferia de la mitocondria es una característica conservada tanto de la levadura como de las células humanas (Sylvestre et al., 2003), y afecta en particular a mRNA de origen procariótico así como a componentes principales (core) de los complejos mitocondriales (García et al., 2007; Marc et al., 2002).

Como se ha comentado (ver 1.3.1), la localización de mRNA en compartimentos subcelulares específicos es un proceso secuencial y que consta de varias etapas e implica elementos *cis* dentro del mRNA, que unen factores *trans*, y que juntos determinan el transporte, anclaje, estabilidad y traducción localizada a los mRNA (Martin y Ephrussi, 2009; Rodriguez et al., 2008). En este sentido, en *S. cerevisiae* se ha descrito que la localización asimétrica de más de 200 mRNA mitocondriales codificados en el núcleo en polisomas unidos a la mitocondria depende de la asociación de la proteína de unión al RNA Puf3p a un elemento de secuencia conservado en el 3'UTR de los mRNA (Gerber et al., 2004; Saint-Georges et al., 2008). De forma coherente, cepas que sobreexpresan Puf3p muestran disfunciones respiratorias y una morfología y motilidad mitocondrial anormales (Garcia-Rodriguez et al., 2007; Gerber et al., 2004). Sorprendentemente, se ha observado también la existencia de un segundo grupo de unos 224 transcritos asociados a la mitocondria que carecen del sitio de unión al Puf3p y que tanto su expresión como su localización no se ve afectada por esta proteína (Saint-Georges et al., 2008), lo que sugiere la existencia de al menos dos vías independientes para que el mRNA sea transportado y localizado específicamente en la mitocondria. Notablemente, la división en estas dos clases de mRNA refleja también una separación en el patrón temporal de expresión así como en la funcionalidad de las proteínas que codifican. Así, el primer grupo de mRNA dependientes de Puf3p codifica componentes básicos para la biogénesis de la mitocondria, tales como proteínas de importación de proteínas, de la maquinaria de traducción o de factores de ensamblado y son transcritos en las fases tempranas del ciclo mitocondrial (Lelandais et al., 2009). Del otro lado, los transcritos del segundo grupo se transcriben más tarde en el ciclo de la mitocondria (Lelandais et al., 2009) y codifican principalmente proteínas de la respiración y morfología mitocondrial (Saint-Georges et al., 2008). En conjunto, estas observaciones sugieren que la localización espacial y temporal de los mRNA mitocondriales codificados en el genoma nuclear determina la biogénesis mitocondrial.

La regulación post-transcripcional del mRNA de la subunidad catalítica de H<sup>+</sup>-ATP sintasa ( $\beta$ -F1-ATPasa) es un caso paradigmático que ha sido ampliamente estudiado tanto en levaduras como en hígado de rata durante el desarrollo (Cuezva et al., 1997; Egea et al., 1997; Garcia et al., 2010; Izquierdo y Cuezva, 1997; Margeot et al., 2002; Margeot et al., 2005). En levaduras, la adecuada localización mitocondrial y traducción del transcrito requiere la participación del 3'UTR (Margeot et al., 2002) y dos elementos reguladores *cis*, localizados en el marco abierto de lectura (open reading frame, ORF) del mRNA (Garcia et al., 2010). La eliminación del 3'UTR en el gen *ATP2* trae como consecuencias una importación deficiente de la proteína, síntesis reducida de ATP, pérdida o depleción de mtDNA y disfunción respiratoria (Margeot et al., 2002; Margeot et al., 2005). Las secuencias del ORF son necesarias para la localización del transcrito en los alrededores de la mitocondria, y la eliminación de éstas probablemente lleva a una fijación fallida del mRNA a la mitocondria (Garcia et al., 2010; Margeot et al., 2002). Se ha propuesto que la traducción de estos elementos en el ORF es necesaria para mantener al transcrito junto a la mitocondria (Garcia et al., 2010; Komili et al., 2007).



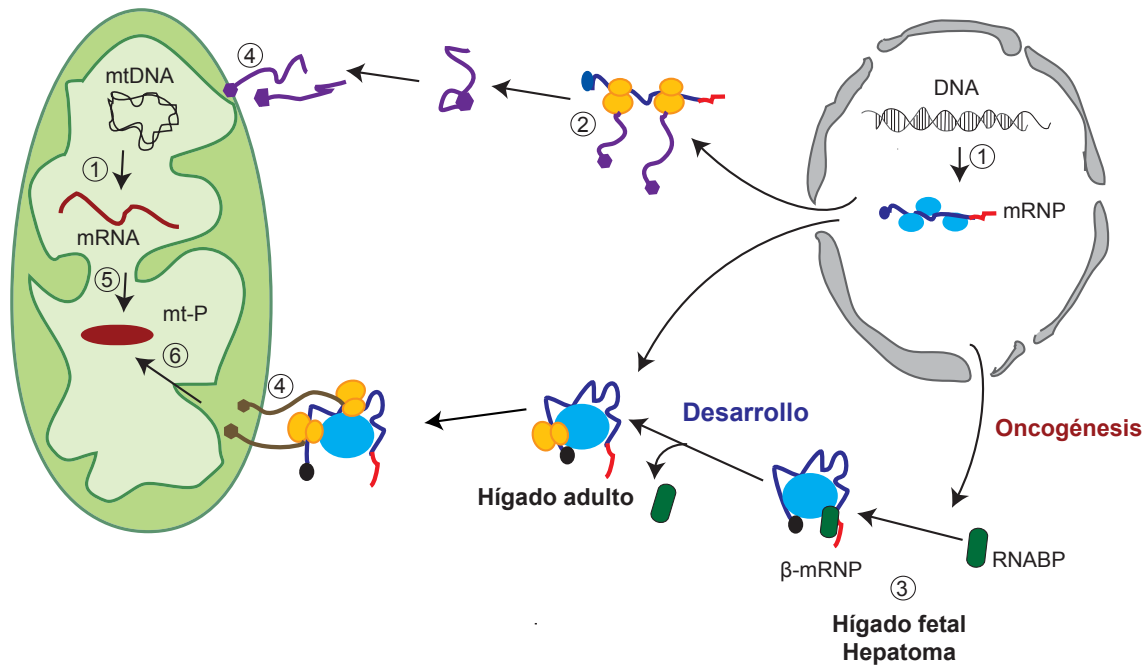


**Figura 1.4. Procesos celulares que controlan la expresión de los genes implicados en la biogénesis mitocondrial.** (1) Transcripción, corte y empalme, y maduración del mtDNA y de los genes mitocondriales codificados en el núcleo. En el núcleo los mRNA son ensamblados en partículas ribonucleoproteicas (mRNP) y exportados al citoplasma. (2) En algunos casos los mRNA codificados en el núcleo son traducidos por ribosomas citoplásmicos, mientras que otros mRNP son transportados a la periferia mitocondrial donde ocurre la traducción localizada del transcrito. (3) El transcrito del  $\beta$ -F1-ATPasa interacciona con proteínas reguladoras (RNABP,  $\beta$ -RNP) que definen el destino metabólico de  $\beta$ -mRNA. Durante el desarrollo de hígado fetal de rata y en hepatocarcinomas de rata (oncogénesis), la traducción de  $\beta$ -mRNA está silenciada por la asociación proteínas de unión específicas (RNABP). En estas situaciones la función bioenergética de la mitocondria se encuentra disminuida. Como resultado de la acción de determinadas señales celulares el enmascaramiento de  $\beta$ -mRNA por las proteínas de unión puede cesar y la traducción por lo tanto completarse. (4) Los precursores proteicos son importados a la mitocondria mediante la maquinaria de importación mitocondrial. (5) La maquinaria de traducción mitocondrial sintetiza polipéptidos codificados en la mitocondria (mt-P) que (6) en algunos casos se ensamblan a complejos mitocondriales mediante proteínas codificadas en el núcleo. ribosoma, naranja; 3'UTR, rojo; RNABP, proteína de unión, verde.

En hepatocitos de rata, el mRNA de  $\beta$ -F1-ATPasa ( $\beta$ -mRNA) está presente en complejos ribonucleoproteicos ( $\beta$ -RNP) grandes (~150 nm) que se encuentran preferencialmente asociados a la membrana mitocondrial externa (Fig. 1.4) (Egea et al., 1997; Ricart et al., 1997). De forma similar a la levadura, un ensamblado y localización subcelular adecuados del  $\beta$ -RNP de mamíferos depende de dos elementos reguladores *cis* situados en el 3'UTR y en el ORF, y de un conjunto de proteínas que interaccionan con estos elementos del mRNA (Ricart et al., 2002). Es interesante señalar que el transcrito de  $\beta$ -F1-ATPasa no ha sido identificado como una diana de la familia PUF ni en levaduras (Saint-Georges et al., 2008) ni en células de mamíferos (Galvano et al., 2008) Éste pertenece al segundo grupo de mRNA mencionado anteriormente, los cuales se encuentran en los alrededores de la mitocondria independientemente de Puf3 (Saint-Georges et al., 2008) y para los que los factores *trans* aún no han sido identificados.

### 1.3.3 Represión de la expresión de $\beta$ -F1-ATPasa en el desarrollo y en cáncer

El control post-transcripcional de la expresión de  $\beta$ -F1-ATPasa es particularmente importante durante el desarrollo de hígado de rata (Luis et al., 1993), oncogénesis (Cuezva et al., 1997; de Heredia et al., 2000) y progresión a lo largo del ciclo celular (Martinez-Diez et al., 2006). En estas situaciones, se ha mostrado que la expresión de  $\beta$ -F1-ATPasa se encuentra especialmente regulada al nivel de la traducción. Durante el desarrollo fetal de la rata, se acumula  $\beta$ -mRNA en el hígado como resultado de un incremento en su estabilidad (Izquierdo et al., 1995; Luis et al., 1993) y se mantiene traduccionalmente reprimido hasta el momento del nacimiento (Fig. 1.4), momento en el que ocurre un rápido incremento en la expresión de la proteína (Luis et al., 1993; Ostronoff et al., 1996; Valcarce et al., 1988). De forma similar, en hepatomas de rata la cantidad de  $\beta$ -F1-ATPasa se encuentra significativamente reducida si lo comparamos con la de un hígado normal adulto, mientras que el nivel de su transcrito no muestra variaciones (de Heredia et al., 2000). El estudio del mecanismo molecular responsable de este efecto mostró que, tanto en hígado fetal como en hepatomas,  $\beta$ -mRNA está traduccionalmente enmascarado como resultado de la interacción con proteínas específicas de unión al RNA (RNABPS) que dificultan una traducción eficiente (Fig. 1.4) (de Heredia et al., 2000; Izquierdo y Cuezva, 1997). En este contexto, se ha mostrado que el 3'UTR de  $\beta$ -mRNA en ratas actúa como un intensificador de la traducción tanto *in vitro* (Izquierdo y Cuezva, 1997; Izquierdo y Cuezva, 2000) como *in vivo* (Di Liegro et al., 2000) y es esencial para la traducción del transcrito debido a su capacidad para interactuar con la maquinaria de traducción (Izquierdo y Cuezva, 1997). Se ha propuesto que la unión de las RNABP al 3'UTR inhibe la actividad intrínseca intensificadora de la traducción del elemento (Izquierdo y Cuezva, 2000), presumiblemente dificultando el acceso de la maquinaria de traducción al mRNA (Di Liegro et al., 2000; Ricart et al., 2002). El hecho de que el mecanismo molecular de represión de la traducción esté conservado para regular la expresión de  $\beta$ -F1-ATPasa en hígado fetal de rata (Izquierdo y Cuezva, 1997) y en hepatomas de rata (de Heredia et al., 2000) sugiere que este mecanismo podría también contribuir al fenotipo bioenergético alterado observado en células de cáncer humanas (ver 1.2.1 y 1.2.2). Este estudio ha sido uno de los objetivos de la presente Tesis Doctoral.

### 1.3.4 Mecanismos y factores *trans* que afectan la expresión/actividad de $H^+$ -ATP sintasa en cáncer

Se han observado múltiples mecanismos independientes que pueden afectar a la actividad bioenergética de la mitocondria en cáncer, entre los que se incluye el control de  $H^+$ -ATP sintasa. En cáncer colorectal el gen *ATP5A1*, que codifica la subunidad  $\alpha$  de la  $H^+$ -ATP sintasa, se encuentra frecuentemente reprimido (Bacolod y Barany, 2010). En células de leucemia mieloide crónica, la expresión de  $\beta$ -F1-ATPasa está limitada por la hipermetilación del promotor del gen codificante *ATP5B*, comprometiendo por tanto la actividad bioenergética de la mitocondria y contribuyendo a la resistencia a la Adriamicina (Li et al., 2010a).

Por otro lado, el péptido inhibidor de la ATPasa mitocondrial, llamado factor inhibidor de la ATPasa 1 o IF1 (Cabezon et al., 2000; Gledhill et al., 2007; Pullman y Monroy, 1963) se encuentra aumentado

en carcinomas de mama, colon y pulmón humanos si lo comparamos con tejidos normales (Sanchez-Cenizo et al., 2010). Originalmente, IF1 fue descrito como un inhibidor de la actividad de la hidrolasa de H<sup>+</sup>-ATP sintasa, es decir, del transporte de protones en contra de gradiente a costa de la hidrólisis de ATP, cuando la respiración mitocondrial se encuentra alterada. En esta situación, el pH de la matriz mitocondrial se vuelve más ácido, IF1 es activado y se une a  $\beta$ -F1-ATPasa para prevenir un gasto innecesario de energía (Cabezon et al., 2000; Gledhill et al., 2007). Ensayos de sobreexpresión de IF1 y de un mutante insensible a la regulación por pH H49K activo de forma constitutiva (Cabezon et al., 2000) en células que expresan bajos niveles de IF1 (Sanchez-Cenizo et al., 2010) mostraron que IF1 desencadena también una reducción en la actividad de H<sup>+</sup>-ATP sintasa, un incremento en la glicólisis aeróbica y, simultáneamente, un incremento en el potencial de la membrana mitocondrial, imitando los efectos de la oligomicina (Sanchez-Cenizo et al., 2010). En cambio, el silenciamiento mediado por siRNA de IF1 en células que expresan altos niveles de IF1 provoca la disminución de la glicólisis aeróbica y un incremento en la actividad de H<sup>+</sup>-ATP sintasa (Sanchez-Cenizo et al., 2010). Por tanto, se sugirió que la inhibición de H<sup>+</sup>-ATP sintasa por IF1 depende también de la relación masa-acción y que en situaciones de expresión aumentada de IF1, como en determinados tumores y células cancerígenas (Sanchez-Cenizo et al., 2010), la proteína inhibe tanto la actividad sintética como la hidrolítica, proporcionando a la célula cancerígena un mecanismo adicional para regular su metabolismo energético (Sanchez-Cenizo et al., 2010).

Finalmente y como se ha comentado con anterioridad, se ha propuesto que las RNABP pueden estar involucradas en el control de la traducción de  $\beta$ -mRNA de rata durante el desarrollo (Izquierdo y Cuezva, 1997; Izquierdo et al., 1995) y oncogénesis (de Heredia et al., 2000) (ver también 1.3.3), así como en la localización de  $\beta$ -mRNA (Ricart et al., 2002). Recientemente, se ha demostrado que HuR, un regulador post-transcripcional central de la expresión génica (Levy et al., 1998) y cuya expresión se encuentra aumentada en la mayoría de tumores humanos (Lopez de Silanes et al., 2003), interacciona con el 3'UTR del  $\beta$ -mRNA humano (Izquierdo, 2006; Ortega et al., 2008). De todas formas, experimentos de silenciamiento y sobreexpresión no revelaron una participación significativa de HuR en el control de la expresión de  $\beta$ -F1-ATPasa (Ortega et al., 2008), lo que sugiere que podría participar en otros sucesos post-transcripcionales tales como la localización y/o el anclaje de  $\beta$ -mRNA (Ortega, et al., 2008).

Aunque las proteínas de unión a  $\beta$ -mRNA podrían, de forma análoga a lo que ocurre durante el desarrollo del hígado de rata, jugar un papel importante en el control del fenotipo bioenergético en cáncer humano, nuestro conocimiento sobre su identidad molecular es escaso. Por tanto, un objetivo primario de nuestro laboratorio ha sido la identificación de posibles proteínas de unión a  $\beta$ -mRNA. Utilizando un procedimiento mejorado de purificación de RNABP basado en el etiquetado del mRNA diana con las horquillas del fago MS2 seguido por cromatografía de afinidad, se identificaron nueve posibles proteínas de unión a  $\beta$ -mRNA que interaccionan *in vitro* con el transcrito humano (Ortega et al., 2010). Estas proteínas están involucradas en la transcripción (DHX9, SFPQ, NONO, ILF3, NCL y NPM1), corte y empalme (SFPQ y NONO), exportación del

RNA al citoplasma (DHX9, NCL, ILF3 e IMP1), procesado de RNA (SFPQ, NONO, NCL y NPM1), localización de RNA (NCL, NPM1, SFPQ, NONO, G3BP1 e IMP1), estabilidad de RNA (IMP1 y G3BP1) y traducción (ILF3, G3BP1, IMP1 y RL8) (Ortega et al., 2010). Más aún, DHX9, NCL, NPM1, ILF3, G3BP1 e IMP1 viajan entre el núcleo y el citoplasma dependiendo de las condiciones ambientales (Gallouzi et al., 1998; Hüttelmaier et al., 2005; Parrott et al., 2005; Tourriere et al., 2001) y forman parte de diferentes RNP que son distribuidas por el citoplasma por las proteínas motoras kinesina y dineína (Elvira et al., 2006; Kanai et al., 2004). El análisis de la interacción *in vivo* y de la relevancia funcional de las tres RNABP (IMP1, NPM1 y G3BP1) en la expresión de  $\beta$ -F1-ATPasa es parte del presente estudio. Un breve resumen de las principales funciones celulares atribuidas a las tres RNABP objeto de estudio se proporciona en el Anexo.



# **OBJECTIVES**



## **2 OBJECTIVES**

The mitochondrial H<sup>+</sup>-ATP synthase is a key element required for the transduction of biological energy. Thus, it is not surprising that mitochondrial deregulated expression of this protein is associated with human pathologies including cancer. In this regard, we have demonstrated that the bioenergetic proteome of tumors differs from that of counterpart normal tissues. In particular, the relative expression of the catalytic subunit of the H<sup>+</sup>-ATP synthase ( $\beta$ -F1-ATPase) is decreased in various human carcinomas and this alteration plays an important role in cancer progression.

The mechanisms that control  $\beta$ -F1-ATPase expression in humans, however, have been poorly characterized. Therefore, the main aim of this study was to characterize the biology of  $\beta$ -mRNA in human cells, which in turn might contribute to explain the altered energetic metabolism of carcinomas and could be beneficial in cancer therapy. In particular, and based on previous data from our laboratory, we have established the following specific objectives:

- (1) Explore the mechanisms that control  $\beta$ -F1-ATPase expression in human breast, colon, esophageal and lung cancer. This objective includes in particular addressing the relevance of translational control in  $\beta$ -F1-ATPase expression in human cancer and the partial characterization that the 3'UTR of  $\beta$ -mRNA has on translation.
- (2) Study the putative interaction and biological relevance of G3BP1, NPM1 and IMP1 with  $\beta$ -mRNA in the cellular context.
- (3) Study the clinical relevance of G3BP1 expression in a cohort of human breast cancer patients.
- (4) Develop cellular systems to analyze the role that miRNAs targeting the 3'UTR of  $\beta$ -mRNA could play as post-transcriptional regulators on  $\beta$ -F1-ATPase expression.





# **MATERIAL AND**

# **METHODS**



## 3 MATERIAL AND METHODS

### 3.1 MATERIAL

#### 3.1.1 Tumor biopsies

Frozen tissue sections obtained from surgical specimens of untreated cancer patients with primary adenocarcinomas of the breast (ductal infiltrating carcinomas), colon, esophageal and lung and squamous lung carcinomas were obtained from the Banco de Tejidos y Tumores, IDIBAPS (Instituto de Investigaciones Biomédicas Pi y Suñer), Hospital Clinic, Barcelona, Spain (Isidoro et al., 2004). See Table A1 in Appendix for a summary of the clinical data of the patients.

The 93 breast tumor samples used for the analysis of G3BP1 expression consisted in tissue samples obtained from patients that had an operation for invasive breast carcinoma at the Hospital Universitario La Paz between 1991 and 2000. For further information see Isidoro et al.; 2005, and Table A2 in Appendix for a summary of the clinical data of the patients of this cohort

All human tissue samples used in this study were anonymized and received in a coded form to protect patient confidentiality. The Institutional Review Board approved the project. Tissue sections of the tumor and normal tissue of each patient were analyzed previously by an expert pathologist.

#### 3.1.2 Human cell lines

BT549 (ATCC HTB-122) Human ductal breast cancer cell line

Hs578T (ATCC HTB-126) Human breast cancer cell line

T47D (ATCC HTB-133) Human ductal breast cancer cell line

HCT116 (ATCC CCL-247) Human colon cancer cell line

Hek293T (ATCC CRL-1573) Human embryonic kidney cell line transformed with adenovirus 5 DNA

HeLa (ATCC CCL-2) Human cervical cancer cell line

Jurkat (ATCC TIB-152) Human T cell leukemia cell line

MCF-12F (ATCC 10783) Normal human breast cell line

NRK (ATCC CRL-6509) Normal rat kidney cell line

C9 (ATCC CRL-1439) Normal rat liver cell line

C4 (Laboratory, AD. Ortega) Derivate of NRK cells that stably express  $\beta$ -F1-ATPase mRNA fused to 3 MS2 hairpins

#### 3.1.3 Bacterial strains

The *E. coli* strains DH5 $\alpha$  and XL-Blue were used for cloning, maintenance and amplification of plasmids. The bacterial culture were grown in Luria-Bertani (LB) media (1% (w/v) bacto-tryptone, 0.5% (w/v) yeast extract and 1% (w/v) NaCl) supplemented with appropriate antibiotics (100  $\mu$ g/ml).

### 3.1.4 Plasmids

Number Name	Insert	Derivate of	Description/Use	Source
pCDNA3			Cloning, pCMV, T7, SP6	Invitrogen, Carlsbad, CA, USA
pBS-SK(+)			Cloning, T7, SP6	Stratagen, LA Jolla, CA, USA
pEGFP-C1			Cloning, mammalian expression (pCMV) of GFP.	Clontech, Mountain View, CA, USA
pGEM T			Cloning, T7, SP6	Promega, Madison, WI, USA
pGEM-PK	PK	pGEM T	Expression of human pyruvate kinase (NM_182471.1) in the eukaryotic TNT expression system.	Lab.
pBS- $\beta$ F1(h)	$\beta$ F1(h)-fl	pBS-SK(+)	Vector coding for full-length human $\beta$ -F1-ATPase mRNA (NM_001686.3).	Lab.: ML. de Heredia
pARF	ARF	pBS-SK(+)	Human ARF mRNA.	Lab.: JM. Izquierdo
pARF-3' $\beta$	ARF-3' $\beta$ (h)	pARF	Human ARF mRNA fused to 3'UTR of human $\beta$ -F1-ATPase.	Lab.: ML. de Heredia
p $\beta$ Gal-3' $\beta$ (r)-MS2	$\beta$ Gal-3' $\beta$ (r)-MS2h(7x)		$\beta$ -galactosidase mRNA fused to rat 3'UTR of $\beta$ -F1-ATPase and seven MS2 hairpins.	Lab.: AD. Ortega (Ortega et al., 2010)
p $\beta$ Gal-MS2	$\beta$ Gal-3' $\beta$ (r)-MS2h(7x)		$\beta$ -galactosidase mRNA fused to seven MS2 hairpins.	Lab.: AD. Ortega (Ortega et al., 2010)
pGFP-CP-nls	GFP-CP-nls	pEGFP-C1	Eukaryotic expression (pCMV) of GFP fused to MS2 coat protein and a nuclear localization signal.	Keneth S. Kosik (Rook et al., 2000)
pIW21	pre $\beta$ (r)-GFP	pCDNA3	Eukaryotic expression (pCMV) or transcription (T7) of pre $\beta$ (rat) fused to GFP.	Lab.: IM. Willers, (this study)
pIW22	pre $\beta$ (r)-GFP-3' $\beta$ F1(h)	pIW21	Eukaryotic expression (pCMV) or transcription (T7,) of pre $\beta$ (rat) fused to GFP and human 3'UTR of $\beta$ -F1-ATPase .	Lab.: IM. Willers, (this study)
pIW23	pre $\beta$ (r)-GFP-3' $\alpha$ F1(h)	pIW21	Eukaryotic expression (pCMV) or transcription (T7) of pre $\beta$ (rat) fused to GFP and human 3'UTR of $\alpha$ -F1-ATPase.	Lab.: IM. Willers, (this study)
pYFP <sub>Ct</sub> -HA-MS2BP	YFP <sub>Ct</sub> -HA-MS2BP	pECFP-C1	Eukaryotic expression (pCMV) of the C-terminal of YFP fused to HA-tagged MS2 coat protein.	S. Hüttelmaier (Stöhr et al., 2006)
pYFP <sub>Nt</sub> -Flag-ZBP1	YFP <sub>Nt</sub> -Flag-ZBP1(ch)	pECFP-C1	Eukaryotic expression (pCMV) of the N-terminal of YFP fused to Flag-tagged chicken Zipcode binding protein.	S.Hüttelmaier (Stöhr et al., 2006)
pIW24	YFP <sub>Nt</sub> -Flag-IMP1(h)	YFP <sub>Nt</sub> -Flag-ZBP1	Eukaryotic expression (pCMV) of the N-terminal of YFP fused to human Flag-tagged IMP1 (NM_006546.3).	Lab.: IM. Willers, (this study)
pIW25	YFP <sub>Nt</sub> -Flag-G3BP1(h)	YFP <sub>Nt</sub> -Flag-ZBP1	Eukaryotic expression (pCMV) of the N-terminal of YFP fused to human Flag-tagged G3BP1 (NM_005754.2).	Lab.: IM. Willers, (this study)
pIW26	YFP <sub>Nt</sub> -Flag-NPM1(h)	YFP <sub>Nt</sub> -Flag-ZBP1	Vector for eukaryotic expression (pCMV) of the N-terminal of YFP fused to human Flag-tagged NPM1 (NM_002520.5).	Lab.: IM. Willers, (this study)
pIW29	pre $\beta$ (r)-GFP-3' $\beta$ MUT	pIW21	Eukaryotic expression (pCMV) or transcription (T7) of pre $\beta$ (rat) fused to GFP and human 3'UTR of $\beta$ -F1-ATPase containing 4 point mutations in the miR-127-5p binding site.	Lab.: IM. Willers, (this study)

**Table 1: Plasmids.** Number/Name, indicates the number of the plasmid or a short description of the insert; Insert, depicts the DNA sequence included in the plasmid (h, human; r, rat; ch, chicken; nls, nucleus localization signal; Nt, n-terminal; Ct, c-terminal); Derivate of, indicates the base vector; Description/Use, indicates the usage and promoter (T7, SP6 and pCMV) present in the plasmid and gives a description of the insert; Source, name of the company or person who provided the plasmid, Lab, laboratory of JM Cuezva. Reference in brackets is referred to the paper where cloning procedure of the plasmid is described.

### 3.1.5 Antibodies

Antigen	Swiss Prot	MW [kDa]	Origen	Use
$\beta$ -F1-ATPase	ATPB_HUMAN (P06576)	52	Rabbit, polyclonal (Lab. JM Cuezva)	WB (1:20000)
GAPDH	G3P_HUMAN (P04406)	35	Mouse monoclonal (Abcam, ab8245)	WB (1:15000)
Hsp60	CH60_HUMAN (P10809)	60	Mouse monoclonal (Stressgen, SPA-807)	WB (1:5000)
G3BP1	G3BP1_HUMAN (Q13283)	55	Mouse, monoclonal (BD Bioscience, 611126)	WB (1:1000) IF (1:200)
G3BP1	G3BP1_HUMAN (Q13283)	55	Rabbit polyclonal (Santa Cruz, sc-985661)	WB (1:1000)
GFP	GFP_AEQVI (P42212)	27	Mouse, monoclonal (Clontech, 8371-2)	WB (1:10000)
$\beta$ -Actin	ACTB_HUMAN (P60709)	42	Mouse monoclonal (Sigma, A1978)	WB (1:100000)
COXI	COX1_HUMAN(P00395)	39	Mouse, monoclonal (Molecular Probes 35-38100)	WB (1:250)
COXIV	COX4_HUMAN (P13073)	17	Mouse, monoclonal (Molecular Probes, A21348)	WB (1:250)
SDH	DHSB_HUMAN (P21912)	32	Mouse, monoclonal (Molecular Probes, A21345)	WB (1:500)
TIA-1	TIA1_HUMAN (P31483)	43	Goat polyclonal (Santa Cruz, sc-1751)	IF (1:200)
ScamC-1	SCMC1_HUMAN (Q6NUK1)	54	Rabbit polyclonal (Lab. J.Satrústegui)	IF (1:200)
$\alpha$ -Tubulin	TBA4A_HUMAN (P68366)	60	Mouse monoclonal (Sigma, T5169)	WB (1:1000)
LDH-A	LDHA_HUMAN (P00338)	37	Mouse, Hybridoma supernatant (Lab. JM Cuezva)	WB (1:1000)
$\gamma$ -F1-ATPase	ATPG_HUMAN (P36542)	33	Mouse, blood serum (Lab. JM Cuezva)	WB (1:1000)
FLAG-M2-tag			Mouse monoclonal (Sigma, F1804)	WB (1:3000) IF (1:1000)

**Table 2: Antibodies.** Antigen, name of the antigen recognized by the antibody; Swiss Prot, accession number and name in Swiss-Prot database (<http://www.uniprot.org/>); MW, molecular weight in kilo Dalton (kDa); Origen, animal used for production and name of the company or laboratory (Lab. followed by name of the leader) where the antibody was produced; Use, WB if used in western blot, IF if used for immunofluorescence, dilution used is indicated in brackets.

### 3.1.6 Oligonucleotides

HPLC purified and lyophilized oligonucleotides were purchased from Invitrogen and resuspended in TE-buffer (Tris-HCl 10 mM pH 8, EDTA 2 mM) to obtain a 100  $\mu$ M solution. The resuspended oligonucleotides were stored at  $-20^{\circ}\text{C}$ . Table 3 contains list of the oligonucleotides used in this study.

### 3.1.7 Radioisotopes

- Redivue-5'-[ $\alpha^{32}$ ]-UTP (Perkin Elmer, Boston, USA), half-life 2 weeks, stored at  $-20^{\circ}\text{C}$
- Easy Tag Express Protein Labeling Mix [ $^{35}\text{S}$ ] (Perkin Elmer, Boston, USA), half-life 3 months, stored at  $4^{\circ}\text{C}$ .

Number	Name	Sense	Sequence 5'-3'	Usage	Tm (°C)	Length (bp)
IW2	R-Egfp-EcoRI	AS	GCGGAATTCACCTTGACAGCTCGTCCATG	C/ piW21,	53	18
IW3	F-3'β-h-EcoRI	SS	GCGGAATTCGGGGTCTTTGTCTCTGTA	C/ piW22	55	19
IW4	R-3'β-h-XhoI	AS	GCGCTCGAGTTTTTTTTTTTTTTGAGGGGTGTA	C/ piW22, piW29	51	19
IW5	F-3'a-h-EcoRI	SS	GCGGAATTCACCTCTGTGGATTACATCAA	C/ piW23, piW29	47	24
IW6	R-3'a-h-XhoI	AS	GCGCTCGAGTTTTTTTTTTAACTATGCATTATG	C/ piW23	41	21
IW7	F-preβ-EGFP-KpnI	SS	GCGGGTACCCGAATCCAGTCTC	C/ piW21	54	24
W14	pCDNA3	AS	CCTTCCAGGGTCAAGGAAG	S: binds in pCDNA3 ~ 80bp after SP6 Promoter	50	20
IW15	pCMV-F	SS	GTCTATATAAGCAGAGCTGG	S: binds in pCMV	53	19
IW22	F-imp1-EcoRI	SS	GCGGAATTCATGAACAAGCTTTACATCGGCAAC	C/ piW24	54	33
IW23	R-imp1-BamHI	AS	GCGGGATCCCTTCTCCGTGCCTGGG	C/ piW24	53	26
IW24	F-G3BP-EcoRI	SS	GCGGAATTCATG GTG ATG GAG AAG CCT AGT C	C/ piW25	54	38
IW25	R-G3BP-BamHI	AS	GCGGGATCCCTGCCGTGGCGCAAAGC	C/ piW25	54	25
IW26	F-NPM1-EcoRI	SS	GCGGAATTCATGGAAAGATTGGATGGACATGG	C/ piW26	53	31
IW27	R-NPM1-BamHI	AS	GCGGGATCCAAGAGACTTCTCCACTGCC	C/ piW26	53	29
IW28	qPCR-IGF2BP1-F	SS	AAGTTCCGGAGGCCCTATGAG	pPCR-SYBR of IMP1 (h) (NM_006546.3)	60	20
IW29	qPCR-IGF2BP1-R	AS	CAGGGATCAGGTGAGACTGC	pPCR-SYBR of IMP1 (h) (NM_006546.3)	59	20
IW30	qPCR-G3BP1-F	SS	CTTTGGTGGGTTTGTCAC TG	pPCR-SYBR of G3BP1(h) (NM_005754.2)	59	20
IW31	qPCR-G3BP1-R	AS	TGCTGTCTTCTTCAGGTTCC	pPCR-SYBR of G3BP1(h) (NM_005754.2)	60	21
IW34	qPCR-NPM1-F	SS	GAAATGAAAAGAACTCAAAACCATCA	pPCR-SYBR of NPM1 (h) (NM_002520.5)	60	25
IW35	qPCR-NPM1-R	AS	ACTTTGGGAAGAGAACCCCTTT	pPCR-SYBR of NPM1 (h) (NM_002520.5)	60	23
IW38	qPCR-cMyc(h)-F	SS	CACAAACTTGACAGCTACGG	pPCR-SYBR of cMYC (h) (NM_002467.3)	60	21
IW39	qPCR-cMyc(h)-R	AS	GGTGATTGCTCAGGACATTC	pPCR-SYBR of cMYC (h) (NM_002467.3)	59	21
IW54	hβF1-1526-1575	SS	TGGTGGACCCATTGAAGAAAGCTGGCAAAAGCTGATAAGCTG GCTGAACCTGTCTC	FISH	64	58
IW55	hβF1-1188-1236	SS	AGCTGTGGATCTCTAGACTCCACTCTGTATCATGGATCCCAAC ATTCCTGTCTC	FISH	70	57
IW56	hβF1-792-838	SS	GGTAGCCGGTATATGGTCAAATGAATGAACCACCTGGTGCTCG TGCTGTCTC	FISH	70	55

Number	Name	Sense	Sequence 5'-3'	Usage	T <sub>m</sub> (°C)	Length (bp)
IW57	hβF1-566-619	SS	GATCTGCTAGCTCCCTCATGCCAAGGTTGGCAAAATTTGGGCTTTTT GGTGCCTGTCTC	FISH	70	57
IW58	hβF1-284-331	SS	TGGTTTTGGAGGTGGCCACGATTTGGGTGAGAGCACAGTAAGG ACTACCTGTCTC	FISH	66	56
IW59	R-3'hBmut-PCR1a	AS	CACAGAAAAAATAAGGGTCTTTGGGTTAGG	C/ pIW29	55	29
IW60	F-3'hBmut-PCR1b	SS	CCTAACCCAAAGACCCCTATTCTCTGTG	C/ pIW29	55	24
IW78	qPCR F-SDH-h	SS	GGGGCCTGCAGTCTTATG	qPCR of SDH-B (NM_003000.2), UPL: #42	60	19
IW79	qPCR R-SDH-h	AS	AGCGTCTCTGTGAAGT	qPCR of SDH-B (NM_003000.2), UPL: #42	60	19
IW96	qPCR F-gF1-h	SS	TTCATCCTCAGACAAGAGTA	qPCR of γ-F1-ATPase (NM_001001973.1), UPL: #74	60	23
IW97	qPCR R-gF1-h	AS	GAGAAACAGTTCTTCGGACA	qPCR of γ-F1-ATPase (NM_001001973.1), UPL: #74	59	21
	h18S-qPCR-L	AS	GCAATTAATCCCCATGAACG	qPCR of 18S (NM_001001973.1), UPL: #48	60	20
	h18S-qPCR-R	SS	GGGACTTAATCAACGCAAGC	qPCR of 18S (NM_001001973.1), UPL: #48	59	20
	SP6	AS	ATTTAGGTGACACTATAG	S: binds in SP6 promoter	41	18
	T7pcmvspport6	SS	TAATACGACTCACTATAGGG	S: binds in T7 promoter, PCR	48	20
	hB-qPCR-R	AS	CTTCAATGGTCCACCACATA	qPCR of β-F1-ATPase (NM_001686.3), UPL #14	52	20
	hB-qPCR-L	SS	CAGCAGATTTTGGCAGGTG	qPCR of β-F1-ATPase (NM_001686.3), UPL: #14	51	19
	hGAPDH-qPCR-R	AS	GCCCAATACGACCAAATCC	qPCR of GAPDH (NM_002046.3), UPL: #60	51	19
	hGAPDH-qPCR-L	SS	AGCCACATCGCTCAGACAC	qPCR of GAPDH (NM_002046.3), UPL: #60	53	19
	GFP-qPCR-R	AS	CCATGCCGAGAGTGATCC	qPCR of GFP, UPL: #67	52	18
	GFP-qPCR-L	SS	GAAGCGGATCACATGGT	qPCR of GFP (gi 13733151), UPL: #67	50	18
	hHSP60-qPCR-R	AS	CAGCAGCATCCAATAAAGCA	qPCR of Hsp60 (NM_002156.4), UPL: #31	50	20
	hHSP60-qPCR-L	SS	TGCTATGGCTGGAGATTTTGT	qPCR of Hsp60 (NM_002156.4), UPL: #31	50	21
	XL39	AS	TAATCCTGTTCCGACCACCC	Molde TNT eukaryotic expression system	54	20
	qPCR-β-actin-F	SS	CAGCCATGTACGTTGCTATCCAGG	qPCR-SYBR of β-actin (h) (NM_001101)	60	24
	qPCR-β-actin-R	AS	AGGTCCAGACCGCAGGATGGCATG	qPCR-SYBR of β-actin (h) (NM_001101)	60	23

**Table 3: Oligonucleotides.** Name, names in short the amplicon (h, human gene; r, rat gene), orientation regarding to the target gene (F, forward orientation; R, reverse orientation), name of restriction enzyme, qPCR if used for quantitative PCR; Sense, orientation regarding to the target gene (SS, same orientation; AS, antisense orientation); Sequence 5'-3', sequence of the oligonucleotide in 5'-3' direction; Usage, C/ cloning and following name of the plasmid, S/ sequencing, quantitative PCR (qPCR) with SYBR green or Universal Library Probe (UPL, Roche, # number of probe), Fluorescence in situ hybridization (FISH); T<sub>m</sub>, annealing temperature for PCR reaction; Length, number of nucleotides.



### 3.1.8 Human Protein and RNA Liver extracts

- Human Fetal liver total RNA (20-44 weeks) (Clontech, Mountain View, CA, USA, #636540)
- Human total RNA (51 year-old man) (Clontech, Mountain View, CA, USA, #636531,)
- Fetal Human Liver Lysate (ProSci Incorporated, Flint Place, CA, USA, #XBL-10409)

### 3.1.9 siRNAs and miRNAs

The siRNAs, pre- and anti-miRNAs used in this study were s19754 (siG3BP#1), s19756 (siG3BP#2), s20917 (siIMP1#1), s20918 (siIMP1#2), s9678 (siNPM1#1), s9678 (siNMP1#2), negative control #1 siRNA (siControl), PM11164 (pre-miRNA hsa-miR-423-5p), PM11414 (pre miRNA hsa-miR-101), PM13001 (pre-miRNA hsa-miR-127-5p), PM11646 (pre-miRNA hsa-miR-581), PM10492 (pre-miRNA hsa-miR-200b), PM11753 (pre-miRNA hsa-miR-186), PM10632 (pre-miRNA hsa-miR-103), AM11164 (anti-miRNA hsa-miR-423-5p), AM11646 (anti-miRNA hsa-miR-581), AM10492 (anti-miRNA hsa-miR-200b), AM11753 (anti-miRNA hsa-miR-186), AM10632 (anti-miRNA hsa-miR-103), AM13001 (anti-miRNA hsa-miR-127-5p) and AM17110 (miRNA negative control #1).

## 3.2 MOLECULAR BIOLOGY METHODS

### 3.2.1 DNA purification from bacterial strain

Plasmid DNA for cloning, sequencing or transfection was isolated using the DNA purification system (Promega, Madison, WI, USA) or Plasmid MAXI Kit (QUIAGEN) according to the instructions provided by the manufacturer.

### 3.2.2 DNA restriction by endonucleases

Plasmid DNA and DNA fragments were digested with sequence specific restriction endonucleases. The digestion was performed in the presence of the enzyme specific buffer and at the temperature recommended by the manufacturer (Roche, Mannheim, Germany).

### 3.2.3 Separation of DNA fragments by gel electrophoresis

Agarose gel electrophoresis was used to separate plasmid DNA and large DNA fragments using TAE (Tris-acetate-EDTA) buffer (40 mM Tris-acetate, 2 mM EDTA) both as a running buffer and in the agarose gels. In order to visualize DNA or RNA, the gel was prepared with 2 µl of ethidium bromide (10 mg/ml), and ϕ29 DNA cut with HindIII was used as a standard marker. Electrophoretic separation of smaller fragments (< 0.2 kb) was performed by native 5% polyacrylamide gel electrophoresis in TAE buffer at 70 V using 1Kb Plus DNA ladder as a standard marker. The polyacrylamide gel was incubated in a 1.5 µg/ml ethidium bromide solution to visualize the bands.

### 3.2.4 Purification of DNA fragments from agarose gels

Isolation and purification of DNA fragments from agarose gels were performed after cutting out the band of interest using the Wizard SV Gel and PCR clean up system (Promega, Madison, WI, USA) according to the instruction manual supplied by the manufacturer.

### 3.2.5 Ligation of DNA fragments

Ligation of DNA fragments was done for 5 min at room temperature in a 1:3 molar ratio of vector and insert using the Quick ligation kit (New England Biolabs, Ipswich, MA, USA).

### 3.2.6 Transformation of competent *E. coli* cells

100  $\mu$ l of competent *E. coli* cells were incubated with DNA and 5  $\mu$ l of  $\beta$ -mercaptoethanol for 30 min on ice. The mixture was heat shocked at 42°C for 45 sec and placed on ice again for 5 min. Cells were resuspended in 950  $\mu$ l LB-media and incubated for at least 30 min at 37°C. Afterwards, 100  $\mu$ l of the bacterial culture was placed on LB-agar plates supplemented with appropriate antibiotics and incubated over night at 37°C.

### 3.2.7 PCR amplification for cloning

The Expand High Fidelity system (Roche, Mannheim, Germany) was used to amplify DNA fragments used in further cloning steps. The amplification reaction was performed in a volume of 50  $\mu$ l in the presence of 3.5 U of high fidelity Tag DNA polymerase, 0.3 mM of each oligo, 0.1 mM dNTP, 1.5 mM MgCl<sub>2</sub> and 10-250 ng of template DNA. The following PCR program was used: 1 cycle of initial denaturation (94°C-2min), 10 cycle of amplification (denaturation: 94°C-15 sec, annealing: lower T<sub>m</sub> of primer-30 sec, elongation 72°C-1 min/1 kb), 25 cycle of amplification (denaturation: 94°C-15 sec, annealing: lower T<sub>m</sub> of primer-30 sec, elongation 72°C-1 min/1 kb +5sec for each successive cycle) and 1 cycle of final elongation (72°C-7 min).

### 3.2.8 PCR to identify recombinant clones

PCR was used to identify positive bacterial clones after plasmid transformation (3.2.6). A tip of bacterial colony grown on LB-agar plates was put directly to the PCR reaction (25  $\mu$ l). The reaction mix contained 2 mM MgCl<sub>2</sub>, 0.2 mM dNTPs, 1 U/ $\mu$ l Taq polymerase (Biotools B&M, Madrid, Spain) and 0.2  $\mu$ M of each oligonucleotide. The following PCR program was used: 1 cycle of initial denaturation (94°C-10min), 25 cycle of amplification (denaturation: 94°C-15 sec, annealing: lower T<sub>m</sub> of primer-30 sec, elongation 72°C-1 min/1 kb) and 1 cycle of final elongation (72°C-7 min).

### 3.2.9 RT-PCR

The High capacity cDNA Reverse Transcription Kit (Applied Biosystems, Foster City, CA, USA) was used to synthesize cDNA from RNA. 1 µg of RNA was diluted in 10 µl of nuclease-free water and combined with 10 µl of reaction mix containing 2 µl of 10X RT buffer, 0.8 µl of dNTP mix (100 mM), 2 µl of 10X RT Random Primers, 1 µl of RNase Inhibitor (20 U/µl) and 1 µl of MultiScribe Reverse Transcriptase (50 U/µl). As a control of DNA contamination always one reaction without addition of MultiScribe Reverse Transcriptase was carried out (RT-). The following PCR-program was used: 25°C/10 min, 37°C/120 min, 85°C/5 min, 4°C/hold.

### 3.2.10 Quantification of RNA by real-time PCR (qPCR)

Quantitative real-time PCR (qPCR) in glass capillaries was done using the Light Cycler Carousel-Based System for Real-Time PCR (Roche) and the LightCycler FastStart DNA MasterPlus SYBR Green (Roche). To quantify RNA in plates the thermocycler ABI PRISM 7900HT SDS and the Power SYBR Green Master Mix (Applied Biosystems) was used. The PCR reactions were carried out in a final volume of 10 µl containing the corresponding SYBR Master mix (1X), 5 ng of cDNA and 0.5 µM of each oligo (Table 3) in the case of qPCR in capillaries, and 0.25 µM of each oligo (Table 3) in the case of qPCR analysis done in plates. The PCR program consisted in one cycle of pre-incubation (95°C/10 min) to activate the enzyme, 40 cycle of amplification (denaturation: 95°C/15 sec; annealing: 60°C/20 sec; extension and single fluorescence acquisition: 72°C/20 sec) and a final step of gradual temperature increase (0.1°C/sec) up to 95°C by continuous fluorescence acquisition (melting curve). Amplification efficiency (E) of the reaction was determined using a standard curve and calculated according to  $E=10^{-1/\text{slope}}$ . The RNA was quantified according to the  $\Delta\Delta\text{Ct}$  method (Livak and Schmittgen, 2001).

#### 3.2.10.1 Quantification of $\beta$ -mRNA in human tissues

Human  $\beta$ -F1-ATPase mRNA level in normal and tumors tissues was determined by qPCR using TissueScan Disease Tissue qPCR panels from OriGene Technologies, Inc (Rockville, MD) and the thermocycler ABI PRISM 7900HT SDS (see 3.2.10). The breast cancer panel (BCRT101) contains cDNA from seven normal and 41 tumor samples. The lung cancer panel (HLRT104) includes cDNA from paired normal and tumor tissues derived from ten adenocarcinomas, eight squamous and six other lung carcinoma patients. The colon (HCRT103) cDNA panel includes paired normal tumor tissue samples from 24 patients. Only samples from clinic stages I, II and III were considered in the analysis. The oligos hB-qPCR-R/hB-qPCR-R (Table 3) were used to amplify human  $\beta$ -F1-ATPase mRNA, and qPCR- $\beta$ -actin-F/qPCR- $\beta$ -actin-R (Table 3) to amplify human  $\beta$ -actin mRNA. The relative expression level of  $\beta$ -mRNA in normal and cancer samples was determined according to the  $\Delta\Delta\text{Ct}$  method (Livak and Schmittgen, 2001) using  $\beta$ -actin as an internal control and relative to the  $\Delta\text{Ct}$  mean value of the normal samples.

### **3.2.10.2 Quantification of immunoprecipitated mRNA**

Quantification of immunoprecipitated mRNA (3.3.6) was performed in glass capillaries (3.2.10) and the relative expression levels of  $\beta$ -mRNA and c-myc mRNA were determined according to the comparative  $\Delta\Delta C_t$  method (Livak and Schmittgen, 2001) with GAPDH as a control and relative to the non-transfected cells. The oligonucleotides used for amplification are indicated in Table 3.

### **3.2.10.3 Quantification of mature miR-127-5p in human cells and during human and rat liver development**

RNA was extracted from cultured cells and rat liver using TRIzol reagent (Invitrogen, Carlsbad, CA) according to the manufacturer's protocol (3.3.1). Human adult (#636540, Lot 1007011A) and fetal (#636531, Lot 9100089A) liver total RNA were purchased from Clontech (Mountain View, CA, USA). The expression level of miRNAs was determined using TagMan MicroRNA Assay from Applied Biosystems, which includes a unique set of RT-PCR primers and a specific TagMan probe. RNA was reverse transcribed using the TagMan MicroRNA Reverse Transcription Kit (Applied Biosystems). Briefly, 10 ng of total RNA was diluted in 5  $\mu$ l nuclease-free water and combined with RT reaction mix containing 1X RT-PCR buffer, 50 U of Multi-Scribe RT enzyme, 0.15  $\mu$ l of 100X dNTP mix, 3.8 U RNase-inhibitor, 4.16  $\mu$ l nuclease-free water and 3  $\mu$ l of 5X specific RT-primer. The RT-primer used in this study were RNU48 (TagMan MicroRNA Assay #001006, Applied Biosystems), U6 snRNA (TagMan MicroRNA Assay #001973, Applied Biosystems) and hsa-miR-127-5p (TagMan MicroRNA Assay #002229, Applied Biosystems). The RT reactions were incubated on a thermocycler: 16°C/30 min, 42°C/30 min, 85°C/5 min and 4°C/hold. Once the RT reaction was completed, the qPCR reaction was assembled containing 5  $\mu$ l of 2X Universal Master Mix without UNG (Applied Biosystems), 0.66  $\mu$ l of the RT product, 0.5  $\mu$ l of the respective (RNU48, hsa-miR-127-5p or U6) 20X TagMan assay and 3.84  $\mu$ l nuclease-free water. qPCR reactions were carried out using ABI PRISM 7900 SDS thermocycler following the instructions provided by the manufacturer. Expression of miR-127-5p was determined according to the  $\Delta\Delta C_t$  method (Livak and Schmittgen, 2001) using RNU48 (human cell lines) or U6 (human and rat tissues) as an internal control.

### **3.2.11 Cloning**

All sequences of the following constructs were verified by direct automated sequencing.

#### **3.2.11.1 pIW21: p $\beta$ GFP / pIW22: p $\beta$ GFP-3' $\beta$ / pIW23: p $\beta$ GFP-3' $\alpha$**

The vectors pIW21, pIW22 and pIW23 encode the mitochondrial targeting sequence of rat  $\beta$ -F1 ATPase (p $\beta$ ) fused in-frame with the GFP coding sequence (pre $\beta$ GFP) and either with or without the 3'UTR of human  $\beta$ -F1-ATPase mRNA (pre $\beta$ GFP-3' $\beta$ ) or  $\alpha$ -F1-ATPase (p $\beta$ GFP-3' $\alpha$ ). The p $\beta$ GFP fragment was obtained from p $\beta$ GFP-3' $\beta$ rat by PCR using the oligos IW2/IW7 (Table 3) and inserted into the pcDNA3 vector at KpnI and EcoRI sites. The 3'UTR sequences of human  $\beta$ -F1-ATPase mRNA or  $\alpha$ -F1-ATPase mRNA were amplified by PCR using human cDNA as a template and respectively the oligos IW3/IW4 and IW5/IW6 (Table 3). The amplified PCR fragments were placed downstream at EcoRI-XhoI site.

**3.2.11.2 pIW24: YFP<sub>Nt</sub>-Flag-IMP1 / pIW25: YFP<sub>Nt</sub>-Flag-G3BP1 / pIW26: YFP<sub>Nt</sub>-Flag-NPM1**

The plasmids coding for the N-terminal of YFP fused to Flag-tagged IMP1 (pIW24: YFP<sub>Nt</sub>-Flag-IMP1), Flag-tagged G3BP1 (pIW25: YFP<sub>Nt</sub>-Flag-G3BP1) or Flag-tagged NPM1 (pIW26: YFP<sub>Nt</sub>-Flag-NPM1) are derivatives of the plasmid YFP<sub>Nt</sub>-Flag-ZBP1 (Table 1), which was kindly provided by Dr. Stefan Hüttelmaier (Martin Luther University, Halle-Wittenberg, Germany) (Stohr et al., 2006). Fragments of IMP1, G3BP1 and NPM1 were generated by PCR using respectively the oligos IW22/IW23, IW24/IW25 and IW26/IW27 (Table 3) and cloned into YFP<sub>Nt</sub>-Flag-ZBP1 at EcoRI-BamHI site replacing ZBP1.

**3.2.11.3 Cloning of preβGFP-3'βMUT (pIW29) by PCR-site directed mutagenesis**

The vector pIW29 expresses the mitochondrial targeting sequence of rat β-F1 ATPase (preβ) fused in-frame with GFP and the 3'UTR of the human β-F1 ATPase containing four point mutations in the seed sequence of the hsa-miR-127-5p binding site (Fig 3.1A). In order to introduce the point mutations, in a first step two overlapping PCR products containing the desired mutations were amplified using the oligos IW7/IW59 and IW3/IW60 (Table 3) (Fig. 3.1B). The mutations were introduced via the two mutated and overlapping oligonucleotides (IW59 and IW60, Table 3) (Fig. 3.1B). Then the two gel purified PCR products were mixed 1:1, incubated for 5 min at 94°C and 30 min at 37°C to separate the double strand PCR products and further allow annealing of the complementary tails (Fig. 3.1B). To extend the annealed fragments and to form one full length

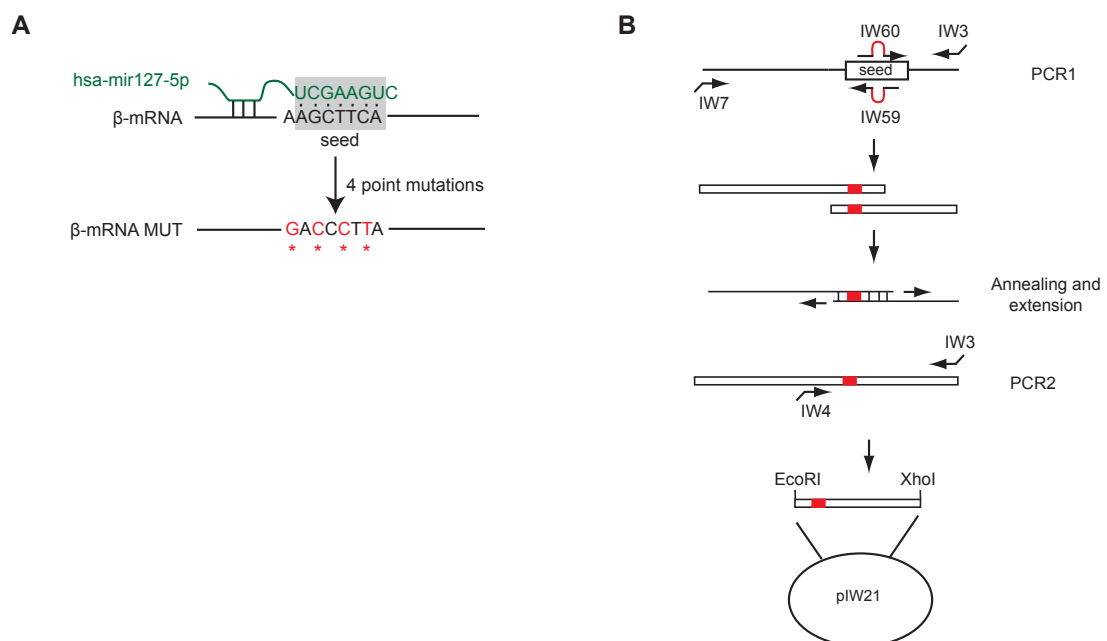


**Figure 3.1: Site directed mutagenesis by PCR mutagenesis for cloning of pβGFP-3'βMUT (pIW29).** (A) Binding of miR-127-5p to β-mRNA. Mutations inserted into the miR-127-5p seed region (highlighted in gray) are marked by red. (B) Mutations (indicated as red bulges) are introduced into two overlapping primers (IW59 and IW60, Table 3) and used for amplifications of two overlapping DNA segments (PCR1). The two PCR products containing the introduced mutations (red) are combined, denatured, allowed to re-anneal and extended. Afterwards, a second DNA segment is amplified by PCR (PCR2) using the outer primer IW3 and IW4 (Table 3). The PCR fragment containing the 3'UTR of human β-F1-ATPase with 4 point mutations in the miR-127-5p binding region is further digested with EcoRI and XhoI and subcloned into the plasmid pIW21 (Table 1) replacing the non-mutated 3'UTR of β-F1-ATPase.

mutated PCR fragment, 1.75 mM dNTPs and 1 U/ $\mu$ l of Klenow DNA polymerase were added and incubated for 30 min at 37°C. The product from this reaction was used as a template for a second PCR reaction using the outer primers IW3/IW4 (Table 2) (Fig. 3.1B). The amplified PCR fragment was purified, digested with the restriction enzymes EcoRI and XhoI and ligated with the plasmid pIW21 (3.1.4 and Table 1) digested with the same enzymes (Fig. 3.1B).

### 3.3 BIOCHEMICAL METHODS

#### 3.3.1 Extraction of RNA and miRNA from cells and tissue samples

Cells were collected as described in 3.4.1 and the cell pellet was lysed for 7 min on ice in RLNT buffer (50 mM Tris-HCl pH 8, NaCl 140 mM, 1.5 mM MgCl<sub>2</sub>, 1 mM DTT, 0.5% Triton X-100) supplemented with protease inhibitor cocktail (Roche). After centrifugation, the supernatant was used to extract RNA with the RNeasy mini kit (QUIAGEN) following the instructions provided by the supplier. When small RNAs (e.g. miRNAs) were extracted from cell cultures and tissue samples TRIzol Reagent (Invitrogen) was used. RNA was precipitated by addition of 1 volume of isopropanol, 0.5 M ammonium acetate and 50  $\mu$ g/ml of GlycoBlue (Ambion/Applied Biosystems Austin, TX, USA) .

#### 3.3.2 Protein extraction from human tissues and cell culture

Cells were collected as described in 3.4.1 and the cell pellet was resuspended in lysis buffer (10 mM Tris pH 8, 140 mM NaCl, 1% Triton X-100) and kept on ice for 7 min. Nuclei and cell debris were pelleted by centrifugation (5 min, 10000 x g, and 4°C). Human tissue samples were homogenized with a glass potter and proteins were extracted as described in Isidoro et al., 2004. Breast tumor tissue samples for analysis of G3BP1 expression were extracted as specified in Isidoro et al., 2005. When protein extracts were used in *in vitro* translation assays (3.3.8), tissue samples were homogenized with a glass potter in extraction buffer containing 20 mM HEPES pH 7.9, 100 mM KCl, 3 mM MgCl<sub>2</sub>, 1 mM DTT, 0.5 mM PMSF and protease inhibitors (Roche) in a 1/5 (w/v) ratio and further freeze-thawed three times in liquid nitrogen. Thereafter, the samples were centrifuged (15000 x g, 4°C, 25 min) and protein extracts were passed through a Centricon YM-10 filter (Amicon). Aliquots of 50  $\mu$ l were frozen in liquid N<sub>2</sub> and stored at -80°C until use. In all cases, protein concentration in the supernatant was determined by Bradford (Bio-Rad, Hercules, CA, USA) following the recommendations supplied by the manufacturer. Solutions containing BSA of known concentrations were used as a standard.

#### 3.3.3 SDS-polyacrylamide gel electrophoresis, western blotting and fluography

Proteins were separated by SDS-polyacrylamide gel electrophoresis according to the method described by Laemmli (Laemmli, 1970). Protein extracts were mixed with Laemmli loading buffer and boiled for 5 min at 95°C. Equal amounts of protein were loaded on the gel and High-Range

Rainbow Molecular Weight Markers (GE Healthcare) were used as standards. After electrophoresis, proteins were transferred to PVDF-membranes using a wet Mini Trans Blot electro-transfer system (Bio-Rad). The transfer was carried out for 1 h at 100 V and 4°C in transfer buffer (39 mM Glycine, 48 mM Tris-HCl, methanol 20% (v/v) and 0.0375% SDS). Before putting the PVDF-membrane in transfer buffer, the membrane was moistened with methanol to make the membrane surface hydrophilic. After transfer, membranes were incubated in blocking solution (5% milk powder diluted in TBST (Tris-HCl 50 mM pH 7.5, 150 mM NaCl and 0.1% Tween-20)). Incubation with the antibody was carried out at room temperature for 1 h or at 4°C over night depending on the antibody used. The antibodies were diluted in TBS, 3% BSA and 1 mM Na<sub>3</sub>N. The antibodies used in this study and the appropriate dilutions are summarized in Table 2. Next, the membrane was washed three times for 5 min with TBST and depending on the primary antibody used peroxidase conjugated anti-rabbit or anti-mouse IgGs (diluted in blocking solution 1:5000) (Nordic immunology) were used as secondary antibodies for detection by chemiluminescence (ECL, Invitrogen). Membranes were exposed to X-ray films and quantification of the immunoreactive bands (arbitrary units) was accomplished using a Kodak DC120 Zoom digital camera and the Kodak 1D Image Analysis Software for Windows.

The detection of proteins labeled with low-energy  $\beta$ -emitting [<sup>35</sup>S] was carried out by fluorography using sodium salicylate as a fluor. After gel electrophoresis the gel was fixed for 30 min in a solution of 25% isopropanol and 10% acetic acid, the fixed gel was washed twice with water, incubated for 1 h in 1 M sodium salicylate and dried under vacuum at 80°C.

### 3.3.4 Determination of G3BP1 expression in human breast tumor biopsies

Expression of G3BP1 in human breast tumor tissue samples (3.1.1) was determined by western blot (3.3.3) using 25  $\mu$ g of protein tumor extracts (for protein extraction see A. Isidoro et al., 2005). A sample of the Hs578T cells was loaded in all gels to allow normalization of the G3BP1 signal between the different gels. Polyclonal G3BP1 antibody (Santa Cruz Biotechnology, Santa Cruz, CA, USA) (Table 2) was used in a dilution of 1:1000. The expression data were analyzed using the statistic software SPSS. The relative expression of G3BP1 was dichotomized by the median (0.92) in low and high G3BP1 expression. Unsupervised hierarchical clustering were performed using Euclidean distances and average linkage method (<http://ep.ebi.ac.uk/EP/EPCLUS>).

### 3.3.5 Distribution of $\beta$ -mRNA in polysomes

Cell-free translation assay of P<sup>32</sup>-labelled  $\beta$ -mRNA (2 x 10<sup>6</sup> cpm) was carried out for 20 min at 30°C in a final volume of 25  $\mu$ l using nuclease-treated rabbit reticulocyte lysate (Promega). Reactions were performed in the presence of G3BP1 and PK, synthesized *in vitro* using the TnT expression system (Promega) (3.3.9). The control reaction includes equivalent amounts of the TnT expression system but without any protein. Following incubation, reactions were stopped by addition of cyclohexamide (100  $\mu$ g/ml) and diluted in 500  $\mu$ l polysome buffer (10 mM Tris-HCl pH 7.4, 80

mM KCl, 5 mM MgCl<sub>2</sub>, 1 mM DTT) supplemented with cyclohexamide (100 µg/ml). The samples were loaded onto a linear 15-40% (w/v) sucrose gradient in polysome buffer and centrifuged at 38000 rpm for 130 min at 4°C in a Beckman Coulter L100-XP ultracentrifuge using a SW41 rotor. Fractions were collected manually from the bottom of the tube and radioactivity in each fraction was determined by scintillating counting.

### 3.3.6 Immunoprecipitation of RNA (RNA-IP) from Flag-RNABP transfected cells

Hek293T cells (~10<sup>6</sup> cells) were transfected with 3 µg of Flag-G3BP1 (pIW25), Flag-IMP1 (pIW24) or Flag-NPM1 (pIW26) in 10 cm dishes. At 48 h post-transfection cells were harvested and washed twice with ice-cold PBS. Next, the cells were lysed in RLNT lysis buffer (50 mM Tris-HCl pH 8, 140 mM NaCl, 1.5 mM MgCl<sub>2</sub>, 0.5% Triton-X-100) supplemented with protease inhibitor cocktail (Roche) and RNase inhibitor (Applied Biosystems), and the lysate was pre-cleared by incubation with protein G-sepharose beads (Sigma, St. Louis, MO, USA) for 2 h at 4°C. One portion (1.5%) of the pre-cleared lysate was set aside as protein input used later in the western blot analysis. The remaining portion was incubated over night at 4°C with monoclonal anti-Flag-M2 (Sigma) or monoclonal anti-G3BP1 (BD Bioscience, Parlo Alto, CA, USA) antibody (Table 2). Thereafter, the lysate was mixed with protein G-sepharose beads (Sigma) and incubated for 2 h at 4°C. The beads were collected by centrifugation (1 min, 8200 x g) and 1.5% of the supernatant was set aside as flow through sample. The beads were washed 4 times with RLNT buffer and 4 times with RLNT buffer supplemented with 1 M Urea. After that, the resin was resuspended in 200 µl RLNT buffer and 10 µl (5%) of the slurry were taken away as immunoprecipitation sample used in the western blot analysis. Finally, the beads were collected by centrifugation (1 min, 8200 x g) and resuspended in 100 µl elution buffer (50 mM Tris-HCl pH 8, 140 mM NaCl, 1.5 mM MgCl<sub>2</sub>, 0.25% Triton-X-100, 0.1% SDS) supplemented with 42 µl (~12-22 mg/ml) of proteinase K (Roche) and incubated for 30 min at 50°C. The elution step was repeated, the two elutes were mixed and the RNA was extracted using TRIzol Reagent (Invitrogen) according to the manufacturer's protocol and precipitated using Glycoblue as a carrier (Ambion/Applied Biosystems). The purified RNA was reverse transcribed (3.2.9) and the relative expression level of c-myc mRNA and β-mRNA was determined by qPCR (3.2.10.2).

### 3.3.7 *In vitro* transcription

*In vitro* transcription was carried out for 2 h at 37°C using 1 µg of linearized plasmid and the MEGAscript T7 High Yield Transcription Kit (Ambion/Applied Biosystems) following the instructions provided by the supplier. The obtained RNA was purified by lithium chloride precipitation. When the synthesized RNA was to be used as a template in *in vitro* translation assays (3.3.8) the m7G(5')ppp(5')G cap analog (Ambion/Applied Biosystems) was included in the reaction at a final concentration of 6 mM. The transcription procedure as well as the quality of the final RNA product were assessed by electrophoresis and quantified by UV absorbance at λ=260 nm. For the synthesis of β-mRNA used in cell-free sucrose density gradient assays (3.3.5) the linearized



plasmid was transcribed by T7 RNA polymerase (Ambion/ Applied Biosystems) for 20 min at 37°C with 0.5 mM ATP, GTP and CTP, 5 µM UTP, 20 µCi α[<sup>32</sup>P]-UTP (0) and 1 U of RNase Inhibitor (Applied Biosystems). To remove the DNA template the reaction was treated for 15 min at 37°C with 2 U TURBO DNase (Ambion/Applied Biosystems). The RNA was purified by phenol/chloroform extraction and unincorporated ribonucleotides were removed using a sepharose G-50 microspin column (GE Healthcare, Waukesha, WI, USA) size exclusion chromatography. Activity of the RNA probe was determined by scintillation counting of a 1 µl aliquot before and after passing the sample through the column.

### 3.3.8 *In vitro* translation

*In vitro* translation assays were performed using rabbit reticulocyte lysates (GE Healthcare or Promega) and 100 ng of *in vitro* synthesized capped mRNA (3.3.7) as a template. The reaction was performed at 30°C for 30-60 min in the presence of 1.6 µCi/µl of [<sup>35</sup>S]-Met labeling mix (Perkin Elmer) (0). When the reticulocyte lysate system from GE Healthcare was used additionally 63 mM KCl and 0.3 mM magnesium acetate were included to the reaction. For *in vitro* translation assays in the presence of human protein extracts the reaction was performed for 1 h at 30°C adding 0-10 µg of protein extracts derived from human tumor and normal tissue sections (3.1.1 and 3.3.2). The protein extracts were appropriately diluted in translation buffer (20 mM HEPES, 20 mM KCl, 1 mM DTT supplemented with protease inhibitor from Roche). The synthesized products were analyzed by SDS-PAGE and fluorography (3.3.3).

### 3.3.9 Eukaryotic cell-free transcription and translation assays

*In vitro* synthesis of PK and G3BP1 was performed using the eukaryotic cell-free TnT T7 (for (G3BP1) or Sp6 (for PK) expression system (Promega). For the synthesis of proteins (PK) transcribed by Sp6 polymerase 0.5 µg of the non-digested plasmid (pGEM-PK) (Table 1) was used as template. To synthesize proteins transcribed by the T7 polymerase (G3BP1), the reaction mix included the T7 PCR enhancer provided by the supplier and 0.5 µg of the PCR product was used a template. The PCR product was amplified by the Expand High fidelity PCR system (3.2.7) using the oligos XL39/T7 Pcmvsport6 (Table 3) and pCMV-sport 6 XL5 (G3BP1) (Invitrogen) as a DNA template. The reaction mix included further 20 µM or 0.4 µCi/µl of [<sup>35</sup>S]-Met to synthesize respectively no labeled or [<sup>35</sup>S]-Met labeled protein. The degree of the incorporation of [<sup>35</sup>S]-methionine was analyzed in a small aliquot by SDS-PAGE and fluorography (1/50) (3.3.3).

## 3.4 CELL BIOLOGY METHODS

### 3.4.1 Cell culture

The human breast cancer cell lines BT549 and the colon cancer cell line HCT116 were cultured in RPMI and McCoys, respectively, supplemented with 10% FBS, 400  $\mu$ M non-essential amino acids, 100 UI/ml penicillin and 0.1mg/ml streptomycine. Hek293T, Hs578T, C9 and NRK were cultured in DMEM supplemented with 10% and 5% FBS, respectively, 2 mM glutamine, 400  $\mu$ M non-essential amino acids 100 UI/ml penicillin and 0.1mg/ml streptomycine. All cell lines were cultured at 37°C, 95% humidity and 7% CO<sub>2</sub>. For longtime storage, cells were frozen gradually (-1°C/min) using a Nalgene “Mr Frosty” freezing container and stored in liquid N<sub>2</sub>. To harvest adherent cells from cell culture plates, plates were washed twice with trypsin (0.25% trypsin 0.02% EDTA) and kept for 3-5 min in the incubator. Cells were rinsed with the appropriate growth medium and collected by centrifugation (1200 rpm, 5 min).

### 3.4.2 Transient plasmid transfections

For transient plasmid transfection cells were seeded at 24 h prior transfection and grown up to 80% confluence. Transfection was performed using Lipofectamine and Plus reagent (Invitrogen) following manufacturer’s instructions. In all cases the cell culture was incubated with the cationic-lipid-DNA complexes for 2 h at 37°C.

### 3.4.3 siRNA and miRNA transfection

MicroRNAs (miRNAs) and siRNAs (3.1.9) were transfected at the time of plating using siPORT NeoFx reagent (Ambion/Applied Biosystems) following manufacturer’s instructions. The medium was changed at 24 h post-transfection and the cells were analyzed at 48-72 h post-transfection. siRNAs and miRNAs were respectively used at a final concentration of 10 nM and 30 nM. MicroRNAs and plasmids were co-transfected in a ratio of 2:1 using Lipofectamine and Plus reagent (Invitrogen) (3.4.2).

### 3.4.4 Generation of stable transfected cell lines

Cells were transfected as described above (3.4.2) with the plasmids pIW22 and pIW23 (Table 1). After 24 h of transfection cells were split 1:10 and 1:20 into 10 cm plates and grown in the appropriate medium (3.4.1) containing 0.3 mg/ml geneticin (G418, GIBCO, Invitrogen) for generation of stable BT549 cells or 4mg/ml geneticin in the case of HCT116 cells. The cells were cultured for several days in medium containing the selection drug G418, changing the medium every 2 days. After 1-2 weeks isolated colonies began to appear and the positive drug resistant and GFP fluorescent clones were isolated with cloning cylinder (8 mm x 8 mm) (Sigma) and sub-cloned into 96-well plate. The clones were expanded and purity of the population derived from one clone was analyzed by flow cytometry (3.4.5).

### 3.4.5 Flow cytometry

Cells were collected as described in 3.4.1 in 1X PBS and centrifuged (5 min, 1200 rpm, 4°C). The cell pellet was resuspended in 200-400 µl FACS solution (1% FBS, 0.1% NaN<sub>3</sub> and 1X PBS) and analyzed in a FACS Calibur (Becton Dickinson, San José, CA, USA) flow cytometry system using the program CellQuest supplied by the manufacturer. The results were analyzed with the program FlowJo.

### 3.4.6 *In vivo* RNA imaging by trimolecular fluorescence complementation (TriFC) assay

The TriFC assay (Stohr et al., 2006) was used to visualize and localize β-mRNA-RNABPs interaction in living cells. C4 and NRK cells were cultured in glass bottom dishes coated with poly-D-lysine (MatTek Corporation, Ashland, OR) and were co-transfected with equal amounts (80 ng) of YFP<sub>ct</sub>-HA-MS2CP and YFP<sub>Nt</sub>-Flag-G3BP1 plasmids (Table 1). NRK cells were cultured and transfected as described above, but additionally co-transfected with the reporter RNA plasmid pβGal-3'β-MS2 or pβGal-MS2 in a ratio 1:5 (400 ng) (Table 1). Cells were visualized 24 h after transfection using an inverted confocal LSM510 META microscope (Zeiss) equipped with 63X1.4 oil Plan-Apocromate objective.

### 3.4.7 Indirect immunofluorescence microscopy

For detection and imaging of subcellular localization of specific proteins, indirect immunofluorescence microscopy was carried using secondary antibodies conjugated with different fluorescence dyes. Cells grown on cover slips were fixed for 20 min at room temperature with 4% (w/v) paraformaldehyde (PFA). Next, cover slips were washed twice with PBS and incubated for 10 min with freshly prepared NaBH<sub>4</sub> (1mg/ml in PBS pH 8.0) to eliminate autofluorescence. Afterwards, cells were permeabilized by incubation with a 0.1% Triton X-100 PBS solution (10 min, room temperature) and blocked for 10 min in 1% FBS, 0.1% Triton X-100 PBS solution. Primary antibodies were appropriately diluted (Table 2) in blocking solution, centrifuged for 5 min at 12000 x g and 4°C and incubated with the cells for 1 h at room temperature under continuous shaking. Then, cover slips were rinsed three times with PBS and incubated for 1 h in the dark with the appropriate secondary antibody conjugated either to Alexa 488, Alexa 594 or Alexa 555 (Molecular Probes, 1:1000). Before use, secondary antibodies diluted in blocking solution were centrifuged for 5 min at 12000 x g and 4°C. Finally, cover slips were rinsed three times in PBS, once in water, once in 100% ethanol and allowed to dry in the air. Cover slips were mounted (cell side down) with mowiol (DABCO) onto slides and dried overnight in the dark at room temperature. Cellular fluorescence was analyzed by confocal microscopy using a vertical LSM510 microscope (Zeiss) equipped with a 63X1.4 oil Plan-Apocromate objective. Cover slips for adherent cells were prepared as followed: Autoclaved cover slips were incubated with polylysine (10 mg/ml) for at least 1 h at 37°C. Afterwards, cover slips were washed 3 times with PBS, 3 times with H<sub>2</sub>O and dried under UV-light. Dried cover slips were stored at -20°C until use.

### 3.4.8 Preparation of riboprobes for fluorescence in situ hybridization (FISH)

Riboprobes for  $\beta$ -mRNA FISH were generated using the mirVANA miRNA probe construction kit (Ambion/Applied Biosystems) and the oligos IW61-IW76 (Table 3). The riboprobes were synthesized by *in vitro* transcription following the instructions provided by the supplier, except that UTP was replaced by aminoallyl-UTP (Sigma). RNA was purified by phenol-chloroform extraction followed by G-50 microspin column (GE-Healthcare) size-exclusion separation. A riboprobe mixture containing 10  $\mu$ g of each probe was vacuum dried, resuspended in 50  $\mu$ l of labeling buffer (0.1 M Na<sub>2</sub>CO<sub>3</sub> pH 9.0) and added to 1 vial of Cy5 dye (GE Healthcare). The labeling reaction was carried for 1 h in the dark at room temperature with additional mixing every 15 min. Labeled probes were purified by G-50 microspin columns (GE-Healthcare).

### 3.4.9 Combined immunofluorescence and FISH

Hek293T cells grown on cover slips were fixed with 4% (w/v) PFA for 20 min at room temperature. Immunofluorescence of G3BP1 preceded FISH of  $\beta$ -mRNA and was performed as described above (3.4.7) using anti-mouse IgGs conjugated to Alexa 488 as a secondary antibody. For *in situ* hybridization of  $\beta$ -mRNA the slides were equilibrated for 10 min at room temperature in a 2X SCC/50% formamide solution. The riboprobe mixture (50 ng) was dissolved in 10  $\mu$ l formamide and incubated for 5 min at 70°C. Afterwards, 10  $\mu$ l of hybridization buffer (4X SCC, 100  $\mu$ g salmon sperm DNA, 100  $\mu$ g of yeast tRNA) was added to the probes and hybridized to the cells over night at 37°C. Cells were washed twice at 37°C for 15 min with 2X SCC/50% formamide and rinsed once in PBS and nuclease-free water. For competition experiments, a 100-fold excess of unlabeled  $\beta$ -mRNA riboprobe mixture was added 1 h before addition of the Cy5-labeled probes. Cellular fluorescence was analyzed by confocal microscopy using a LSM510 META microscope equipped with a 63X1.4 oil Plan-Apocromate objective.

### 3.4.10 High-resolution immunoelectron microscopy

Transfected cells were fixed at 30 h post-transfection in freshly prepared 4% (w/v) PFA in 0.1 M Sørensen phosphate buffer (pH 7.4) for 1 h at room temperature and further incubated over night in 8% PFA at 4°C. Fixed cells were washed in the culture dishes, scrapped and embedded in 10% gelatin in PBS. 0.5-1mm<sup>3</sup> cubes of gelatin embedded cells were cryoprotected with 30% glycerol for 15 min, plunge frozen in liquid propane and immediately transferred to an Automatic Freeze-Substitution System (AFS, Leica microsystems, Wetzlar, Germany). Freeze substitution was carried out at -85°C in methanol containing 0.5% uranyl acetate for 54 h. After raising the temperature to -45°C at a rate of 5°C/h and washing several times with pure methanol, the samples were infiltrated with Lowicryl HM20 and polymerized by UV light radiation at -45°C for two days. Ultrathin Lowicryl

sections were cut in a Reichert-Jung Ultracut E ultramicrotome. Grids were incubated 1 min in TBS (30 mM Tris-HCl pH 8, 150 mM NaCl) and then transferred to 0.2 M ammonium chloride in PBS (2 x 15 min) to quench free-aldehyde groups. Afterwards, grids were blocked for 10 min in blocking buffer (TBS + 0.1% bovine serum albumin and 1% gelatin) and incubated for 1 h at RT onto a drop of anti-GFP antibody (1:50, Clontech). Then, grids were washed with TBS and incubated for 1 h at RT with protein A conjugated to 15 nm gold particles. After incubation, grids were washed once in TBG, once in TBS and finally in water and air-dried. Counterstaining was performed with 2% aqueous uranyl acetate (6 min) and 1% lead citrate (25 sec). Standard controls were carried to assess the specificity of the immunoreactive signals (Egea et al., 1997). Grids were examined at 80 KV in a JEM1010 electron microscope (Jeol, Japan).

### **3.4.11 Screening for miRNA that affect $\beta$ -F1-ATPase expression using a fluorescence plate reader**

BT549 clones stably expressing mitochondria localized GFP fused either to the 3'UTR of  $\alpha$ -F1-ATPase (BT549:p $\beta$ GFP-3' $\alpha$ ) or  $\beta$ -F1-ATPase (BT549:p $\beta$ GFP-3' $\beta$ ) were used to identify those miRNAs that could be relevant in controlling  $\beta$ -mRNA translation. Over-expression and silencing assays of the selected miRNAs were performed by transfection of miRNAs precursors (pre-miRNA) and anti-miRNAs as described in 3.4.3. The assays were carried out in 96-well plates with a black border and a clear flat bottom (Corning, NY, USA). After 48 h and 72 h of transfection cells were stained for 10 min at 37°C with 5  $\mu$ g/ml of Hoechst (Sigma) diluted in cell culture medium. The medium was changed for medium without phenol red and the plate was analyzed using a FLUOstar Omega Microplate Reader (BMG Labtech, Offenbach, Germany) measuring the fluorescence intensity of Hoechst (Filter: excitation. 340-10 nm, emission. 470-10 nm) and GFP (Filter: excitation . 485nm, emission. 510-10). The GFP fluorescence intensity was normalized to the number of cells as determined by Hoechst fluorescence intensity, and quantified relative the cells transfected with a non-relevant miRNA (control).

### **3.4.12 Measurement of oxygen consumption rates in adherent cells**

The XF24 Extracellular Flux Analyzer (SeahorseBioscience, Billerica, MA, USA) measures in real time the oxygen consumption rate (OCR) in attached cells. To analyze the effect of miRNAs on mitochondrial bioenergetic functions, BT549 cells were transfected as described above (3.4.3) and at 48 h of transfection cells were seeded in a specific XF24 cell culture microplate (Seahorse Bioscience) that contains the fluorescent biosensors ( $O_2$  and  $H^+$ ) and 4 ports to inject different compounds. The XF24 cell culture microplate was incubated for additional 24 h at 37°C and 7%  $CO_2$ . In order to assure a uniform distribution of the cells, seeding into the XF24 cell culture microplate was carried out in two steps. First, the appropriate cell number of cells was seeded in a volume of 100  $\mu$ l of growth medium (3.4.1) and incubated for 1-5 h in the incubator to allow cell adhesion, and then 150  $\mu$ l of growth medium were added to reach a final volume of 250  $\mu$ l. Before each assay the biosensors of the XF24 Analyzer were calibrated with a standard solution containing known

concentrations of oxygen and protons, and 1 h before measurement plated cells were incubated at 37°C in 700 µl of non buffered growth medium in order to equilibrate both the temperature and the pH. OCR values, measured as pmols of oxygen consumed per min, were normalized to the respective cellular protein concentration (µg/µl) and to the OCR/(µg/µl) value of the control cells transfected with a non-relevant miRNA.



# **RESULTS**

---

---





## 4 RESULTS

### 4.1 POST-TRANSCRIPTIONAL CONTROL OF $\beta$ -F1-ATPase EXPRESSION

Recently, we have shown that the alteration of energetic metabolism is a phenotypic trait of most human tumors (Cuezva et al., 2004; Cuezva et al., 2002; Isidoro et al., 2005; Isidoro et al., 2004). Changes in this particular phenotype were determined by quantification of the relative expression level of  $\beta$ -F1-ATPase, a key enzyme of oxidative phosphorylation. Additional proteins studied were Hsp60, a structural mitochondrial protein and GAPDH, a glycolytic enzyme. It was demonstrated that concurrent with the upregulation of glycolytic GAPDH, the normalized expression of  $\beta$ -F1-ATPase is significantly diminished in several human tumors including colon (Bi et al., 2006; Cuezva et al., 2002) (Fig. 4.1), lung (Cuezva et al., 2004; Isidoro et al., 2004; Lopez-Rios et al., 2007) (Fig. 4.1), breast (Isidoro et al., 2005) (Fig. 4.1), renal (Cuezva et al., 2002; Unwin et al., 2003) and gastric (Chen et al., 2004; Isidoro et al., 2004) cancer, providing a bioenergetic signature of energetic metabolism of potential relevance in clinical practice. Notably, the bioenergetic signature provides a marker for the response to chemotherapy (Hernlund et al., 2009; Sanchez-Arago and Cuezva, 2011; Santamaria et al., 2006; Shin et al., 2005) as well as an indicator of disease progression (Cuezva et al., 2004; Cuezva et al., 2002; Lin et al., 2008). The biology of the  $\beta$ -F1-ATPase transcript ( $\beta$ -mRNA) in rodents has been partially characterized (de Heredia et al., 2000; Izquierdo and Cuezva, 1997; Ricart et al., 2002). In contrast, the mechanisms that control human  $\beta$ -F1-ATPase expression and localization have been poorly analyzed.

#### 4.1.1 Evidence of post-transcriptional regulation of $\beta$ -F1-ATPase expression in human colon, lung and breast cancer

The results in Figure 4.1 illustrate the significant down-regulation of the bioenergetic signature ( $\beta$ -F1-ATPase/GAPDH ratio) in breast, colon, and lung adenocarcinomas as well as in squamous lung carcinomas when compared to the bioenergetic signature in paired normal tissues. These findings raised the question of the mechanism(s) that could control  $\beta$ -F1-ATPase expression in human tumors.

First, we determined by real time PCR (qPCR)  $\beta$ -mRNA expression in breast, colon and lung cancer arrays (Fig. 4.1). We used commercial panels that included cDNA obtained from normal and tumor biopsies derived from patients with histopathological confirmed cancer and representing all clinical stages. The expression of  $\beta$ -mRNA in cancer varied depending upon the tissue being considered (Fig. 4.1). Expression of  $\beta$ -mRNA in breast (Fig. 4.1A) and lung adenocarcinomas (Fig. 4.1C) was not significantly different from normal tissues. In contrast, its expression was significantly augmented in adenocarcinomas of the colon (Fig. 4.1B) and squamous carcinomas of the lung (Fig. 4.1C) when compared to paired normal samples. Together, these findings indicate that the decreased expression of  $\beta$ -F1-ATPase in human tumors (Fig. 4.1) could not be ascribed to a limitation in

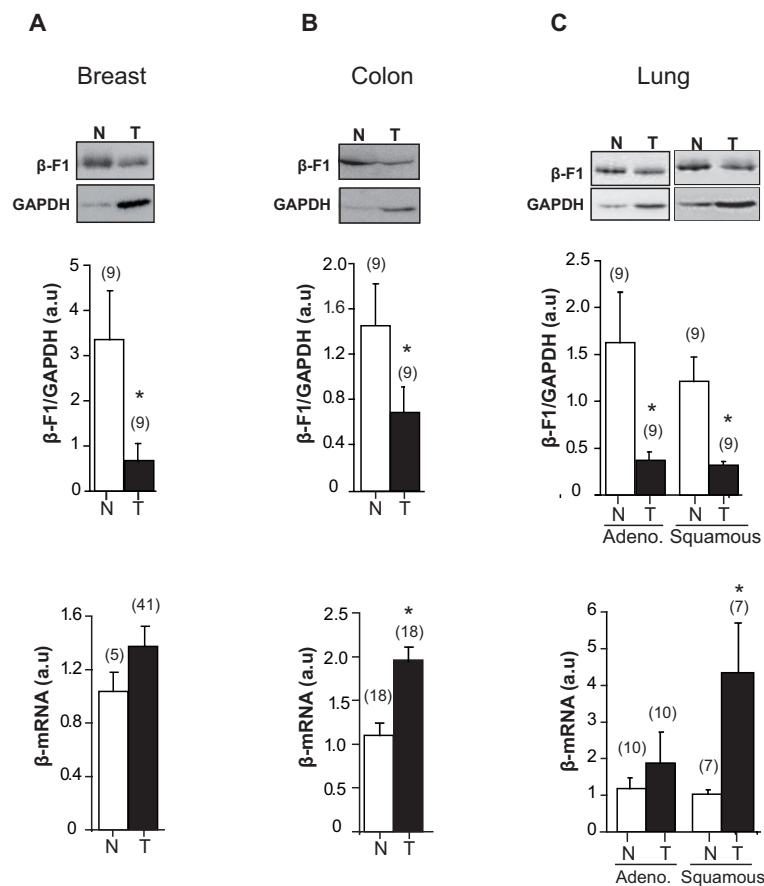


**Figure 4.1: Expression of  $\beta$ -mRNA in human breast, colon and lung tumors.** The bioenergetic signature ( $\beta$ -F1-ATPase/GAPDH ratio) was determined by western blotting in human (A) breast, (B) colon, (C) lung adenocarcinomas (Adeno.) and squamous carcinomas (T, black bars) and in paired normal tissues (N, white bars) of the same patients. A representative western blot of one patient is shown. Expression of  $\beta$ -mRNA was assessed by qPCR in human (A) breast, (B) colon, and (C) lung normal (N, white bars) and tumor (T, black bars) biopsies.  $\beta$ -mRNA expression level was quantified relative to the  $\Delta$ Ct mean value of normal samples and  $\beta$ -actin mRNA. The number of patients analyzed is shown in brackets. The results shown are means  $\pm$  SEM. \*,  $p < 0.05$  when compared with normal tissues by Student's t-test.

the availability of  $\beta$ -mRNA due to an impaired transcription and/or increased degradation of the transcript. Otherwise, the results suggest that the lower content of  $\beta$ -F1-ATPase could originate from translational silencing of  $\beta$ -mRNA as it has been previously documented in rat liver during development (Izquierdo and Cuezva, 1997; Luis et al., 1993), in brown adipose tissue (Tvrđik et al., 1992) and in rat hepatocarcinomas (de Heredia et al., 2000).

#### 4.1.2 The 3'UTR of human $\beta$ -mRNA is a *cis*-acting element involved in the control of its translation

Previous studies have demonstrated a relevant role for the 3'UTR of rat  $\beta$ -mRNA in the control of its translation (Di Liegro et al., 2000; Izquierdo and Cuezva, 1997; Izquierdo and Cuezva, 2000; Ricart et al., 2002). Therefore, a first question was to verify whether the human 3'UTR is also necessary for efficient translation of the transcript. *In vitro* translation of the human  $\beta$ -mRNA (h $\beta$ F1) and of a truncated version of the mRNA that lacks the 3'UTR (h $\beta$ F1-3' $\Delta$ ) revealed a significant two-fold decrease in the amount of synthesized  $\beta$ -F1-ATPase when the 3'UTR is missing (Fig. 4.2A). To

further confirm the need of the human 3'UTR in translation we fused the human 3'UTR of  $\beta$ -mRNA to GFP mRNA and tested the *in vitro* translation efficiency of the reporter constructs (Fig. 4.2B). The results revealed an autonomous translation enhancing activity of the human 3'UTR as the amount of GFP derived from the GFP-3' $\beta$  reporter was ~2-fold higher than that derived from GFP chimeras that lack any 3'UTR (GFP-3' $\Delta$ ) or contained the 3'UTR of  $\alpha$ -F1-ATPase (GFP-3' $\alpha$ ), a partner subunit of  $\beta$ -F1-ATPase in the H<sup>+</sup>-ATP synthase complex (Fig. 4.2B). The same result was obtained when the 3'UTR was fused to ARF (data not shown). Overall, these results demonstrate *in vitro* that the human 3'UTR of  $\beta$ -mRNA is also necessary for efficient translation of the transcript and that it might act as a relevant element in the control of  $\beta$ -mRNA translation (Di Liegro et al., 2000; Ricart et al., 2002).

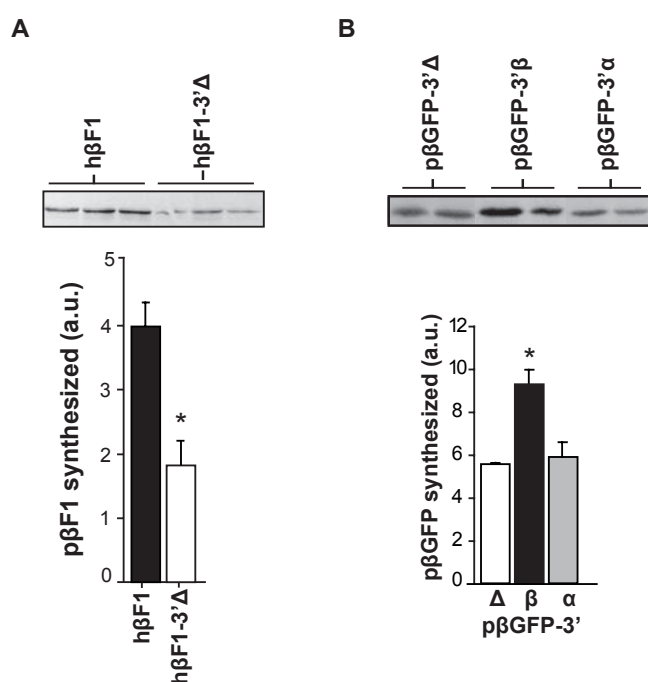


**Figure 4.2: The 3'UTR of the  $\beta$ -mRNA is required for efficient translation.** (A) *In vitro* translation of human capped  $\beta$ -mRNA containing (h $\beta$ F1) or not-containing (h $\beta$ F1-3' $\Delta$ ) the 3'UTR of the transcript. Fluorogram of the synthesized protein products is illustrated and the relative amount of the synthesized protein is indicated in the histogram. (B) The *in vitro* synthesized GFP mRNA containing (p $\beta$ GFP-3' $\beta$ ) or not (p $\beta$ GFP-3' $\Delta$ ) the 3'UTR of  $\beta$ -mRNA were translated in a cell-free system. The p $\beta$ GFP-3' $\alpha$  chimera containing the 3'UTR of  $\alpha$ -F1-ATPase mRNA, a partner subunit of the H<sup>+</sup>-ATP synthase, was used as an additional control. Fluorograms of the synthesized protein products are shown and the relative amounts of the synthesized proteins are illustrated in the histogram. The results shown are means  $\pm$  SEM. \*,  $p < 0.05$  when compared to h $\beta$ F1 and p $\beta$ GFP-3' $\Delta$ , respectively, by Student's t-test.

#### 4.1.3 Human tumor extracts promote the specific repression of $\beta$ -mRNA translation

The lower relative cellular content of  $\beta$ -F1-ATPase despite an increased or unchanged level of its mRNA in human breast, lung and colon cancer (Fig. 4.1) suggested that translation of  $\beta$ -mRNA might be repressed in cancer. Antonio Isidoro, a former member of our laboratory, analyzed whether the amount of the  $\beta$ -F1-ATPase protein synthesized *in vitro* could be modified by the presence of exogenously added protein extracts derived from paired normal and tumor tissues obtained from different cancer patients. Using cell-free translation assays, it was observed that in seven out of the eleven breast cancer patients studied (64 %), the addition of carcinoma extracts promoted a dose dependent reduction in the amount of  $\beta$ -F1-ATPase synthesized when compared to assays in which normal breast extracts were added (Fig. 4.3A). Similar findings were obtained in six out of the eight (75 %) lung cancer patients analyzed (Fig. 4.4A). In both cases breast and

## Results

lung tumor extracts exhibited a higher inhibitory activity on the synthesis of the protein when compared to normal tissue extracts (Histogram in Fig. 4.3B and 4.4B). It should be noted that differences in  $\beta$ -F1-ATPase synthesized are not the result of an increased degradation of  $\beta$ -mRNA in the presence of tumor extract, because when we determined the recovery of the transcript at the end of translation assays it was found to be the same irrespective of the extract added (Histogram in Fig. 4.3A and 4.4A).

To substantiate these findings, we analyzed the *in vitro* synthesis of  $\beta$ -F1-ATPase in the presence of normal and tumor extracts derived from esophageal cancer patients. Similar to breast and lung, three out of four esophageal tumor extracts provoked a significant decrease in the amount of  $\beta$ -F1-ATPase synthesized when compared to paired extracts derived from normal tissue biopsies (Fig. 4.5).

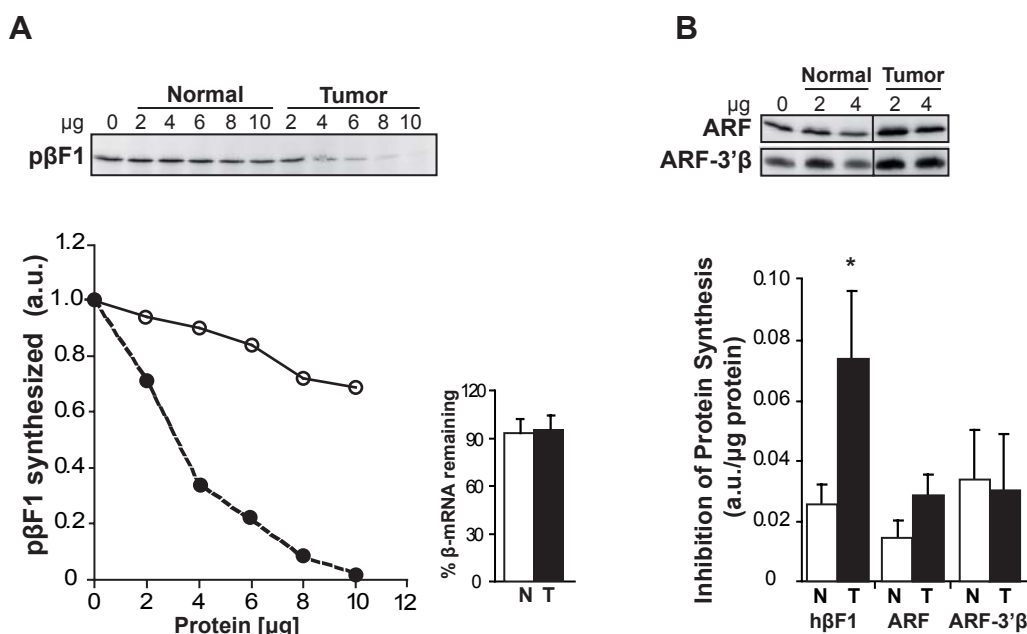


**Figure 4.3: Human breast tumor extracts specifically repress  $\beta$ -mRNA translation.** (A) *In vitro* synthesized and capped full-length human  $\beta$ -mRNA was translated in a cell-free system ( $\beta$ F1) in the presence of different amounts of human breast tissue extracts ( $\mu$ g) derived from normal and tumor biopsies. A representative fluorogram and plot illustrates the relative amount of  $\beta$ -F1-ATPase synthesized in the presence of different  $\mu$ g of protein derived from normal (open circle and continuous line) or tumor (closed circle and discontinuous line) tissue of one patient. The histogram shows the quantity of  $\beta$ -mRNA recovered after translation assays with normal (N, white bar) and tumor (T, black bar) extracts. (B) Translation of *in vitro* synthesized full-length ARF mRNA and ARF-3' $\beta$ UTR mRNA in the presence of normal and tumor breast extracts. A representative experiment illustrates the ARF protein in the presence of different protein inputs ( $\mu$ g). The histogram summarizes the quantification of the inhibitory activity of normal (N, white bars) and tumor (T, black bars) extracts for  $\beta$ F1, ARF and ARF-3' $\beta$  translation. The results shown are means  $\pm$  SEM of seven patients. \*,  $p < 0.05$  when compared with normal extracts by Student's t-test. (Part of the data in this figure were supplied by Antonio Isidoro.)

Next, in order to assess the specificity of the inhibitory effect of tumor extracts on  $\beta$ -mRNA translation, we studied the effect of tumor extracts on the translation of an unrelated mRNA such as ARF. The results showed no relevant effect of breast (Fig. 4.3B), lung (Fig. 4.4B) and esophageal (Fig. 4.5) tumor extracts on the synthesis of ARF compared to paired normal extracts (Fig. 4.3B, 4.4B and 4.5), illustrating the specific inhibition of  $\beta$ -mRNA translation exerted by tumor extracts.

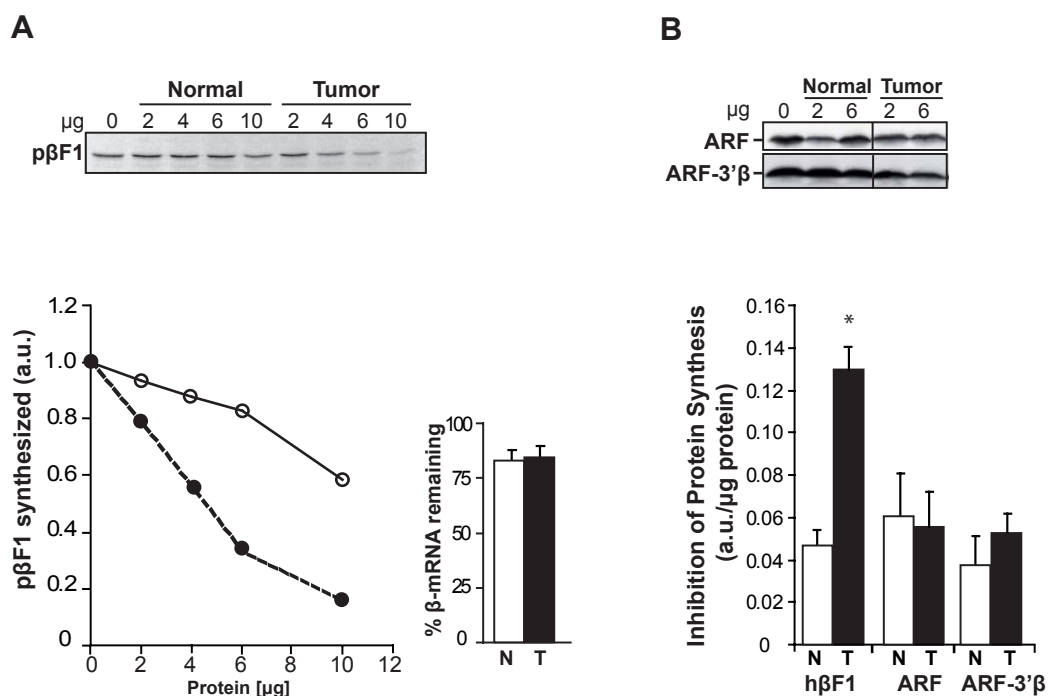


**Figure 4.4: Human lung tumor extracts specifically repress  $\beta$ -mRNA translation.** (A) *In vitro* synthesized and capped full-length human  $\beta$ -mRNA was translated in a cell-free system (p $\beta$ F1) in the presence of different amounts of human lung tissue extracts ( $\mu$ g) derived from normal and tumor biopsies. A representative fluorogram and plot illustrates the relative amount of  $\beta$ -F1-ATPase synthesized in the presence of different  $\mu$ g of protein derived from normal (open circle and continuous line) or tumor (closed circles and discontinuous line) lung biopsies from one patient. The histogram shows the quantity of  $\beta$ -mRNA recovered after translation assays with normal (N, white bar) and tumor (T, black bar) extracts. (B) Translation of *in vitro* synthesized full-length ARF mRNA and ARF-3'UTR mRNA in the presence of normal and tumor lung extracts. A representative experiment illustrates the ARF protein in the presence of different protein inputs ( $\mu$ g). The histogram summarizes the quantification of the inhibitory activity of normal (N, white bars) and tumor (T, black bars) extracts for p $\beta$ F1, ARF and ARF-3' $\beta$ . The results shown are means  $\pm$  SEM of six patients. \*,  $p < 0.05$  when compared with normal extracts by Student's t-test. (Part of the data in this figure were supplied by Antonio Isidoro.)

Since the 3'UTR is a relevant *cis*-acting element in controlling translation of  $\beta$ -mRNA (Fig. 4.2 and de Heredia et al., 2000; Izquierdo and Cuezva, 1997), next we examined the effect of the extracts on the translational efficiency of a chimeric reporter construct that contain the sequence of ARF fused to the human 3'UTR (ARF-3' $\beta$ ). Interestingly, and at variance with previous findings in rat liver and hepatoma extracts (de Heredia et al., 2000; Izquierdo and Cuezva, 1997), the synthesis of ARF derived from ARF-3' $\beta$  transcript is not affected by the presence of human tumor extracts when compared to normal (Fig. 4.3B, 4.4B and 4.5). These results suggest the existence of mechanistic differences in mammals for controlling the expression of  $\beta$ -mRNA. Moreover, it indicates that the inhibitory effect of the lung, breast and esophageal tumor extracts on the synthesis of  $\beta$ -F1-ATPase in human tissues requires, in addition to the 3'UTR, other *cis*-acting elements of the  $\beta$ -F1-ATPase transcript.

Taken together, the results hint that the decreased  $\beta$ -F1-ATPase expression in human breast, lung and esophageal cancer could originate from a specific translation repression event on  $\beta$ -mRNA, as it was previously documented in development and in hepatocarcinogenesis of the rat (Cuezva et al., 1997; de Heredia et al., 2000; Izquierdo and Cuezva, 1997; Luis et al., 1993).

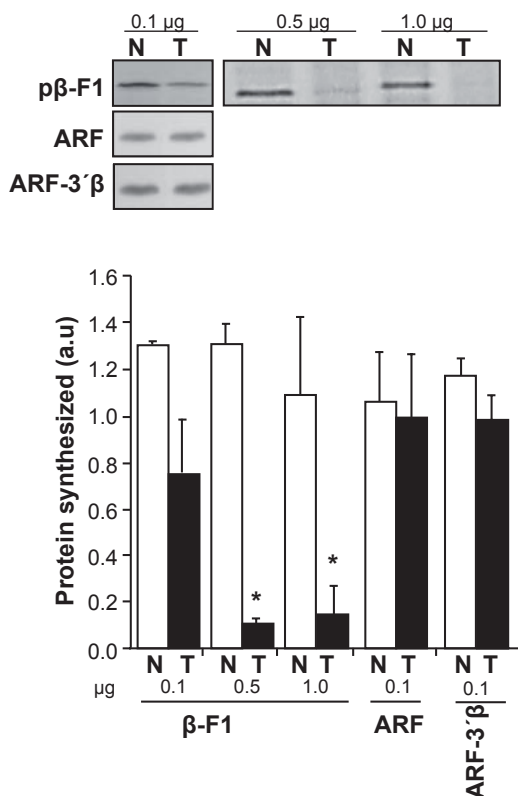


**Figure 4.5: Human esophageal tumor extracts specifically repress  $\beta$ -mRNA translation.** (A) *In vitro* synthesized and capped full-length human  $\beta$ -mRNA, ARF mRNA and ARF-3'  $\beta$ UTR mRNA were translated in a cell-free system in the presence of different amounts of human esophageal tissue extracts ( $\mu$ g) derived from paired normal (N) and tumor biopsies (T) of the same patient. A representative fluorogram of one cancer patient is illustrated. The histogram shows the quantification of p $\beta$ F1, ARF and ARF-3'  $\beta$  synthesized in the presence of normal (N, white bars) and tumor (T, black bars) extracts. The results shown are means  $\pm$  SEM of three patients. \*,  $p < 0.05$  when compared with normal extracts by Student's t-test.

## 4.2 MOLECULAR AND FUNCTIONAL CHARACTERIZATION OF $\beta$ -mRNA BINDING PROTEINS

Previous studies of the laboratory indicated that expression of  $\beta$ -F1-ATPase is stringently controlled at the level of translation by the binding of RNABPs onto the mRNA (de Heredia et al., 2000; Izquierdo and Cuezva, 1997). This mechanism of regulation of gene expression was found to be operative during development of rat liver (Izquierdo and Cuezva, 1997), in rat hepatocarcinogenesis (de Heredia et al., 2000) and during cell cycle progression (Martinez-Diez et al., 2006). The result in part 4.1 of this thesis indicated that also human  $\beta$ -F1-ATPase expression is controlled at the level of translation in human cancer. In this regard, a main objective of our laboratory has been the identification of the RNABPs that could regulate  $\beta$ -F1-ATPase expression.

Dr. Álvaro Ortega, a former member of our laboratory was able, using an improved RNABP affinity purification assay (Bardwell and Wickens, 1990; Zhou et al., 2002; Ortega et al., 2010) to identify nine bonafide RNABPs that interact *in vitro* with full-length human  $\beta$ -mRNA (Ortega et al., 2010). Consequently, our first aim was to verify *in vivo* the interaction of some of these RNABPs with the human  $\beta$ -mRNA. A further aim was to characterize the physiological relevance that the identified proteins could have on  $\beta$ -F1-ATPase biology. From the nine proteins identified, we focused our study on three proteins (IMP1, NPM1 and G3BP1) due to the following criterions: (I) The size of the proteins should be in the range of 50-70 kDa, since the previously described most relevant  $\beta$ -F1-ATPase RNABPs ( $\beta$ -RNABPs) present in rat and human cellular extracts were in that range (de Heredia et al., 2000; Izquierdo and Cuezva, 1997; Izquierdo and Cuezva, 2005; Ortega et al.,

2010; Ricart et al., 2002). (II) The selected proteins should be able to shuttle between the nucleus and the cytoplasm, because in rat hepatocytes we have described that the  $\beta$ -RNP complex is first formed in the nucleus and then exported to the cytoplasm, from where it is preferentially sorted to the vicinity of mitochondria (Egea et al., 1997). (III) Finally, the proteins should be involved in some aspects of tumorigenesis. A brief summary of the biological role of IMP1, NPM1 and G3BP1 is provided in the Appendix.

## 4.2.1 G3BP1 interacts *in vivo* with $\beta$ -mRNA

### 4.2.1.1 $\beta$ -mRNA pull-down assays

To verify *in vivo* the putative interaction of G3BP1, IMP1 and NPM1 with  $\beta$ -mRNA, we transfected Hek293T cells with Flag-tagged IMP1, NPM1 and G3BP1 and immunoprecipitated the mRNA-RNABP complex using monoclonal anti-Flag antibodies. Subsequently, the co-immunoprecipitated mRNA was isolated and analyzed by RT-qPCR for the presence of  $\beta$ -mRNA. Western blot analysis confirmed the expression and immunoprecipitation (IP) of the three tagged proteins (Fig. 4.6). The RT-qPCR analysis of the IPs indicated that IMP1 does not interact with  $\beta$ -mRNA (Fig. 4.6B), because

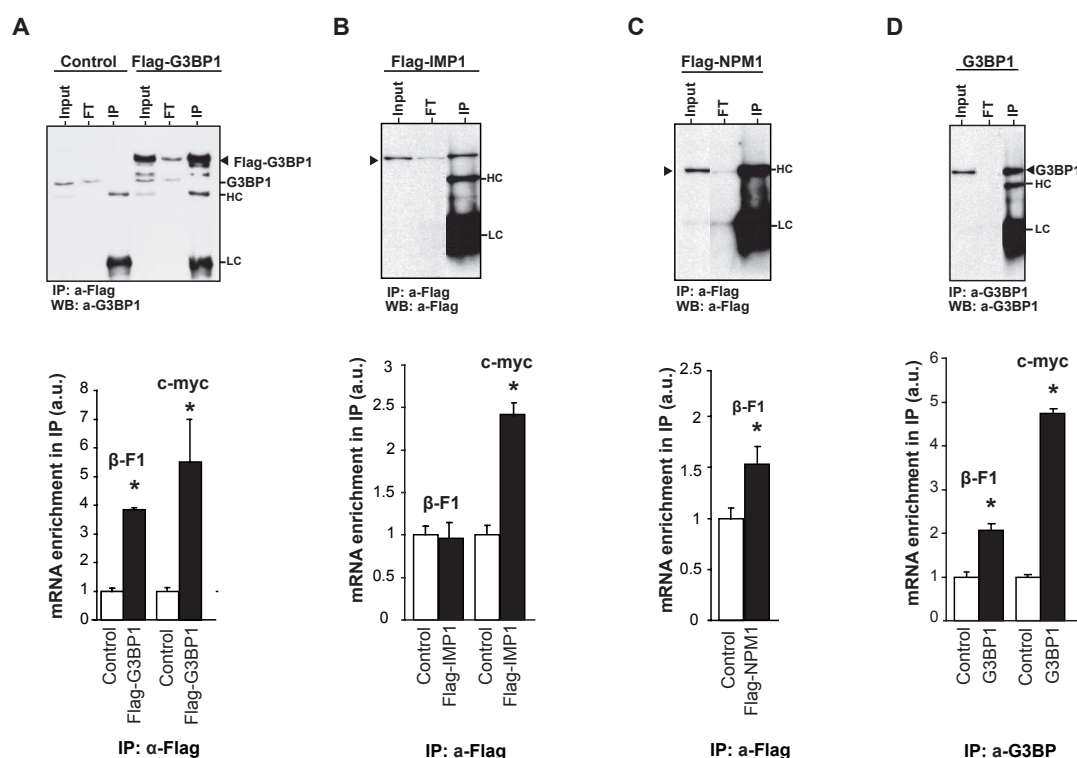


**Figure 4.6: Co-immunoprecipitation of  $\beta$ -mRNA with G3BP1.** (A-C) Non-transfected (control) and transfected Hek293T cells with plasmids encoding (A) Flag-G3BP1, (B) Flag-IMP1 or (C) Flag-NPM1 were subjected to immunoprecipitation (IP) using monoclonal anti-Flag antibody. The input, flow through (FT) and immunoprecipitates (IP) were subsequently analyzed by western blot (WB) using the indicated antibody. (D) Immunoprecipitation of endogenous G3BP1 using the monoclonal anti-G3BP1 antibody. Arrowheads indicate the corresponding proteins. HC and LC indicate the migration of the heavy and light chain of the IgGs used for immunoprecipitation. The histograms show the quantification of the mRNA amplified by RT-qPCR in the different IPs (black bars) relative to that of non-transfected cells (control, white bars) and GAPDH used as an internal control. The quantification of *c-myc* mRNA was assessed as a positive control of G3BP1 (A, D) and IMP1 (B). The results shown are the means  $\pm$  SEM. \*,  $p < 0.05$  compared with control IP using Student's t-test.



the  $\beta$ -F1-ATPase transcript is not enriched in the IPs of Flag-IMP1. In contrast, c-myc mRNA, which is known to be bound by IMP1 (Doyle et al., 1998; Bernstein et al., 1992) is clearly increased when compared to the IPs of control cells (Fig. 4.6B). Likewise, NPM1 seems to associate only marginally with  $\beta$ -mRNA (Fig. 4.6C). However, cells over-expressing G3BP1 (Fig. 4.6A) illustrated a  $\sim$ 4-fold enrichment of  $\beta$ -mRNA in the IPs when compared to control non-transfected cells. The enrichment of  $\beta$ -mRNA in the IPs of Flag-G3BP1 was similar to that of c-myc mRNA, which is a known RNA target of G3BP1 (Gallouzi et al., 1998; Tourriere et al., 2001), suggesting the interaction of G3BP1 and  $\beta$ -mRNA in the cellular context.

Since the over-expression of G3BP1 has been shown to promote the assembly of stress granules (SGs) (Tourriere et al., 2003), we wanted to rule out the possibility that the observed  $\beta$ -mRNA-G3BP1 interaction (Fig. 4.6A) could be artificially mediated by the over-expression of G3BP1. Remarkably, immunoprecipitation of endogenous G3BP1 in non-transfected cells with an antibody against G3BP1 revealed the co-immunoprecipitation of  $\beta$ -mRNA with the protein (Fig. 4.6D), demonstrating the specificity of this interaction within the cellular context.

### 4.2.1.2 Fluorescence *in situ* hybridization

The *in vivo*  $\beta$ -mRNA-G3BP1 interaction was further confirmed by fluorescence *in situ* hybridization of  $\beta$ -mRNA (red) combined with immunofluorescence of G3BP1 (green) (Fig. 4.7). The partial co-localization of the endogenous G3BP1 with  $\beta$ -mRNA (yellow dots) was extinct when the cells were incubated with an excess of unlabeled riboprobes (Fig. 4.7). Overall, these data demonstrate that G3BP1 interacts *in vivo* with  $\beta$ -mRNA.

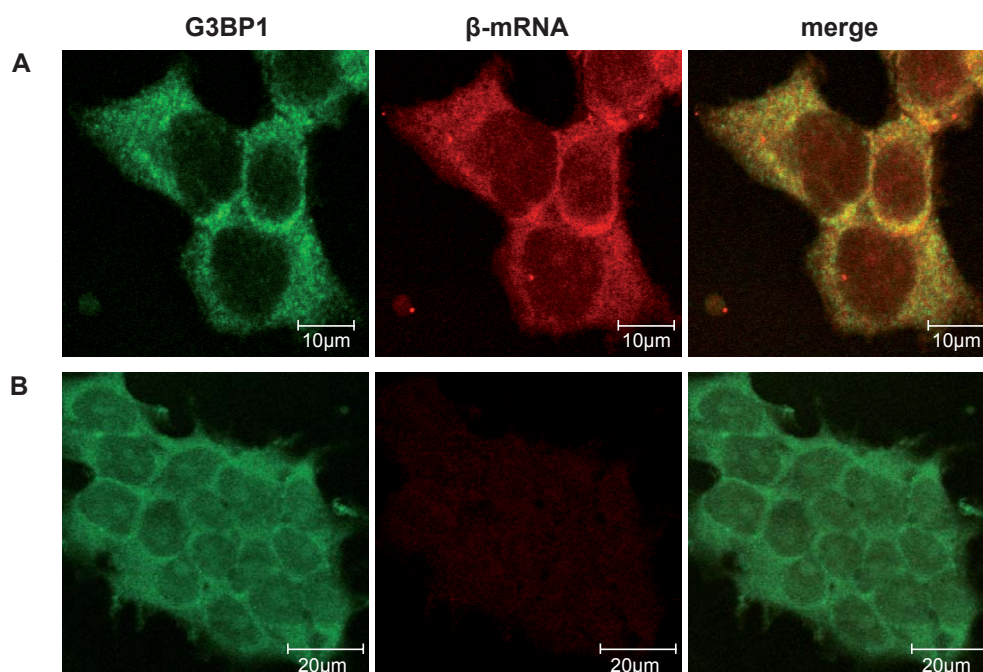


**Figure 4.7: Fluorescence *in situ* hybridization of  $\beta$ -mRNA.** (A) Co-localization of endogenous G3BP1 and  $\beta$ -mRNA was analyzed in Hek293T cells by combined immunofluorescence and FISH. Fixed cells were immunostained with anti-G3BP1 antibody (green, G3BP1) and further hybridized with a mixture of Cy5-labeled  $\beta$ -mRNA riboprobes (red,  $\beta$ -mRNA). Yellow signals in the merged image indicate co-localization of both molecules. (B) After immunostaining with anti-G3BP1 antibody, cells were incubated with a 100-fold excess of unlabeled riboprobes and further hybridized with Cy5-labeled  $\beta$ -mRNA riboprobes.

#### 4.2.2 Visualizing RNA-protein interactions *in vivo* (TriFC)

The putative *in vivo* interaction of G3BP1, NPM1 and IMP1 with  $\beta$ -mRNA was further analyzed by RNA-bridged trimolecular fluorescence complementation assay (TriFC), a technique that allows the visualization and localization of RNA-protein interactions in living cells (Bertrand et al., 1998; Rackham and Brown, 2004; Stohr et al., 2006). In this system, the C-terminal domain of the yellow fluorescence protein (YFP) is fused to the MS2-coat-protein (YFP<sub>Ct</sub>-HA-MS2CP) and is tethered to the RNA of interest due to the high affinity of the bacteriophage MS2-coat-protein (CP or MS2CP) to its MS2-RNA-hairpins (Peabody, 1993). The complementary N-terminal domain of YFP is fused to the RNABP of interest (YFP<sub>Nt</sub>-Flag-RNABP). If the RNABP associates with  $\beta$ -mRNA, the two YFP domains will come in close proximity and consequently the fluorescent complex is reconstituted and the subcellular localization of this interaction is revealed. No reconstitution of fluorescence will occur when the two domains of YFP do not get in close contact. For this study we used NRK cells that stably express the  $\beta$ -mRNA fused to three MS2-hairpins (C4) (Ortega et al., 2010) co-transfected with YFP<sub>Nt</sub>-RNABP and YFP<sub>Ct</sub>-MS2CP in a 1:1 ratio.

##### 4.2.2.1 G3BP1 binds $\beta$ -mRNA *in vivo* in small fluorescence foci

RNA-bridged TriFC system revealed specific cytoplasmic fluorescent foci in C4 cells (Fig. 4.8A) and the absence of fluorescent complexes after equimolar transfection of YFP<sub>Nt</sub>-Flag-G3BP1 and YFP<sub>Ct</sub>-HA-MS2CP in the parental NRK cell line (Fig. 4.8B). Interestingly, YFP fluorescence was found

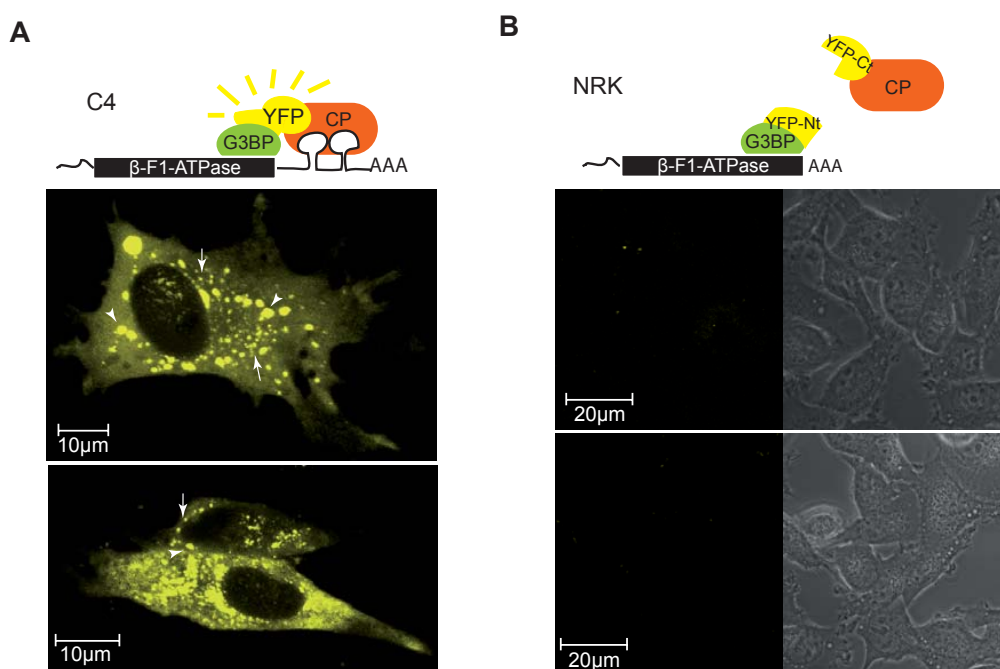


**Figure 4.8: G3BP1 interacts with  $\beta$ -mRNA.** RNA-bridged trimolecular fluorescent complementation assay performed *in vivo* by equimolar co-transfection with YFP<sub>Ct</sub>-HA-MS2CP (orange, CP) and YFP<sub>Nt</sub>-Flag-G3BP1 (green) in (A) C4 cells and (B) NRK cells. (A) C4 cells stably express  $\beta$ -mRNA (black) fused to MS2-RNA-hairpins (shown as two hairpins in black upstream poly-A tail). G3BP1 binds  $\beta$ -mRNA so that both N- and C-terminal YFP domains (yellow) come together and reconstitute fluorescence. (B) Formation of the fluorescent complex is hampered in NRK cells, because  $\beta$ -mRNA lacks the MS2 hairpins and MS2CP cannot bind to the mRNA. White arrows and arrowheads denote small and large  $\beta$ -mRNA granules, respectively. The right panels in B show phase contrast images of the respective fluorescence fields.

clustered in both large (see arrowhead in Fig. 4.8A) and small (see arrow in Fig. 4.8A) cytoplasmic granules, which might illustrate two different cytoplasmic compartments for the  $\beta$ -mRNA. The large cytoplasmic granules might illustrate the accumulation of  $\beta$ -mRNA in SGs, because over-expression of G3BP1 provokes the assembly of SGs (Tourriere et al., 2003).

Consistently, a partial co-localization of G3BP1 with the prominent SG marker TIA1 (Kedersha et al., 1999) was observed (see arrowhead in Fig. 4.9) when using both anti-Flag (Fig. 4.9A) and anti-G3BP1 (Fig. 4.9B) antibodies. However, in agreement with the small  $\beta$ -mRNA granules observed in C4 cells (Fig. 4.8A), G3BP1 was also found in tiny, TIA1-negative granules (see arrow in Fig. 4.9). All in all, these findings suggest together with the RNA-IP results (Fig. 4.6 A,D) and the co-localization images of endogenous G3BP1 with  $\beta$ -mRNA (Fig. 4.7) that  $\beta$ -mRNA-G3BP1 specifically interact in those small TIA1-negative granules, whereas sorting of  $\beta$ -mRNA into SGs might be the result of cellular stressful conditions.

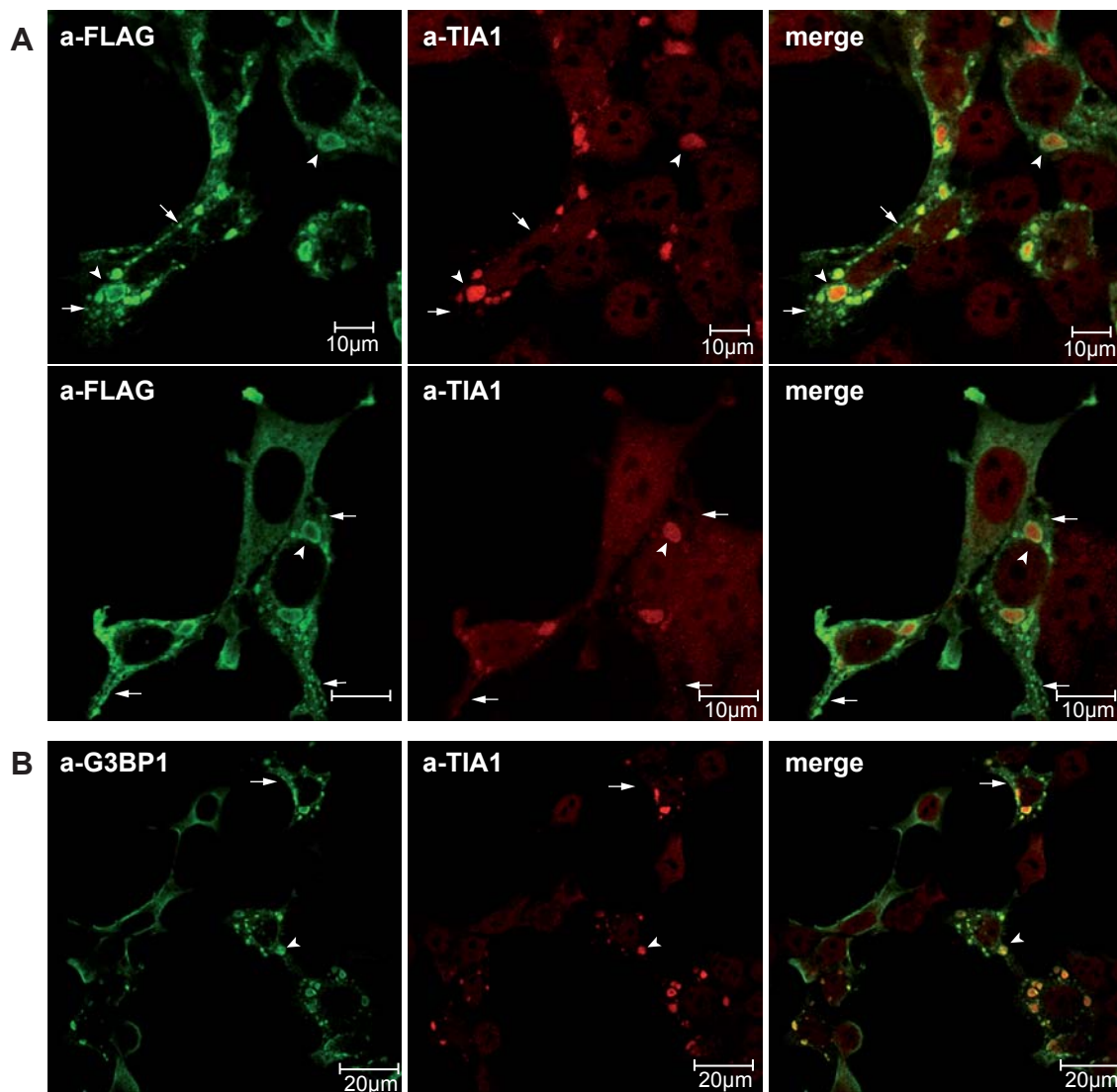


**Figure 4.9: G3BP1 is localized both in TIA1-positive (SGs) and negative cytoplasmic granules.** Hek293T cells were transfected with the Flag-G3BP1 plasmid, fixed and immunostained with (A) anti-TIA1 (red, TIA1) and anti-Flag (green, FLAG) or (B) anti-G3BP1 (green, G3BP1) antibodies. White arrows and arrowheads denote respectively small (TIA1-negative) and large (TIA1-positive, SGs) granules. Fluorescence was analyzed *in vivo* by confocal microscopy.

#### 4.2.2.2 No evidence that IMP1 and NPM1 associate with $\beta$ -mRNA

When YFP<sub>Nt</sub>-Flag-IMP1 and YFP<sub>Ct</sub>-HA-MS2CP are co-expressed, a bright fluorescence signal with large cytoplasmic perinuclear clustering is detected (Fig. 4.10) in both C4 and NRK cells, indicating the lack of specific interaction of IMP1 and  $\beta$ -mRNA. Fluorescent granules in these cells could result from an artificial interaction and accumulation of YFP in agglomeration bodies. Similar negative findings were obtained when YFP<sub>Nt</sub>-Flag-NPM1 and YFP<sub>Ct</sub>-HA-MS2CP are co-expressed in C4 and NRK cells (Fig. 4.10). In both cell lines reconstitution of the fluorescent signal was observed in the nucleus (Fig. 4.10). NPM1 is a shuttle protein that is mainly nucleolarly localized (Borer et al., 1989), therefore it is possible that expression of the YFP<sub>Nt</sub>-Flag-NPM1 and YFP<sub>Ct</sub>-HA-MS2CP fusion proteins could lead to a non-specific assembly of YFP in the cytoplasm and its further transport by means of NPM1 into the nucleus. Taken together, these results underline (Fig. 4.6B, C) that IMP1 and NPM1 do not associate *in vivo* with  $\beta$ -mRNA and suggest no role for these proteins in controlling  $\beta$ -F1-ATPase biology.

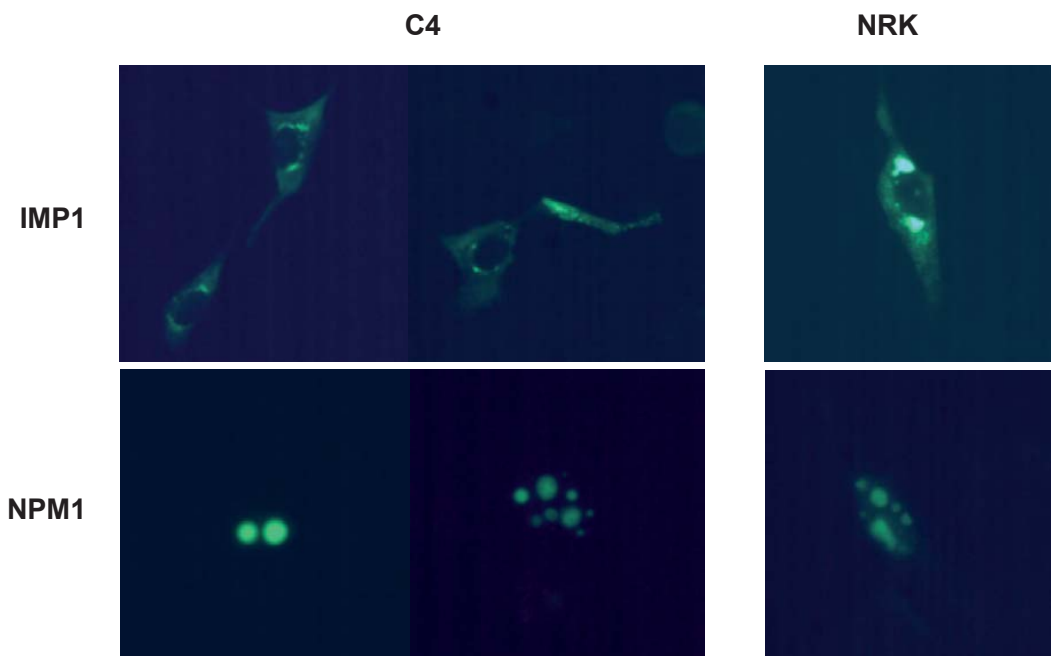


**Figure 4.10: Analysis of IMP1 and NPM1 interaction with  $\beta$ -mRNA by TriFC.** RNA-bridged trimolecular fluorescent complementation assay (TriFC) was performed in NRK and C4 cells co-transfected with YFP<sub>Ct</sub>-HA-MS2CP and YFP<sub>Nt</sub>-Flag-IMP1 (IMP1, upper panels) or YFP<sub>Nt</sub>-Flag-NPM1 (NPM1, lower panel). Fluorescence was analyzed *in vivo* using a Leica DM IRB microscope.

#### 4.2.2.3 G3BP1 binds *in vivo* the 3'UTR of $\beta$ -mRNA

Because the 3'UTR is an essential regulatory element required for efficient translation of the transcript (Fig. 4.2 and Di Liegro et al., 2000; Izquierdo and Cuezva, 1997), next we analyzed whether G3BP1 could interact *in vivo* with the 3'UTR of human  $\beta$ -mRNA. To this aim, we studied the reconstitution of YFP fluorescence in NRK cells transiently expressing a chimeric RNA reporter made of the  $\beta$ -galactosidase sequence fused to seven MS2CP binding sites containing (Fig. 4.11A) or not (Fig. 4.11B) the 3'UTR of  $\beta$ -mRNA (black in 4.11A). Remarkably, the  $\beta$ -galactosidase bearing the 3'UTR of  $\beta$ -mRNA recapitulates essentially the same cytoplasmic fluorescent pattern observed

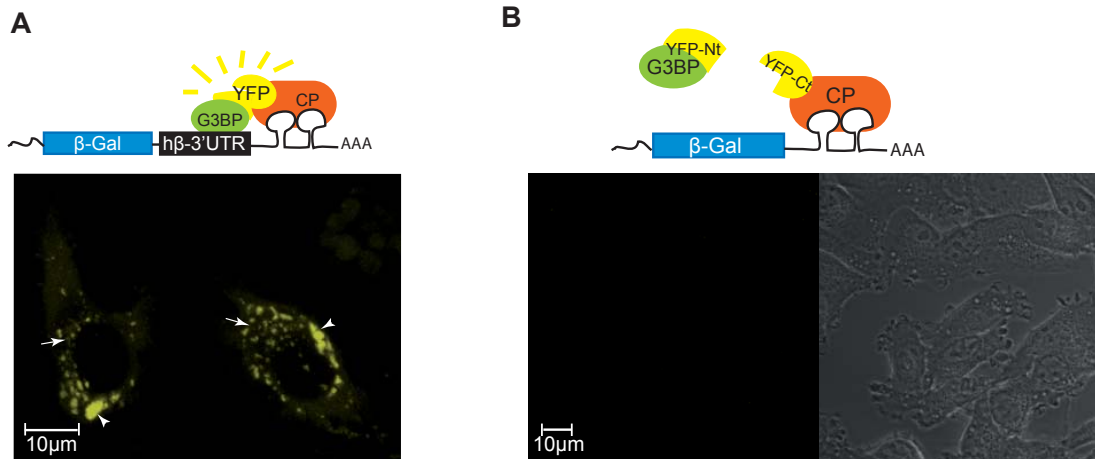


**Figure 4.11: G3BP1 interacts with 3'UTR of  $\beta$ -mRNA.** (A), (B) NRK cells were co-transfected with plasmids encoding the fusion proteins YFP<sub>Ct</sub>-HA-MS2CP (orange, CP) and YFP<sub>Nt</sub>-Flag-G3BP1 (green) and a plasmid encoding a hybrid reporter mRNA consisting of (A)  $\beta$ -galactosidase ( $\beta$ -Gal, blue) fused to MS2-RNA-hairpins (shown as two hairpins in black upstream poly-A tail) containing or (B) not containing the human 3'UTR (h $\beta$ -3'UTR, black) of the  $\beta$ -F1-ATPase. Fusion proteins were transfected at a molar 1:5 ratio with regard to hybrid RNA. (A) MS2CP binds with high affinity the MS2-RNA-hairpins and G3BP1 binds the h $\beta$ -3'UTR (black) bringing YFP domains closer enough to reconstitute fluorescence. (B) The  $\beta$ -Gal reporter RNA lacking the 3'-UTR of  $\beta$ -mRNA is unable to recruit G3BP1 and thus reconstitution of fluorescence is not detected (right panel). White arrows and arrowheads denote respectively small and large  $\beta$ -mRNA granules. The right panels in B show phase contrast images of the respective fluorescence fields. Fluorescence was analyzed *in vivo* by confocal microscopy.

with the full-length MS2-tagged  $\beta$ -mRNA (Fig. 4.8A), whereas the control RNA chimera that lacked the 3'UTR of  $\beta$ -mRNA was unable to regenerate YFP fluorescence. Interestingly, the number, size and fluorescence intensity of reconstituted YFP in NRK cells using the  $\beta$ -galactosidase reporter (Fig. 4.11A) are less than those observed with the tagged  $\beta$ -mRNA in C4 cells (Fig. 4.8A). This might result from differences in the cellular abundance of the  $\beta$ -mRNA probe (Ortega et al., 2010) and/or from the involvement of additional *cis*-acting elements and/or  $\beta$ -RNABPs that might stabilize the G3BP1 interaction in the RNA-protein complex. Overall, these results demonstrate that G3BP1 associates *in vivo* with the 3'UTR of  $\beta$ -mRNA and that the determinants for the cytoplasmic subcellular localization of human  $\beta$ -mRNA reside in the 3'UTR.

### 4.2.3 $\beta$ -mRNA is sorted to the vicinity of mitochondria

Next, we questioned about the possible mitochondrial localization of the fluorescent granules containing  $\beta$ -mRNA. For this purpose, C4 cells that stably express MS2-tagged  $\beta$ -mRNA were transfected with both YFP<sub>Nt</sub>-Flag-G3BP1 and YFP<sub>Ct</sub>-HA-MS2CP and mitochondria were stained with MitotrackerRed (Fig. 4.12). Both large (arrowhead in Fig. 4.12) and small (arrows in Fig. 4.12)  $\beta$ -mRNA granules were shown to co-localize with mitochondria. To substantiate this finding, we transfected C4 cells with a vector expressing GFP fused to the MS2CP. The GFP fusion protein contains a nuclear retention signal (Rook et al., 2000) so that cytoplasmic localization of GFP is only possible when the fusion protein is exported from the nucleus tethering the MS2-tagged  $\beta$ -mRNA. High-resolution immunoelectron microscopy of C4 cells with an antibody against GFP revealed the specific labeling of the cytoplasm with both scattered and clustered gold signals (Fig. 4.13A,

B). Interestingly, there was also specific and significant GFP labeling of mitochondria in its outer membrane (Fig. 4.13A, B), suggesting the spatial association between  $\beta$ -mRNA and mitochondria in the C4 cell line.

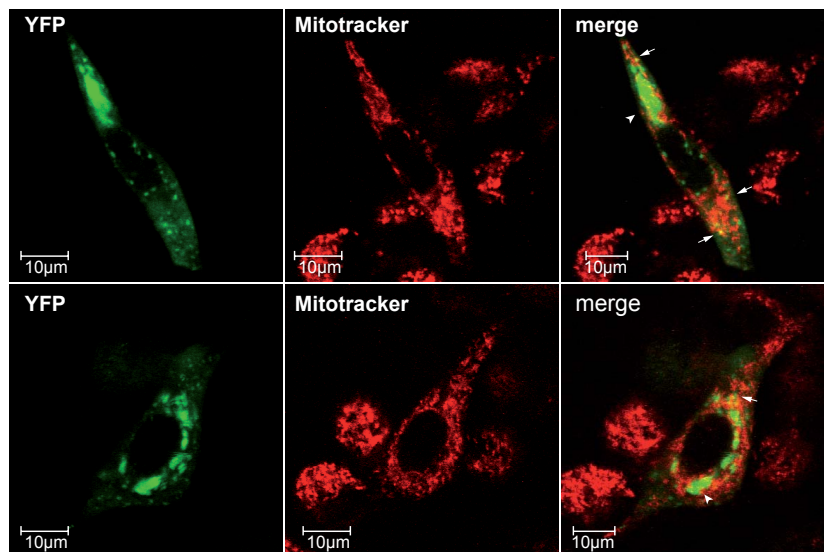


**Figure 4.12:  $\beta$ -mRNA granules co-localize with mitochondria.**  $\beta$ -RNA bridged TriFC assays were performed as in Fig 4.8. Cells were stained with MitotrackerRed (200 nM) and analyzed *in vivo* by confocal microscopy. White arrows and arrowheads denote respectively small and large  $\beta$ -mRNA granules.

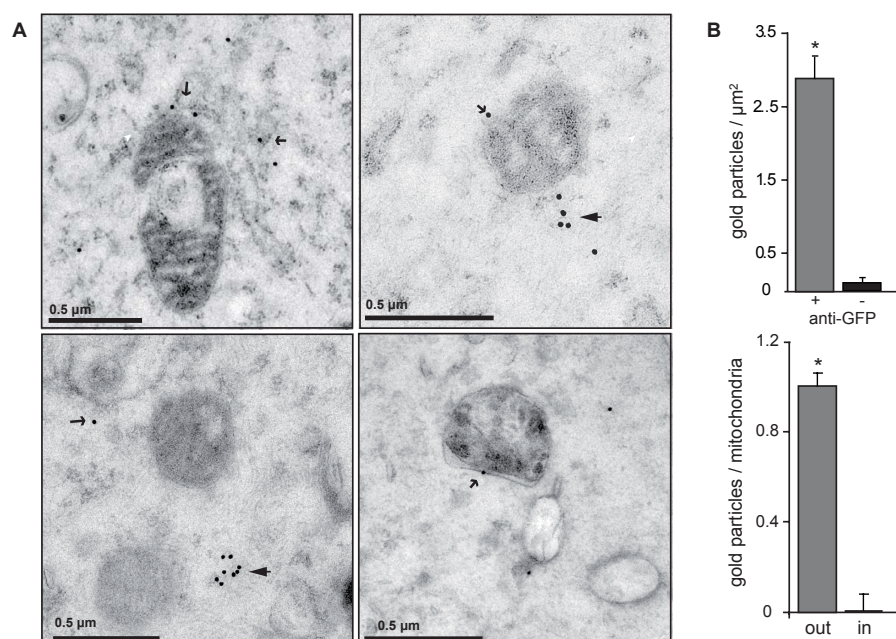


**Figure 4.13:  $\beta$ -mRNA is sorted to the vicinity of mitochondria.** (A) Subcellular localization of  $\beta$ -mRNA in C4 cells was analyzed by immunoelectron microscopy after transfection of GFP-CP-nls using anti-GFP antibody. The GFP-CP-nls fusion protein is localized into the nucleus due to the nucleus localization signal (nls) where it binds to the MS2 hairpins of  $\beta$ -mRNA. The  $\beta$ -mRNA-GFP complex is transported into the cytoplasm and indicates the localization of  $\beta$ -mRNA. Single (arrow) or clustered (arrowhead) appearance of  $\beta$ -mRNA can be observed in the vicinity of mitochondria. (B) Upper histogram shows the number of gold particles/ $\mu\text{m}^2$  of ultrathin sections incubated with (+) or without (-) the primary antibody revealing the specificity of the gold signal. The results are means  $\pm$  SEM of gold particles in ten different fields of 5  $\mu\text{m}^2$ . Lower histogram shows the quantification of gold particles attached to the outside of mitochondria compared to the number of gold particles localized within the mitochondrial interior. The results shown are the means  $\pm$  SEM of the gold particle counted in 50 mitochondria.

#### 4.2.4 G3BP1 inhibits the synthesis of $\beta$ -F1-ATPase

To address the putative functional role that G3BP1 could have on  $\beta$ -F1-ATPase expression, we performed in collaboration with Dr. Álvaro Ortega over-expression and siRNA mediated silencing assays in Hek293T cells. Interestingly, cellular silencing of G3BP1 cells had no effect on  $\beta$ -mRNA levels and on the relative rates of  $\beta$ -F1-ATPase synthesis (data not shown). In contrast, over-expression of G3BP1 (Fig. 4.14A) promoted a significant reduction in the *in vivo* rate of  $\beta$ -F1-ATPase synthesis without relevant changes in the steady state level of the  $\beta$ -mRNA (Fig. 4.14B). Notably, G3BP1 expression had no influence on the synthesis of Hsp60, suggesting a specific role for G3BP1 in the control of  $\beta$ -mRNA translation.

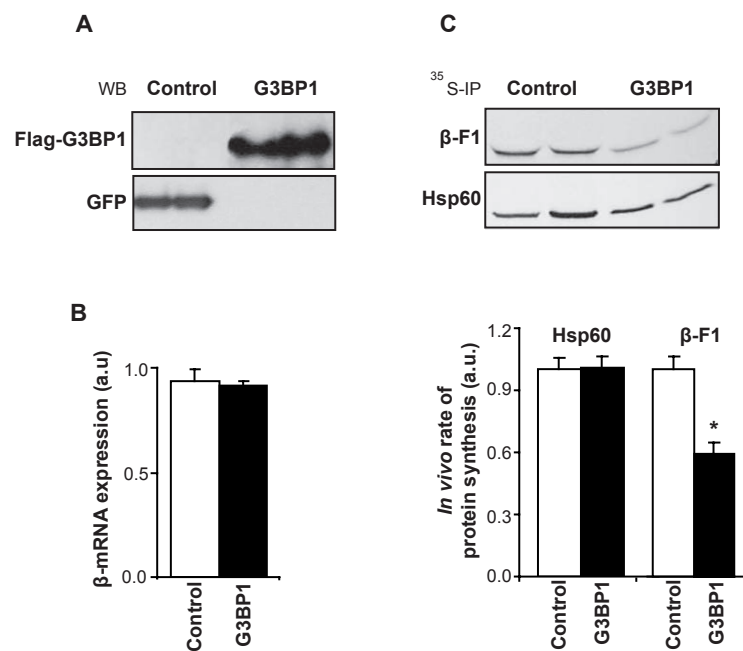


**Figure 4.14: G3BP1 inhibits the translation of  $\beta$ -mRNA *in vivo*.** (A) Western blot analysis of Hek293T cells transfected either with Flag-G3BP1 or GFP (control) to assess over-expression. (B)  $\beta$ -mRNA expression in both control and G3BP1 over-expressing cells was assessed by RT-qPCR. Histogram shows the mean  $\pm$  SEM of three independent experiments of  $\beta$ -mRNA quantification relative to mock transfected cells. GAPDH mRNA used as an internal control. (C) Determination of the *in vivo* rate of the  $\beta$ -F1-ATPase synthesis after metabolic labeling with  $^{35}$ S-methionine followed by immunoprecipitation (35S-IP) in both control and G3BP1 over-expressing cells. The histogram shows the mean  $\pm$  SEM of the quantification of the bands normalized to the mean value in control cells from six independent experiments. \*, when  $p < 0.05$  when compared to control cells by Student's t-test. (Data in this figure were supplied by Dr. Álvaro Ortega.)

The specific repression of  $\beta$ -mRNA translation exerted by G3BP1 was further confirmed in an *in vitro* system (Fig. 4.15). Addition of *in vitro* synthesized G3BP1 (Fig. 4.15A) to cell-free translation assays triggered a repression of the synthesis of  $\beta$ -F1-ATPase when compared to the translation that lacked the inclusion of any protein (control) or in the presence of equivalent amounts of pyruvate kinase (PK), a non relevant protein in this study (Fig. 4.15). Notably, addition of G3BP1 had no effect on the translation of luciferase mRNA when compared to control (Fig. 4.15B), underlining the specific regulatory effect of G3BP1 on the translation of  $\beta$ -mRNA. Overall, these results support the idea that G3BP1 represents a negative regulator of the translation of  $\beta$ -mRNA.

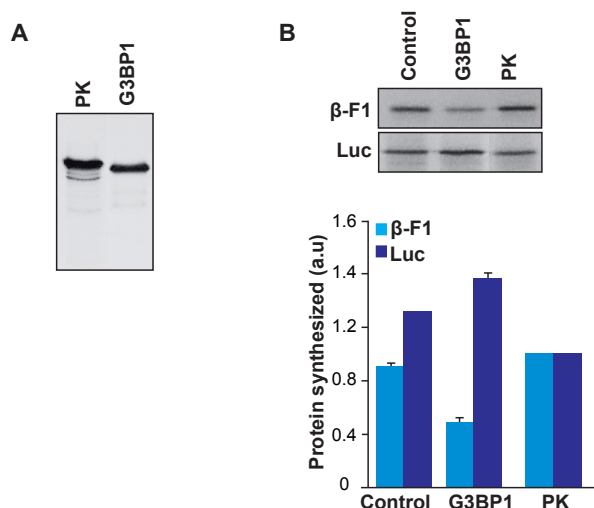


**Figure 4.15: G3BB1 inhibits translation of  $\beta$ -mRNA *in vitro*.** (A) G3BP1 and pyruvate kinase (PK) were synthesized in a cell-free system. The fluorography shows an aliquot of the *in vitro* synthesis. (B) *In vitro* translation of  $\beta$ -mRNA and luciferase (Luc) mRNA using rabbit reticulocyte lysate in the absence (control) or presence of equivalent amounts of PK and G3BP1. The histogram shows the mean  $\pm$  SEM of the quantification of the bands normalized to the mean value in the presence of PK.

Over-expression and silencing of NPM1 and IMP1 did not affect the expression of  $\beta$ -mRNA and the rates of  $\beta$ -F1-ATPase synthesis (data not shown), supporting the lack of functional roles for IMP1 and NPM1 in post-transcriptional expression of  $\beta$ -F1-ATPase.

#### 4.2.5 G3BP1 inhibits translation initiation of $\beta$ -mRNA

Next, we pursued the characterization of the mechanism by which G3BP1 interferes with the translation of  $\beta$ -mRNA. For this purpose, we analyzed the interaction of the  $\beta$ -mRNA with the translational machinery using sucrose-density gradient centrifugation under the same conditions as for *in vitro* translations (Fig. 4.15). Interestingly, the presence of G3BP1 caused a shift of a great part of  $\beta$ -mRNA into the less dense region of the gradient, preventing its recruitment into the 80S complex (Fig. 4.16). Contrary, the absence of G3BP1 (control) or presence of PK allowed the assembly of  $\beta$ -mRNA into the 80S complex (Fig. 4.16). These results indicate that G3BP1 could act as a negative regulator of  $\beta$ -F1-ATPase expression by interfering with the initiation step of  $\beta$ -mRNA translation.

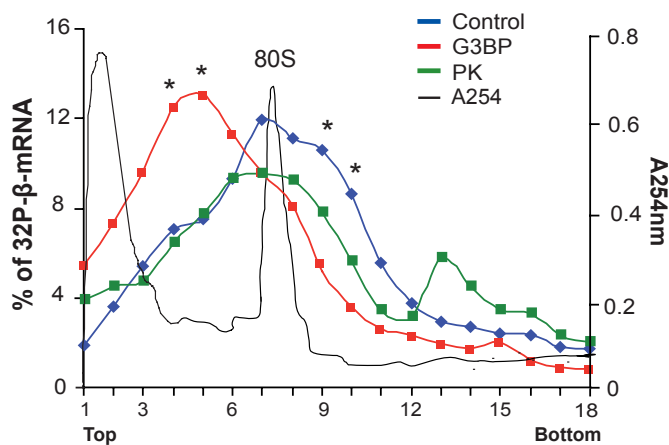


**Figure 4.16: G3BB1 inhibits translation initiation of  $\beta$ -mRNA.**  $^{32}$ P-labeled  $\beta$ -mRNA was incubated as in Fig. 4.15 and further fractionated on 15-40% sucrose gradients. The radioactivity recovered in each fraction is represented as percentage of the total. Red (G3BP1), blue (control) and green (PK) graphs show the mean value of four independent experiments. \*,  $p < 0.05$  statistical significance of  $\beta$ -mRNA fractionation in the presence of G3BP1 compared with its absence (control, PK) using Student's t-test. Black continuous line illustrates absorbance at 254 nm. Top, bottom and fractions of the sucrose gradient as well as migration of the 80S monosome are indicated.



### 4.3 THE RELEVANCE OF G3BP1 IN HUMAN BREAST CANCER

We have demonstrated that G3BP1 interacts with  $\beta$ -mRNA and inhibits its translation. At the same time previous studies have shown that G3BP1 is over-expressed in several human cancer cell lines as well as in breast and head and neck tumors (Barnes et al., 2002; French et al., 2002; Guitard et al., 2001), suggesting that G3BP1 might be a relevant factor in controlling the down-regulation of the mitochondrial protein in human cancer and thus could be partially responsible for the distinctive bioenergetic phenotype that characterize most human neoplasias (Cuezva et al., 2002; Isidoro et al., 2004).

#### 4.3.1 G3BP1 is a marker of breast cancer progression

A first step was to analyze the expression of G3BP1 in tumor and normal biopsies derived from the same cancer patients operated from breast, colon and lung adenocarcinomas as well as from squamous lung carcinomas. Previous studies indicated that the relative  $\beta$ -F1-ATPase expression in these human carcinomas is regulated at post-transcriptional levels (4.1 and Willers et al., 2010). We observed that the steady state level of G3BP1 in colon and lung carcinomas was not significantly different from paired normal tissues (Fig. 4.17 A and B). In contrast, expression of G3BP1 was increased in 7 out of 8 human breast tumor patients analyzed when compared to normal tissue, although this difference did not reached the level of statistical significance (Fig. 4.17A and B). The latter finding supports previous studies that have demonstrated by western blot and immunohistochemistry the over-expression of G3BP1 in human breast carcinomas (Guitard et al., 2001; Barnes et al., 2002; French, et al.,2002).

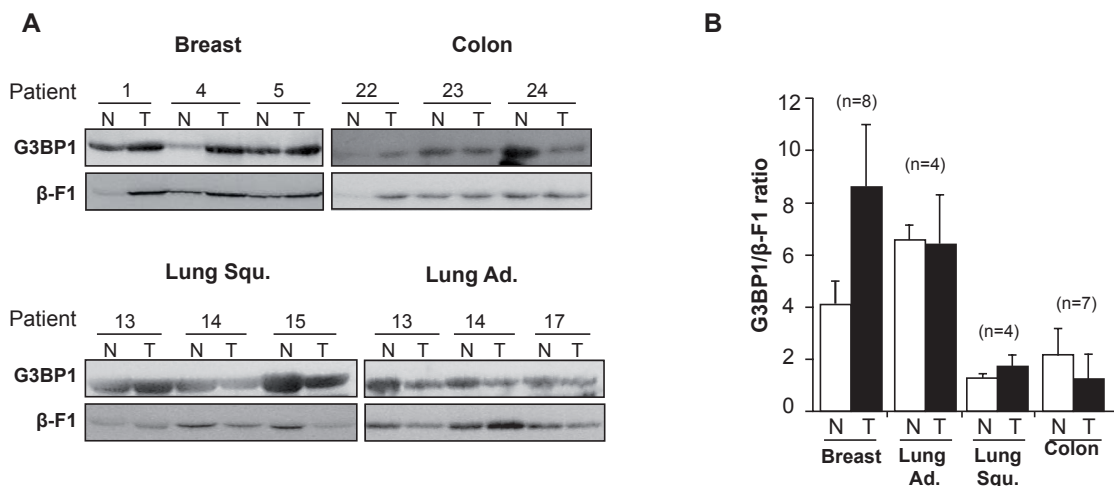


**Figure 4.17: G3BP1 is over-expressed in human breast cancer.** (A) Expression of G3BP1 and  $\beta$ -F1-ATPase ( $\beta$ -F1) were analyzed by immunoblotting in normal (N) and tumor (T) tissue biopsies derived from the same patients of breast, colon, lung adenocarcinomas (Ad.) and squamous (Squ.) lung carcinomas. Representative examples obtained from 3 patients are shown. (B) The histogram shows the means  $\pm$  SEM of the quantification of the G3BP1/ $\beta$ -F1 ratio. The number of patients analyzed is indicated in brackets.

To analyze the relationship that might exist between G3BP1 and the bioenergetic phenotype of breast cancer, we determined the expression level of G3BP1 in a cohort of 93 breast tumor samples (Table A2 in the Appendix), in which the bioenergetic signature was previously analyzed and for which the clinicopathological characteristics as well as follow-up data are available (Isidoro et al., 2005; Ortega et al., 2008). The previous study demonstrated that a profound shift towards an enhanced glycolytic phenotype occurs in breast cancer concurrent with down-regulation of the expression of  $\beta$ -F1-ATPase (Isidoro et al., 2005). Furthermore, the alteration of the bioenergetic phenotype was associated with the progression of the disease (Isidoro et al., 2005).

In agreement with the down-regulation of  $\beta$ -F1-ATPase by G3BP1 (Fig. 4.14 and 4.15) a significant inverse correlation was observed between the expression of G3BP1 and  $\beta$ -F1-ATPase in breast cancer samples ( $R=-0.2172$ ,  $p=0.041$ ). Consistently, Kaplan-Meier survival analysis showed that patients with a high expression of G3BP1 have both a significant greater chance of disease recurrence (Fig. 4.18A) and worse overall prognosis (Fig. 4.18B), even though the latter did not reach the level of statistical significance. Univariate Cox survival analysis (Table A3 in the Appendix) revealed that a high expression of G3BP1 is associated with a two-fold higher risk of death (HR= 2.4 CI: 0.83-6.92,  $p=0.094$ ) and relapse of the tumor (HR=2.05 CI: 0.98-4.32,  $p=0.058$ ), further emphasizing that a high expression of G3BP1 is associated with breast tumor progression.

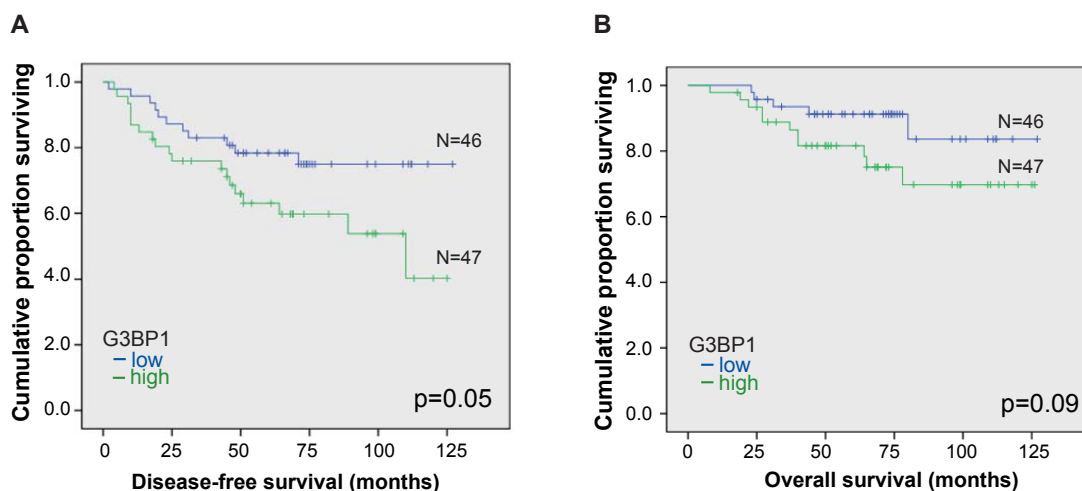


**Figure 4.18: A high expression of G3BP1 predicts a worse prognosis in human breast cancer patients.** Kaplan-Meier (A) disease-free survival and (B) overall survival analysis in 93 breast cancer patients. G3BP1 was dichotomized by the median in high (green) and low (blue) G3BP1 expression levels. N indicates the number of patients in each group. p-value as determined by log-rank test.

Interestingly, it was observed that both the 5 year overall (OS) and disease-free survival (DFS) in low risk patients, as assessed by the bioenergetic phenotype of the tumor (L+M groups in Fig. 1 in Isidoro et al., 2005), was significantly reduced if G3BP1 expression was high (L+M in Table 4 and Table 5). These results were confirmed by unsupervised hierarchical cluster presentation of G3BP1 and the cellular bioenergetic signature ( $\beta$ -F1/GAPDH ratio) (Fig. 4.19A) of the low risk patients (L+M). This analysis discriminated the patients into two main groups C1 and C2 differing in the

Parameter	G3BP1	N (%)	Events	OS 5 years (proportion)	SEM	95% CI	p
Nodes 0-3	Low	38 (51)	2	0.95	0.04	0.87-1.03	0.083
	High	37 (49)	7	0.89	0.06	0.74-1.01	
Stage I + II	Low	37 (52)	2	0.94	0.04	0.86-1.02	0.111
	High	34 (48)	6	0.88	0.06	0.76-1.00	
Grade 1 + 2	Low	20 (56)	1	0.94	0.06	0.82-1.06	0.346
	High	16 (44)	0				
L+M	Low	27 (53)	1	0.96	0.04	0.88-1.04	<b>0.029</b>
	High	24 (47)	6	0.86	0.08	0.70-1.02	

**Table 4: Univariate overall survival analysis of patients stratified by tumor expression of G3BP1.** Breast cancer patients with good prognosis as assessed both by clinical and molecular marker (L+M) were selected to study the association of G3BP1 expression and patients outcome by Kaplan-Meier overall survival (OS) analysis. The molecular marker L+M identifies the patients with less alteration of the bioenergetic signature when compared to normal biopsies (Isidoro et al., 2005). Low and high expression of G3BP1 is referred to the dichotomization by the median of G3BP1 expression. N (%), number and percentage of patients in each group. Events, number of patients dead in each group. OS 5 years, cumulated proportion of patients with 5 year overall survival with the standard error of the mean (SEM) and the 95% confidence interval (CI). p-value was determined by log-rank test, in bold if p<0.05.

Parameter	G3BP1	N (%)	Events	DFS 5 years (proportion)	SEM	95% CI	p
Nodes 0-3	Low	38 (51)	7	0.81	0.06	0.69-0.92	0.088
	High	37 (49)	13	0.68	0.08	0.52-0.84	
Stage I + II	Low	37 (52)	7	0.81	0.07	0.67-0.95	0.174
	High	34 (48)	11	0.72	0.08	0.56-0.88	
Grade 1 + 2	Low	20 (56)	3	0.85	0.08	0.69-1.01	0.509
	High	16 (44)	4	0.86	0.09	0.68-1.04	
L+M	Low	27 (53)	5	0.81	0.08	0.65-0.97	<b>0.009</b>
	High	24 (47)	12	0.47	0.12	0.23-0.71	

**Table 5: Univariate disease-free survival analysis of patients stratified by tumor expression of G3BP1.** Breast cancer patients with good prognosis as assessed both by clinical and molecular markers (L+M) were selected to study the association of G3BP1 expression and patient's outcome by Kaplan-Meier disease-free survival (DFS) analysis. The molecular marker L+M identifies the patients with less alteration of the bioenergetic signature when compared to normal biopsies (Isidoro et al., 2005). Low and high expression of G3BP1 is referred to the dichotomization by the median of G3BP1 expression. N (%), number and percentage of patients in each group. Events, number of patients with recurrence of disease in each group. DFS 5 years, cumulated proportion of patients with 5 years distant disease-free survival with the standard error of the mean (SEM) and the 95% confidence interval (CI). p-value was determined by log-rank test, in bold if p<0.05.

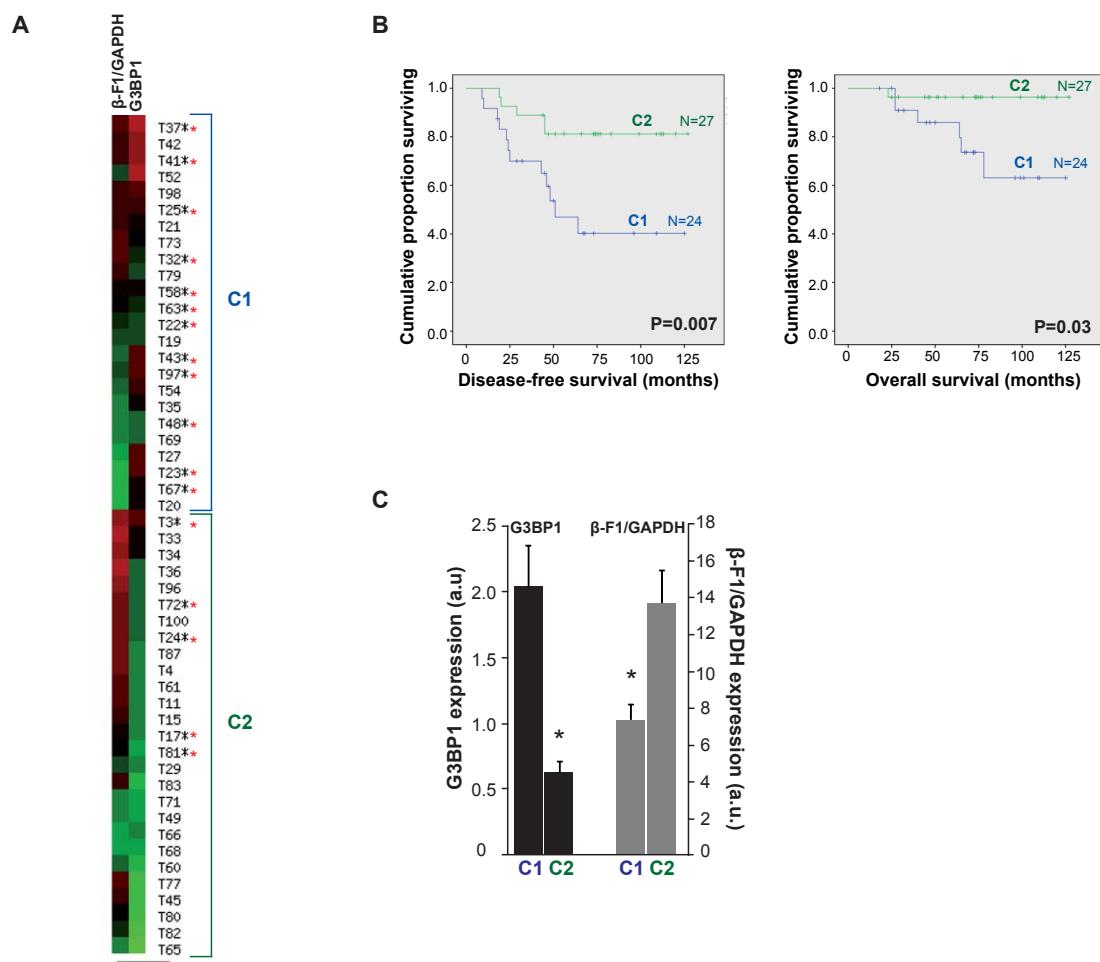


**Figure 4.19: Expression of G3BP1 in good prognosis patients defines a group of patients with higher probability of developing metastasis.** (A) Unsupervised hierarchical cluster analysis (<http://ep.ebi.ac.uk/EP/EPCLUST> using Euclidean distances and average linkage method) of G3BP1 and the cellular bioenergetic signature ( $\beta$ -F1/GAPDH) in 51 low risk breast tumor patients as assessed by the bioenergetic signature (see L+M groups in Fig.1 in Isidoro et al., 2005). Rows, samples; columns, markers. Color scale: red, high; black, normal and green, low. The dendrogram represents overall similarities in the expression profiles providing two clusters C1 and C2 differing in the expression of G3BP1 and the bioenergetic signature ( $\beta$ -F1/GAPDH). Red asterisks identify the patients who developed metastasis. (B) Kaplan-Meier disease-free and overall survival analysis of C1 and C2 patients. p-value as determined by log-rank test. N indicates the number of patients in each group. (C) The histogram shows the mean  $\pm$  SEM of the relative expression level of G3BP1 and  $\beta$ -F1/GAPDH ratio in clusters C1 and C2. \*, p<0.05 by Student's t-test.

bioenergetic signature and the level of G3BP1 expression (Fig. 4.19A and C). C1 is characterized by higher levels of G3BP1 expression, whereas C2 exhibits low G3BP1 expressions (Fig. 4.19C). The analysis indicated that the patients with a high expression of G3BP1 (C1) have a lower bioenergetic signature (Fig. 4.19C) and a higher probability to develop metastatic disease (red asterisk in Fig. 4.19A). Kaplan-Meier analysis confirmed the risk differences between C1 and C2 patients in both OS and DFS (Fig. 4.19B).

In agreement with other studies (French et al., 2002; Guitard et al., 2001; Zhang et al., 2007c) no significant differences and correlations were found between G3BP1 expression and clinicopathological parameters of breast tumors (Table A4 in the Appendix).

## Results

Univariate Cox regression analysis (Table A3 in the Appendix) and Kaplan-Meier DFS analysis (Table A5 in the Appendix) demonstrated that nodal affectation, the clinical state and the histological grade are the clinicopathological parameters that are significantly associated with the progression of breast cancer. Furthermore, previous studies analyzing the same cohort of breast cancer patients demonstrated, that in addition to the clinicopathological parameters, the expression of HuR, GAPDH and a subset of 17 patients with an abnormal high expression of  $\beta$ -F1-ATPase ( $\beta$ -cluster) are molecular variables associated with progression of the disease (Isidoro et al., 2005; Ortega et al., 2008) (Table A3 and Table A5 in the Appendix).

We performed multivariate Cox regression survival analysis including G3BP1, the molecular markers and only one clinopathological variable, because nodal status, clinical stage and histological grade are not independent variables (Isidoro et al., 2005; Ortega et al., 2008). The analysis revealed that G3BP1 is a significant independent prognostic marker of DFS when it is subjected to a multivariate

Disease-free survival			
	Parameter	HR (95% CI)	p
Clinicopathological	G3BP1	1.90 (0.90-4.01)	0.0911
	Stage II	2.85(0.65-12.42)	0.1642
	Stage III	6.59 (1.47-29.63)	<b>0.0139</b>
	G3BP1	3.09 (1.36-7.02)	<b>0.0069</b>
	Grade 3	3.26 (1.35-7.87)	<b>0.0085</b>
	G3BP1	1.79 (0.83-3.83)	0.1367
	Nodes 1-3	2.27 (0.91-5.69)	0.0785
	Nodes >3	4.19 (1.64-10.69)	<b>0.0027</b>
	Molecular	G3BP1	3.40 (1.51-7.64)
GAPDH		2.33 (1.10-4.92)	<b>0.027</b>
$\beta$ -cluster		4.35 (1.88-10.07)	<b>0.001</b>
G3BP1		1.63 (0.66-4.21)	0.308
GAPDH		2.43 (1.02-5.80)	<b>0.046</b>
$\beta$ -cluster		3.78 (1.55-9.21)	<b>0.003</b>
HuR		2.95(1.16-7.42)	<b>0.023</b>
Molecular and clinicopathological	G3BP1	4.77 (1.95-11.70)	<b>0.001</b>
	GAPDH	2.63 (1.06-5.28)	<b>0.036</b>
	$\beta$ -cluster	4.05 (1.64-10.02)	<b>0.002</b>
	Grade 3	2.77 (1.15-6.27)	<b>0.024</b>
	G3BP1	2.01 (0.75-5.71)	0.160
	GAPDH	2.84 (1.10-7.31)	<b>0.031</b>
	$\beta$ -cluster	2.94 (1.06-8.15)	<b>0.039</b>
	HuR	4.41 (1.54-12.61)	<b>0.006</b>
	Grade 3	2.57 (0.93-7.04)	0.068

**Table 6: Multivariate disease-free survival analysis.** Proportional multivariate Cox regression analyses were performed in combination with different clinicopathological as well as with the molecular markers (GAPDH,  $\beta$ -cluster, HuR and G3BP1) shown to be significant in univariate analysis (Table A3). The hazard ratio (HR) and the 95% confidence interval (95% CI) are shown. The p-value indicates the independence of each co-parameter as a prognostic marker and was determined by Wald test, in bold when  $p < 0.05$ .

analysis with the histological grade as well as the molecular markers GAPDH and  $\beta$ -cluster (Table 6). Interestingly, when a multivariate Cox survival analysis is performed combining the molecular markers (G3BP1, HuR,  $\beta$ -cluster and GAPDH) with or without the significant independent clinicopathological variable Grade 3, it turns out that the significance of G3BP1 is lost when HuR is included in the analysis (Table 6). This finding could indicate that there might be a functional relationship between the RNABPs, G3BP1 and HuR. Within this context it is noteworthy that HuR and G3BP1 significantly correlate inversely with each other ( $R=-0.3382$ ,  $p=0.0019$ ), what is consistent with the fact that contrary to the high expression of G3BP1 (Fig. 4.18) a low expression of HuR is an independent marker of breast prognosis predicting a higher risk of disease recurrence (Ortega et al., 2008). In conclusion, these findings demonstrate that a high expression of G3BP1 predicts a higher risk of disease recurrence in breast cancer patients and supports its usage as an additional prognostic marker further providing a potential target for future anticancer therapies.

#### **4.4 THE ROLE OF miRNAs AS POST-TRANSCRIPTIONAL REGULATORS OF $\beta$ -F1-ATPase EXPRESSION**

To date our laboratory has concentrated most efforts in finding and identifying proteins that could be involved in the control of  $\beta$ -mRNA translation. In recent years, however, it has become apparent that also miRNAs play an important role in post-transcriptional regulation of mRNA expression. Generally, miRNAs regulate gene expression by imperfectly base pairing to the 3'-UTR of target mRNAs inhibiting protein synthesis or inducing the degradation of the target mRNAs (Filipowicz et al., 2008). MicroRNAs are involved in almost all cell physiological processes, and their aberrant expression has been related to human pathologies including cancer (Garzon et al., 2009). Because the expression of  $\beta$ -F1-ATPase has been shown to be post-transcriptional regulated during development of the liver (Izquierdo and Cuezva, 1997; Izquierdo et al., 1995; Luis et al., 1993), progression through the cell cycle (Martinez-Diez et al., 2006) and in carcinogenesis (de Heredia et al., 2000; Willers et al., 2010) by mechanism that affect the subcellular localization, the stability and translation of the transcript, we questioned whether miRNAs might also be involved in controlling  $\beta$ -F1-ATPase expression.

##### **4.4.1 *In silico* approach to identify miRNA candidates that might be involved in $\beta$ -F1-ATPase expression**

In order to identify miRNAs that could bind to the 3' UTR of the human  $\beta$ -mRNA and might influence the bioenergetic activity of mitochondria, we have performed a bioinformatic study using the available online miRNA target prediction software TargetScan5.1 (<http://www.targetscan.org/>). The target prediction algorithm of TargetScan is essentially based on a few binding rules that were established according to previous experimental and bioinformatic data (Brennecke et al., 2005; Grimson et al., 2007; Lewis et al., 2005). The most important requirement seems to be a contiguous and perfect Watson-Crick base pairing of the 5'-miRNAs "seed" region (nucleotides 2-8), providing

## Results

most of the pairing specificity (Fig. 4.20A). Matching of the mRNA to the miRNA seed can be divided into 8mer sites, 7mer sites and 6mer sites, that differ in their effectiveness of miRNA action (Fig. 4.20A) (Grimson et al., 2007). In addition, an A residue at position 1 (7mer-A1) and an A or U at position 9 of the miRNA improves the miRNA activity. Complementarity to the 3' region of the miRNA, usually occurring to the miRNA nucleotides 13-16, is not necessary but supports the miRNA-mRNA interaction, in particular if the interaction in the seed region is not perfect (Fig. 4.20A). Generally, the central region at miRNA position 10-12 contains mismatches forming a bulge in the miRNA-mRNA duplex (Fig. 4.20A) (Brennecke et al., 2005; Grimson et al., 2007; Lewis et al., 2005). In addition to these binding rules, miRNAs that were conserved among different species were preferentially selected, and we pursued to cover the whole 3'UTR of  $\beta$ -mRNA. Overall, the *in silico* study provided miR-101, miR-103, miR-127-5p, miR-186, miR-200b, miR-423-5p and miR-581 as the strongest candidates which were chosen for subsequent *in vivo* studies (Fig. 4.20B).

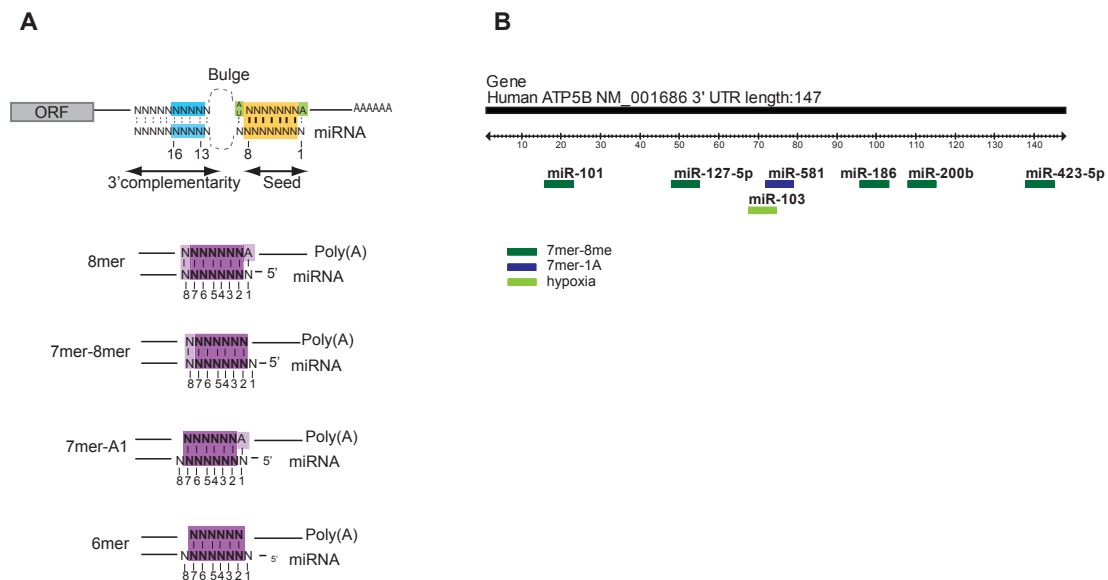


**Figure 4.20: miRNAs that are predicted to bind to the 3'UTR of human  $\beta$ -F1-ATPase.** (A) Schematic illustration of miRNA binding to target mRNA. The miRNA target mRNA pairing in the seed region (2-7 nucleotides, highlighted in yellow) is usually perfect and contiguous. An A or U nucleotide (shown in green) at position 9 or an A-residue (shown in green) at position 1 of the miRNA improves the site efficiency. miRNA binding to the mRNA exhibits generally bulges and mismatches in the central region. Complementarity to the 3' region (particularly residues 13-16, blue) becomes important when matching in seed region is suboptimal. The complementary seed binding can be divided into four preferential subtypes: 8mer, 7mer-8mer, 7mer-A1 and 6mer sites. (Figure adapted from Grimson et al.; 2007) (B) Schematic illustration of the 3'UTR of  $\beta$ -mRNA along with the miRNAs that have been predicted to bind to the 3'UTR of the transcript. Binding sites and types of the miRNAs are indicated. The light green miR-103 is none of the indicated binding types, but was involved in the study for the putative relevance that hypoxia might play in regulation of  $\beta$ -F1-ATPase expression

#### 4.4.2 Generation of stable cell lines expressing p $\beta$ GFP-3' $\alpha$ and p $\beta$ GFP-3' $\beta$

First of all, and in order to analyze the influence of miRNAs on the translation of  $\beta$ -F1-ATPase, we generated cell lines that stably express a GFP reporter bearing either the 3'UTR of the  $\alpha$ - or  $\beta$ -F1-ATPase mRNA. The pre-sequence of the  $\beta$ -F1-ATPase (p $\beta$ ) was fused in frame upstream of GFP to localize the protein into the mitochondria (Martinez-Diez et al., 2006). For generation of the stable cell lines we have chosen the breast cancer cell line BT549 and the colon cancer cell line HCT116, because in those tumor tissues expression of  $\beta$ -F1-ATPase has been shown to be post-transcriptional regulated (Fig. 4.1).

Analysis of the BT549 cell clones by flow cytometry demonstrated that the selected p $\beta$ GFP-3' $\alpha$  clones ( $\alpha$ 2 and  $\alpha$ 4) and p $\beta$ GFP-3' $\beta$  clones ( $\beta$ 2 and  $\beta$ 10) have a very high purity (>98%) and a well defined and unique peak of GFP fluorescence (Fig. 4.21A). In contrast, the stable cell clones  $\beta$ 8 and  $\beta$ 9 displayed a wide range of GFP intensity (Fig. 4.21A), indicating that they do not derive from one single clone. Therefore, in the following studies we have used clones BT549:p $\beta$ GFP-3' $\beta$ 2 and  $\beta$ 10. The stable HCT116 cell lines expressing p $\beta$ GFP-3' $\alpha$  or  $\beta$  exhibited also a high grade (>98%) of purity and showed narrow as well as nearly identical peaks of GFP fluorescence (Fig. 4.22A).

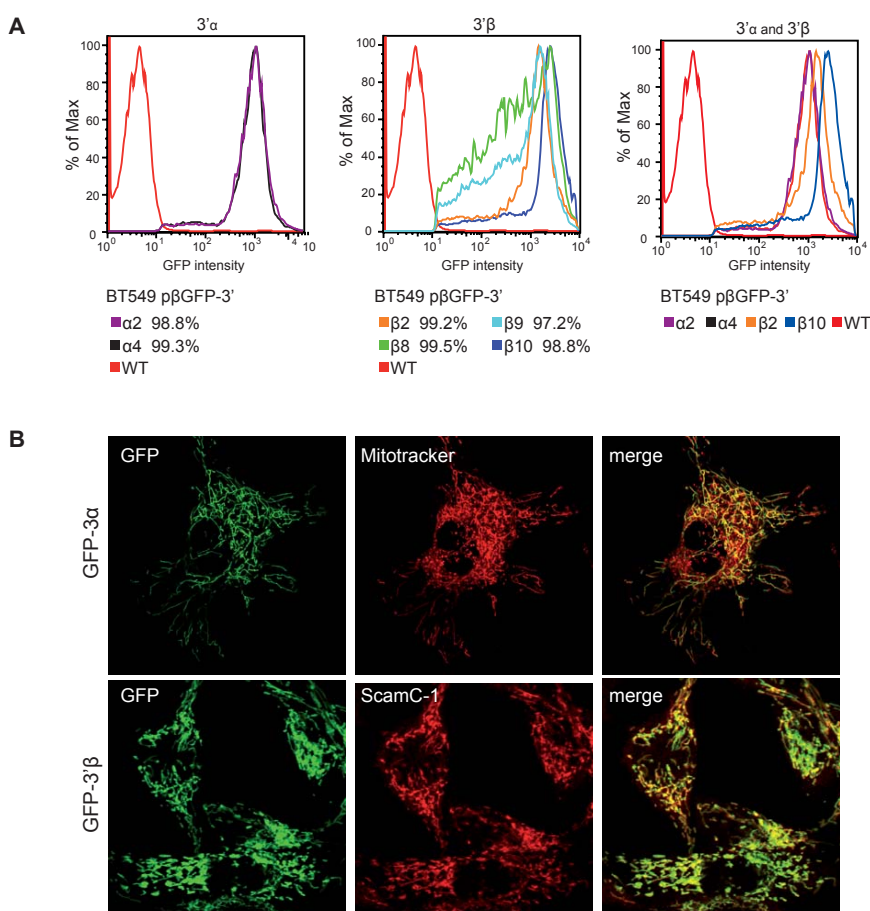


**Figure 4.21: Analysis of stable BT549:p $\beta$ GFP-3' $\beta$  and BT549:p $\beta$ GFP-3' $\alpha$  cell lines.** (A) Analysis of GFP fluorescence by flow cytometry in BT549 clones that stably express mitochondrial GFP fused to the 3'UTR of human  $\beta$ -F1-ATPase (clone  $\beta$ 2,  $\beta$ 8,  $\beta$ 9 and  $\beta$ 10) or to the 3'UTR of the partner  $\alpha$ -F1-ATPase subunit (clone  $\alpha$ 2 and  $\alpha$ 4). The percentage of GFP expressing cells is indicated. (B) A representative example of immunofluorescence of a BT549:p $\beta$ GFP-3' $\alpha$  (upper panel, GFP-3' $\alpha$ ) and BT549:p $\beta$ GFP-3' $\beta$  (lower panel, GFP-3' $\beta$ ) cell lines illustrates the mitochondrial localization of GFP using ScamC-1 and MitotrackerRed as a mitochondrial marker. WT, wild type.



## Results

In both cell lines the mitochondrial localization of GFP was confirmed by immunofluorescence microscopy using MitotrackerRed or anti-ScamC-1 (del Arco and Satrustegui, 2004) as a mitochondrial marker (Fig. 4.21B and 4.22B).

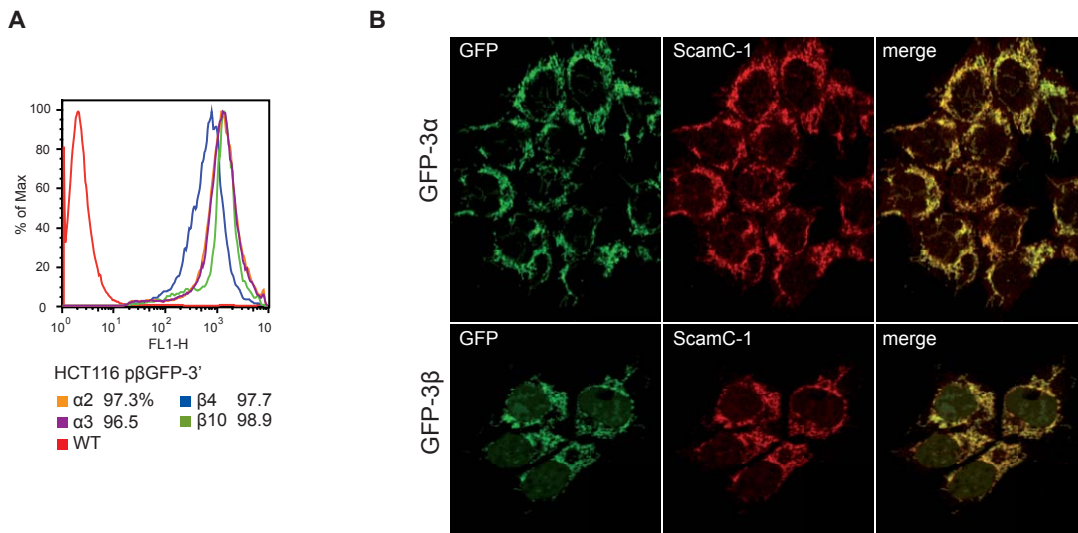


**Figure 4.22: Analysis of stable HCT116:pβGFP-3'β and HCT116:pβGFP-3'α cell lines.** (A) Analysis of GFP fluorescence by flow cytometry in HCT116 clones that stably express mitochondrial GFP fused to the 3'UTR of human β-F1-ATPase (clone β4 and β10) or to the 3'UTR of the partner α-F1-ATPase subunit (clone α2 and α3). The percentage of GFP expressing cells is indicated. (B) A representative example of immunofluorescence of a HCT116:pβGFP-3'α (upper panel, GFP-3'α) and HCT116:pβGFP-3'β (lower panel, GFP-3'β) cell lines illustrates the mitochondrial localization of GFP using ScamC-1 as a mitochondrial marker. WT, wild type.

Importantly, in both cell lines (BT549 and HCT116) the relative protein level of GFP derived from pβGFP-3'β did not differ from pβGFP-3'α (Fig. 4.23A and B), even though in both cell lines the relative steady state level of pβGFP-3'β mRNA exhibited approximately a two-fold increase when compared to the amount of the pβGFP-3'α mRNA (Histogram in Fig. 4.23A and B). The higher cellular availability of pβGFP-3'β mRNA suggests that the β-3'UTR might either increase the stability of the transcript or its rate of transcription when compared to the α-3'UTR. Furthermore,

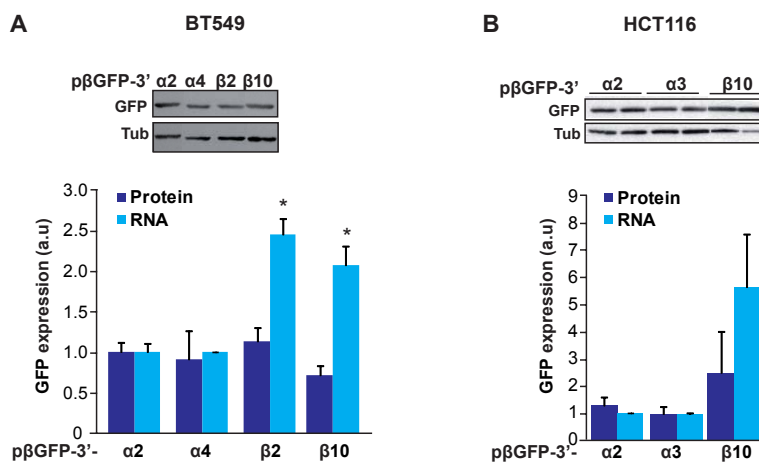


**Figure 4.23: Expression level of GFP in BT549 and HCT116 clones.** Protein extracts of (A) BT549 and (B) HCT116 clones stably expressing either pβGFP-3'α (GFP fused to the 3'UTR of human α-F1-ATPase) or pβGFP-3'β (GFP fused to the 3'UTR of human β-F1-ATPase) were analyzed by western blot using monoclonal anti-GFP antibody and anti-tubulin antibody (Tub) to normalize GFP expression. A representative western blot is shown. The histogram in A and B

summarizes the quantification of the relative steady state level of GFP (dark blue bars, relative to tubulin) and GFP mRNA (light blue bars, relative to GAPDH mRNA) expression. The data were normalized with respect to α2 in A and α3 in B. Expression of GAPDH mRNA was used as an internal control. The results shown are the means ± SEM. \*, p<0.05 when compared to GFP protein level by Student's t test.

the result suggests that the *in vivo* synthesis of ectopically expressed p $\beta$ GFP-3 $\beta$  mRNA is also controlled at the translation level, what is in agreement with previous findings of our laboratory (Ortega et al., 2010 and data not shown).

#### 4.4.3 miR-127-5p is identified as a potential regulator of $\beta$ -F1-ATPase expression in a screening for miRNAs in BT549 cells

In order to identify in a cellular context, which miRNA might be relevant in controlling  $\beta$ -F1-ATPase translation and therefore in triggering changes in the bioenergetic phenotype of the cell, we carried out miRNA over-expression and silencing experiments. To this aim, the stable BT549:p $\beta$ GFP-3' $\beta$  (clones  $\beta$ 2 and  $\beta$ 10) and BT549:p $\beta$ GFP-3' $\alpha$  cell lines (clone  $\alpha$ 4) were transfected with miRNA precursors and anti-miRNAs (complementary to the mature miRNA) to respectively over-express and silence the expressed miRNAs. Changes in expression of the GFP reporters were measured by determining the relative GFP fluorescence intensity of the cell. The study revealed that from all the miRNAs studied only miR-127-5p triggered a significant decrease in the expression of p $\beta$ GFP-3' $\beta$ 2 and  $\beta$ 10 when compared to p $\beta$ GFP-3' $\alpha$ 4 and the cells transfected with a non-relevant miRNA

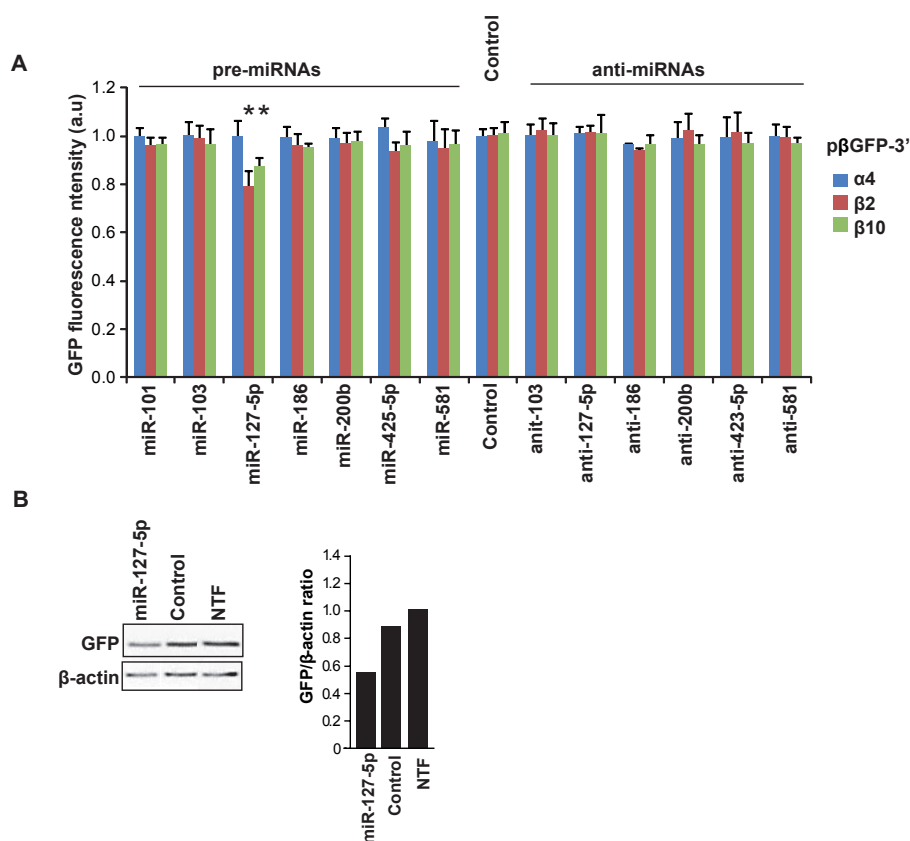


**Figure 4.24: Screening for miRNAs that affect expression of p $\beta$ GFP-3' $\beta$  in BT549 cells.** (A) GFP fluorescence intensity of p $\beta$ GFP-3' $\beta$  (clon  $\beta$ 2, red bars; clon  $\beta$ 10, green bars) was determined after 48 h of transfection with the indicated anti-miRNAs and pre-miRNAs using a fluorescence luminometer. Data were normalized with respect to the number of cells as determined by Hoescht fluorescence intensity, and quantified relative to the mean GFP fluorescence of control cells transfected with a non-relevant miRNA. The fluorescence intensity of BT549 cells stably expressing p $\beta$ GFP-3' $\alpha$  (clone  $\alpha$ 4, blue bars) was used as an additional control. The results shown are the means  $\pm$  SEM of three independent experiments. \*,  $p < 0.05$  when compared to p $\beta$ GFP-3' $\alpha$  level by Student's t test. (B) Western blot of BT549:p $\beta$ GFP-3' $\beta$ 2 cells non-transfected (NTF) or transfected with pre-miR-127-5p and a scramble miRNA (control) using anti-GFP and anti- $\beta$ -actin antibodies. The histogram displays the quantification of p $\beta$ GFP- $\beta$ 2 relative to  $\beta$ -actin.

## Results

(control) (Fig. 4.24A). Western blot analysis of transfected BT549:p $\beta$ GFP-3'UTR cells confirmed the reduced GFP reporter level in the presence of miR-127-5p (Fig. 4.24B). Notably, anti-miR-127-5p expression had no effect on the fluorescence intensity of p $\beta$ GFP-3'UTR (Fig. 4.24A).

In order to determine a possible effect of these miRNAs on the bioenergetic activity of the mitochondria, we examined the oxygen consumption rate (OCR) in the parental BT549 cell line in the presence of pre- and anti-miRNAs (Fig. 4.25A). Silencing of miR-103 (anti-103) triggered a significant increase in both the basal and oligomycin sensitive respiration (OSR) of the cells when compared to mock transfected cells (control) (Fig. 4.25A). This finding suggests that miR-103, although it does not affect  $\beta$ -F1-ATPase expression (Fig. 4.24A), in some way is involved in hampering the bioenergetic activity of mitochondria in BT549 cancer cells. Surprisingly, miR-127-5p expressing cells (Fig. 4.25A) did not reveal changes in both basal and OSR when compared to control cells.

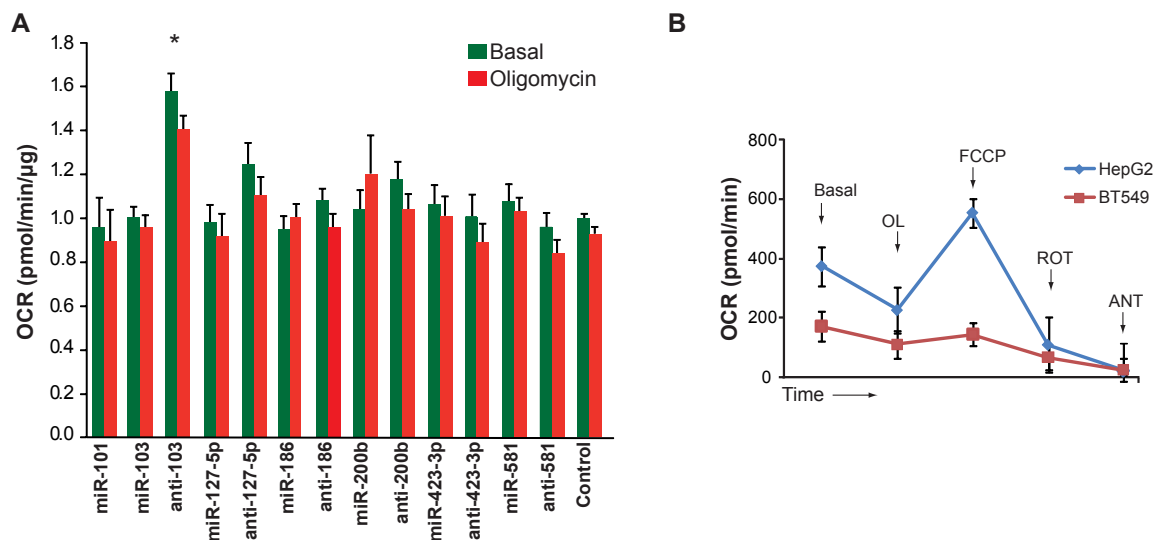


**Figure 4.25: Analysis of the oxygen consumption rate after over-expression and silencing of miRNAs.** (A) Seahorse Bioscience extracellular flux analyzer was used to measure the oxygen consumption rate (OCR) of BT549 cells transfected with miRNA precursors (miR-), anti-miRNAs and scramble miRNAs (control) before (basal, green bars) and after addition of oligomycin (red bars). The miRNA used are indicated. The results shown are the means  $\pm$  SEM of 4 independent experiments relative to mock transfected cells after 72 h of transfection. \*,  $p < 0.05$  when compared to control by Student's t test. (B) Oxygen consumption rate (OCR) of HepG2 (blue line) and control-miRNA transfected BT549 cells (red line) without (Basal) and after addition of 6  $\mu$ M oligomycin (OL), 1  $\mu$ M FCCP, 1  $\mu$ M rotenone (ROT) and 1  $\mu$ M antimycin A (ANT). The OCR profile of a representative experiment is shown.

In this regard, it should be noted that the OCR profile of mock BT549 transfected cells in the presence of regulators of OXPHOS such as oligomycin, FCCP, rotenone and antimycin hardly changed and responded to the added drugs (Fig. 4.25B). This finding is at variance with the OCR profile displayed by the human liver cancer HepG2 cell line (Fig. 4.25B), indicating that the OXPHOS activity in the breast cancer cell line BT549 is almost obliterated. Indeed, studies of our laboratory analyzing the metabolic activity of different cancer cell lines of the NCI-60 panel demonstrated that breast cancer cells had a significant higher glycolytic flux than any other examined cell line. Therefore, it is tempting to suggest that the bioenergetic phenotype of BT549 cells could not be converted to be more glycolytic through a miR-127-5p mediated down-regulation of  $\beta$ -F1-ATPase.

#### 4.4.4 miR-127-5p binds to the 3'UTR of $\beta$ -mRNA and inhibits its translation

Next, we questioned about the inhibitory effect of miR-127-5p on the expression of endogenous  $\beta$ -F1-ATPase. Transfection of miR-127-5p precursors in parental BT549 cells provoked a significant decrease in the expression of  $\beta$ -F1-ATPase when compared to mock transfected cells (Fig. 4.26A, B). Furthermore, the relative expression level of the  $\beta$ -F1-ATPase was restored to that of control cells when miR-127-5p expression was silenced by co-transfection with the anti-miR-127-5p (Fig. 4.26B yellow bar). However, and concurrent with the aforementioned results (Fig. 4.24A) silencing of miR-127-5p has no effect on the synthesis of  $\beta$ -F1-ATPase (Fig. 4.26B green bar).

To verify that the observed decreased  $\beta$ -F1-ATPase level is due to a specific binding of the miR-127-5p to its binding site in the 3' UTR of the  $\beta$ -mRNA, we generated a mutated p $\beta$ GFP-3' $\beta$  version (p $\beta$ GFP-3' $\beta$ MUT) that contains 4 point mutations in miR-127-5p binding region (Fig. 4.26C). BT549 cells were co-transfected with miR-127-5p and p $\beta$ GFP-3' $\beta$  or p $\beta$ GFP-3' $\beta$ MUT, and the GFP fluorescence intensity was analyzed by flow cytometry (Fig. 4.26D). The analysis confirmed the 50% reduced expression of p $\beta$ GFP-3' $\beta$  by miR-127-5p, whereas expression of the mutated GFP reporter was not affected (Fig. 4.26D). Similar results were obtained by western blot analysis (Fig. 4.26D). Together, these results illustrate that miR-127-5p binds directly to the 3'UTR of  $\beta$ -mRNA and inhibits the expression of  $\beta$ -F1-ATPase.

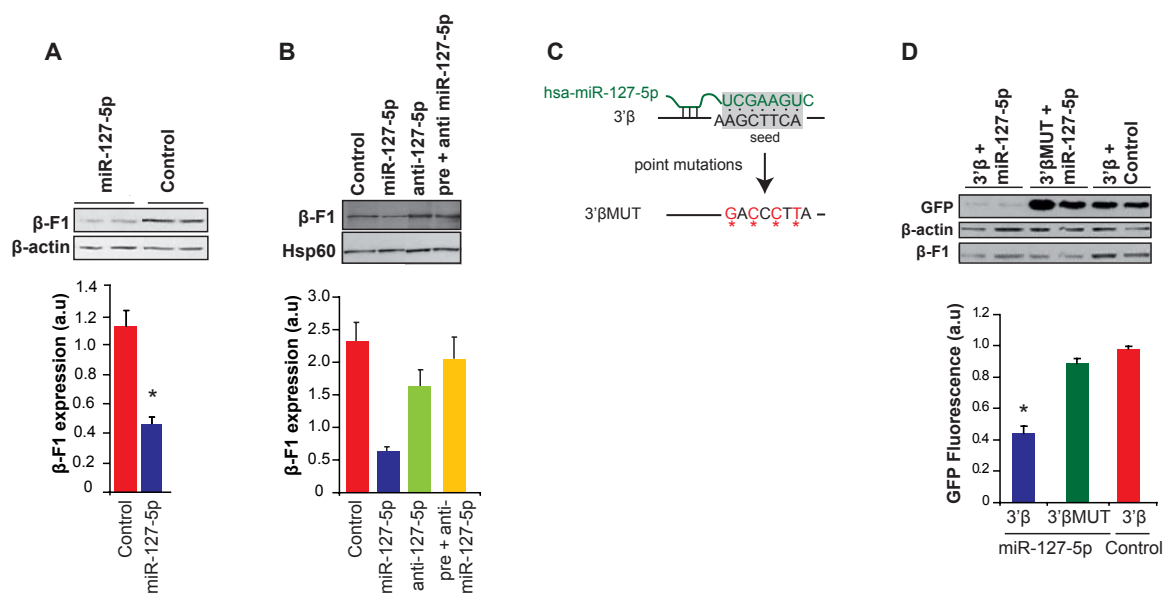


**Figure 4.26: miR-127-5p down-regulates endogenous  $\beta$ -F1-ATPase expression.** (A) Western blot analysis of BT549 cells transfected with miR-127-5p precursors (miR-127-5p, blue bar) or scramble miRNA precursors (control, red bar) using polyclonal anti- $\beta$ -F1-ATPase and monoclonal anti- $\beta$ -actin antibodies. The histogram illustrates the means  $\pm$  SEM of the quantification of the bands of  $\beta$ -F1-ATPase relative to  $\beta$ -actin of four independent experiments. (B) Analysis of BT549 cells transfected with miR-127-5p precursor (blue bar), anti-miR-127-5p (green bar), both (pre + anti-127-5p, yellow bar) or a negative control miRNA (control, red bar). Quantification of  $\beta$ -F1-ATPase expression using Hsp60 as a reference gene is illustrated in the histogram. (C) Schematic illustration of insertion of four point mutations (red, asterisks) in the 3'UTR of  $\beta$ -mRNA (3' $\beta$ MUT) at the miR-127-5p seed matching side (highlighted in gray) (3' $\beta$ MUT) (D) Western blot and flow cytometry (histogram) analysis of BT549 cells co-transfected with miR-127-5p or a negative control miRNA (control, red bar), and a reporter plasmid expressing GFP fused either to the 3'UTR of  $\beta$ -mRNA (3' $\beta$ , blue bar) or to the mutant (3' $\beta$ MUT, green bar). The histogram illustrates the mean GFP fluorescence intensity as determined by flow cytometry. The results shown are the means  $\pm$  SEM of three independent experiments. \*,  $p < 0.05$  when compared to control cells by Student's t-test.

The lower expression of  $\beta$ -F1-ATPase in miR-127-5p expressing cells might be caused by a miR-127-5p mediated induction of  $\beta$ -mRNA degradation or by inhibition of its translation. Therefore, we determined the cellular content of  $\beta$ -mRNA in cells expressing miR-127-5p or control miRNA. As expected, the protein level of  $\beta$ -F1-ATPase was significantly reduced (Fig. 4.27A and C) in the presence of miR-127-5p, whereas the level of  $\beta$ -mRNA was not affected by miR-127-5p over-expression when compared to cells transfected with a non relevant miRNA (Fig. 4.27B and C), indicating that miR-127-5p inhibits the translation of  $\beta$ -mRNA. Taken together, these findings point out that miR-127-5p binds directly and specifically to the 3'UTR of the  $\beta$ -mRNA and interferes with the synthesis of  $\beta$ -F1-ATPase.

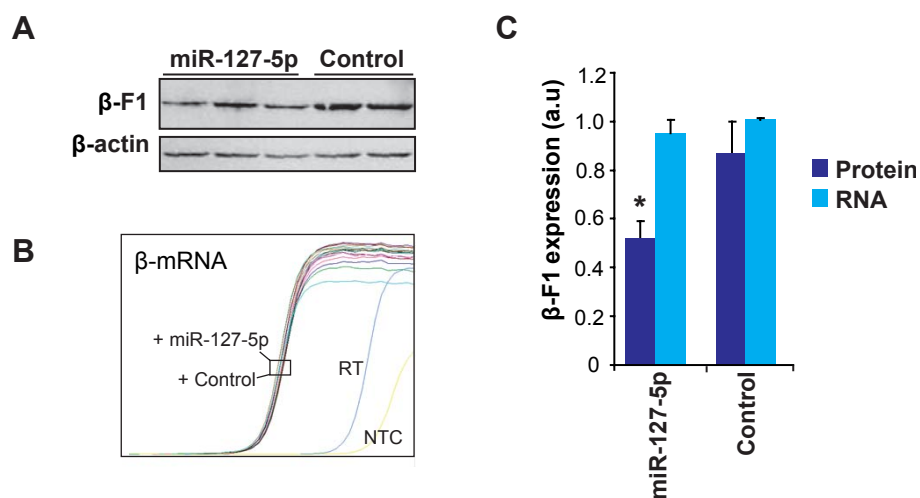


**Figure 4.27: miR-127-5p inhibits translation of  $\beta$ -F1-ATPase.** BT549 cells were transfected with miR-127-5p precursors (miR-127-5p) and scramble miRNA precursors (control) and expression of (A)  $\beta$ -F1-ATPase and (B)  $\beta$ -mRNA was analyzed. (A) Western blot analysis of BT549 transfected cells using polyclonal anti- $\beta$ -F1-ATPase and monoclonal anti- $\beta$ -actin antibodies. (B) Quantitative polymerase chain reaction amplification curves of  $\beta$ -mRNA. Each curve designates an independent experiment of BT549 transfected cells. RT, minus reverse transcriptase sample; NTC, non-template control sample (C) The histogram summarizes the quantification of  $\beta$ -F1-ATPase (dark blue bars) and  $\beta$ -mRNA expression (light blue bars). Expression data were normalized with respect to the mean value of control transfected cells and  $\beta$ -actin used as a reference gene. The results shown are the means  $\pm$  SEM of three independent experiments. \*,  $p < 0.05$  when compared to control transfected cells by Student's t-test.

#### 4.4.5 miR-127-5p might be involved in controlling $\beta$ -F1-ATPase expression during liver development in humans

##### 4.4.5.1 No expression of miR-127-5p in human cancer cell lines

As mentioned previously, when BT549 cells were transfected with anti-miR-127-5p to silence miR-127-5p no changes in the steady state level of p $\beta$ GFP-3' $\beta$  (Fig. 4.24) and  $\beta$ -F1-ATPase (Fig. 4.26B) could be detected. Therefore, we questioned about the presence of miR-127-5p in BT549 cells and analyzed by RT-qPCR the relative expression level of mature miR-127-5p. In fact, the analysis revealed that miR-127-5p is not expressed in BT549 cells (Fig. 4.28A). This finding is consistent with our results, because we were not able to silence miR-127-5p. An effect of miR-127-5p on  $\beta$ -F1-ATPase expression could only be detected when miR-127-5p was over-expressed (Fig. 4.24A and 4.26A, B).

To identify in which cellular context the silencing of  $\beta$ -mRNA translation by miR-127-5p might be of physiological relevance, we further analyzed the expression of miR-127-5p in different human cancer cell lines (T47, HCT116, Hela, Hop62, Jurkat), in Hek239T cells and the normal breast cell line MCF12F. The results obtained revealed that none of the analyzed cell lines exhibited a significant expression of miR-127-5p (Fig. 4.28A black bars).

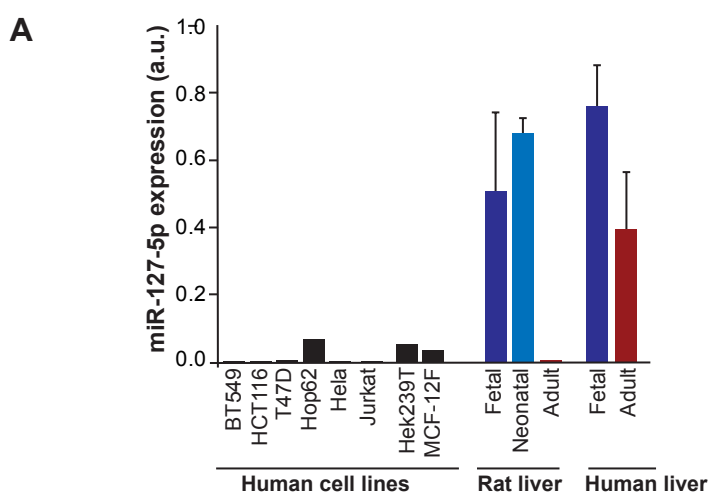
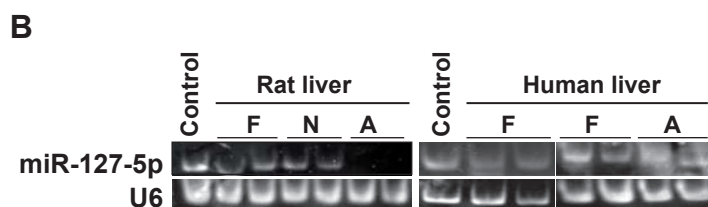


**Figure 4.28: miR-127-5p is expressed in human and rat fetal liver.** (A) Quantification of miR-127-5p expression by qPCR in human cancer (BT549, T47D, HCT116, Hop62, Jurkat and Hela) and normal (Hek239T, MCF12F) cell lines. For quantification of miR-127-5p during liver development of the rat, RNA was extracted from the fetus (Fetal) at day 21 of gestation, from 2-6 h old neonates (Neonatal) and from adult rat liver. Human fetal RNA derives from 63 spontaneously aborted fetuses with an age of 22-40 weeks and human adult liver RNA derives from a 51 year-old man. miR-127-5p expression in the cell lines and during liver development was normalized, respectively, to RNU48 and U6 RNA. (B) After qPCR, miR-127-5p expression in fetal (F), neonatal (N) and adult (A) liver was analyzed on a 5% polyacrylamide gel. RNA from BT549 cells transfected with miR-127-5p precursors was used as positive control for miR-127-5p expression. U6 RNA was used as a reference RNA.



### **4.4.5.2 Potential role of *mir127-5p* as a regulator of $\beta$ -F1-ATPase expression during human liver development**

In addition to neoplastic cells, previous studies characterizing the biogenesis of mitochondria during rat liver development demonstrated that  $\beta$ -mRNA is accumulated in the fetal liver in a translational repressed state until the time of birth, when a rapid increase in its translation occurred (Luis et al., 1993; Izquierdo and Cuezva, 1997; Izquierdo et al., 1995). Thus, to assess whether miR-127-5p might be involved in the down-regulation of  $\beta$ -F1-ATPase during liver development, we analyzed the expression of miR-127-5p in both human and rat livers. RNA from BT549 cells transfected with miR-127-5p precursors was used as a positive control of miR-127-5p expression. Remarkably, RT-qPCR analysis revealed the expression of miR-127-5p in both the human and rat livers as well as in the liver from 2-6 hours-old rat neonates (Fig. 4.28A and B). Importantly, no expression of miR-127-5p was observed in liver from adult rats (Fig. 4.28A and B).

The latter findings suggest a possible role for miR-127-5p in controlling  $\beta$ -F1-ATPase expression during liver development. However, and because mitochondrial biogenesis and the expression pattern of  $\beta$ -F1-ATPase during liver development has been mainly studied in rat (Luis et al., 1993; Ostronoff et al., 1996; Valcarce et al., 1988), in a next step we studied the expression of  $\beta$ -F1-ATPase and of other mitochondrial proteins such as Hsp60,  $\gamma$ -F1-ATPase ( $\gamma$ -F1), subunit b of succinate dehydrogenase complex (SDH-B), COX1 and COX4 of complex IV and GAPDH and LDH-A from the glycolytic pathway in human fetal and adult liver tissue lysates (Fig. 4.29A).

The analysis revealed that the mitochondrial proteins involved in oxidative phosphorylation such as COX4,  $\beta$ -F1-ATPase,  $\gamma$ -F1-ATPase, SDH-B and COX1 were barely expressed in human fetal liver (Fig. 4.29A and B). In adult liver, however, their expression increased significantly and in particular the steady state level of  $\beta$ -F1-ATPase and SDH-B rose up distinctively compared to fetal liver (Fig. 4.29A and B). Remarkably, expression of the structural mitochondrial protein Hsp60 did not differ significantly between fetal and human adult liver (Fig. 4.29A and B). Furthermore, the  $\beta$ -F1/Hsp60 ratio (an index of the bioenergetic competence of mitochondria) increased significantly in adult liver (Fig. 4.29B), suggesting in agreement with similar findings in rat (Cuezva et al., 1997) that human fetal liver mitochondria are structurally existent yet incomplete in their functional ability to perform oxidative phosphorylation. Interestingly, expression of the glycolytic enzymes GAPDH and LDH-A was also elevated in adult liver when compared to fetal liver (Fig. 4.29A and B).

Analysis of developmental changes of liver  $\beta$ -mRNA in humans revealed that the transcript level was 2.5-fold higher in the fetal than in the adult liver (Fig. 4.29C). Likewise, the mRNA of the  $\gamma$ -F1-ATPase subunit ( $\gamma$ -mRNA) of the same OXPHOS complex (complex V) was 10-fold increased in the fetal liver when compared to the transcript level in adult liver (Fig. 4.29C). Considering the low  $\beta$ -F1-ATPase and  $\gamma$ -F1-ATPase expression in fetal liver (Fig. 4.29A and B), the latter observations indicate an accumulation of both transcripts in human liver, strongly suggesting in agreement with previous findings in rat (Izquierdo et al., 1990; Luis et al., 1993; Izquierdo et al., 1995) that synthesis of  $\beta$ - and  $\gamma$ -F1-ATPase is post-transcriptional inhibited during the fetal stage of liver

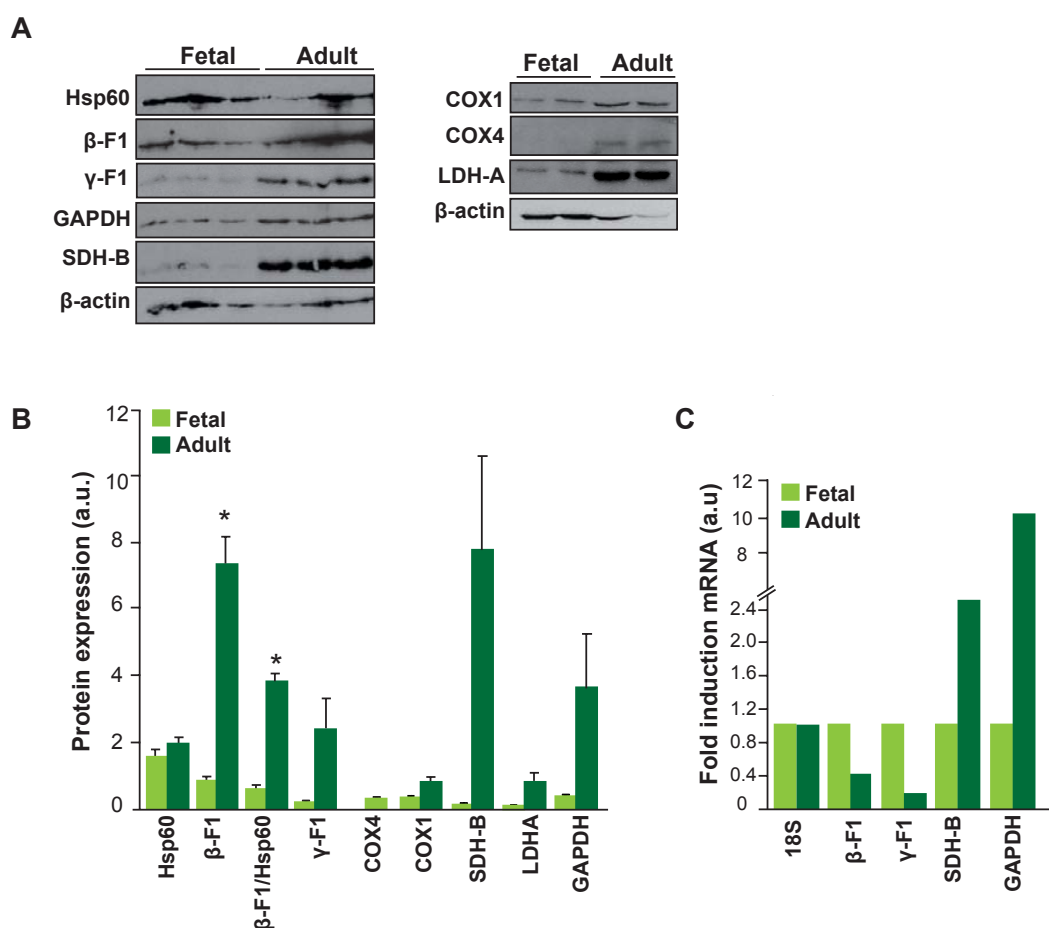


**Figure 4.29: OXPHOS during human liver development.** (A) Western blot analysis of the mitochondrial proteins Hsp60,  $\beta$ -F1-ATPase ( $\beta$ -F1),  $\gamma$ -F1-ATPase ( $\gamma$ -F1), subunit B of the succinate dehydrogenase (SDH-B), subunits COX1 and COX4 of cytochrome c oxidase, and GAPDH and lactate dehydrogenase A (LDH-A) of the glycolytic pathway in human fetal and adult liver. Expression of  $\beta$ -actin was used as a reference gene. (B) The histogram summarizes the quantification of the relative expression level of the proteins relative to  $\beta$ -actin in human fetal (light green bars) and adult (dark green bars) liver extracts. \*,  $p < 0.05$  as determined by Student's t-test. (C) qPCR analysis of 18S,  $\beta$ -F1-ATPase mRNA,  $\gamma$ -F1-ATPase mRNA, SDH-B mRNA, and GAPDH mRNA in human fetal (light green bars) and adult (dark green bars) liver. Data were normalized relative to  $\beta$ -actin mRNA and are illustrated as fold induction relative to fetal liver.

development. In contrast, the content of the mRNAs of the mitochondrial protein SDH-B and of the glycolytic enzyme GAPDH experienced an increase in their steady state level (Fig. 4.29C), while the ribosomal 18S RNA showed no changes during human liver development (Fig. 4.29C).

In summary, these results indicate that human fetal liver mitochondria are bioenergetically undeveloped when compared to adult liver mitochondria. Since  $\beta$ -F1-ATPase protein is significantly reduced in human fetal liver despite a higher abundance of its transcript when compared to adult liver (Fig. 4.29), we suggest that a bottle-neck for functional differentiation of human liver mitochondria is exerted by translational control of  $\beta$ -mRNA. In this regard miR-127-5p, which is expressed in human liver (Fig. 4.28), might be involved in controlling the expression of  $\beta$ -F1-ATPase and thus the acquisition of functional oxidative phosphorylation during liver development.



**4.4.5.3 miR-127-5p does not control rat  $\beta$ -F1-ATPase expression**

The miR-127 precursor sequence is fundamentally preserved beyond species (Song and Wang, 2009), and we observed that miR-127-5p is expressed in fetal rat liver and in 2-6 h old rat neonates (Fig. 4.28A and B), whereas no expression of miR-127-5p was detectable in the liver from adult rats (Fig. 4.28A and B). This finding suggested the participation of this miRNA in controlling  $\beta$ -F1-ATPase expression during functional differentiation of mitochondria in developing liver. However, when compared to human  $\beta$ -mRNA the miR-127-5p target site in the 3'UTR of rat  $\beta$ -mRNA lacks one nucleotide (Fig. 4.30A), which would result in an imperfect and discontinuous pairing between miR-127-5p and the rat  $\beta$ -mRNA, a phenomenon rarely detected in miRNA target sites (Hafner et al., 2010). Consistent with the "relaxed" matching of miR-127-5p and the 3'UTR of rat  $\beta$ -mRNA,

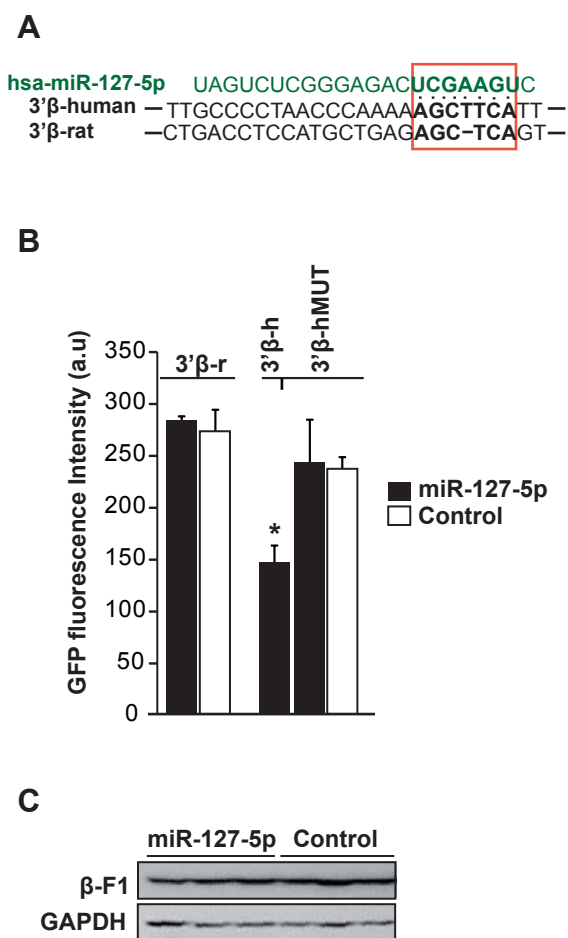


**Figure 4.30: miR-127-5p has no effect on rat  $\beta$ -mRNA.** (A) Schematic illustration of miR-127-5p (green) matching to the 3'UTR of human (3'β-human) and rat  $\beta$ -F1-ATPase (3'β-rat). Seed region is highlighted by red box. (B) C9 rat liver cells were co-transfected with miR-127-5p (black bar) or control miRNA (control, white bar), and a reporter plasmid expressing GFP fused to the 3'UTR of rat  $\beta$ -mRNA (3'β-rat), to the 3'UTR of human  $\beta$ -mRNA (3'β-h) or to the 3'UTR of human  $\beta$ -mRNA containing 4 point mutations in the miR-127-5p matching side (3'β-hMUT). The histogram illustrates the mean GFP fluorescence intensity as determined by flow cytometry. The results shown are the means  $\pm$  SEM of three independent experiments. (C) Western blot analysis of  $\beta$ -F1-ATPase ( $\beta$ -F1) and GAPDH in C9 cells transfected with miR-127-5p or control miRNA.

transient expression of miR-127-5p and a GFP reporter fused to the 3'UTR of rat  $\beta$ -F1-ATPase (3'β-r) in C9 rat liver cells revealed no significant effect on GFP fluorescence (Fig. 4.30B) or on endogenous rat  $\beta$ -F1-ATPase expression (Fig. 4.30C). As a control, C9 cells were additionally co-transfected with miR-127-5p and a GFP chimera fused to the 3'UTR of human  $\beta$ -F1-ATPase, containing (3'β-hMUT) or not (3'β-h) 4 point mutations in the miR-127-5p target site. Flow cytometry analysis (Fig. 4.30B)

demonstrated as shown above (Fig. 4.26D) that human 3'UTR of the  $\beta$  F1-ATPase is a target of miR-127-5p (Fig. 4.30B). Overall, these findings demonstrate that in contrast to human cells miR-127-5p plays no relevant role in the post-transcriptional regulation of rat  $\beta$ -F1-ATPase expression.



# **DISCUSSION**



## 5 DISCUSSION

A fundamental characteristic of cancer cells is the metabolic switch from oxidative phosphorylation to enhanced glycolysis (Hanahan and Weinberg, 2011). Otto Warburg, who first described the high aerobic glycolysis of cancer cells (Warburg effect) suggested that this decisive phenotype was a result of an impaired oxidative phosphorylation (Warburg, 1956a). In fact, several transcriptomic, genetic and proteomic studies aimed at explaining the Warburg effect have demonstrated that tumors and cancer cells in addition to the induction of glycolytic genes exhibit a malfunctioning of the bioenergetic activity of mitochondria (for review see Cuezva et al., 2009; Ortega et al., 2009). Importantly, studies in our laboratory and in others have demonstrated profound proteomic changes in the bioenergetic metabolism of human tumors. In particular the normalized expression of  $\beta$ -F1-ATPase is down-regulated in human breast, colon, lung, esophageal, gastric and kidney tumors (Bi et al., 2006; Cuezva et al., 2002; Chen et al., 2004; Isidoro et al., 2005; Isidoro et al., 2004; Unwin et al., 2003). Additionally, changes in the expression level of  $\beta$ -F1-ATPase are linked to the glycolytic switch experienced by the tumors, in such a way that a reduction in the activity of oxidative phosphorylation significantly correlates with an increase in the rate of glucose consumption by aerobic glycolysis (Isidoro et al., 2005; Lopez-Rios et al., 2007; Sanchez-Arago et al., 2010). This proteomic feature was called the bioenergetic signature of cancer and notably affords potential clinical utility as a diagnostic marker in breast, colon and lung cancer patients (Cuezva et al., 2004; Cuezva et al., 2002; Isidoro et al., 2005; Lin et al., 2008; Lopez-Rios et al., 2007) as well as a marker for the response to chemotherapy (Hernlund et al., 2009; Hernlund et al., 2008; Sanchez-Arago and Cuezva, 2011; Sanchez-Arago et al., 2010; Santamaria et al., 2006; Shin et al., 2005). In the present study, we have contributed to the so far largely unexplored characterization of the molecular mechanisms that control the expression of human  $\beta$ -F1-ATPase by (i) demonstrating that control of  $\beta$ -F1-ATPase translation is a crucial mechanism operating during human oncogenesis as well as development, and (ii) identifying G3BP1 and miR-127-5p as factors that interact and regulate  $\beta$ -F1-ATPase expression. Moreover, we have demonstrated that G3BP1 could provide a promising diagnostic marker for breast cancer progression, suggesting that G3BP1 is a relevant actor mediating  $\beta$ -F1-ATPase down-regulation in human breast cancer.

### 5.1 TRANSLATION OF $\beta$ -mRNA IS SELECTIVELY DOWN-REGULATED IN HUMAN CANCER

The enforced aerobic glycolysis is not an exclusive feature of tumor cells, but also a characteristic trait of normal highly proliferating cells, including embryonic cells (Cuezva et al., 2009; Ortega et al., 2009). Remarkably, biochemical and mechanistic similarities exist between tumors and embryonic tissues, such as expression of isoforms of glycolytic enzymes (Mazurek et al., 2005) and the control of mitochondrial biogenesis (Cuezva et al., 1997). In this regard, during fetal rat liver development mitochondria are hampered in their production of energy, due to reduced levels of components of

the oxidative respiration system such as  $\beta$ -F1-ATPase, whose transcript is translationally repressed in both fetal rat liver and in rat hepatomas (Luis et al., 1993; Izquierdo et al., 1995; de Heredia et al., 2000). In the present study we have shown that also in human breast, colon and lung tumors (Willers et al., 2010) as well as in human liver development the decreased amount of  $\beta$ -F1-ATPase originates from specific translation silencing of the transcript, supporting the idea that  $\beta$ -mRNA translation is a molecular mechanism that participates in defining the bioenergetic phenotype.

Every cell type exhibits a specific molecular composition and function of their mitochondria (Fernandez-Vizarra et al., 2011; Pagliarini et al., 2008). Concurrently, we observed with regard to  $\beta$ -mRNA expression that different tissues respond differently to the drop in the bioenergetic signature during tumorigenesis. Whereas in breast and lung adenocarcinomas  $\beta$ -mRNA expression remained unchanged, in colon adenocarcinomas and lung squamous carcinomas revealed a significant increase in  $\beta$ -mRNA expression (Willers et al., 2010). Changes in the cellular availability of  $\beta$ -mRNA might result from an increased mRNA stability and/or transcription rate of the transcript, because both mechanisms have been shown to control the expression of mammalian *ATP5B* gene in order to compensate for the energetic imbalance (de Heredia et al., 2000; Izquierdo et al., 1995).

Consistent with previous findings regarding rat  $\beta$ -mRNA (Izquierdo and Cuezva, 1997), we have shown that the 3'UTR of human  $\beta$ -F1-ATPase is required for efficient translation of the transcript, acting as a translational enhancer of reporter constructs (Willers et al., 2010). In fetal rat liver and in rat hepatomas  $\beta$ -mRNA is translationally masked by the binding of specific RNABPs (Izquierdo and Cuezva, 1997; de Heredia et al., 2000; Izquierdo and Cuezva, 2005). Analogously, in this investigation we have shown that synthesis of human  $\beta$ -F1-ATPase is specifically inhibited in the presence of lung, breast and esophageal tumor extracts. During rat development and in carcinogenesis it is assumed that binding of specific proteins to the 3'UTR of  $\beta$ -mRNA sterically hinder the initiation of translation by preventing the access of the translational machinery to the enhancer region of the mRNA (Izquierdo and Cuezva, 1997; de Heredia et al., 2000; Izquierdo and Cuezva, 2000). However, in contrast to rat  $\beta$ -mRNA no inhibitory effect of the human tumor extracts was observed when a reporter construct containing the 3'UTR of  $\beta$ -F1-ATPase transcript was used. Consistent with this observation the 3'UTR of human  $\beta$ -mRNA does not interact specifically with breast and lung tumor proteins (Willers et al., 2010). Therefore, in humans the control of  $\beta$ -mRNA translation appears to be more complex, and although the 3'UTR is a sequence element required for efficient translation of the mRNA, further *cis*-acting elements seem to be required to effectively inhibit  $\beta$ -mRNA translation. The additional *cis*-acting factors required could be located in the 5'UTR or in the ORF, and the *trans*-acting factors involved might be necessary for intramolecular cross-talk to stabilize interactions of RNABPs with the 3'UTR, among RNABPs and/or to support the inhibition of the ribosomal recruitment to the transcript. Consistently, in yeast combination of two *cis*-acting elements located in the ORF and in the 3'UTR of  $\beta$ -mRNA is required to confer appropriate cellular localization and translation of the mRNA (Garcia et al., 2010). Assembly of

rat  $\beta$ -mRNA into a ribonucleoprotein complex along with its association with the translational machinery equally requires the cross-talk of the 3'UTR with a *cis*-acting element located in the ORF (Ricart et al., 2002).

Overall, the findings of the present study indicate that down-regulation of the bioenergetic activity of mitochondria in human tumors is exerted by translational silencing of  $\beta$ -mRNA.

## 5.2 G3BP1, A REGULATOR OF $\beta$ -mRNA TRANSLATION

The full-length  $\beta$ -mRNA is able to recruit RNABPs from human cell extracts to form a  $\beta$ -mRNP complex (Ortega et al., 2010), and human breast, lung and esophageal tumor extracts specifically masked translation only of the full-length  $\beta$ -mRNA (Willers et al., 2010). In order to understand the molecular mechanisms that regulate the translational repression of  $\beta$ -F1-ATPase in cancer, it is essential to identify the regulatory factors that interact with the mRNA and potentially define its cellular fate.

In this investigation, we have analyzed the biological relevance of three putative  $\beta$ -mRNA binding proteins: NPM1, IMP1 and G3BP1 (Ortega et al., 2010). We have demonstrated that neither IMP1 nor NPM1 associate *in vivo* with  $\beta$ -mRNA. Moreover, over-expression and silencing assays do not reveal significant changes on expression of  $\beta$ -F1-ATPase, strongly suggesting that IMP1 and NPM1 are not involved in  $\beta$ -F1-ATPase biology. In contrast, we have demonstrated that G3BP1 interacts *in vivo* with  $\beta$ -mRNA and in particular with the 3'UTR of the transcript. Furthermore, we have shown that G3BP1 exerts the activity of a repressor of  $\beta$ -mRNA translation both *in vivo* and *in vitro*, providing a potent candidate of the  $\beta$ -mRNP complex (Ortega et al., 2010) that might control the bioenergetic phenotype of the cell.

G3BP1 is a ubiquitously expressed and evolutionary conserved protein among eukaryotes that has been involved in multiple cellular processes such as Ras signaling and proliferation, RNA metabolism and SGs assembly (Irvine et al., 2004). In the present work, we documented by RNA-IP and FISH assays that endogenous G3BP1 directly interacts with  $\beta$ -mRNA, revealing the specificity of the G3BP1- $\beta$ -mRNA interaction in a normal cellular context. We observed the interaction of G3BP1 with  $\beta$ -mRNA in SGs as a consequence of G3BP1 over-expression and its unspecific recruitment (Tourriere et al., 2003). However, additionally we observed the G3BP1- $\beta$ -mRNA interaction in tiny, TIA1-negative cytoplasmic granules, suggesting that these small G3BP1- $\beta$ -mRNA granules represent the site of its natural cytoplasmic fate.

G3BP1 harbors a RNA binding domain and associates selectively with mRNAs such as c-myc mRNA (Gallouzi et al., 1998), cdk7 mRNA (Lypowy et al., 2005), tau mRNA (Atlas et al., 2007) and in a complex with Caprin-1 cyclinD2 mRNA (Solomon et al., 2007). Binding of G3BP1 to the mRNAs, however, affects in different ways the cellular fate of the transcripts. In quiescent cells, hyperphosphorylation of G3BP1 causes the activation of its intrinsic phosphorylation-dependent endonuclease activity promoting the degradation of c-myc mRNA (Gallouzi et al., 1998; Tourriere



et al., 2001). Contrary, interaction of G3BP1 with cdk7 and tau mRNAs favors the stabilization of the transcripts (Atlas et al., 2007; Lypowy et al., 2005) and influences the localization of tau mRNA in neurons (Atlas et al., 2007). In this study, we observed that inhibition of  $\beta$ -F1-ATPase synthesis in G3BP1 expressing cells is exerted in the absence of relevant changes in the cellular availability of  $\beta$ -mRNA. Moreover, we report that the synthesis of  $\beta$ -F1-ATPase is repressed in the presence of G3BP1 and prevents *in vitro* the recruitment of  $\beta$ -mRNA into the translational competent 80S ribosome, demonstrating that G3BP1 inhibits expression of  $\beta$ -F1-ATPase at the level of translation initiation.

We documented the presence of  $\beta$ -mRNA on the outer mitochondrial membrane, suggesting that the  $\beta$ -mRNP is transported and anchored within the periphery of the mitochondria. This result is in agreement with findings in yeast and mammalian cells, demonstrating that many nucleus-encoded mRNAs of mitochondrial proteins, in particular those encoding core components of mitochondrial complexes (Egea et al., 1997; Garcia et al., 2007; Marc et al., 2002), are specifically sorted to the vicinity of mitochondria (Lithgow et al., 1997; Marc et al., 2002; Sylvestre et al., 2003). Moreover, the clustered and granular  $\beta$ -mRNA localization underlines previous data in rat hepatocytes, which have illustrated that  $\beta$ -mRNA is present in large  $\sim$ 150 nm  $\beta$ -mRNP complexes preferentially associated to the outer mitochondrial membrane (Egea et al., 1997).

Direct and active mRNP localization, which is carried out by specific motor proteins such as kinesin, dynein and myosin that transport mRNPs along the cytoskeleton to their subcellular destination, represents a widespread mechanism to establish site-specific translation to generate different cellular compartments and functions (Lithgow et al., 1997; Lopez de Heredia and Jansen, 2004; Martin and Ephrussi, 2009). In this regard, G3BP1 has been shown to co-localize with Caprin-1 in microtubule associated RNA granules concentrated in the leading and trailing edge of migrating cells (Solomon et al., 2007). Furthermore, G3BP1 was found in a RNP that controls the localization and translation of the tau mRNA in neurons (Atlas et al., 2007). Therefore, and similar to the control of  $\beta$ -actin mRNA by ZBP1 (Hüttelmaier et al., 2005), we suggest that G3BP1 might inhibit  $\beta$ -mRNA translation while the  $\beta$ -mRNP is transported along the cytoskeleton to mitochondria (Fig. 1.4) where its spatially restricted translation by mitochondrial bound ribosomes will take place (Kellems et al., 1975; MacKenzie and Payne, 2004; Martin and Ephrussi, 2009). Alternatively, the observed cytoplasmic G3BP1- $\beta$ -mRNA foci might represent repositories of translational repressed  $\beta$ -mRNA in order to assure a rapid response to cell physiological demands.

We have seen that G3BP1 binds *in vivo* specifically to reporter mRNAs bearing the  $\beta$ -F1-ATPase 3'UTR. In rat, binding of RNABPs to the 3'UTR has been shown to inhibit translation (de Heredia et al., 2000; Izquierdo and Cuezva, 1997) presumably by interfering with the intrinsic enhancer activity of the 3'UTR hindering the access of the translational machinery onto the mRNA (Izquierdo and Cuezva, 1997; Di Liegro et al., 2000; Izquierdo and Cuezva, 2000; Willers et al., 2010). Herein, we show that binding of G3BP1 to  $\beta$ Gal-3' $\beta$  mRNA chimeras in cells is less efficient than that to the full length  $\beta$ -mRNA. Moreover, G3BP1 over-expression did not affect the expression of

GFP reporters fused to the 3'UTR of human  $\beta$ -F1-ATPase (data not shown), suggesting that other *cis*-elements and/or RNABPs associated to other regions within the transcript contribute to the stabilization and functionality of the complex. This idea is consistent with the results that illustrate that translation masking of  $\beta$ -mRNA in human cancer depends on the full length  $\beta$ -mRNA (Willers et al., 2010). Furthermore, several studies have shown that the effect of G3BP1 on the target mRNA is influenced and/or depends on other proteins (Atlas et al., 2007; Lypowy et al., 2005). Overall, these findings suggest the existence of an intramolecular cross-talk between the different  $\beta$ -mRNP components and the transcript, which is necessary for the efficient association with the translation machinery.

Generally, in the canonical cap-dependent way of translation initiation recruitment of the ribosomes to the mRNA is facilitated by binding of the eIF4F complex to the 5' cap of the mRNA and its subsequent interaction with the poly(A) binding protein (PABP), bringing about the circularization of the mRNA to enhance translation initiation (Gallie, 1991; Svitkin and Sonenberg, 2006) (Fig. 5.1A). It is thought that the combined cooperative interactions within the closed mRNA loop increase the affinity of the eIF4F complex for the 5' cap by lowering its dissociation and stimulate the joining of the 43S ribosomal subunit to the mRNA (Tarun and Sachs, 1995; Tarun and Sachs, 1996; Wei et al., 1998; Sachs and Varani, 2000; Kahvejian et al., 2005). Thus, and considering that G3BP1 represses  $\beta$ -mRNA translation at the level of initiation, G3BP1 as part of the  $\beta$ -mRNP could impede the recruitment of the 43S ribosome to the mRNA or interfere with the 5' to 3' circularization of the mRNA (Fig. 5.1A). The loss of mRNA circularization would consequently lead to a lower affinity of eIF4F for the cap, a hampered ribosome binding and polysome re-cycling and ultimately a decrease in the efficiency of translation initiation.

RNPs are dynamic structures that act constantly as a platform for the association of proteins and small non-coding RNAs. In fact, interactions between the regulatory factors and the RNA might be transitional and constantly changed in response to environmental and cellular demands (Moore, 2005), allowing in this way a coordinated and flexible regulation of genetic expression and ensuring a rapid and versatile answer to changing conditions of the system. Within this context, the observation that siRNA mediated silencing of G3BP1 did not affect  $\beta$ -F1-ATPase protein or mRNA levels, suggests a possible redundancy in the control of  $\beta$ -mRNA expression to ensure normal steady state levels of the  $\beta$ -F1-ATPase, a bottle-neck component required for functional OXPHOS. Alternatively, the effect of G3BP1 on  $\beta$ -F1-ATPase expression may not be exerted constitutively in the cell and might be influenced by specific cellular signaling events. In this regard, it is possible that post-translational modifications following specific stimuli, and which are abrogated in over-expression experiments, could modify the activity of G3BP1. Indeed, post-translational regulatory events such as phosphorylation and the control of subcellular localization play a relevant role on G3BP1 activity (Gallouzi et al., 1998; Tourriere et al., 2001; Tourriere et al., 2003).

G3BP1 harbors 3 phosphorylation sites and Ser-149 phosphorylation in quiescent fibroblasts is critical for G3BP1 translocation into the nucleus where it mediates selective RNA degradation

(Gallouzi et al., 1998; Tourriere et al., 2001). In contrast, in growth factor stimulated cells G3BP1 associates with RasGAP (P120-Ras GTPase activating protein) and localizes at the plasma membrane (Gallouzi et al., 1998; Tourriere et al., 2001). Furthermore, hyperphosphorylation of G3BP1 activates its intrinsic endonuclease activity (Gallouzi et al., 1998) and de-phosphorylation of Ser-149 is critical for SGs assembly by G3BP1 due to a necessary multimerization of G3BP1 to cross-link RNA molecules (Tourriere et al., 2003). Thus, repression/activation of  $\beta$ -mRNA translation by G3BP1 might be promoted by certain stimuli that could modify G3BP1 activity. We suggest that among these stimuli could be metabolic indicators such as the energetic charge and the REDOX state of the cell (Izquierdo and Cuezva, 2005), which could participate in controlling G3BP1 activity. In this situation, G3BP1 might play a role as a sensor that integrates cellular and extracellular signaling events and adapts the mitochondrial phenotype of the cell to different bioenergetic demands through controlling the spatial and temporal expression of  $\beta$ -F1-ATPase.

Accumulating evidence suggests the participation of G3BP1 in promoting cell growth, proliferation and survival and as such may influence tumorigenesis. Historically, G3BP1 was detected in a screen for RasGAP binding proteins (Parker et al., 1996), which is known as a negative regulator of Ras activity (McCormick, 1995). The involvement of deregulated Ras signal transduction pathways in tumorigenesis and metastasis is well established. In this regard, the interaction of G3BP1 with RasGAP may suggest a role for G3BP1 in the signaling pathways that control tumor cell proliferation and survival. Indeed, G3BP1 is up-regulated in proliferating retinal pigment epithelia cells (Kociok et al., 1999) and G3BP1 has been found over-expressed in head and neck (Guitard et al., 2001) and breast (Barnes et al., 2002; French et al., 2002) carcinomas as well as in several human cancer cell lines (Guitard et al., 2001). G3BP1 over-expression in fibroblasts has also been shown to increase S-phase entry (Guitard et al., 2001) and G3BP1 binds and regulates c-myc mRNA (Gallouzi et al., 1998; Tourriere et al., 2001), which is an important transcription factor involved in the regulation of cell growth and proliferation. Most convincingly, microarray analysis of G3BP1 knock out MEFs demonstrated that 70% of the deregulated genes are implicated in cell signaling and control of cellular proliferation (Zekri et al., 2005), and inactivation of the G3BP1 encoding gene in mice leads to embryonic lethality and growth retardation (Zekri et al., 2005). Altogether, these data support a participation of G3BP1 in tumorigenesis, nevertheless exactly how G3BP1 may contribute to cancer formation or progression is still elusive.

In this regard, expression of  $\beta$ -F1-ATPase as well as its activity has consistently been reported to be down-regulated in most human carcinomas (Cuezva et al., 2002; Cuezva et al., 2004; Isidoro et al., 2004; Isidoro et al., 2005; Sanchez-Cenizo et al., 2010). In chronic-myeloid leukemia  $\beta$ -F1-ATPase expression is down-regulated due to promoter hypermethylation of the *ATP5B* gene (Li et al., 2010a). In contrast, as shown in the present study, down-regulation of  $\beta$ -F1-ATPase in colon, lung, breast and esophageal cancer is exerted at the level of translation (Willers et al., 2010). Thus, the opposite relation of G3BP1 over-expression found in cancer (Guitard et al., 2001; Barnes et al., 2002; French et al., 2002; Zhang et al., 2007c) to a diminished expression of  $\beta$ -F1-ATPase

in most human carcinomas (Cuezva et al., 2002; Cuezva et al., 2004; Isidoro et al., 2004; Isidoro et al., 2005) along with the finding that G3BP1 inhibits  $\beta$ -mRNA translation strongly suggest that G3BP1 could play a relevant role in defining the bioenergetic phenotype of cancer cells and thus regulate the glycolytic switch that occurs during cellular transformation (Fig. 5.1B). In this situation, and consistent with the abovementioned idea, the tumoral microenvironment could lead to selective metabolic constraints caused by nutrient limitation, limited oxygen supply and the build-up of potentially toxic molecules such as lactic acid (Fang et al., 2008), which in turn could determine G3BP1 activity and its inhibitory activity on  $\beta$ -mRNA translation. Interestingly, a recent report demonstrated that G3BP1 interacts with MK-STYX (Hinton et al., 2010), a MAPK homologue and catalytically inactive phosphatase that localizes to mitochondria and is specifically involved in signaling the mitochondrial-dependent apoptotic program (Niemi et al., 2011). This finding might suggest another link between G3BP1 and mitochondria and the promotion of an apoptotic resistant phenotype (see 5.5).

In conclusion, we suggest that  $\beta$ -F1-ATPase expression is controlled by specific interaction of RNABPs with the transcript as well as with other RNABPs within the  $\beta$ -mRNP complex, and that masking of  $\beta$ -mRNA translation in cancer could be mediated by signaling through G3BP1. Thus, G3BP1 could play a relevant role in the glycolytic switch that occurs in cellular transformation, thereby contributing to the establishment of the Warburg phenotype that characterizes the cancer cell.

### 5.3 G3BP1, A $\beta$ -mRNABP INVOLVED IN BREAST CANCER PROGRESSION

Albeit G3BP1 is apparently involved in tumorigenesis, to date there has been only one study (Zhang et al., 2007c) exploring the potential prognostic impact of G3BP1 in patients with cancer. The data presented by Zhang et al. indicated that G3BP1 is a prognostic factor in esophageal squamous carcinomas, because a high G3BP1 expression in the tumor correlates with reduced overall survival rate of the patients (Zhang et al., 2007c).

In the present study, we have analyzed the clinical relevance of G3BP1 in human breast cancer. We underlined the tissue specific over-expression of G3BP1 in human breast cancer (Barnes et al., 2002; French et al., 2002). Moreover, we found that G3BP1 is a prognostic factor of breast tumor progression, as a high expression of G3BP1 correlates with reduced overall survival and predicts a significant higher risk of disease recurrence for the patients. Importantly, cluster analysis of a group of patients with good prognosis, as assessed by the bioenergetic signature of their tumors, revealed that a high G3BP1 expression determines both a worse prognosis and a significant higher risk of disease recurrence. This finding suggests that G3BP1 expression may be switched on early in the progress of tumorigenesis, indicating that G3BP1 could be a useful marker for the detection of early stage breast cancer patients with worse prognosis. In addition, the normalized expression of  $\beta$ -F1-ATPase was significantly reduced in these patients. The latter

finding, together with the observation that  $\beta$ -F1-ATPase and G3BP1 inversely correlate with each other in the cohort of cancer patients analyzed further supports the assumption that G3BP1 represses translationally the expression of  $\beta$ -F1-ATPase in breast cancer, contributing in this way to the metabolic reprogramming experienced by this tumor tissue (Isidoro et al., 2005).

Interestingly, in the cohort of breast cancer patients analyzed we observed a significant inverse correlation between the expression of G3BP1 and HuR. Multivariate Cox survival analysis leads us to speculate that the influence of G3BP1 on tumor progression might be indirectly influenced and/or superposed by the effect of a low HuR expression. A previous study from our laboratory analyzing the same breast cancer biopsies found that a low expression of HuR predicts a higher risk of disease recurrence and identified HuR as an independent marker of breast cancer prognosis (Ortega et al., 2008). An increased cytoplasmic expression of HuR in several tumor types has been reported to predict a worse prognosis for the patients (Erkinheimo et al., 2003; Heinonen et al., 2005; Mrena et al., 2005). Ortega et al. however, suggested that similar to a population of breast cancer cells that are neither dividing nor apoptotic, but are intensely motile and exhibit a decreased expression of IMP1 (Wang et al., 2004), a low expression of HuR could identify a subgroup of breast cancer patients with a high metastatic potential (Ortega et al., 2008). A recent report underlines this assumption, showing that high HuR expression in human breast cancer patients predicts a favorable prognosis, and remarkably those patients who died of breast cancer and developed metastasis revealed significantly lowers levels of HuR transcripts (Yuan et al., 2011). Consistent with Ortega's findings and suggestions (Ortega et al., 2008), HuR over-expressing cells transplanted into nude mice significantly reduced tumor growth presumably by blocking angiogenesis (Gubin et al., 2010).

The existence of a connection between G3BP1 and HuR in human breast cancer might not be surprising, given the functional and molecular similarities that exist between both RNABPs. G3BP1 and HuR are ubiquitously expressed RNABPs and, remarkably, both were identified as  $\beta$ -RNABPs (Ortega et al., 2008, Ortega, et al., 2010), even though the effect of HuR on  $\beta$ -F1-ATPase expression is controversial (Izquierdo, 2006; Ortega et al., 2008). Ortega et al. could not identify any specific influence of HuR on  $\beta$ -F1-ATPase expression (Ortega et al., 2008), whereas other authors reported a reduced expression of the protein after knocking down endogenous HuR (Izquierdo, 2006). In addition, HuR and G3BP1 are both involved in regulating c-myc mRNA expression (Ma et al., 1996; Tourriere et al., 2001), they form part of SGs (Gallouzi et al., 2000; Tourriere et al., 2003), co-purified with FMRP-RNP (Khandjian et al., 2004) and with a RNP particle that contains tau mRNA (Atlas et al., 2004) and controls tau mRNA translation and location (Atlas et al., 2007). Altogether, it is tempting to speculate that G3BP1 and HuR might influence in opposite ways the activity of a not yet identified protein and/or signaling pathway that favors breast tumorigenesis. Within this context, G3BP1 has been implicated in pathways involving cytoskeletal dynamics (Leblanc et al., 1998; Meng et al., 2004; Atlas et al., 2007; Hara et al., 2007; Solomon et al., 2007; Anderson and Kedersha, 2009), and it is well established that cytoskeletal rearrangement is involved in tumor

metastasis. Intriguingly, a recent paper indicates a link between G3BP1 and cell invasion, because BART (Binder of Arl 2) mRNA can be cleaved *in vitro* by G3BP1, and siRNA mediated knock down of BART increases cell motility and invasion (Taniuchi et al., 2011). Thus, G3BP1 might be involved in supporting the proposed high metastatic phenotype of low expressing HuR breast cancer patients (Ortega et al., 2008). In this regard, it would be interesting to analyze the effect of G3BP1 expression on cellular invasion and metastatic behavior.

Still, one of the principal challenges in cancer pathology is the identification of cancer type specific biomarkers that could provide reliable prognostic and predictive information. In this regard, the data presented in this study indicate that G3BP1 might be used as a potential diagnostic marker identifying in particular breast cancer patients on the early stage of disease that have higher chances of developing metastasis. Furthermore, and together with the recently suggested strategies aimed at targeting the energetic metabolism of tumors (Cuezva et al., 2009; Hanahan and Weinberg, 2011), our finding that G3BP1 participates in the regulation of cellular energetic metabolism makes of G3BP1 a strong candidate for novel anti-cancer therapy.

#### **5.4 THE ROLE OF miR-127-5p IN CONTROLLING $\beta$ -F1-ATPase EXPRESSION: THE BIOGENESIS OF MITOCHONDRIA DURING HUMAN LIVER DEVELOPMENT**

Translational control of specific mRNAs could be explained by the action of regulatory proteins as well as by miRNAs, both binding *cis*-acting elements within the mRNA. Therefore, in the present thesis we questioned whether in addition to the reported participation of RNABPs (Izquierdo and Cuezva, 1997; Ricart et al., 2002; Ortega et al., 2010) miRNAs might be involved in the post-transcriptional control of  $\beta$ -F1-ATPase expression. miRNAs were first discovered in *C. elegans* as important regulators of developmental timing (Lee et al., 1993; Reinhart et al., 2000). Nowadays, it has become apparent that miRNAs are as RNABPs important post-transcriptional regulatory factors that are involved in multiple biological processes including proliferation, apoptosis and cellular differentiation. Moreover, changes in miRNA expression are associated with pathogenesis in various human diseases such as cancer. (Alvarez-Garcia and Miska, 2005; Zhang et al., 2007a; Garzon et al., 2009; Krol et al., 2010).

Of the seven miRNAs chosen according to the bioinformatic study as putative  $\beta$ -mRNA miRNAs, in the present study we found that only miR-127-5p interferes with  $\beta$ -F1-ATPase expression and binds to the 3'UTR of human  $\beta$ -mRNA. In contrast to a recent report in HeLa cells, we have not identified a role of miR-101 as a post-transcriptional regulator of  $\beta$ -F1-ATPase expression (Zheng et al., 2011) perhaps due to differences in the cell type and/or the methodology used. Generally, miRNAs silence gene expression post-transcriptionally either by induction of mRNA degradation or by inhibition of translation (Humphreys et al., 2005; Lim et al., 2005; Bagga et al., 2005; Eulalio et al., 2009; Fabian et al., 2010). We illustrate that expression of miR-127-5p brings about a profound

decrease in the steady state level of endogenous  $\beta$ -F1-ATPase without changes in the mRNA level, demonstrating that miR-127-5p represses  $\beta$ -mRNA translation (Fig. 5.1A). Interestingly, transfection of miR-127-5p in BT549 cells had no effect on the oxygen consumption rate, maybe due the highly glycolytic phenotype of this cell line that may superimpose the changes in mitochondrial respiration.

So far, functional studies have been performed on miR-127-3p that derives from the 3'arm of the pre-miRNA hairpin precursor. These studies demonstrated a role for miR-127-3p in fetal lung development of the rat (Bhaskaran et al., 2009), B-cell differentiation (Leucci et al., 2010) and in down-regulating the proto-oncogene BCL6 (Saito et al., 2006). The miR-127 gene is embedded in a CpG island (Saito et al., 2006). Therefore, and contrary to miR-127-3p expression in normal fibroblasts, its expression was shown to be silenced in some cancer cell lines probably due to hypermethylation of the promoter (Saito et al., 2006). In agreement with this observation, we were not able to detect any significant miR-127-5p expression in the human cancer cell lines examined in this study, suggesting that miR-127-5p plays no relevant role in controlling  $\beta$ -F1-ATPase expression during oncogenesis, and thus in promoting the bioenergetic switch that occurs during cellular transformation in these cancer cell lines. Nevertheless, it should be noted that cancer is a set of heterogenous diseases with vast molecular and biological differences and causes, and even though the miR-127 is localized within a CpG island (Saito et al., 2006), over-expression of the miR-127-3p has been reported in invasive squamous cell carcinomas (Lee et al., 2008; Zhang et al., 2010) and miR-127-5p expression was shown to be upregulated in melanoma progression (Philippidou et al., 2010).

In addition to neoplastic cells,  $\beta$ -mRNA was shown to accumulate in fetal rat liver in a translational repressed state until the time of birth, when its translation is activated (1995; Luis et al., 1993; Izquierdo et al., Ostronoff et al., 1996) to promote transformation of pre-existent fetal mitochondria into fully active organelles (Valcarce et al., 1988; Izquierdo et al., 1995; Ostronoff et al., 1996; Cuezva et al., 1997; Lin et al., 2003).

Remarkably, we observed that miR-127-5p is expressed in fetal human and rat liver, suggesting that attenuation of  $\beta$ -mRNA translation by miR-127-5p might be of physiological relevance during liver development. Indeed, fetal rat tissues are highly glycolytic (Burch et al., 1963; Hommes, 1975; Cuezva et al., 1997), and both the number and the bioenergetic activity of fetal mitochondria are very low (Valcarce et al., 1988; Cuezva et al., 1997). Birth triggers the adaption to an increased aerobic environment by promoting the differentiation of mitochondria and the rapid onset of oxidative phosphorylation (Cuezva et al., 1997; Izquierdo et al., 1995; Nakai et al., 2000; Valcarce et al., 1988) by concerted transcriptional and post-transcriptional activation of the nuclear and mitochondrial genomes (Luis et al., 1993; Izquierdo et al., 1995; Ostronoff et al., 1995; Ostronoff et al., 1996). Consistent with these findings in rat, the present study illustrates that OXPHOS proteins were hardly expressed in fetal liver experiencing an increase in their expression in adult liver. Importantly, the  $\beta$ -F1-ATPase/Hsp60 ratio, which illustrates the energetic competence of the mitochondria, increased significantly postnatal, indicating that pre-existent human fetal liver

mitochondria are deficient in their functionality resembling very much the findings obtained previously in developing rat liver (Cuezva et al., 1997). Interestingly, we observed that the steady state level of the glycolytic enzymes GAPDH and LDH-A also increased in adult liver. This may suggest a general metabolic activation in the adult hepatocyte as a result of cellular hypertrophy.

Recent reports demonstrated that the activity of OXPHOS complexes increase significantly in postnatal liver, brain, muscle and heart tissues of humans (Minai et al., 2008; Pejznochova et al., 2010). In this work, we found hints that in humans, as it is the case in rat, transcriptional and post-transcriptional levels of regulation control the gene expression program that accounts for the differentiation of mitochondria. In this regard, SDH-B that is responsible for the transfer of electrons from succinate to coenzyme Q at complex II experienced a burst in its expression in adult liver. Concurrently, adult liver SDH-B mRNA level was increased indicating an enhanced transcription rate and/or increased mRNA half-life that in turn favors a higher synthesis rate of the mitochondrial protein in adult liver. On the other hand, and consistent with findings in rat liver (Luis et al., 1993; Izquierdo et al., 1995), we observed a high steady state  $\beta$ - and  $\gamma$ -F1-ATPase mRNA level in contrast to a low protein expression during the fetal stage of liver development, indicating the relevance of post-transcriptional regulation for the expression of proteins of complex V in humans. In particular, this observation demonstrates that  $\beta$ -mRNA expression is not only translationally silenced in fetal rat liver (Luis et al., 1993; Izquierdo et al., 1995), but also in human hepatocytes during fetal development.

Thus, considering the expression of miR-127-5p in human fetal liver, we suggest that binding of miR-127-5p to the 3'UTR of  $\beta$ -mRNA (maybe in co-operation with RNABPs) mediates the silencing of  $\beta$ -F1-ATPase in human liver until the time of birth (Fig. 5.1A). After birth miR-127-5p and repressor RNABPs should be released to allow  $\beta$ -mRNA translation and the functional differentiation of mitochondria. In other words, we suggest that miR-127-5p is a likely candidate involved in the establishment of the bioenergetic function of the mitochondria in human hepatocytes during development (Fig. 5.1A). However, the proposed action of miR-127-5p appears to be specific for expression in humans as functional assays with the rat transcript revealed no effect of miR-127-5p in this species, most likely because the rat  $\beta$ -mRNA lacks one matching nucleotide in the seed of miR-127-5p (Hafner et al., 2010).

Remarkably, the promoters of human, rat and dog miR-127 gene can be activated by estrogen related receptor gamma ( $ERR\gamma$ ) and alpha ( $ERR\alpha$ ) transcription factors (Song and Wang, 2009) that are nuclear receptors acting as transcriptional activators. Functional and biochemical studies have shown that  $ERR\alpha$  is involved in several aspects of energy metabolism and mitochondrial biogenesis (Scarpulla, 2008). Together with PGC-1 $\alpha$ ,  $ERR\alpha$  is involved in the induction of the *ATP5B* gene that encodes  $\beta$ -F1-ATPase (Mootha et al., 2004; Schreiber et al., 2004). Thus, one can speculate that during the fetal stages of liver development,  $ERR\alpha$  simultaneously activates the transcription of  $\beta$ -F1-ATPase and miR-127-5p gene expression. This would promote the onset of mitochondrial biogenesis during development, yet ensuring at the same time a less functionality



of the organelles through translational repression of  $\beta$ -mRNA by miR-127-5p. After birth, cellular signaling might induce the release of miR-127-5p mediated silencing of  $\beta$ -mRNA translation. In this regard, miR-127-5p could be part of a cellular bioenergetic fine tuning program, operating in development as well as in human adult liver for adjusting the cell to changing energetic demands.

Taken together, translational control of  $\beta$ -mRNA in mammals is a general mechanism regulating its expression and thus controlling the energetic phenotype of the cell during proliferation (Martinez-Diez et al., 2006), development (Izquierdo et al., 1995; Luis et al., 1993) and oncogenesis (de Heredia et al., 2000; Willers et al., 2010). Translational masking of  $\beta$ -F1-ATPase mRNA is controlled by RNABPs like G3BP1 in neoplasia and/or miRNAs such as miR-127-5p during human liver development.

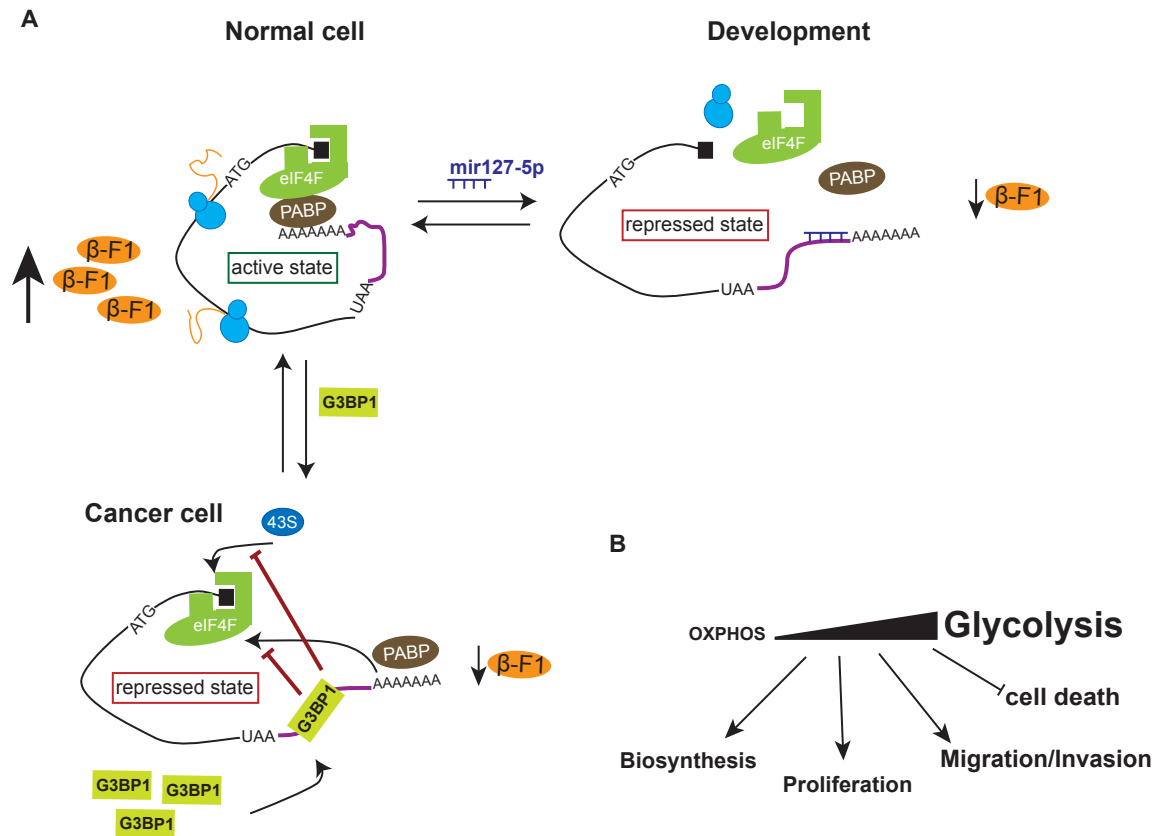


**Figure 5.1: Mechanisms that regulate  $\beta$ -mRNA translation in humans.** (A) The mRNA is efficiently translated in a circular way by the 5'–3' communication established by the interaction of the scaffolding eIF4F complex (green) and PABP (brown) (active state). Low  $\beta$ -F1-ATPase expression ( $\beta$ -F1, orange) in human fetal hepatocytes could result from binding of miR-127-5p (blue) to the 3'UTR (purple) of  $\beta$ -mRNA provoking the inhibition of  $\beta$ -mRNA translation (repressed state). G3BP1 plays a relevant role in mediating translational masking of  $\beta$ -mRNA in human cancer cells provoking the down-regulation of  $\beta$ -F1-ATPase. G3BP1 binds to the 3'UTR of  $\beta$ -mRNA inhibiting the translation of the transcript at the level of initiation. Mechanistically, G3BP1 binding could prevent either the interaction of the mRNA with the 43S ribosome and/or hindering mRNA circularization. Ribosome, blue; 5'cap, black square (B) Down-regulation of  $\beta$ -F1-ATPase contributes to the reprogramming of cellular energy metabolism from oxidative phosphorylation (OXPHOS) to an enhanced glycolysis, which supports biosynthetic processes and proliferation, migration, invasion and an apoptotic resistant phenotype. Overall the control of  $\beta$ -mRNA translation is a complex network of regulatory factors that allow the fine-tuning of energetic metabolism to changing cellular constitions.

## 5.5 WHY IS THE BIOENERGETIC FUNCTION OF MITOCHONDRIA REPRESSED IN CANCER?

Apparently, the enhanced aerobic glycolysis and a repressed bioenergetic function of mitochondria confer to the transformed cancer cell a significant growth advantage (Cuezva et al., 2009; Gatenby and Gillies, 2004; Sanchez-Arago et al., 2010). But why is it advantageous for the tumor cell to change the energetic metabolism and repress selectively the expression of  $\beta$ -F1-ATPase?

Although glycolysis is the less efficient way to produce energy, it is sufficient to cover the energetic demands of a cell as long as the supply of glucose is not restricted. Moreover glycolysis is the pathway that supplies metabolic intermediates to allow proliferation (Plas and Thompson, 2005; Cuezva et al., 2009; Ortega et al., 2009). In fact, glycolysis supports the anabolic demands of highly proliferating cells by providing precursors and reducing power needed for the augmented biosynthetic processes (DeBerardinis et al., 2008; Ortega et al., 2009) (Fig. 5.1B and Fig. 1.1). Furthermore, genetic and chemical induced mitochondrial dysfunction (Amuthan et al., 2001; Guha et al., 2010; Moro et al., 2009; Pelicano et al., 2009; Sanchez-Arago et al., 2010) as well as acidification of the microenvironment caused by an increased lactate production (Gatenby and Gillies, 2004) are known to favor tumor invasion and progression (Fig. 5.1B). A lesser dependence on oxidative phosphorylation becomes in fact advantageous in the generally hypoxic and acidic tumor microenvironment (Gatenby and Gillies, 2004; Sanchez-Arago et al., 2010). Furthermore, and perhaps most importantly, increased glycolysis and a silenced oxidative phosphorylation confer the cells with an apoptotic resistant phenotype (Park et al., 2004; Santamaria et al., 2006; Vander Heiden et al., 2001; Vaughn and Deshmukh, 2008) (Fig. 5.1B). In fact, cell death after acute growth factor withdrawal can be suppressed by upregulation of glycolysis (Vander Heiden et al., 2001; Plas et al., 2001; Rathmell et al., 2003), and notably it has been demonstrated in yeast, mammalian and plant cells that the execution of cell death requires a functional oxidative phosphorylation (Chivasa et al., 2011; Dey and Moraes, 2000; Matsuyama et al., 1998; Santamaria et al., 2006; Tomiyama et al., 2006). In particular, the molecular components and activity of the  $H^+$ -ATP synthase are needed to execute efficient cell death (Matsuyama et al., 1998; Harris et al., 2000; Santamaria et al., 2006; Sanchez-Arago and Cuezva, 2011; Chivasa et al., 2011). In this regard, Bax toxicity was reduced in yeast strains lacking the ability of oxidative phosphorylation (Harris et al., 2000) and Bax induced cell killing was dependent upon the  $\beta$ -F1-ATPase and other mitochondrial components (Gross et al., 2000). Likewise,  $\beta$ -F1-ATPase knocked out plants were resistant to drug-induced cell death (Chivasa et al., 2011) and treatment of yeast and mammalian cells with OXPHOS inhibitors delays or inhibits apoptosis (Matsuyama et al., 1998; Santamaria et al., 2006; Sanchez-Arago and Cuezva, 2011; Sanchez-Arago et al., 2010).

Mechanistically, our group has proposed that the  $H^+$ -ATP synthase controls the generation of ROS after priming the cells with death-inducing agents (Santamaria et al., 2006; Sanchez-Arago et al., 2010). The generated ROS in turn promote severe oxidative damage on cellular and mitochondrial proteins and contribute to effectively swamp the cell into death (Sanchez-Arago et al., 2010;

Santamaria et al., 2006). However, it should be noted that ROS act as a double-edged sword in cell physiology, and the cell fate appears to depend upon the level and duration of the ROS signal (Hamanaka and Chandel, 2010). Large amounts of ROS can be detrimental and trigger cell death (Santamaria et al., 2006; Vaughn and Deshmukh, 2008; Sanchez-Arago et al., 2010), whereas a transient ROS signal tolerated by the antioxidant defense of the cell can signal to pathways that allow proliferation and survival (Brunelle et al., 2005; Giannoni et al., 2005; Guzy and Schumacker, 2006; Morgan and Liu, 2011) and might favor the tumorigenic and metastatic potential of the cancer cell (Szatrowski and Nathan, 1991; Ishikawa et al., 2008; Pelicano et al., 2009).

Recently we have demonstrated that IF1, which is over-expressed in different human tumors (Sanchez-Cenizo et al., 2010), triggers a decrease in the activity of the H<sup>+</sup>-ATP synthase (Sanchez-Cenizo et al., 2010) provoking an increase of the mitochondrial membrane potential and a concurrent a higher production of ROS (Sanchez-Cenizo et al., 2010; Formentini et al., 2011). The higher levels of ROS, however, have been associated with activation of the NF-κB pathway and the induction of anti-apoptotic genes, strongly suggesting the participation of IF1 in generating a retrograde ROS signaling to the nucleus (Butow and Avadhani, 2004) to mediate cell survival (Formentini et al., 2011). Within this context, tumor cells have developed mechanisms to balance toxic ROS levels. Especially HIF1α, which is activated as a result of the limited oxygen conditions in the tumor microenvironment, reduces by several mechanisms mitochondrial oxidative phosphorylation and regulates the production of ROS (Semenza, 2010). Otherwise, exposure of HIF1α-deficient fibroblasts to chronic hypoxia results in cell death due to excessive levels of ROS (Kim et al., 2006). Furthermore, transformed cells counteract the accumulation of ROS by upregulating the antioxidant defense, such as glutathion (GSH) and thioredoxin (TRX) systems (Vaughn and Deshmukh, 2008). Importantly, activity of the GSH and TRX systems is driven by NADPH that is generated by metabolism of glucose in the pentose phosphate pathway. Consistently, upregulation of the glycolytic pathway in cancer cells triggers the production of NADPH by the PPP counteracting thereby oxidative stress induced apoptosis and promoting cell survival (Bolanos et al., 2008; Kim et al., 2007; Vaughn and Deshmukh, 2008).

Taken together, we assume that down-regulation of oxidative phosphorylation, specifically through selective translational repression of the catalytic subunit of the H<sup>+</sup>-ATP synthase (β-F1-ATPase) and/or by inhibition of its activity through IF1 (Sanchez-Cenizo et al., 2010) is advantageous to cancer growth making the cancer cell resistant to ROS mediated mitochondria dependent cell death contributing to the promotion of tumor progression.





# **CONCLUSIONS**

---

**A translation of this chapter into spanish can be found on page 131.**



## 6 CONCLUSIONS

1. Inhibition of the translation of  $\beta$ -F1-ATPase mRNA promotes the down-regulation of its expression in human breast, lung, esophageal and colon cancer.
2. The 3'UTR of human  $\beta$ -mRNA is a relevant *cis*-acting element required for its efficient translation, yet inhibition of human  $\beta$ -mRNA requires the participation additional *cis*-elements of the full-length transcript.
3. RNA-immunoprecipitation, fluorescence *in situ* hybridization and trimolecular fluorescence complementation assay demonstrate that RasGAP SH3 binding protein 1 (G3BP1) interacts with  $\beta$ -mRNA in the cellular context. G3BP1 binds the 3'UTR of the transcript and inhibits  $\beta$ -mRNA translation both *in vitro* and *in vivo* assays. Inhibition of  $\beta$ -mRNA translation by G3BP1 is exerted at the initiation step. We suggest that G3BP1 is a likely candidate participating in modifying the bioenergetic signature of the cell and thus in promoting the metabolic switch that occurs in cancer.
4. We confirmed that G3BP1 is over-expressed in human breast cancer. Furthermore, a high G3BP1 expression in a cohort of breast tumors predicts a worse overall and disease-free survival for the patients. Moreover, a high expression of G3BP1 is associated with a greater chance of developing metastatic disease in good prognosis patients, as assessed by the bioenergetic phenotype. Overall, G3BP1 could provide a relevant target for the anti-cancer therapy.
5. We have developed cellular systems to analyze the role of miRNAs in  $\beta$ -F1-ATPase expression. We show that miR-127-5p targets the 3'UTR of human  $\beta$ -mRNA and inhibits its translation. miR-127-5p is expressed in fetal liver but not in human cancer cells. miR-101, miR-103, miR-186, miR-200b, miR-423-5p and miR-581 have no effect on  $\beta$ -F1-ATPase expression.
6. In human fetal liver the expression of  $\beta$ -F1-ATPase appears to be controlled at post-transcriptional levels. The expression of miR-127-5p in fetal liver strongly suggests a potential regulatory role for this miRNA in controlling the translation of  $\beta$ -mRNA. In this situation, miR-127-5p could represent a relevant regulator of the bioenergetic differentiation of human liver mitochondria after birth.





# **CONCLUSIONES**

---



## 6 CONCLUSIONES

1. La inhibición de la traducción del mRNA de  $\beta$ -F1-ATPasa promueve la disminución de su expresión en cáncer de mama humano, pulmón, esófago y colon.
2. El 3'UTR del  $\beta$ -mRNA humano es un elemento de secuencia relevante necesario para una traducción eficiente, aunque la inhibición del  $\beta$ -mRNA humano requiere la participación de otros elementos *cis* adicionales del transcrito completo.
3. Ensayos de inmunoprecipitación de RNA, de hibridación *in situ* con sondas fluorescentes y de complementación trimolecular de fluorescencia han mostrado que la proteína de unión RasGAP SH3 1 (G3BP1) interacciona con  $\beta$ -mRNA en el contexto celular. G3BP1 se une al 3'UTR del transcrito e inhibe la traducción de  $\beta$ -mRNA tanto en ensayos *in vitro* como *in vivo*. La inhibición de la traducción de  $\beta$ -mRNA por G3BP1 se lleva a cabo en la fase de iniciación. A la luz de estos resultados, sugerimos la participación de G3BP1 en la modificación de la huella bioenergética de la célula y, por lo tanto, en la promoción del cambio metabólico que ocurre en cáncer.
4. Confirmamos que G3BP1 se encuentra sobreexpresada en cáncer humano de mama. Más aún, una alta expresión de G3BP1 se relaciona con un pronóstico desfavorable de los pacientes, mostrando una menor supervivencia global y supervivencia libre de enfermedad. Además, una alta expresión de G3BP1 está relacionada con una mayor probabilidad de desarrollo de metástasis en pacientes de buen pronóstico, evaluado éste mediante el fenotipo bioenergético. En resumen, G3BP1 podría ser una diana molecular relevante para la terapia contra el cáncer.
5. Hemos desarrollado sistemas celulares para analizar el papel de los miRNA en la expresión de  $\beta$ -F1-ATPasa. Demostramos que miR-127-5p inhibe la traducción de  $\beta$ -mRNA a través de su unión al 3'UTR. miR-127-5p se expresa en hígado fetal pero no en líneas celulares humanas de cáncer. miR-101, miR-103, miR-186, miR-200b, miR-423-5p y miR-581 no tienen ningún efecto en la expresión de  $\beta$ -F1-ATPasa.
6. En hígado fetal humano la expresión de  $\beta$ -F1-ATPasa está controlada a nivel post transcripcional. La expresión de miR-127-5p en hígado fetal sugiere un potencial papel regulador de este miRNA en el control de la traducción de  $\beta$ -mRNA. En este caso, miR-127-5p podría ser un regulador relevante de la diferenciación bioenergética de las mitocondrias del hígado humano tras el nacimiento.



# **BIBLIOGRAPHY**

---

---



- Abrahams, J. P., Leslie, A. G., Lutter, R. and Walker, J. E.** (1994). Structure at 2.8 Å resolution of F1-ATPase from bovine heart mitochondria. *Nature* **370**, 621-628
- Adereth, Y., Dammai, V., Kose, N., Li, R. and Hsu, T.** (2005). RNA-dependent integrin alpha3 protein localization regulated by the Muscleblind-like protein MLP1. *Nat Cell Biol* **7**, 1240-7.
- Alvarez-Garcia, I. and Miska, E. A.** (2005). MicroRNA functions in animal development and human disease. *Development* **132**, 4653-62.
- Amuthan, G., Biswas, G., Zhang, S. Y., Klein-Szanto, A., Vijayasarathy, C. and Avadhani, N. G.** (2001). Mitochondria-to-nucleus stress signaling induces phenotypic changes, tumor progression and cell invasion. *EMBO J* **20**, 1910-20.
- Anderson, P. and Kedersha, N.** (2009). RNA granules: post-transcriptional and epigenetic modulators of gene expression. *Nat Rev Mol Cell Biol* **10**, 430-6.
- Atlas, R., Behar, L., Elliott, E. and Ginzburg, I.** (2004). The insulin-like growth factor mRNA binding-protein IMP-1 and the Ras-regulatory protein G3BP associate with tau mRNA and HuD protein in differentiated P19 neuronal cells. *J Neurochem* **89**, 613-26.
- Atlas, R., Behar, L., Sapoznik, S. and Ginzburg, I.** (2007). Dynamic association with polysomes during P19 neuronal differentiation and an untranslated-region-dependent translation regulation of the tau mRNA by the tau mRNA-associated proteins IMP1, HuD, and G3BP1. *J Neurosci Res* **85**, 173-83.
- Bacolod, M. D. and Barany, F.** (2010). Gene dysregulations driven by somatic copy number aberrations-biological and clinical implications in colon tumors: a paper from the 2009 William Beaumont Hospital Symposium on Molecular Pathology. *J Mol Diagn* **12**, 552-61.
- Bagga, S., Bracht, J., Hunter, S., Massirer, K., Holtz, J., Eachus, R. and Pasquinelli, A. E.** (2005). Regulation by let-7 and lin-4 miRNAs results in target mRNA degradation. *Cell* **122**, 553-63.
- Baggetto, L. G.** (1992). Deviant energetic metabolism of glycolytic cancer cells. *Biochimie* **74**, 959-74.
- Bardwell, V. J. and Wickens, M.** (1990). Purification of RNA and RNA-protein complexes by an R17 coat protein affinity method. *Nucleic Acids Res* **18**, 6587-94.
- Barnes, C. J., Li, F., Mandal, M., Yang, Z., Sahin, A. A. and Kumar, R.** (2002). Heregulin induces expression, ATPase activity, and nuclear localization of G3BP, a Ras signaling component, in human breast tumors. *Cancer Res* **62**, 1251-5.
- Benard, G., Bellance, N., James, D., Parrone, P., Fernandez, H., Letellier, T. and Rossignol, R.** (2007). Mitochondrial bioenergetics and structural network organization. *J Cell Sci* **120**, 838-48.
- Bensaad, K., Tsuruta, A., Selak, M. A., Vidal, M. N., Nakano, K., Bartrons, R., Gottlieb, E. and Vousden, K. H.** (2006). TIGAR, a p53-inducible regulator of glycolysis and apoptosis. *Cell* **126**, 107-20.



- Bernstein, P. L., Herrick, D. J., Prokipcak, R. D. and Ross, J.** (1992). Control of c-myc mRNA half-life in vitro by a protein capable of binding to a coding region stability determinant. *Genes Dev.* **6**, 642-654.
- Bertrand, E., Chartrand, P., Schaefer, M., Shenoy, S. M., Singer, R. H. and Long, R. M.** (1998). Localization of ASH1 mRNA particles in living yeast. *Mol. Cell* **2**, 437-445.
- Bhaskaran, M., Wang, Y., Zhang, H., Weng, T., Baviskar, P., Guo, Y., Gou, D. and Liu, L.** (2009). MicroRNA-127 modulates fetal lung development. *Physiol Genomics* **37**, 268-78.
- Bi, X., Lin, Q., Foo, T. W., Joshi, S., You, T., Shen, H. M., Ong, C. N., Cheah, P. Y., Eu, K. W. and Hew, C. L.** (2006). Proteomic analysis of colorectal cancer reveals alterations in metabolic pathways: mechanism of tumorigenesis. *Mol Cell Proteomics* **5**, 1119-30.
- Bolanos, J. P., Delgado-Esteban, M., Herrero-Mendez, A., Fernandez-Fernandez, S. and Almeida, A.** (2008). Regulation of glycolysis and pentose-phosphate pathway by nitric oxide: impact on neuronal survival. *Biochim Biophys Acta* **1777**, 789-93.
- Bonnet, S., Archer, S. L., Allalunis-Turner, J., Haromy, A., Beaulieu, C., Thompson, R., Lee, C. T., Lopaschuk, G. D., Puttagunta, L., Bonnet, S. et al.** (2007). A mitochondria-K<sup>+</sup> channel axis is suppressed in cancer and its normalization promotes apoptosis and inhibits cancer growth. *Cancer Cell* **11**, 37-51.
- Bonora E, Porcelli AM, Gasparre G, Biondi A, Ghelli A, Carelli V, Baracca A, Tallini G, Martinuzzi A, Lenaz G, Rugolo M, Romeo G.** (2006) Defective oxidative phosphorylation in thyroid oncocyctic carcinoma is associated with pathogenic mitochondrial DNA mutations affecting complexes I and III. *Cancer Res.* **66**, 6087-96.
- Borer, R. A., Lehner, C. F., Eppenberger, H. M. and Nigg, E. A.** (1989). Major nucleolar proteins shuttle between nucleus and cytoplasm. *Cell* **56**, 379-90.
- Boyer, P. D.** (1993). The binding change mechanism for ATP synthase--some probabilities and possibilities. *Biochim. Biophys. Acta* **1140**, 215-250.
- Boyer, P. D.** (1997). The ATP synthase. A splendid molecular machine. *Annu. Rev. Biochem.* **66**, 717-749.
- Brady, S. N., Yu, Y., Maggi, L. B., Jr. and Weber, J. D.** (2004). ARF impedes NPM/B23 shuttling in an Mdm2-sensitive tumor suppressor pathway. *Mol Cell Biol* **24**, 9327-38.
- Brand, K., Aichinger, S., Forster, S., Kupper, S., Neumann, B., Nurnberg, W. and Ohrisch, G.** (1988). Cell-cycle-related metabolic and enzymatic events in proliferating rat thymocytes. *Eur J Biochem* **172**, 695-702.
- Brand, K. A. and Hermfisse, U.** (1997). Aerobic glycolysis by proliferating cells: a protective strategy against reactive oxygen species. *FASEB J.* **11**, 388-395.

- Brandon, M., Baldi, P. and Wallace, D. C.** (2006). Mitochondrial mutations in cancer. *Oncogene* **25**, 4647-62.
- Brennecke, J., Stark, A., Russell, R. B. and Cohen, S. M.** (2005). Principles of microRNA-target recognition. *PLoS Biol* **3**, e85.
- Brunelle, J. K., Bell, E. L., Quesada, N. M., Vercauteren, K., Tiranti, V., Zeviani, M., Scarpulla, R. C. and Chandel, N. S.** (2005). Oxygen sensing requires mitochondrial ROS but not oxidative phosphorylation. *Cell Metab* **1**, 409-14.
- Burch, H. B., Lowry, O. H., Kuhlman, A. M., Skerjance, J., Diamant, E. J., Lowry, S. R. and Von Dippe, P.** (1963). Changes in patterns of enzymes of carbohydrate metabolism in the developing rat liver. *J Biol Chem* **238**, 2267-73.
- Butow, R. A. and Avadhani, N. G.** (2004). Mitochondrial signaling: the retrograde response. *Mol Cell* **14**, 1-15.
- Cabezón, E., Butler, P. J., Runswick, M. J. and Walker, J. E.** (2000). Modulation of the oligomerization state of the bovine F1-ATPase inhibitor protein, IF1, by pH. *J Biol Chem* **275**, 25460-4.
- Capaldi, R. A. and Aggeler, R.** (2002). Mechanism of the F(1)F(0)-type ATP synthase, a biological rotary motor. *Trends Biochem Sci* **27**, 154-60.
- Carew, J. S. and Huang, P.** (2002). Mitochondrial defects in cancer. *Mol Cancer* **1**, 9.
- Carew, J. S., Zhou, Y., Albitar, M., Carew, J. D., Keating, M. J. and Huang, P.** (2003). Mitochondrial DNA mutations in primary leukemia cells after chemotherapy: clinical significance and therapeutic implications. *Leukemia* **17**, 1437-47.
- Colombo, E., Marine, J. C., Danovi, D., Falini, B. and Pelicci, P. G.** (2002). Nucleophosmin regulates the stability and transcriptional activity of p53. *Nat Cell Biol* **4**, 529-33.
- Copeland, W. C., Wachsman, J. T., Johnson, F. M. and Penta, J. S.** (2002). Mitochondrial DNA alterations in cancer. *Cancer Invest* **20**, 557-69.
- Corral-Debrinski, M., Blugeon, C. and Jacq, C.** (2000). In yeast, the 3' untranslated region or the presequence of ATM1 is required for the exclusive localization of its mRNA to the vicinity of mitochondria. *Mol Cell Biol* **20**, 7881-7892.
- Cuezva, J. M., Chen, G., Alonso, A. M., Isidoro, A., Misek, D. E., Hanash, S. M. and Beer, D. G.** (2004). The bioenergetic signature of lung adenocarcinomas is a molecular marker of cancer diagnosis and prognosis. *Carcinogenesis* **25**, 1157-63.
- Cuezva, J. M., Krajewska, M., de Heredia, M. L., Krajewski, S., Santamaria, G., Kim, H., Zapata, J. M., Marusawa, H., Chamorro, M. and Reed, J. C.** (2002). The bioenergetic signature of cancer: a marker of tumor progression. *Cancer Res* **62**, 6674-81.

- Cuezva, J. M., Ortega, A. D., Willers, I., Sanchez-Cenizo, L., Aldea, M. and Sanchez-Arago, M.** (2009). The tumor suppressor function of mitochondria: Translation into the clinics. *Biochim Biophys Acta* **1792**, 1145-1158.
- Cuezva, J. M., Ostronoff, L. K., Ricart, J., Lopez de Heredia, M., Di Liegro, C. M. and Izquierdo, J. M.** (1997). Mitochondrial biogenesis in the liver during development and oncogenesis. *J Bioenerg Biomembr* **29**, 365-77.
- Cuezva, J. M., Sanchez-Arago, M., Sala, S., Blanco-Rivero, A. and Ortega, A. D.** (2007). A message emerging from development: the repression of mitochondrial beta-F1-ATPase expression in cancer. *J Bioenerg Biomembr* **39**, 259-65.
- Czech, B., Zhou, R., Erlich, Y., Brennecke, J., Binari, R., Villalta, C., Gordon, A., Perrimon, N. and Hannon, G. J.** (2009). Hierarchical rules for Argonaute loading in Drosophila. *Mol Cell* **36**, 445-56.
- Chan, W. Y., Liu, Q. R., Borjigin, J., Busch, H., Rennert, O. M., Tease, L. A. and Chan, P. K.** (1989). Characterization of the cDNA encoding human nucleophosmin and studies of its role in normal and abnormal growth. *Biochemistry* **28**, 1033-9.
- Chan S.Y., Zhang Y.Y., Hemann C., Mahoney C.E., Zweier J.L., Loscalzo J.** (2009) MicroRNA-210 controls mitochondrial metabolism during hypoxia by repressing the iron-sulfur cluster assembly proteins ISCU1/2. *Cell Metab.* **10**, 273-84.
- Chen, J., Kahne, T., Rocken, C., Gotze, T., Yu, J., Sung, J. J., Chen, M., Hu, P., Malfertheiner, P. and Ebert, M. P.** (2004). Proteome analysis of gastric cancer metastasis by two-dimensional gel electrophoresis and matrix assisted laser desorption/ionization-mass spectrometry for identification of metastasis-related proteins. *J Proteome Res* **3**, 1009-16.
- Chen, Z., Li, Y., Zhang, H., Huang, P. and Luthra, R.** (2010). Hypoxia-regulated microRNA-210 modulates mitochondrial function and decreases ISCU and COX10 expression. *Oncogene* **29**, 4362-8.
- Chen, Z., Odstrcil, E. A., Tu, B. P. and McKnight, S. L.** (2007). Restriction of DNA replication to the reductive phase of the metabolic cycle protects genome integrity. *Science* **316**, 1916-9.
- Chiche, J., Rouleau, M., Gounon, P., Brahimi-Horn, M. C., Pouyssegur, J. and Mazure, N. M.** (2010). Hypoxic enlarged mitochondria protect cancer cells from apoptotic stimuli. *J Cell Physiol* **222**, 648-57.
- Chivasa, S., Tome, D. F., Hamilton, J. M. and Slabas, A. R.** (2011). Proteomic Analysis of Extracellular ATP-Regulated Proteins Identifies ATP Synthase {beta}-Subunit as a Novel Plant Cell Death Regulator. *Mol Cell Proteomics* **10**, M110 003905.
- Christofk, H. R., Vander Heiden, M. G., Harris, M. H., Ramanathan, A., Gerszten, R. E., Wei, R., Fleming, M. D., Schreiber, S. L. and Cantley, L. C.** (2008a). The M2 splice isoform of pyruvate kinase is important for cancer metabolism and tumour growth. *Nature* **452**, 230-3.

- Christofk, H. R., Vander Heiden, M. G., Wu, N., Asara, J. M. and Cantley, L. C.** (2008b). Pyruvate kinase M2 is a phosphotyrosine-binding protein. *Nature* **452**, 181-6.
- David, C. J., Chen, M., Assanah, M., Canoll, P. and Manley, J. L.** (2010). HnRNP proteins controlled by c-Myc deregulate pyruvate kinase mRNA splicing in cancer. *Nature* **463**, 364-8.
- de Groof, A. J., te Lindert, M. M., van Dommelen, M. M., Wu, M., Willemse, M., Smift, A. L., Winer, M., Oerlemans, F., Pluk, H., Fransen, J. A. et al.** (2009). Increased OXPHOS activity precedes rise in glycolytic rate in H-RasV12/E1A transformed fibroblasts that develop a Warburg phenotype. *Mol Cancer* **8**, 54.
- de Heredia, M. L., Izquierdo, J. M. and Cuezva, J. M.** (2000). A conserved mechanism for controlling the translation of beta-F1-ATPase mRNA between the fetal liver and cancer cells. *J Biol Chem* **275**, 7430-7.
- de Moor, C. H., Meijer, H. and Lissenden, S.** (2005). Mechanisms of translational control by the 3' UTR in development and differentiation. *Semin Cell Dev Biol* **16**, 49-58.
- DeBerardinis, R. J., Lum, J. J., Hatzivassiliou, G. and Thompson, C. B.** (2008). The biology of cancer: metabolic reprogramming fuels cell growth and proliferation. *Cell Metab* **7**, 11-20.
- DeBerardinis, R. J., Lum, J. J. and Thompson, C. B.** (2006). Phosphatidylinositol 3-kinase-dependent modulation of carnitine palmitoyltransferase 1A expression regulates lipid metabolism during hematopoietic cell growth. *J Biol Chem* **281**, 37372-80.
- DeBerardinis, R. J., Mancuso, A., Daikhin, E., Nissim, I., Yudkoff, M., Wehrli, S. and Thompson, C. B.** (2007). Beyond aerobic glycolysis: transformed cells can engage in glutamine metabolism that exceeds the requirement for protein and nucleotide synthesis. *Proc Natl Acad Sci U S A* **104**, 19345-50.
- del Arco, A. and Satrustegui, J.** (2004). Identification of a novel human subfamily of mitochondrial carriers with calcium-binding domains. *J Biol Chem* **279**, 24701-13.
- Deng, Y., Singer, R. H. and Gu, W.** (2008). Translation of ASH1 mRNA is repressed by Puf6p-Fun12p/eIF5B interaction and released by CK2 phosphorylation. *Genes Dev* **22**, 1037-50.
- Derdak, Z., Mark, N. M., Beldi, G., Robson, S. C., Wands, J. R. and Baffy, G.** (2008). The mitochondrial uncoupling protein-2 promotes chemoresistance in cancer cells. *Cancer Res* **68**, 2813-9.
- Deshler, J. O., Highett, M. I., Abramson, T. and Schnapp, B. J.** (1998). A highly conserved RNA-binding protein for cytoplasmic mRNA localization in vertebrates. *Curr. Biol.* **8**, 489-496.
- Dey, R. and Moraes, C. T.** (2000). Lack of oxidative phosphorylation and low mitochondrial membrane potential decrease susceptibility to apoptosis and do not modulate the protective effect of Bcl-x(L) in osteosarcoma cells. *J Biol Chem* **275**, 7087-94.

- Di Liegro, C. M., Bellafiore, M., Izquierdo, J. M., Rantanen, A. and Cuezva, J. M.** (2000). 3'-untranslated regions of oxidative phosphorylation mRNAs function in vivo as enhancers of translation. *Biochem J* **352 Pt 1**, 109-15.
- Dimitriadis, E., Trangas, T., Milatos, S., Foukas, P. G., Gioulbasanis, I., Courtis, N., Nielsen, F. C., Pandis, N., Dafni, U., Bardi, G. et al.** (2007). Expression of oncofetal RNA-binding protein CRD-BP/IMP1 predicts clinical outcome in colon cancer. *Int J Cancer* **121**, 486-94.
- Ding, D., Parkhurst, S. M., Halsell, S. R. and Lipshitz, H. D.** (1993). Dynamic Hsp83 RNA localization during *Drosophila* oogenesis and embryogenesis. *Mol Cell Biol* **13**, 3773-81.
- Doyle, G. A., Betz, N. A., Leeds, P. F., Fleisig, A. J., Prokipcak, R. D. and Ross, J.** (1998). The c-myc coding region determinant-binding protein: a member of a family of KH domain RNA-binding proteins. *Nucleic Acids Res* **26**, 5036-44.
- Driever, W. and Nusslein-Volhard, C.** (1988). The bicoid protein determines position in the *Drosophila* embryo in a concentration-dependent manner. *Cell* **54**, 95-104.
- Dumbar, T. S., Gentry, G. A. and Olson, M. O.** (1989). Interaction of nucleolar phosphoprotein B23 with nucleic acids. *Biochemistry* **28**, 9495-501.
- Ebert, B. L., Firth, J. D. and Ratcliffe, P. J.** (1995). Hypoxia and mitochondrial inhibitors regulate expression of glucose transporter-1 via distinct Cis-acting sequences. *J Biol Chem* **270**, 29083-9.
- Edinger, A. L. and Thompson, C. B.** (2002). Akt maintains cell size and survival by increasing mTOR-dependent nutrient uptake. *Mol Biol Cell* **13**, 2276-88.
- Egea, G., Izquierdo, J. M., Ricart, J., San Martin, C. and Cuezva, J. M.** (1997). mRNA encoding the beta-subunit of the mitochondrial F1-ATPase complex is a localized mRNA in rat hepatocytes. *Biochem J* **322 ( Pt 2)**, 557-65.
- Eliyahu, E., Pnueli, L., Melamed, D., Scherrer, T., Gerber, A. P., Pines, O., Rapaport, D. and Arava, Y.** (2010). Tom20 mediates localization of mRNAs to mitochondria in a translation-dependent manner. *Mol Cell Biol* **30**, 284-94.
- Elstrom, R. L., Bauer, D. E., Buzzai, M., Karnauskas, R., Harris, M. H., Plas, D. R., Zhuang, H., Cinalli, R. M., Alavi, A., Rudin, C. M. et al.** (2004). Akt stimulates aerobic glycolysis in cancer cells. *Cancer Res* **64**, 3892-9.
- Elvira, G., Wasiak, S., Blandford, V., Tong, X. K., Serrano, A., Fan, X., del Rayo Sanchez-Carbente, M., Servant, F., Bell, A. W., Boismenu, D. et al.** (2006). Characterization of an RNA granule from developing brain. *Mol Cell Proteomics* **5**, 635-51.
- Ephrussi, A., Dickinson, L. K. and Lehmann, R.** (1991). Oskar organizes the germ plasm and directs localization of the posterior determinant nanos. *Cell* **66**, 37-50.

- Erkinheimo, T. L., Lassus, H., Sivula, A., Sengupta, S., Furneaux, H., Hla, T., Haglund, C., Butzow, R. and Ristimaki, A.** (2003). Cytoplasmic HuR expression correlates with poor outcome and with cyclooxygenase 2 expression in serous ovarian carcinoma. *Cancer Res* **63**, 7591-4.
- Eulalio, A., Tritschler, F. and Izaurralde, E.** (2009). The GW182 protein family in animal cells: new insights into domains required for miRNA-mediated gene silencing. *RNA* **15**, 1433-42.
- Fabian, M. R., Sonenberg, N. and Filipowicz, W.** (2010). Regulation of mRNA translation and stability by microRNAs. *Annu Rev Biochem* **79**, 351-79.
- Fang, J. S., Gillies, R. D. and Gatenby, R. A.** (2008). Adaptation to hypoxia and acidosis in carcinogenesis and tumor progression. *Semin Cancer Biol* **18**, 330-7.
- Fantin, V. R., St-Pierre, J. and Leder, P.** (2006). Attenuation of LDH-A expression uncovers a link between glycolysis, mitochondrial physiology, and tumor maintenance. *Cancer Cell* **9**, 425-34.
- Fernandez-Vizarra, E., Enriquez, J. A., Perez-Martos, A., Montoya, J. and Fernandez-Silva, P.** (2011). Tissue-specific differences in mitochondrial activity and biogenesis. *Mitochondrion* **11**, 207-13.
- Feuerstein, N., Spiegel, S. and Mond, J. J.** (1988). The nuclear matrix protein, numatrin (B23), is associated with growth factor-induced mitogenesis in Swiss 3T3 fibroblasts and with T lymphocyte proliferation stimulated by lectins and anti-T cell antigen receptor antibody. *J Cell Biol* **107**, 1629-42.
- Filipowicz, W., Bhattacharyya, S. N. and Sonenberg, N.** (2008). Mechanisms of post-transcriptional regulation by microRNAs: are the answers in sight? *Nat Rev Genet* **9**, 102-14.
- Formentini, L., Sanchez-Aarago, M., Sanchez-Cenizo, L. and Cuezva, J. M.** (2011). The mitochondrial ATPase Inhibitory Factor 1 (IF1) triggers a ROS-mediated retrograde pro-survival and proliferative response. *Mol Cell* submitted.
- Forrest, K. M. and Gavis, E. R.** (2003). Live imaging of endogenous RNA reveals a diffusion and entrapment mechanism for nanos mRNA localization in *Drosophila*. *Curr Biol* **13**, 1159-68.
- French, J., Stirling, R., Walsh, M. and Kennedy, H. D.** (2002). The expression of Ras-GTPase activating protein SH3 domain-binding proteins, G3BPs, in human breast cancers. *Histochem J* **34**, 223-31.
- Fukuda, R., Zhang, H., Kim, J. W., Shimoda, L., Dang, C. V. and Semenza, G. L.** (2007). HIF-1 regulates cytochrome oxidase subunits to optimize efficiency of respiration in hypoxic cells. *Cell* **129**, 111-22.
- Funes, J. M., Quintero, M., Henderson, S., Martinez, D., Qureshi, U., Westwood, C., Clements, M. O., Bourbouli, D., Pedley, R. B., Moncada, S. et al.** (2007). Transformation of human mesenchymal stem cells increases their dependency on oxidative phosphorylation for energy production. *Proc Natl Acad Sci U S A* **104**, 6223-8.

- Galgano, A., Forrer, M., Jaskiewicz, L., Kanitz, A., Zavolan, M. and Gerber, A. P.** (2008). Comparative analysis of mRNA targets for human PUF-family proteins suggests extensive interaction with the miRNA regulatory system. *PLoS One* **3**, e3164.
- Gallardo, M. E., Moreno-Loshuertos, R., Lopez, C., Casqueiro, M., Silva, J., Bonilla, F., Rodriguez de Cordoba, S. and Enriquez, J. A.** (2006). m.6267G>A: a recurrent mutation in the human mitochondrial DNA that reduces cytochrome c oxidase activity and is associated with tumors. *Hum Mutat* **27**, 575-82.
- Gallie, D. R.** (1991). The cap and poly(A) tail function synergistically to regulate mRNA translational efficiency. *Genes Dev* **5**, 2108-16.
- Gallouzi, I. E., Brennan, C. M., Stenberg, M. G., Swanson, M. S., Eversole, A., Maizels, N. and Steitz, J. A.** (2000). HuR binding to cytoplasmic mRNA is perturbed by heat shock. *Proc Natl Acad Sci U S A* **97**, 3073-8.
- Gallouzi, I. E., Parker, F., Chebli, K., Maurier, F., Labourier, E., Barlat, I., Capony, J. P., Tocque, B. and Tazi, J.** (1998). A novel phosphorylation-dependent RNase activity of GAP-SH3 binding protein: a potential link between signal transduction and RNA stability. *Mol Cell Biol* **18**, 3956-65.
- Gao, P., Tchernyshyov, I., Chang, T. C., Lee, Y. S., Kita, K., Ochi, T., Zeller, K. I., De Marzo, A. M., Van Eyk, J. E., Mendell, J. T. et al.** (2009). c-Myc suppression of miR-23a/b enhances mitochondrial glutaminase expression and glutamine metabolism. *Nature* **458**, 762-5.
- Garber, K.** (2006). Energy deregulation: licensing tumors to grow. *Science* **312**, 1158-9.
- Garcia-Rodriguez, L. J., Gay, A. C. and Pon, L. A.** (2007). Puf3p, a Pumilio family RNA binding protein, localizes to mitochondria and regulates mitochondrial biogenesis and motility in budding yeast. *J Cell Biol* **176**, 197-207.
- Garcia, M., Darzacq, X., Delaveau, T., Jourden, L., Singer, R. H. and Jacq, C.** (2007). Mitochondria-associated yeast mRNAs and the biogenesis of molecular complexes. *Mol Biol Cell* **18**, 362-8.
- Garcia, M., Delaveau, T., Goussard, S. and Jacq, C.** (2010). Mitochondrial presequence and open reading frame mediate asymmetric localization of messenger RNA. *EMBO Rep* **11**, 285-91.
- Garesse, R. and Vallejo, C. G.** (2001). Animal mitochondrial biogenesis and function: a regulatory cross-talk between two genomes. *Gene* **263**, 1-16.
- Garzon, R., Calin, G. A. and Croce, C. M.** (2009). MicroRNAs in Cancer. *Annu Rev Med* **60**, 167-79.
- Gatenby, R. A. and Gillies, R. J.** (2004). Why do cancers have high aerobic glycolysis? *Nat Rev Cancer* **4**, 891-9.
- Gavis, E. R. and Lehmann, R.** (1992). Localization of nanos RNA controls embryonic polarity. *Cell* **71**, 301-13.

- Gerber, A. P., Herschlag, D. and Brown, P. O.** (2004). Extensive association of functionally and cytotopically related mRNAs with Puf family RNA-binding proteins in yeast. *PLoS Biol* **2**, E79.
- Ghildiyal, M., Xu, J., Seitz, H., Weng, Z. and Zamore, P. D.** (2009). Sorting of Drosophila small silencing RNAs partitions microRNA\* strands into the RNA interference pathway. *RNA* **16**, 43-56.
- Giannoni, E., Buricchi, F., Raugei, G., Ramponi, G. and Chiarugi, P.** (2005). Intracellular reactive oxygen species activate Src tyrosine kinase during cell adhesion and anchorage-dependent cell growth. *Mol Cell Biol* **25**, 6391-403.
- Gledhill, J. R., Montgomery, M. G., Leslie, A. G. and Walker, J. E.** (2007). How the regulatory protein, IF(1), inhibits F(1)-ATPase from bovine mitochondria. *Proc Natl Acad Sci U S A* **104**, 15671-6.
- Grimson, A., Farh, K. K., Johnston, W. K., Garrett-Engele, P., Lim, L. P. and Bartel, D. P.** (2007). MicroRNA targeting specificity in mammals: determinants beyond seed pairing. *Mol Cell* **27**, 91-105.
- Grisendi, S., Bernardi, R., Rossi, M., Cheng, K., Khandker, L., Manova, K. and Pandolfi, P. P.** (2005). Role of nucleophosmin in embryonic development and tumorigenesis. *Nature* **437**, 147-53.
- Gross, A., Pilcher, K., Blachly-Dyson, E., Basso, E., Jockel, J., Bassik, M. C., Korsmeyer, S. J. and Forte, M.** (2000). Biochemical and genetic analysis of the mitochondrial response of yeast to BAX and BCL-X(L). *Mol Cell Biol* **20**, 3125-36.
- Gu, L., Shigemasa, K. and Ohama, K.** (2004). Increased expression of IGF II mRNA-binding protein 1 mRNA is associated with an advanced clinical stage and poor prognosis in patients with ovarian cancer. *Int J Oncol* **24**, 671-8.
- Gubin, M. M., Calaluce, R., Davis, J. W., Magee, J. D., Strouse, C. S., Shaw, D. P., Ma, L., Brown, A., Hoffman, T., Rold, T. L. et al.** (2010). Overexpression of the RNA binding protein HuR impairs tumor growth in triple negative breast cancer associated with deficient angiogenesis. *Cell Cycle* **9**, 3337-46.
- Guha, M., Tang, W., Sondheimer, N. and Avadhani, N. G.** (2010). Role of calcineurin, hnRNPA2 and Akt in mitochondrial respiratory stress-mediated transcription activation of nuclear gene targets. *Biochim Biophys Acta* **1797**, 1055-65.
- Guitard, E., Parker, F., Millon, R., Abecassis, J. and Tocque, B.** (2001). G3BP is overexpressed in human tumors and promotes S phase entry. *Cancer Lett* **162**, 213-21.
- Gullino, P. M., Grantham, F. H. and Courtney, A. H.** (1967). Glucose consumption by transplanted tumors in vivo. *Cancer Res* **27**, 1031-40.
- Guzy, R. D., Hoyos, B., Robin, E., Chen, H., Liu, L., Mansfield, K. D., Simon, M. C., Hammerling, U. and Schumacker, P. T.** (2005). Mitochondrial complex III is required for hypoxia-induced ROS production and cellular oxygen sensing. *Cell Metab* **1**, 401-8.



- Guzy, R. D. and Schumacker, P. T.** (2006). Oxygen sensing by mitochondria at complex III: the paradox of increased reactive oxygen species during hypoxia. *Exp Physiol* **91**, 807-19.
- Hafner, M., Landthaler, M., Burger, L., Khorshid, M., Hausser, J., Berninger, P., Rothballer, A., Ascano, M., Jr., Jungkamp, A. C., Munschauer, M. et al.** (2010). Transcriptome-wide identification of RNA-binding protein and microRNA target sites by PAR-CLIP. *Cell* **141**, 129-41.
- Hamanaka, R. B. and Chandel, N. S.** (2010). Mitochondrial reactive oxygen species regulate cellular signaling and dictate biological outcomes. *Trends Biochem Sci.*
- Han, J., Lee, Y., Yeom, K. H., Nam, J. W., Heo, I., Rhee, J. K., Sohn, S. Y., Cho, Y., Zhang, B. T. and Kim, V. N.** (2006). Molecular basis for the recognition of primary microRNAs by the Drosha-DGCR8 complex. *Cell* **125**, 887-901.
- Hanahan, D. and Weinberg, R. A.** (2000). The hallmarks of cancer. *Cell* **100**, 57-70.
- Hanahan, D. and Weinberg, R. A.** (2011). Hallmarks of cancer: the next generation. *Cell* **144**, 646-74.
- Hansen, T. V., Hammer, N. A., Nielsen, J., Madsen, M., Dalbaeck, C., Wewer, U. M., Christiansen, J. and Nielsen, F. C.** (2004). Dwarfism and impaired gut development in insulin-like growth factor II mRNA-binding protein 1-deficient mice. *Mol Cell Biol* **24**, 4448-64.
- Hara, T., Honda, K., Shitashige, M., Ono, M., Matsuyama, H., Naito, K., Hirohashi, S. and Yamada, T.** (2007). Mass spectrometry analysis of the native protein complex containing actinin-4 in prostate cancer cells. *Mol Cell Proteomics* **6**, 479-91.
- Harris, M. H., Vander Heiden, M. G., Kron, S. J. and Thompson, C. B.** (2000). Role of oxidative phosphorylation in Bax toxicity. *Mol Cell Biol* **20**, 3590-6.
- Hatzivassiliou, G., Zhao, F., Bauer, D. E., Andreadis, C., Shaw, A. N., Dhanak, D., Hingorani, S. R., Tuveson, D. A. and Thompson, C. B.** (2005). ATP citrate lyase inhibition can suppress tumor cell growth. *Cancer Cell* **8**, 311-21.
- Havin, L., Git, A., Elisha, Z., Oberman, F., Yaniv, K., Schwartz, S. P., Standart, N. and Yisraeli, J. K.** (1998). RNA-binding protein conserved in both microtubule- and microfilament-based RNA localization. *Genes Dev* **12**, 1593-8.
- He, Q. Y., Chen, J., Kung, H. F., Yuen, A. P. and Chiu, J. F.** (2004). Identification of tumor-associated proteins in oral tongue squamous cell carcinoma by proteomics. *Proteomics* **4**, 271-8.
- Heinonen, M., Bono, P., Narko, K., Chang, S. H., Lundin, J., Joensuu, H., Furneaux, H., Hla, T., Haglund, C. and Ristimaki, A.** (2005). Cytoplasmic HuR expression is a prognostic factor in invasive ductal breast carcinoma. *Cancer Res* **65**, 2157-61.
- Henke, J. I., Goergen, D., Zheng, J., Song, Y., Schuttler, C. G., Fehr, C., Junemann, C. and Niepmann, M.** (2008). microRNA-122 stimulates translation of hepatitis C virus RNA. *EMBO J* **27**, 3300-10.

- Hernlund, E., Hjerpe, E., Avall-Lundqvist, E. and Shoshan, M.** (2009). Ovarian carcinoma cells with low levels of beta-F1-ATPase are sensitive to combined platinum and 2-deoxy-D-glucose treatment. *Mol Cancer Ther* **8**, 1916-23.
- Hernlund, E., Ihlund, L. S., Khan, O., Ates, Y. O., Linder, S., Panaretakis, T. and Shoshan, M. C.** (2008). Potentiation of chemotherapeutic drugs by energy metabolism inhibitors 2-deoxyglucose and etomoxir. *Int J Cancer* **123**, 476-83.
- Hervouet, E., Demont, J., Pecina, P., Vojtiskova, A., Houstek, J., Simonnet, H. and Godinot, C.** (2005). A new role for the von Hippel-Lindau tumor suppressor protein: stimulation of mitochondrial oxidative phosphorylation complex biogenesis. *Carcinogenesis* **26**, 531-9.
- Hieronymus, H. and Silver, P. A.** (2004). A systems view of mRNP biology. *Genes Dev* **18**, 2845-60.
- Hinton, S. D., Myers, M. P., Roggero, V. R., Allison, L. A. and Tonks, N. K.** (2010). The pseudophosphatase MK-STYX interacts with G3BP and decreases stress granule formation. *Biochem J* **427**, 349-57.
- Holt, C. E. and Bullock, S. L.** (2009). Subcellular mRNA localization in animal cells and why it matters. *Science* **326**, 1212-6.
- Hommes, F. A.** (1975). In *Energetic aspects of late fetal and neonatal metabolism.*, pp. 1-7. London: Academic Press.
- Hume, D. A., Radik, J. L., Ferber, E. and Weidemann, M. J.** (1978). Aerobic glycolysis and lymphocyte transformation. *Biochem J* **174**, 703-9.
- Humphreys, D. T., Westman, B. J., Martin, D. I. and Preiss, T.** (2005). MicroRNAs control translation initiation by inhibiting eukaryotic initiation factor 4E/cap and poly(A) tail function. *Proc Natl Acad Sci U S A* **102**, 16961-6.
- Hüttelmaier, S., Zenklusen, D., Lederer, M., Dichtenberg, J., Lorenz, M., Meng, X., Bassell, G. J., Condeelis, J. and Singer, R. H.** (2005). Spatial regulation of beta-actin translation by Src-dependent phosphorylation of ZBP1. *Nature* **438**, 512-5.
- Ioannidis, P., Mahaira, L., Papadopoulou, A., Teixeira, M. R., Heim, S., Andersen, J. A., Evangelou, E., Dafni, U., Pandis, N. and Trangas, T.** (2003). CRD-BP: a c-Myc mRNA stabilizing protein with an oncofetal pattern of expression. *Anticancer Res* **23**, 2179-83.
- Ioannidis, P., Trangas, T., Dimitriadis, E., Samiotaki, M., Kyriazoglou, I., Tsiapalis, C. M., Kittas, C., Agnantis, N., Nielsen, F. C., Nielsen, J. et al.** (2001). C-MYC and IGF-II mRNA-binding protein (CRD-BP/IMP-1) in benign and malignant mesenchymal tumors. *Int J Cancer* **94**, 480-4.
- Irvine, K., Stirling, R., Hume, D. and Kennedy, D.** (2004). Rasputin, more promiscuous than ever: a review of G3BP. *Int J Dev Biol* **48**, 1065-77.

- Isaacs, J. S., Jung, Y. J., Mole, D. R., Lee, S., Torres-Cabala, C., Chung, Y. L., Merino, M., Trepel, J., Zbar, B., Toro, J. et al.** (2005). HIF overexpression correlates with biallelic loss of fumarate hydratase in renal cancer: novel role of fumarate in regulation of HIF stability. *Cancer Cell* **8**, 143-53.
- Ishikawa, H. and Barber, G. N.** (2008). STING is an endoplasmic reticulum adaptor that facilitates innate immune signalling. *Nature* **455**, 674-8.
- Ishikawa, K., Takenaga, K., Akimoto, M., Koshikawa, N., Yamaguchi, A., Imanishi, H., Nakada, K., Honma, Y. and Hayashi, J.** (2008). ROS-generating mitochondrial DNA mutations can regulate tumor cell metastasis. *Science* **320**, 661-4.
- Isidoro, A., Casado, E., Redondo, A., Acebo, P., Espinosa, E., Alonso, A. M., Cejas, P., Hardisson, D., Fresno Vara, J. A., Belda-Iniesta, C. et al.** (2005). Breast carcinomas fulfill the Warburg hypothesis and provide metabolic markers of cancer prognosis. *Carcinogenesis* **26**, 2095-104.
- Isidoro, A., Martinez, M., Fernandez, P. L., Ortega, A. D., Santamaria, G., Chamorro, M., Reed, J. C. and Cuezva, J. M.** (2004). Alteration of the bioenergetic phenotype of mitochondria is a hallmark of breast, gastric, lung and oesophageal cancer. *Biochem J* **378**, 17-20.
- Izquierdo, J. M.** (2006). Control of the ATP synthase beta subunit expression by RNA-binding proteins TIA-1, TIAR, and HuR. *Biochem Biophys Res Commun* **348**, 703-11.
- Izquierdo, J. M. and Cuezva, J. M.** (1997). Control of the translational efficiency of beta-F1-ATPase mRNA depends on the regulation of a protein that binds the 3' untranslated region of the mRNA. *Mol Cell Biol* **17**, 5255-68.
- Izquierdo, J. M. and Cuezva, J. M.** (2000). Internal-ribosome-entry-site functional activity of the 3'-untranslated region of the mRNA for the beta subunit of mitochondrial H<sup>+</sup>-ATP synthase. *Biochem J* **346 Pt 3**, 849-55.
- Izquierdo, J. M. and Cuezva, J. M.** (2005). Epigenetic regulation of the binding activity of translation inhibitory proteins that bind the 3' untranslated region of beta-F1-ATPase mRNA by adenine nucleotides and the redox state. *Arch Biochem Biophys* **433**, 481-6.
- Izquierdo, J. M., Luis, A. M. and Cuezva, J. M.** (1990). Postnatal mitochondrial differentiation in rat liver. Regulation by thyroid hormones of the beta-subunit of the mitochondrial F1-ATPase complex. *J Biol Chem* **265**, 9090-7.
- Izquierdo, J. M., Ricart, J., Ostronoff, L. K., Egea, G. and Cuezva, J. M.** (1995). Changing patterns of transcriptional and post-transcriptional control of beta-F1-ATPase gene expression during mitochondrial biogenesis in liver. *J Biol Chem* **270**, 10342-50.
- Johnson, M. T., Mahmood, S. and Patel, M. S.** (2003). Intermediary metabolism and energetics during murine early embryogenesis. *J Biol Chem* **278**, 31457-60.

- Jonson, L., Vikesaa, J., Krogh, A., Nielsen, L. K., Hansen, T., Borup, R., Johnsen, A. H., Christiansen, J. and Nielsen, F. C.** (2007). Molecular composition of IMP1 ribonucleoprotein granules. *Mol Cell Proteomics* **6**, 798-811.
- Kahvejian, A., Svitkin, Y. V., Sukarieh, R., M'Boutchou, M. N. and Sonenberg, N.** (2005). Mammalian poly(A)-binding protein is a eukaryotic translation initiation factor, which acts via multiple mechanisms. *Genes Dev* **19**, 104-13.
- Kallinowski, F., Vaupel, P., Runkel, S., Berg, G., Fortmeyer, H. P., Baessler, K. H., Wagner, K., Mueller-Klieser, W. and Walenta, S.** (1988). Glucose uptake, lactate release, ketone body turnover, metabolic micromilieu, and pH distributions in human breast cancer xenografts in nude rats. *Cancer Res* **48**, 7264-72.
- Kanai, Y., Dohmae, N. and Hirokawa, N.** (2004). Kinesin transports RNA: isolation and characterization of an RNA-transporting granule. *Neuron* **43**, 513-25.
- Karrasch, S. and Walker, J. E.** (1999). Novel features in the structure of bovine ATP synthase. *J. Mol. Biol.* **290**, 379-384.
- Kedersha, N., Stoecklin, G., Ayodele, M., Yacono, P., Lykke-Andersen, J., Fritzler, M. J., Scheuner, D., Kaufman, R. J., Golan, D. E. and Anderson, P.** (2005). Stress granules and processing bodies are dynamically linked sites of mRNP remodeling. *J Cell Biol* **169**, 871-84.
- Kedersha, N. L., Gupta, M., Li, W., Miller, I. and Anderson, P.** (1999). RNA-binding proteins TIA-1 and TIAR link the phosphorylation of eIF-2 alpha to the assembly of mammalian stress granules. *J Cell Biol* **147**, 1431-42.
- Keene, J. D. and Tenenbaum, S. A.** (2002). Eukaryotic mRNPs may represent posttranscriptional operons. *Mol Cell* **9**, 1161-7.
- Kellems, R. E., Allison, V. F. and Butow, R. A.** (1975). Cytoplasmic type 80S ribosomes associated with yeast mitochondria. IV. Attachment of ribosomes to the outer membrane of isolated mitochondria. *J Cell Biol* **65**, 1-14.
- Khandjian, E. W., Huot, M. E., Tremblay, S., Davidovic, L., Mazroui, R. and Bardoni, B.** (2004). Biochemical evidence for the association of fragile X mental retardation protein with brain polyribosomal ribonucleoparticles. *Proc Natl Acad Sci U S A* **101**, 13357-62.
- Khvorova, A., Reynolds, A. and Jayasena, S. D.** (2003). Functional siRNAs and miRNAs exhibit strand bias. *Cell* **115**, 209-16.
- Kim, J. W., Tchernyshyov, I., Semenza, G. L. and Dang, C. V.** (2006). HIF-1-mediated expression of pyruvate dehydrogenase kinase: a metabolic switch required for cellular adaptation to hypoxia. *Cell Metab* **3**, 177-85.

- Kim, S. J., Yune, T. Y., Han, C. T., Kim, Y. C., Oh, Y. J., Markelonis, G. J. and Oh, T. H.** (2007). Mitochondrial isocitrate dehydrogenase protects human neuroblastoma SH-SY5Y cells against oxidative stress. *J Neurosci Res* **85**, 139-52.
- King, A., Selak, M. A. and Gottlieb, E.** (2006). Succinate dehydrogenase and fumarate hydratase: linking mitochondrial dysfunction and cancer. *Oncogene* **25**, 4675-82.
- Kobel, M., Weidensdorfer, D., Reinke, C., Lederer, M., Schmitt, W. D., Zeng, K., Thomssen, C., Hauptmann, S. and Huttelmaier, S.** (2007). Expression of the RNA-binding protein IMP1 correlates with poor prognosis in ovarian carcinoma. *Oncogene* **26**, 7584-9.
- Kociok, N., Esser, P., Unfried, K., Parker, F., Schraermeyer, U., Grisanti, S., Toque, B. and Heimann, K.** (1999). Upregulation of the RAS-GTPase activating protein (GAP)-binding protein (G3BP) in proliferating RPE cells. *J Cell Biochem* **74**, 194-201.
- Komili, S., Farny, N. G., Roth, F. P. and Silver, P. A.** (2007). Functional specificity among ribosomal proteins regulates gene expression. *Cell* **131**, 557-71.
- Kondoh, H., Leonart, M. E., Nakashima, Y., Yokode, M., Tanaka, M., Bernard, D., Gil, J. and Beach, D.** (2007). A high glycolytic flux supports the proliferative potential of murine embryonic stem cells. *Antioxid Redox Signal* **9**, 293-9.
- Krieg, R. C., Knuechel, R., Schiffmann, E., Liotta, L. A., Petricoin, E. F., 3rd and Herrmann, P. C.** (2004). Mitochondrial proteome: cancer-altered metabolism associated with cytochrome c oxidase subunit level variation. *Proteomics* **4**, 2789-95.
- Kroemer, G. and Pouyssegur, J.** (2008). Tumor cell metabolism: cancer's Achilles' heel. *Cancer Cell* **13**, 472-82.
- Krol, J., Loedige, I. and Filipowicz, W.** (2010). The widespread regulation of microRNA biogenesis, function and decay. *Nat Rev Genet* **11**, 597-610.
- Kuo, M. L., den Besten, W., Bertwistle, D., Roussel, M. F. and Sherr, C. J.** (2004). N-terminal polyubiquitination and degradation of the Arf tumor suppressor. *Genes Dev* **18**, 1862-74.
- Laemmli, U. K.** (1970). Cleavage of structural proteins during the assembly of the head of bacteriophage T4. *Nature* **227**, 680-685.
- Lawrence, J. B. and Singer, R. H.** (1986). Intracellular localization of messenger RNAs for cytoskeletal proteins. *Cell* **45**, 407-15.
- Le, A., Cooper, C. R., Gouw, A. M., Dinavahi, R., Maitra, A., Deck, L. M., Royer, R. E., Vander Jagt, D. L., Semenza, G. L. and Dang, C. V.** (2010). Inhibition of lactate dehydrogenase A induces oxidative stress and inhibits tumor progression. *Proc Natl Acad Sci U S A* **107**, 2037-42.
- Leblanc, V., Tocque, B. and Delumeau, I.** (1998). Ras-GAP controls Rho-mediated cytoskeletal reorganization through its SH3 domain. *Mol Cell Biol* **18**, 5567-78.

- Lecuyer, E., Yoshida, H., Parthasarathy, N., Alm, C., Babak, T., Cerovina, T., Hughes, T. R., Tomancak, P. and Krause, H. M. (2007). Global analysis of mRNA localization reveals a prominent role in organizing cellular architecture and function. *Cell* **131**, 174-87.
- Lee, J. W., Choi, C. H., Choi, J. J., Park, Y. A., Kim, S. J., Hwang, S. Y., Kim, W. Y., Kim, T. J., Lee, J. H., Kim, B. G. et al. (2008). Altered MicroRNA expression in cervical carcinomas. *Clin Cancer Res* **14**, 2535-42.
- Lee, R. C., Feinbaum, R. L. and Ambros, V. (1993). The *C. elegans* heterochronic gene *lin-4* encodes small RNAs with antisense complementarity to *lin-14*. *Cell* **75**, 843-54.
- Lelandais, G., Saint-Georges, Y., Geneix, C., Al-Shikhley, L., Dujardin, G. and Jacq, C. (2009). Spatio-temporal dynamics of yeast mitochondrial biogenesis: transcriptional and post-transcriptional mRNA oscillatory modules. *PLoS Comput Biol* **5**, e1000409.
- Leucci, E., Onnis, A., Cocco, M., De Falco, G., Imperatore, F., Giuseppina, A., Costanzo, V., Cerino, G., Mannucci, S., Cantisani, R. et al. (2010). B-cell differentiation in EBV-positive Burkitt lymphoma is impaired at posttranscriptional level by miRNA-altered expression. *Int J Cancer* **126**, 1316-26.
- Levy, N. S., Chung, S., Furneaux, H. and Levy, A. P. (1998). Hypoxic stabilization of vascular endothelial growth factor mRNA by the RNA-binding protein HuR. *J Biol Chem* **273**, 6417-23.
- Lewis, B. P., Burge, C. B. and Bartel, D. P. (2005). Conserved seed pairing, often flanked by adenosines, indicates that thousands of human genes are microRNA targets. *Cell* **120**, 15-20.
- Li, F., Wang, Y., Zeller, K. I., Potter, J. J., Wonsey, D. R., O'Donnell, K. A., Kim, J. W., Yustein, J. T., Lee, L. A. and Dang, C. V. (2005). Myc stimulates nuclearly encoded mitochondrial genes and mitochondrial biogenesis. *Mol Cell Biol* **25**, 6225-34.
- Li, R. J., Zhang, G. S., Chen, Y. H., Zhu, J. F., Lu, Q. J., Gong, F. J. and Kuang, W. Y. (2010a). Down-regulation of mitochondrial ATPase by hypermethylation mechanism in chronic myeloid leukemia is associated with multidrug resistance. *Ann Oncol* **7**, 1506-14.
- Li, Y., Liang, Q., Wen, Y. Q., Chen, L. L., Wang, L. T., Liu, Y. L., Luo, C. Q., Liang, H. Z., Li, M. T. and Li, Z. (2010b). Comparative proteomics analysis of human osteosarcomas and benign tumor of bone. *Cancer Genet Cytogenet* **198**, 97-106.
- Li, Z., Okamoto, K., Hayashi, Y. and Sheng, M. (2004). The importance of dendritic mitochondria in the morphogenesis and plasticity of spines and synapses. *Cell* **119**, 873-87.
- Lim, L. P., Lau, N. C., Garrett-Engele, P., Grimson, A., Schelter, J. M., Castle, J., Bartel, D. P., Linsley, P. S. and Johnson, J. M. (2005). Microarray analysis shows that some microRNAs downregulate large numbers of target mRNAs. *Nature* **433**, 769-73.
- Lin, J., Tarr, P. T., Yang, R., Rhee, J., Puigserver, P., Newgard, C. B. and Spiegelman, B. M. (2003). PGC-1beta in the regulation of hepatic glucose and energy metabolism. *J Biol Chem* **278**, 30843-8.

- Lin, P. C., Lin, J. K., Yang, S. H., Wang, H. S., Li, A. F. and Chang, S. C.** (2008). Expression of beta-F1-ATPase and mitochondrial transcription factor A and the change in mitochondrial DNA content in colorectal cancer: clinical data analysis and evidence from an in vitro study. *Int J Colorectal Dis* **23**, 1223-32.
- Lithgow, T.** (2000). Targeting of proteins to mitochondria. *FEBS Lett* **476**, 22-6.
- Lithgow, T., Cuezva, J. M. and Silver, P. A.** (1997). Highways for protein delivery to the mitochondria. *Trends Biochem. Sci.* **22**, 110-113.
- Livak, K. J. and Schmittgen, T. D.** (2001). Analysis of relative gene expression data using real-time quantitative PCR and the 2(-Delta Delta C(T)) Method. *Methods* **25**, 402-8.
- Lopez-Rios, F., Sanchez-Arago, M., Garcia-Garcia, E., Ortega, A. D., Berrendero, J. R., Pozo-Rodriguez, F., Lopez-Encuentra, A., Ballestin, C. and Cuezva, J. M.** (2007). Loss of the mitochondrial bioenergetic capacity underlies the glucose avidity of carcinomas. *Cancer Res* **67**, 9013-7.
- Lopez de Heredia, M. and Jansen, R. P.** (2004). mRNA localization and the cytoskeleton. *Curr Opin Cell Biol* **16**, 80-5.
- Lopez de Silanes, I., Fan, J., Yang, X., Zonderman, A. B., Potapova, O., Pizer, E. S. and Gorospe, M.** (2003). Role of the RNA-binding protein HuR in colon carcinogenesis. *Oncogene* **22**, 7146-54.
- Lu, Y., Yi, Y., Liu, P., Wen, W., James, M., Wang, D. and You, M.** (2007). Common human cancer genes discovered by integrated gene-expression analysis. *PLoS One* **2**, e1149.
- Luis, A. M., Izquierdo, J. M., Ostronoff, L. K., Salinas, M., Santaren, J. F. and Cuezva, J. M.** (1993). Translational regulation of mitochondrial differentiation in neonatal rat liver. Specific increase in the translational efficiency of the nuclear-encoded mitochondrial beta-F1-ATPase mRNA. *J Biol Chem* **268**, 1868-75.
- Lypowy, J., Chen, I. Y. and Abdellatif, M.** (2005). An alliance between Ras GTPase-activating protein, filamin C, and Ras GTPase-activating protein SH3 domain-binding protein regulates myocyte growth. *J Biol Chem* **280**, 25717-28.
- Ma, W. J., Cheng, S., Campbell, C., Wright, A. and Furneaux, H.** (1996). Cloning and characterization of HuR, a ubiquitously expressed Elav-like protein. *J Biol Chem* **271**, 8144-51.
- MacKenzie, J. A. and Payne, R. M.** (2004). Ribosomes specifically bind to mammalian mitochondria via protease-sensitive proteins on the outer membrane. *J Biol Chem* **279**, 9803-10.
- Maggi, L. B., Jr., Kuchenruether, M., Dadey, D. Y., Schwoppe, R. M., Grisendi, S., Townsend, R. R., Pandolfi, P. P. and Weber, J. D.** (2008). Nucleophosmin serves as a rate-limiting nuclear export chaperone for the Mammalian ribosome. *Mol Cell Biol* **28**, 7050-65.
- Mansfield, K. D., Guzy, R. D., Pan, Y., Young, R. M., Cash, T. P., Schumacker, P. T. and Simon, M. C.** (2005). Mitochondrial dysfunction resulting from loss of cytochrome c impairs cellular oxygen sensing and hypoxic HIF-alpha activation. *Cell Metab* **1**, 393-9.

- Marc, P., Margeot, A., Devaux, F., Blugeon, C., Corral-Debrinski, M. and Jacq, C.** (2002). Genome-wide analysis of mRNAs targeted to yeast mitochondria. *EMBO Rep* **3**, 159-64.
- Margeot, A., Blugeon, C., Sylvestre, J., Vialette, S., Jacq, C. and Corral-Debrinski, M.** (2002). In *Saccharomyces cerevisiae*, ATP2 mRNA sorting to the vicinity of mitochondria is essential for respiratory function. *EMBO J* **21**, 6893-904.
- Margeot, A., Garcia, M., Wang, W., Tetaud, E., di Rago, J. P. and Jacq, C.** (2005). Why are many mRNAs translated to the vicinity of mitochondria: a role in protein complex assembly? *Gene* **354**, 64-71.
- Martin, K. C. and Ephrussi, A.** (2009). mRNA localization: gene expression in the spatial dimension. *Cell* **136**, 719-30.
- Martinez-Diez, M., Santamaria, G., Ortega, A. D. and Cuezva, J. M.** (2006). Biogenesis and Dynamics of Mitochondria during the Cell Cycle: Significance of 3'UTRs. *PLoS One* **1**, e107.
- Mathupala, S. P., Heese, C. and Pedersen, P. L.** (1997). Glucose catabolism in cancer cells. The type II hexokinase promoter contains functionally active response elements for the tumor suppressor p53. *J Biol Chem* **272**, 22776-80.
- Matoba, S., Kang, J. G., Patino, W. D., Wragg, A., Boehm, M., Gavrilova, O., Hurley, P. J., Bunz, F. and Hwang, P. M.** (2006). p53 regulates mitochondrial respiration. *Science* **312**, 1650-3.
- Matsuyama, S., Xu, Q., Velours, J. and Reed, J. C.** (1998). The Mitochondrial FOF1-ATPase proton pump is required for function of the proapoptotic protein Bax in yeast and mammalian cells. *Mol Cell* **1**, 327-36.
- Mazurek, S., Boschek, C. B., Hugo, F. and Eigenbrodt, E.** (2005). Pyruvate kinase type M2 and its role in tumor growth and spreading. *Semin Cancer Biol* **15**, 300-8.
- McCormick, F.** (1995). Ras-related proteins in signal transduction and growth control. *Mol Reprod Dev* **42**, 500-6.
- McFate, T., Mohyeldin, A., Lu, H., Thakar, J., Henriques, J., Halim, N. D., Wu, H., Schell, M. J., Tsang, T. M., Teahan, O. et al.** (2008). Pyruvate dehydrogenase complex activity controls metabolic and malignant phenotype in cancer cells. *J Biol Chem* **283**, 22700-8.
- Meierhofer, D., Mayr, J. A., Foetschl, U., Berger, A., Fink, K., Schmeller, N., Hacker, G. W., Hauser-Kronberger, C., Kofler, B. and Sperl, W.** (2004). Decrease of mitochondrial DNA content and energy metabolism in renal cell carcinomas. *Carcinogenesis* **25**, 1005-1010.
- Meng, X., Krishnan, J., She, Y., Ens, W., Standing, K. and Wilkins, J. A.** (2004). Association of rasGAPSH3 binding protein 1, G3BP1, and rasGap120 with integrin containing complexes induced by an adhesion blocking antibody. *J Proteome Res* **3**, 506-16.



**Michelakis, E. D., Sutendra, G., Dromparis, P., Webster, L., Haromy, A., Niven, E., Maguire, C., Gammer, T. L., Mackey, J. R., Fulton, D. et al. (2010).** Metabolic modulation of glioblastoma with dichloroacetate. *Sci Transl Med* **2**, 31-34.

**Michelakis, E. D., Webster, L. and Mackey, J. R. (2008).** Dichloroacetate (DCA) as a potential metabolic-targeting therapy for cancer. *Br J Cancer* **99**, 989-94.

**Minai, L., Martinovic, J., Chretien, D., Dumez, F., Razavi, F., Munnich, A. and Rotig, A. (2008).** Mitochondrial respiratory chain complex assembly and function during human fetal development. *Mol Genet Metab* **94**, 120-6.

**Mingle, L. A., Okuhama, N. N., Shi, J., Singer, R. H., Condeelis, J. and Liu, G. (2005).** Localization of all seven messenger RNAs for the actin-polymerization nucleator Arp2/3 complex in the protrusions of fibroblasts. *J Cell Sci* **118**, 2425-33.

**Modica-Napolitano, J. S., Kulawiec, M. and Singh, K. K. (2007).** Mitochondria and human cancer. *Curr Mol Med* **7**, 121-31.

**Modica-Napolitano, J. S. and Singh, K. (2002).** Mitochondria as targets for detection and treatment of cancer. *Expert Rev Mol Med* **2002**, 1-19.

**Moore, M. J. (2005).** From birth to death: the complex lives of eukaryotic mRNAs. *Science* **309**, 1514-8.

**Mootha, V. K., Handschin, C., Arlow, D., Xie, X., St Pierre, J., Sihag, S., Yang, W., Altshuler, D., Puigserver, P., Patterson, N. et al. (2004).** Erralpha and Gabpa/b specify PGC-1alpha-dependent oxidative phosphorylation gene expression that is altered in diabetic muscle. *Proc Natl Acad Sci U S A* **101**, 6570-5.

**Morgan, M. J. and Liu, Z. G. (2011).** Crosstalk of reactive oxygen species and NF-kappaB signaling. *Cell Res* **21**, 103-15.

**Moro, L., Arbini, A. A., Yao, J. L., di Sant'Agnesse, P. A., Marra, E. and Greco, M. (2009).** Mitochondrial DNA depletion in prostate epithelial cells promotes anoikis resistance and invasion through activation of PI3K/Akt2. *Cell Death Differ* **16**, 571-83.

**Moulin, S., Llanos, S., Kim, S. H. and Peters, G. (2008).** Binding to nucleophosmin determines the localization of human and chicken ARF but not its impact on p53. *Oncogene* **27**, 2382-9.

**Mrena, J., Wiksten, J. P., Thiel, A., Kokkola, A., Pohjola, L., Lundin, J., Nordling, S., Ristimaki, A. and Haglund, C. (2005).** Cyclooxygenase-2 is an independent prognostic factor in gastric cancer and its expression is regulated by the messenger RNA stability factor HuR. *Clin Cancer Res* **11**, 7362-8.

**Muckenthaler, M., Gray, N. K. and Hentze, M. W. (1998).** IRP-1 binding to ferritin mRNA prevents the recruitment of the small ribosomal subunit by the cap-binding complex eIF4F. *Mol Cell* **2**, 383-8.

- Murano, K., Okuwaki, M., Hisaoka, M. and Nagata, K.** (2008). Transcription regulation of the rRNA gene by a multifunctional nucleolar protein, B23/nucleophosmin, through its histone chaperone activity. *Mol Cell Biol* **28**, 3114-26.
- Nakai, A., Taniuchi, Y., Asakura, H., Oya, A., Yokota, A., Koshino, T. and Araki, T.** (2000). Developmental changes in mitochondrial activity and energy metabolism in fetal and neonatal rat brain. *Brain Res Dev Brain Res* **121**, 67-72.
- Nakamura, A., Sato, K. and Hanyu-Nakamura, K.** (2004). Drosophila cup is an eIF4E binding protein that associates with Bruno and regulates oskar mRNA translation in oogenesis. *Dev Cell* **6**, 69-78.
- Nielsen, F. C., Nielsen, J., Kristensen, M. A., Koch, G. and Christiansen, J.** (2002). Cytoplasmic trafficking of IGF-II mRNA-binding protein by conserved KH domains. *J Cell Sci* **115**, 2087-97.
- Nielsen, J., Christiansen, J., Lykke-Andersen, J., Johnsen, A. H., Wewer, U. M. and Nielsen, F. C.** (1999). A family of insulin-like growth factor II mRNA-binding proteins represses translation in late development. *Mol Cell Biol* **19**, 1262-70.
- Niemi, N. M., Lanning, N. J., Klomp, J. A., Tait, S. W., Xu, Y., Dykema, K. J., Murphy, L. O., Gaither, L. A., Xu, H. E., Furge, K. A. et al.** (2011). MK-STYX, a catalytically inactive phosphatase regulating mitochondrial dependent apoptosis. *Mol Cell Biol*.
- Nozawa, Y., Van Belzen, N., Van der Made, A. C., Dinjens, W. N. and Bosman, F. T.** (1996). Expression of nucleophosmin/B23 in normal and neoplastic colorectal mucosa. *J Pathol* **178**, 48-52.
- O'Connell, B. C., Cheung, A. F., Simkevich, C. P., Tam, W., Ren, X., Mateyak, M. K. and Sedivy, J. M.** (2003). A large scale genetic analysis of c-Myc-regulated gene expression patterns. *J Biol Chem* **278**, 12563-73.
- Okada, M., Jang, S. W. and Ye, K.** (2007). Ebp1 association with nucleophosmin/B23 is essential for regulating cell proliferation and suppressing apoptosis. *J Biol Chem* **282**, 36744-54.
- Okamura, K., Phillips, M. D., Tyler, D. M., Duan, H., Chou, Y. T. and Lai, E. C.** (2008). The regulatory activity of microRNA\* species has substantial influence on microRNA and 3' UTR evolution. *Nat Struct Mol Biol* **15**, 354-63.
- Okuwaki, M., Matsumoto, K., Tsujimoto, M. and Nagata, K.** (2001). Function of nucleophosmin/B23, a nucleolar acidic protein, as a histone chaperone. *FEBS Lett* **506**, 272-6.
- Oleynikov, Y. and Singer, R. H.** (2003). Real-time visualization of ZBP1 association with beta-actin mRNA during transcription and localization. *Curr Biol* **13**, 199-207.
- Olson, M. O., Wallace, M. O., Herrera, A. H., Marshall-Carlson, L. and Hunt, R. C.** (1986). Preribosomal ribonucleoprotein particles are a major component of a nucleolar matrix fraction. *Biochemistry* **25**, 484-91.

- Orom, U. A., Nielsen, F. C. and Lund, A. H.** (2008). MicroRNA-10a binds the 5'UTR of ribosomal protein mRNAs and enhances their translation. *Mol Cell* **30**, 460-71.
- Ortega, A. D., Sala, S., Espinosa, E., Gonzalez-Baron, M. and Cuezva, J. M.** (2008). HuR and the bioenergetic signature of breast cancer: a low tumor expression of the RNA-binding protein predicts a higher risk of disease recurrence. *Carcinogenesis* **29**, 2053-61.
- Ortega, A. D., Sanchez-Arago, M., Giner-Sanchez, D., Sanchez-Cenizo, L., Willers, I. and Cuezva, J. M.** (2009). Glucose avidity of carcinomas. *Cancer Lett* **276**, 125-35.
- Ortega, A. D., Willers, I. M., Sala, S. and Cuezva, J. M.** (2010). Human G3BP1 interacts with the  $\beta$ -F'-ATPase mRNA and inhibits its translation. *J. Cell. Science*, in press.
- Osthus, R. C., Shim, H., Kim, S., Li, Q., Reddy, R., Mukherjee, M., Xu, Y., Wonsey, D., Lee, L. A. and Dang, C. V.** (2000). Deregulation of glucose transporter 1 and glycolytic gene expression by c-Myc. *J Biol Chem* **275**, 21797-800.
- Ostronoff, L. K., Izquierdo, J. M. and Cuezva, J. M.** (1995). mt-mRNA stability regulates the expression of the mitochondrial genome during liver development. *Biochem Biophys Res Commun* **217**, 1094-8.
- Ostronoff, L. K., Izquierdo, J. M., Enriquez, J. A., Montoya, J. and Cuezva, J. M.** (1996). Transient activation of mitochondrial translation regulates the expression of the mitochondrial genome during mammalian mitochondrial differentiation. *Biochem J* **316 ( Pt 1)**, 183-91.
- Pagliarini, D. J., Calvo, S. E., Chang, B., Sheth, S. A., Vafai, S. B., Ong, S. E., Walford, G. A., Sugiana, C., Boneh, A., Chen, W. K. et al.** (2008). A mitochondrial protein compendium elucidates complex I disease biology. *Cell* **134**, 112-23.
- Palaniswamy, V., Moraes, K. C., Wilusz, C. J. and Wilusz, J.** (2006). Nucleophosmin is selectively deposited on mRNA during polyadenylation. *Nat Struct Mol Biol* **13**, 429-35.
- Papandreou, I., Cairns, R. A., Fontana, L., Lim, A. L. and Denko, N. C.** (2006). HIF-1 mediates adaptation to hypoxia by actively downregulating mitochondrial oxygen consumption. *Cell Metab* **3**, 187-97.
- Paris, J., Osborne, H. B., Couturier, A., Le Guellec, R. and Philippe, M.** (1988). Changes in the polyadenylation of specific stable RNA during the early development of *Xenopus laevis*. *Gene* **72**, 169-76.
- Park, S. Y., Chang, I., Kim, J. Y., Kang, S. W., Park, S. H., Singh, K. and Lee, M. S.** (2004). Resistance of mitochondrial DNA-depleted cells against cell death: role of mitochondrial superoxide dismutase. *J Biol Chem* **279**, 7512-20.
- Parker, F., Maurier, F., Delumeau, I., Duchesne, M., Faucher, D., Debussche, L., Dugue, A., Schweighoffer, F. and Tocque, B.** (1996). A Ras-GTPase-activating protein SH3-domain-binding protein. *Mol Cell Biol* **16**, 2561-9.

- Parlo, R. A. and Coleman, P. S.** (1984). Enhanced rate of citrate export from cholesterol-rich hepatoma mitochondria. The truncated Krebs cycle and other metabolic ramifications of mitochondrial membrane cholesterol. *J Biol Chem* **259**, 9997-10003.
- Parrott, A. M., Walsh, M. R., Reichman, T. W. and Mathews, M. B.** (2005). RNA binding and phosphorylation determine the intracellular distribution of nuclear factors 90 and 110. *J Mol Biol* **348**, 281-93.
- Peabody, D. S.** (1993). The RNA binding site of bacteriophage MS2 coat protein. *EMBO J* **12**, 595-600.
- Pedersen, P. L.** (1978). Tumor mitochondria and the bioenergetics of cancer cells. *Prog Exp Tumor Res* **22**, 190-274.
- Pejznochova, M., Tesarova, M., Hansikova, H., Magner, M., Honzik, T., Vinsova, K., Hajkova, Z., Havlickova, V. and Zeman, J.** (2010). Mitochondrial DNA content and expression of genes involved in mtDNA transcription, regulation and maintenance during human fetal development. *Mitochondrion* **10**, 321-9.
- Pelicano, H., Lu, W., Zhou, Y., Zhang, W., Chen, Z., Hu, Y. and Huang, P.** (2009). Mitochondrial dysfunction and reactive oxygen species imbalance promote breast cancer cell motility through a CXCL14-mediated mechanism. *Cancer Res* **69**, 2375-83.
- Petros, J. A., Baumann, A. K., Ruiz-Pesini, E., Amin, M. B., Sun, C. Q., Hall, J., Lim, S., Issa, M. M., Flanders, W. D., Hosseini, S. H. et al.** (2005). mtDNA mutations increase tumorigenicity in prostate cancer. *Proc Natl Acad Sci U S A* **102**, 719-24.
- Philippidou, D., Schmitt, M., Moser, D., Margue, C., Nazarov, P. V., Muller, A., Vallar, L., Nashan, D., Behrmann, I. and Kreis, S.** (2010). Signatures of microRNAs and selected microRNA target genes in human melanoma. *Cancer Res* **70**, 4163-73.
- Plas, D. R., Talapatra, S., Edinger, A. L., Rathmell, J. C. and Thompson, C. B.** (2001). Akt and Bcl-xL promote growth factor-independent survival through distinct effects on mitochondrial physiology. *J Biol Chem* **276**, 12041-8.
- Plas, D. R. and Thompson, C. B.** (2005). Akt-dependent transformation: there is more to growth than just surviving. *Oncogene* **24**, 7435-42.
- Plathow, C. and Weber, W. A.** (2008). Tumor cell metabolism imaging. *J Nucl Med* **49 Suppl 2**, 43S-63S.
- Polyak, K., Li, Y., Zhu, H., Lengauer, C., Willson, J. K., Markowitz, S. D., Trush, M. A., Kinzler, K. W. and Vogelstein, B.** (1998). Somatic mutations of the mitochondrial genome in human colorectal tumours. *Nat. Genet.* **20**, 291-293.
- Pullman, M. E. and Monroy, G. C.** (1963). A Naturally Occurring Inhibitor of Mitochondrial Adenosine Triphosphatase. *J Biol Chem* **238**, 3762-9.

- Rackham, O. and Brown, C. M.** (2004). Visualization of RNA-protein interactions in living cells: FMRP and IMP1 interact on mRNAs. *EMBO J* **23**, 3346-55.
- Ramanathan, A., Wang, C. and Schreiber, S. L.** (2005). Perturbational profiling of a cell-line model of tumorigenesis by using metabolic measurements. *Proc Natl Acad Sci U S A* **102**, 5992-7.
- Rathmell, J. C., Fox, C. J., Plas, D. R., Hammerman, P. S., Cinalli, R. M. and Thompson, C. B.** (2003). Akt-directed glucose metabolism can prevent Bax conformation change and promote growth factor-independent survival. *Mol Cell Biol* **23**, 7315-28.
- Rebagliati, M. R., Weeks, D. L., Harvey, R. P. and Melton, D. A.** (1985). Identification and cloning of localized maternal RNAs from *Xenopus* eggs. *Cell* **42**, 769-77.
- Reinhart, B. J., Slack, F. J., Basson, M., Pasquinelli, A. E., Bettinger, J. C., Rougvie, A. E., Horvitz, H. R. and Ruvkun, G.** (2000). The 21-nucleotide let-7 RNA regulates developmental timing in *Caenorhabditis elegans*. *Nature* **403**, 901-6.
- Ricart, J., Egea, G., Izquierdo, J. M., San Martín, C. and Cuezva, J. M.** (1997). Subcellular structure containing mRNA for beta subunit of mitochondrial H<sup>+</sup>-ATP synthase in rat hepatocytes is translationally active. *Biochem J* **324 ( Pt 2)**, 635-43.
- Ricart, J., Izquierdo, J. M., Di Liegro, C. M. and Cuezva, J. M.** (2002). Assembly of the ribonucleoprotein complex containing the mRNA of the beta-subunit of the mitochondrial H<sup>+</sup>-ATP synthase requires the participation of two distal cis-acting elements and a complex set of cellular trans-acting proteins. *Biochem J* **365**, 417-28.
- Richter, J. D. and Sonenberg, N.** (2005). Regulation of cap-dependent translation by eIF4E inhibitory proteins. *Nature* **433**, 477-80.
- Riechmann, V. and Ephrussi, A.** (2001). Axis formation during *Drosophila* oogenesis. *Curr Opin Genet Dev* **11**, 374-83.
- Rigo, P., Paulus, P., Kaschten, B. J., Hustinx, R., Bury, T., Jerusalem, G., Benoit, T. and Foidart-Willems, J.** (1996). Oncological applications of positron emission tomography with fluorine-18 fluorodeoxyglucose. *Eur J Nucl Med* **23**, 1641-74.
- Ro, S., Park, C., Young, D., Sanders, K. M. and Yan, W.** (2007). Tissue-dependent paired expression of miRNAs. *Nucleic Acids Res* **35**, 5944-53.
- Rodriguez, A. J., Czaplinski, K., Condeelis, J. S. and Singer, R. H.** (2008). Mechanisms and cellular roles of local protein synthesis in mammalian cells. *Curr Opin Cell Biol* **20**, 144-9.
- Rook, M. S., Lu, M. and Kosik, K. S.** (2000). CaMKIIalpha 3' untranslated region-directed mRNA translocation in living neurons: visualization by GFP linkage. *J Neurosci* **20**, 6385-93.
- Ross, A.F., Oleynikov Y., Kislauskis E.H., Taneja K.L., Singer R.H.** (1997). Characterization of beta-actin mRNA zipcode binding protein. *Mol. Cell. Biol.* **17**, 2158-2165.

- Ross, J., Lemm, I. and Berberet, B.** (2001). Overexpression of an mRNA-binding protein in human colorectal cancer. *Oncogene* **20**, 6544-50.
- Sachs, A. B. and Varani, G.** (2000). Eukaryotic translation initiation: there are (at least) two sides to every story. *Nat Struct Biol* **7**, 356-61.
- Saint-Georges, Y., Garcia, M., Delaveau, T., Jourden, L., Le Crom, S., Lemoine, S., Tanty, V., Devaux, F. and Jacq, C.** (2008). Yeast mitochondrial biogenesis: a role for the PUF RNA-binding protein Puf3p in mRNA localization. *PLoS One* **3**, e2293.
- Saito, Y., Liang, G., Egger, G., Friedman, J. M., Chuang, J. C., Coetzee, G. A. and Jones, P. A.** (2006). Specific activation of microRNA-127 with downregulation of the proto-oncogene BCL6 by chromatin-modifying drugs in human cancer cells. *Cancer Cell* **9**, 435-43.
- Sanchez-Arago, M. and Cuezva, J. M.** (2011). The bioenergetic signature of isogenic colon cancer cells predicts the cell death response to treatment with 3-bromopyruvate, iodoacetate or 5-fluorouracil. *J Transl Med* **9**, 19.
- Sanchez-Arago, M., Chamorro, M. and Cuezva, J. M.** (2010). Selection of cancer cells with repressed mitochondria triggers colon cancer progression. *Carcinogenesis* **31**, 567-76.
- Sanchez-Cenizo, L., Formentini, L., Aldea, M., Ortega, A. D., Garcia-Huerta, P., Sanchez-Arago, M. and Cuezva, J. M.** (2010). The up-regulation of the ATPase Inhibitory Factor 1 (IF1) of the mitochondrial H<sup>+</sup>-ATP synthase in human tumors mediates the metabolic shift of cancer cells to a Warburg phenotype. *J Biol Chem*.
- Santamaria, G., Martinez-Diez, M., Fabregat, I. and Cuezva, J. M.** (2006). Efficient execution of cell death in non-glycolytic cells requires the generation of ROS controlled by the activity of mitochondrial H<sup>+</sup>-ATP synthase. *Carcinogenesis* **27**, 925-35.
- Satrustegui, J., Pardo, B. and Del Arco, A.** (2007). Mitochondrial transporters as novel targets for intracellular calcium signaling. *Physiol Rev* **87**, 29-67.
- Sauer, L. A., Stayman, J. W., 3rd and Dauchy, R. T.** (1982). Amino acid, glucose, and lactic acid utilization in vivo by rat tumors. *Cancer Res* **42**, 4090-7.
- Scarpulla, R. C.** (2008). Transcriptional paradigms in mammalian mitochondrial biogenesis and function. *Physiol Rev* **88**, 611-38.
- Schreiber, S. N., Emter, R., Hock, M. B., Knutti, D., Cardenas, J., Podvinec, M., Oakeley, E. J. and Kralli, A.** (2004). The estrogen-related receptor alpha (ERRalpha) functions in PPARgamma coactivator 1alpha (PGC-1alpha)-induced mitochondrial biogenesis. *Proc Natl Acad Sci U S A* **101**, 6472-7.
- Schulz, T. J., Thierbach, R., Voigt, A., Drewes, G., Mietzner, B., Steinberg, P., Pfeiffer, A. F. and Ristow, M.** (2006). Induction of oxidative metabolism by mitochondrial frataxin inhibits cancer growth: Otto Warburg revisited. *J Biol Chem* **281**, 977-81.

- Schwartzberg-Bar-Yoseph, F., Armoni, M. and Karnieli, E.** (2004). The tumor suppressor p53 down-regulates glucose transporters GLUT1 and GLUT4 gene expression. *Cancer Res* **64**, 2627-33.
- Selak, M. A., Armour, S. M., MacKenzie, E. D., Boulahbel, H., Watson, D. G., Mansfield, K. D., Pan, Y., Simon, M. C., Thompson, C. B. and Gottlieb, E.** (2005). Succinate links TCA cycle dysfunction to oncogenesis by inhibiting HIF- $\alpha$  prolyl hydroxylase. *Cancer Cell* **7**, 77-85.
- Semenza, G. L.** (2003). Targeting HIF-1 for cancer therapy. *Nat Rev Cancer* **3**, 721-32.
- Semenza, G. L.** (2010). Hypoxia-inducible factor 1: Regulator of mitochondrial metabolism and mediator of ischemic preconditioning. *Biochim Biophys Acta*.
- Semenza, G. L., Roth, P. H., Fang, H. M. and Wang, G. L.** (1994). Transcriptional regulation of genes encoding glycolytic enzymes by hypoxia-inducible factor 1. *J Biol Chem* **269**, 23757-63.
- Seth, R. B., Sun, L., Ea, C. K. and Chen, Z. J.** (2005). Identification and characterization of MAVS, a mitochondrial antiviral signaling protein that activates NF- $\kappa$ B and IRF 3. *Cell* **122**, 669-82.
- Shakya, A., Cooksey, R., Cox, J. E., Wang, V., McClain, D. A. and Tantin, D.** (2009). Oct1 loss of function induces a coordinate metabolic shift that opposes tumorigenicity. *Nat Cell Biol* **11**, 320-7.
- Shim, H., Dolde, C., Lewis, B. C., Wu, C. S., Dang, G., Jungmann, R. A., Dalla-Favera, R. and Dang, C. V.** (1997). c-Myc transactivation of LDH-A: implications for tumor metabolism and growth. *Proc Natl Acad Sci U S A* **94**, 6658-63.
- Shin, Y. K., Yoo, B. C., Chang, H. J., Jeon, E., Hong, S. H., Jung, M. S., Lim, S. J. and Park, J. G.** (2005). Down-regulation of mitochondrial F1F0-ATP synthase in human colon cancer cells with induced 5-fluorouracil resistance. *Cancer Res* **65**, 3162-70.
- Simonnet, H., Alazard, N., Pfeiffer, K., Gallou, C., Beroud, C., Demont, J., Bouvier, R., Schagger, H. and Godinot, C.** (2002). Low mitochondrial respiratory chain content correlates with tumor aggressiveness in renal cell carcinoma. *Carcinogenesis* **23**, 759-68.
- Simonnet, H., Demont, J., Pfeiffer, K., Guenaneche, L., Bouvier, R., Brandt, U., Schagger, H. and Godinot, C.** (2003). Mitochondrial complex I is deficient in renal oncocytomas. *Carcinogenesis* **24**, 1461-6.
- Smith, T. A., Sharma, R. I., Thompson, A. M. and Paulin, F. E.** (2006). Tumor 18F-FDG incorporation is enhanced by attenuation of P53 function in breast cancer cells in vitro. *J Nucl Med* **47**, 1525-30.
- Solomon, S., Xu, Y., Wang, B., David, M. D., Schubert, P., Kennedy, D. and Schrader, J. W.** (2007). Distinct structural features of caprin-1 mediate its interaction with G3BP-1 and its induction of phosphorylation of eukaryotic translation initiation factor 2 $\alpha$ , entry to cytoplasmic stress granules, and selective interaction with a subset of mRNAs. *Mol Cell Biol* **27**, 2324-42.
- Sonenberg, N. and Hinnebusch, A. G.** (2009). Regulation of translation initiation in eukaryotes: mechanisms and biological targets. *Cell* **136**, 731-45.

- Song, G. and Wang, L.** (2009). A conserved gene structure and expression regulation of miR-433 and miR-127 in mammals. *PLoS One* **4**, e7829.
- Springer, E. L.** (1980). Comparative study of the cytoplasmic organelles of epithelial cell lines derived from human carcinomas and nonmalignant tissues. *Cancer Res* **40**, 803-17.
- St Johnston, D.** (2005). Moving messages: the intracellular localization of mRNAs. *Nat Rev Mol Cell Biol* **6**, 363-75.
- Stohr, N., Lederer, M., Reinke, C., Meyer, S., Hatzfeld, M., Singer, R. H. and Huttelmaier, S.** (2006). ZBP1 regulates mRNA stability during cellular stress. *J Cell Biol* **175**, 527-34.
- Subong, E. N., Shue, M. J., Epstein, J. I., Briggman, J. V., Chan, P. K. and Partin, A. W.** (1999). Monoclonal antibody to prostate cancer nuclear matrix protein (PRO:4-216) recognizes nucleophosmin/B23. *Prostate* **39**, 298-304.
- Suen, D. F., Norris, K. L. and Youle, R. J.** (2008). Mitochondrial dynamics and apoptosis. *Genes Dev* **22**, 1577-90.
- Svitkin, Y. V. and Sonenberg, N.** (2006). [Translational control by the poly(A) binding protein: a check for mRNA integrity]. *Mol Biol (Mosk)* **40**, 684-93.
- Sylvestre, J., Margeot, A., Jacq, C., Dujardin, G. and Corral-Debrinski, M.** (2003). The role of the 3' untranslated region in mRNA sorting to the vicinity of mitochondria is conserved from yeast to human cells. *Mol Biol Cell* **14**, 3848-56.
- Szabadkai, G., Simoni, A. M., Chami, M., Wieckowski, M. R., Youle, R. J. and Rizzuto, R.** (2004). Drp-1-dependent division of the mitochondrial network blocks intraorganellar Ca<sup>2+</sup> waves and protects against Ca<sup>2+</sup>-mediated apoptosis. *Mol Cell* **16**, 59-68.
- Szatrowski, T. P. and Nathan, C. F.** (1991). Production of large amounts of hydrogen peroxide by human tumor cells. *Cancer Res* **51**, 794-8.
- Szebeni, A. and Olson, M. O.** (1999). Nucleolar protein B23 has molecular chaperone activities. *Protein Sci* **8**, 905-12.
- Tanaka, M., Sasaki, H., Kino, I., Sugimura, T. and Terada, M.** (1992). Genes preferentially expressed in embryo stomach are predominantly expressed in gastric cancer. *Cancer Res* **52**, 3372-7.
- Taniuchi, K., Nishimori, I. and Hollingsworth, M. A.** (2011). Intracellular CD24 Inhibits Cell Invasion by Posttranscriptional Regulation of BART through Interaction with G3BP. *Cancer Res* **71**, 895-905.
- Tarun, S. Z., Jr. and Sachs, A. B.** (1995). A common function for mRNA 5' and 3' ends in translation initiation in yeast. *Genes Dev* **9**, 2997-3007.
- Tarun, S. Z., Jr. and Sachs, A. B.** (1996). Association of the yeast poly(A) tail binding protein with translation initiation factor eIF-4G. *EMBO J.* **15**, 7168-7177.



- Tessier, C. R., Doyle, G. A., Clark, B. A., Pitot, H. C. and Ross, J.** (2004). Mammary tumor induction in transgenic mice expressing an RNA-binding protein. *Cancer Res* **64**, 209-14.
- Thierbach, R., Schulz, T. J., Isken, F., Voigt, A., Mietzner, B., Drewes, G., von Kleist-Retzow, J. C., Wiesner, R. J., Magnuson, M. A., Puccio, H. et al.** (2005). Targeted disruption of hepatic frataxin expression causes impaired mitochondrial function, decreased life span and tumor growth in mice. *Hum Mol Genet* **14**, 3857-64.
- Tomiya, A., Serizawa, S., Tachibana, K., Sakurada, K., Samejima, H., Kuchino, Y. and Kitanaka, C.** (2006). Critical role for mitochondrial oxidative phosphorylation in the activation of tumor suppressors Bax and Bak. *J Natl Cancer Inst* **98**, 1462-73.
- Tourriere, H., Chebli, K., Zekri, L., Courselaud, B., Blanchard, J. M., Bertrand, E. and Tazi, J.** (2003). The RasGAP-associated endoribonuclease G3BP assembles stress granules. *J Cell Biol* **160**, 823-31.
- Tourriere, H., Gallouzi, I. E., Chebli, K., Capony, J. P., Mouaikel, J., van der Geer, P. and Tazi, J.** (2001). RasGAP-associated endoribonuclease G3BP: selective RNA degradation and phosphorylation-dependent localization. *Mol Cell Biol* **21**, 7747-60.
- Tsai, N. P., Bi, J. and Wei, L. N.** (2007). The adaptor Grb7 links netrin-1 signaling to regulation of mRNA translation. *EMBO J* **26**, 1522-31.
- Tsui, K. H., Cheng, A. J., Chang, P. L., Pan, T. L. and Yung, B. Y.** (2004). Association of nucleophosmin/B23 mRNA expression with clinical outcome in patients with bladder carcinoma. *Urology* **64**, 839-44.
- Tu, B. P., Kudlicki, A., Rowicka, M. and McKnight, S. L.** (2005). Logic of the yeast metabolic cycle: temporal compartmentalization of cellular processes. *Science* **310**, 1152-8.
- Tu, B. P. and McKnight, S. L.** (2006). Metabolic cycles as an underlying basis of biological oscillations. *Nat Rev Mol Cell Biol*.
- Tvrđik, P., Kuzela, S. and Houstek, J.** (1992). Low translational efficiency of the F1-ATPase beta-subunit mRNA largely accounts for the decreased ATPase content in brown adipose tissue mitochondria. *FEBS Lett.* **313**, 23-26.
- Unwin, R. D., Craven, R. A., Harnden, P., Hanrahan, S., Totty, N., Knowles, M., Eardley, I., Selby, P. J. and Banks, R. E.** (2003). Proteomic changes in renal cancer and co-ordinate demonstration of both the glycolytic and mitochondrial aspects of the Warburg effect. *Proteomics* **3**, 1620-32.
- Valcarce, C., Navarrete, R. M., Encabo, P., Loeches, E., Satrustegui, J. and Cuezva, J. M.** (1988). Postnatal development of rat liver mitochondrial functions. The roles of protein synthesis and of adenine nucleotides. *J Biol Chem* **263**, 7767-75.
- van Waveren, C., Sun, Y., Cheung, H. S. and Moraes, C. T.** (2006). Oxidative phosphorylation dysfunction modulates expression of extracellular matrix--remodeling genes and invasion. *Carcinogenesis* **27**, 409-18.

- Vander Heiden, M. G., Cantley, L. C. and Thompson, C. B.** (2009). Understanding the Warburg effect: the metabolic requirements of cell proliferation. *Science* **324**, 1029-33.
- Vander Heiden, M. G., Locasale, J. W., Swanson, K. D., Sharfi, H., Heffron, G. J., Amador-Noguez, D., Christofk, H. R., Wagner, G., Rabinowitz, J. D., Asara, J. M. et al.** (2010). Evidence for an alternative glycolytic pathway in rapidly proliferating cells. *Science* **329**, 1492-9.
- Vander Heiden, M. G., Plas, D. R., Rathmell, J. C., Fox, C. J., Harris, M. H. and Thompson, C. B.** (2001). Growth factors can influence cell growth and survival through effects on glucose metabolism. *Mol Cell Biol* **21**, 5899-912.
- Vassalli, J. D., Huarte, J., Belin, D., Gubler, P., Vassalli, A., O'Connell, M. L., Parton, L. A., Rickles, R. J. and Strickland, S.** (1989). Regulated polyadenylation controls mRNA translation during meiotic maturation of mouse oocytes. *Genes Dev* **3**, 2163-71.
- Vasudevan, S., Tong, Y. and Steitz, J. A.** (2007). Switching from repression to activation: microRNAs can up-regulate translation. *Science* **318**, 1931-4.
- Vaughn, A. E. and Deshmukh, M.** (2008). Glucose metabolism inhibits apoptosis in neurons and cancer cells by redox inactivation of cytochrome c. *Nat Cell Biol* **10**, 1477-83.
- Wallace, D. C.** (2005). Mitochondria and cancer: Warburg addressed. *Cold Spring Harb Symp Quant Biol* **70**, 363-74.
- Wang, T., Marquardt, C. and Foker, J.** (1976). Aerobic glycolysis during lymphocyte proliferation. *Nature* **261**, 702-5.
- Wang, W., Goswami, S., Lapidus, K., Wells, A. L., Wyckoff, J. B., Sahai, E., Singer, R. H., Segall, J. E. and Condeelis, J. S.** (2004). Identification and testing of a gene expression signature of invasive carcinoma cells within primary mammary tumors. *Cancer Res* **64**, 8585-94.
- Wang, X.** (2001). The expanding role of mitochondria in apoptosis. *Genes Dev* **15**, 2922-33.
- Warburg, O.** (1956a). On respiratory impairment in cancer cells. *Science* **124**, 269-70.
- Warburg, O.** (1956b). On the origin of cancer cells. *Science* **123**, 309-14.
- Wei, C. C., Balasta, M. L., Ren, J. and Goss, D. J.** (1998). Wheat germ poly(A) binding protein enhances the binding affinity of eukaryotic initiation factor 4F and (iso)4F for cap analogues. *Biochemistry* **37**, 1910-6.
- Weinhouse, S.** (1956). On respiratory impairment in cancer cells. *Science* **124**, 267-9.
- Weinhouse, S.** (1976). The Warburg hypothesis fifty years later. *Z Krebsforsch Klin Onkol Cancer Res Clin Oncol* **87**, 115-26.
- West A.P., Brodsky I.E., Rahner C., Woo D.K., Erdjument-Bromage H., Tempst P., Walsh M.C., Choi Y., Shadel G.S., Ghosh S.** (2011) TLR signalling augments macrophage bactericidal activity through mitochondrial ROS. *Nature* **472**, 476-80.

**Westermann, B.** (2010). Mitochondrial fusion and fission in cell life and death. *Nat Rev Mol Cell Biol* **11**, 872-84.

**White, J. P., Cardenas, A. M., Marissen, W. E. and Lloyd, R. E.** (2007). Inhibition of cytoplasmic mRNA stress granule formation by a viral proteinase. *Cell Host Microbe* **2**, 295-305.

**Willers, I. M., Isidoro, A., Ortega, A. D., Fernandez, P. L. and Cuezva, J. M.** (2010). Selective inhibition of beta-F1-ATPase mRNA translation in human tumours. *Biochem J* **426**, 319-26.

**Yin, P. H., Lee, H. C., Chau, G. Y., Wu, Y. T., Li, S. H., Lui, W. Y., Wei, Y. H., Liu, T. Y. and Chi, C. W.** (2004). Alteration of the copy number and deletion of mitochondrial DNA in human hepatocellular carcinoma. *Br J Cancer* **90**, 2390-6.

**Yoshida, M., Muneyuki, E. and Hisabori, T.** (2001). ATP synthase--a marvellous rotary engine of the cell. *Nat Rev Mol Cell Biol* **2**, 669-77.

**Yu, T., Robotham, J. L. and Yoon, Y.** (2006). Increased production of reactive oxygen species in hyperglycemic conditions requires dynamic change of mitochondrial morphology. *Proc Natl Acad Sci U S A* **103**, 2653-8.

**Yuan, Z., Sanders, A. J., Ye, L., Wang, Y. and Jiang, W. G.** (2011). Prognostic value of the human antigen R (HuR) in human breast cancer: high level predicts a favourable prognosis. *Anticancer Res* **31**, 303-10.

**Zekri, L., Chebli, K., Tourriere, H., Nielsen, F. C., Hansen, T. V., Rami, A. and Tazi, J.** (2005). Control of fetal growth and neonatal survival by the RasGAP-associated endoribonuclease G3BP. *Mol Cell Biol* **25**, 8703-16.

**Zhang, B., Pan, X., Cobb, G. P. and Anderson, T. A.** (2007a). microRNAs as oncogenes and tumor suppressors. *Dev Biol* **302**, 1-12.

**Zhang, C., Wang, C., Chen, X., Yang, C., Li, K., Wang, J., Dai, J., Hu, Z., Zhou, X., Chen, L. et al.** (2010). Expression profile of microRNAs in serum: a fingerprint for esophageal squamous cell carcinoma. *Clin Chem* **56**, 1871-9.

**Zhang, H., Gao, P., Fukuda, R., Kumar, G., Krishnamachary, B., Zeller, K. I., Dang, C. V. and Semenza, G. L.** (2007b). HIF-1 inhibits mitochondrial biogenesis and cellular respiration in VHL-deficient renal cell carcinoma by repression of C-MYC activity. *Cancer Cell* **11**, 407-20.

**Zhang, H. L., Eom, T., Oleynikov, Y., Shenoy, S. M., Liebelt, D. A., Dictenberg, J. B., Singer, R. H. and Bassell, G. J.** (2001). Neurotrophin-induced transport of a beta-actin mRNP complex increases beta-actin levels and stimulates growth cone motility. *Neuron* **31**, 261-75.

**Zhang, H. Z., Liu, J. G., Wei, Y. P., Wu, C., Cao, Y. K. and Wang, M.** (2007c). Expression of G3BP and RhoC in esophageal squamous carcinoma and their effect on prognosis. *World J Gastroenterol* **13**, 4126-30.

**Zheng, S. Q., Li, Y. X., Zhang, Y., Li, X. and Tang, H.** (2011). MiR-101 regulates HSV-1 replication by targeting ATP5B. *Antiviral Res* **89**, 219-26.

**Zhong, B., Yang, Y., Li, S., Wang, Y. Y., Li, Y., Diao, F., Lei, C., He, X., Zhang, L., Tien, P. et al.** (2008). The adaptor protein MITA links virus-sensing receptors to IRF3 transcription factor activation. *Immunity* **29**, 538-50.

**Zhou, S., Kachhap, S., Sun, W., Wu, G., Chuang, A., Poeta, L., Grumbine, L., Mithani, S. K., Chatterjee, A., Koch, W. et al.** (2007). Frequency and phenotypic implications of mitochondrial DNA mutations in human squamous cell cancers of the head and neck. *Proc Natl Acad Sci U S A* **104**, 7540-5.

**Zhou, Z., Sim, J., Griffith, J. and Reed, R.** (2002). Purification and electron microscopic visualization of functional human spliceosomes. *Proc Natl Acad Sci U S A* **99**, 12203-7.

**Zu, X. L. and Guppy, M.** (2004). Cancer metabolism: facts, fantasy, and fiction. *Biochem Biophys Res Commun* **313**, 459-65.



# **APPENDIX**

---

---



## APPENDIX

**Nucleophosmine** (NPM1, also called nuclear phosphoprotein B23 and numatrin) is a ubiquitously expressed and highly conserved protein of ~37 kDa that is mainly localized in the nucleolus even though it constantly shuttles between the nucleolus and the cytoplasm (Borer et al., 1989). NPM1 is a multifunctional protein that can function as molecular chaperone binding directly nucleic acids and histones and mediating the assembly of histones and nucleosomes (Dumbar et al., 1989; Okuwaki et al., 2001; Szébeni and Olson, 1999). In addition, NPM1 is able to regulate the transcription rate of rRNA genes (Murano et al., 2008), is involved in the maturation of pre-ribosomal particles (Olson et al., 1986) and directs the nuclear export of the ribosomes to the cytoplasm. The capacity of NPM1 to shuttle the ribosomes to the cytoplasm is rate limiting providing a mechanism to regulate the rate of protein synthesis and cell growth given (Maggi et al., 2008). Furthermore, NPM1 is highly expressed in proliferating and cancerous cells (Chan et al., 1989; Nozawa et al., 1996; Subong et al., 1999; Tanaka et al., 1992; Tsui et al., 2004) and plays a role in cell cycle progression and tumorigenesis (Atlas et al., 2007; Brady et al., 2004; Feuerstein et al., 1988; Grisendi et al., 2005; Okada et al., 2007) regulating the stability of p53 (Colombo et al., 2002) and ARF (Kuo et al., 2004; Moulin et al., 2008). NPM1 binds to poly(A) tails of mRNAs as a result of 3' end formation, suggesting that NPM1 could play a role in the quality control of mRNAs or other post-transcriptional processes (Palaniswamy et al., 2006). Studies in NPM1-deficient mice have shown that loss of NPM1 leads to embryonic lethality, unrestricted centrosome duplication and genomic instability (Grisendi et al., 2005; Okada et al., 2007).

**IMP1** belongs to the conserved VICKZ family of mRNA binding proteins (**Vg1 RBP**, **IMP1-3**, **CRB-BP**, **KOC**, **ZBP-1**) that have amino acid identity of ~70%, contain two RNA recognition motifs (RRMs) and four hnRNP K homology domains (Nielsen et al., 1999). The VICKZ family is involved in post-transcriptional processes, such as mRNA localization, turnover and translational control. The IMP1 orthologue in chicken, the zipcode binding protein (ZBP-1), localizes the  $\beta$ -actin mRNA to the leading edge of fibroblasts and prevents translation of the transcript until the ZBP1 mRNA reaches its destination at the periphery of the cell (Deshler et al., 1998; Hüttelmaier et al., 2005; Oleynikov and Singer, 2003; Ross, 1997). The mouse orthologue CRD-BP binds to c-myc mRNA protecting the transcript in this way from endonucleatic cleavage (Bernstein et al., 1992; Doyle et al., 1998). The human IMP family (IMP1-3) is implicated in translational repression of the IGF-II leader mRNA during late development (Nielsen et al., 1999). In mice, a burst of expression of all three IMPs (IMP1-3) occurs at embryonic day 12.5 (E12.5) and declines towards birth (Hansen et al., 2004; Nielsen et al., 1999). Moreover, knock out of the IMP1 encoding gene in mice (*IMP1*<sup>-/-</sup>) provokes a reduced growth rate and perinatal lethality (Hansen et al., 2004). The IMP3 orthologue in *Xenopus* is the Vg1 RNA-binding protein (Vg1-BP), which localizes the Vg1 mRNA to the vegetal pole of the oocyte (Havin et al., 1998). IMP1 is mainly localized in the cytoplasm where it can show a distinct localization pattern depending on the cell type and growth conditions (Nielsen et al., 1999). In motile cells IMP1 is present in the leading edge of the lamellopodia, but can also



be found in discrete perinuclear foci (Nielsen et al., 1999) and/or in large cytoplasmatic granules distributed along microtubules (Jonson et al., 2007; Nielsen et al., 2002). In addition, *de novo* activation and/or over-expression of IMP1 occur in a variety of human tumors (Ioannidis et al., 2003; Ioannidis et al., 2001; Ross et al., 2001). A study in a transgenic mice model evidenced that over expression of IMP1/CRD-BP in adulthood induces the development of tumors (Tessier et al., 2004). Furthermore, in ovarian carcinomas high IMP1 levels are associated with advanced clinical stage and poor prognosis (Gu et al., 2004; Kobel et al., 2007), and in colon cancer IMP1 expression was found to be a predictor of survival (Dimitriadis et al., 2007).

**G3BP1** (Ras-GAP SH3 binding protein 1) is a ubiquitous protein of around 52 kDA that is evolutionary conserved throughout eukaryotes. G3BP1 contains a carboxy terminal RRM-type RNA binding domain, a central domain rich in acidic residues and an N-terminal Nuclear Transport Factor 2-like (NTF2-like) domain, (Parker et al., 1996; Tourriere et al., 2003). The name of G3BP1 originates from its co-immunoprecipitation with Ras GTPase activating protein p120 (RasGAP) in a screen for potential RasGAP effectors (Parker et al., 1996). G3BP1 forms a complex with RasGAP only in growing cells and dependent on Ras activation (Gallouzi et al., 1998; Parker et al., 1996). G3BP1 is primarily localized in the cytoplasm, but the association of G3BP1 with RasGAP in dividing cells provokes its localization to the plasma membrane probably through recruitment of both proteins by activated Ras (Gallouzi et al., 1998; Parker et al., 1996). G3BP1 harbors three phosphorylation sites (Gallouzi et al., 1998) and both localization and function of G3BP1 are specifically modified by phosphorylation. In proliferating cells the intrinsic phosphorylation-dependent endonuclease activity of G3BP1 is negatively regulated by Ras signaling, whereas in quiescent cells hyperphosphorylation of G3BP1 activates its intrinsic RNase activity that in turn catalyzes cleavage of the 3' UTR of c-myc mRNA (Gallouzi et al., 1998; Tourriere et al., 2001). Furthermore, in quiescent fibroblasts S149 phosphorylation is critical for G3BP1 translocation into the nucleus (Tourriere et al., 2001). Ultimately, a role of G3BP1 in conditions of cellular stress has been revealed. In situations of oxidative, heat, metabolic or mitochondrial stress as well as viral infections G3BP1 is localized in stress granules (SGs) (Kedersha et al., 2005; White et al., 2007). The role of G3BP1 during SG formation/recruitment depends on the de-phosphorylation of S149, and G3BP1 over-expression *per se* promotes the assembly of SGs (Tourriere et al., 2003). G3BP1 could present a first cellular barrier in response to viral infection, as G3BP1 is targeted by the poliovirus protease C3 in order to prevent SG assembly while a cleavage resistant G3BP1 form inhibits viral infection and restores SG formation (White et al., 2007). Furthermore, G3BP1 is up-regulated in proliferating pigmental epithelial cells (Kociok et al., 1999) and over-expressed in various human cancer cell lines and tumors, including head and neck and breast cancer (Barnes et al., 2002; French et al., 2002; Guitard et al., 2001). Knock out of the G3BP1 encoding gene in mice is linked to embryonic lethality and growth retardation, and is associated with an altered expression of genes implicated in the regulation of proliferation (Zekri et al., 2005, Lypowiy et al., 2005).

Breast cancer		Lung cancer		Colon cancer	
<b>Histology</b>	<b>N</b>	<b>Histology</b>	<b>N</b>	<b>Histology</b>	<b>N</b>
Normal	14	Normal	35	Normal	27
DIC	50	AC	19	AC	27
		SCC	16		
<b>Stage</b>	<b>N</b>	<b>Stage</b>	<b>N</b>	<b>Stage</b>	<b>N</b>
I	11	IA	4	I	5
IIA	20	IB	8	IIA	10
IIB	10	IIA	9	IIB	5
III	11	IIB	8	IIIA	2
		IIIA	3	IIIB	3
		IIIB	3	IIIC	1
				N/R	1
<b>Grade</b>	<b>N</b>	<b>Grade</b>	<b>N</b>	<b>Grade</b>	<b>N</b>
1	4	1	3	1	4
2	18	2	17	2	17
3		3	12	3	4
		N/R	3	N/R	2
<b>Lymph node metastasis</b>	<b>N</b>	<b>Lymph node metastasis</b>	<b>N</b>	<b>Lymph node metastasis</b>	<b>N</b>
NO	24	NO	13	NO	17
YES	24	YES	22	YES	9
N/R	4	N/R	3	N/R	1

**Table A1: Summary of clinicopathological characteristics of the patients studied for analysis of post-transcriptional mechanism(s) controlling  $\beta$ -F1-ATPase expression.** N, number of patients AC, adenocarcinoma; DIC, ductal infiltrating carcinoma; N/R, non-registered; SCC, squamous cell carcinoma.

<b>Characteristic</b>	<b>N</b>	<b>%</b>	<b>G3BP1</b>
<b>Age</b>			
<50	33	35	1.53 ± 0.31
>50	60	65	1.21 ± 0.13
<b>Size</b>			
<20mm	29	31	0.97 ± 0.16
>20mm	64	69	1.48 ± 0.19
<b>Nodes</b>			
0	45	48	1.19 ± 0.19
1-3	30	32	1.41 ± 0.22
>3	18	19	1.51 ± 0.39
<b>Grade</b>			
1	8	9	1.14 ± 0.42
2	28	30	1.32 ± 0.25
3	43	46	1.19 ± 0.20
N/A	14	15	1.84 ± 0.41
<b>Histology</b>			
Ductal	79	85	1.26 ± 0.15
Lobular	9	10	1.98 ± 0.60
Others	5	5	1.08 ± 0.36
<b>Stage</b>			
I	17	18	1.00 ± 0.25
II	54	58	1.35 ± 0.18
III	22	24	1.15 ± 0.32
<b>Metastasis</b>			
No	63	68	1.18 ± 0.14
Yes	30	32	1.63 ± 0.30

**Table A2: Summary of clinicopathological characteristics and G3BP1 expression level in the cohort of breast cancer patients studied.** N and %, indicates the number and percentage of breast cancer patients in each group. The expression level of G3BP1 is expressed in arbitrary units as the mean ± SEM.

Parameter	N	Overall survival		Disease-free survival	
		HR (95% CI)	p	HR (95% CI)	p
<b>Nodes</b>					
0	50	1		1	
1-3	32	3.51 (0.88-14.06)	0.076	2.76 (1.13-6.76)	<b>0.026</b>
>3	19	8.50 (2.26-38.00)	<b>0.002</b>	5.16 (2.07-12.88)	<b>0.000</b>
<b>Grade</b>					
1/2	38	1		1	
3	48	13.65 (2.77-246.89)	<b>0.011</b>	2.88 (1.21-6.81)	<b>0.017</b>
<b>Stage</b>					
I	21	1		1	
II	57	31716.48 (0.00-∞)	0.915	3.51 (0.81-15.29)	0.094
III	23	97105.70 (0.00-∞)	0.906	9.06 (2.04-40.26)	<b>0.004</b>
<b>Size</b>					
<20mm	34	1		1	
>20mm	67	3.98 (0.91-17.40)	0.067	1.63 (0.73-3.65)	0.233
<b>β-cluster</b>					
C1	81	1		1	
C2	17	3.19 (1.17-8.69)	<b>0.023</b>	2.98 (1.39-6.37)	<b>0.005</b>
<b>GAPDH</b>					
Low	72	1		1	
High	29	2.43 (0.94-6.31)	0.068	1.98 (0.67-4.033)	0.062
<b>HuR</b>					
High	52	1		1	
Low	37	1.60 (0.52-4.97)	0.417	2.19 (0.98-4.94)	0.060
<b>G3BP1</b>					
Low	47	1		1	
High	46	2.4 (0.83-6.92)	0.094	2.05 (0.98-4.32)	0.058

**Table A3: Univariate Cox regression analysis of breast cancer patients.** Univariate Cox regression analyses were performed with different clinicopathological parameters (number of nodes, histological grade, clinical stage and size of the tumor) and molecular variables (β-F1-ATPase (β-cluster), GAPDH, HuR and G3BP1), whose expression was analyzed in the cohort of patients (Isidoro et al., 2005; Ortega et al., 2008). The low and high expression of the variable is referred to the dichotomization cut point. G3BP1 was dichotomized by median, for HuR see Ortega et al., 2008 and for β-cluster and GAPDH see Isidoro et al., 2005. N indicates the number of breast cancer patients. HR, hazard ratio or relative risk of the parameter with the 95% confidence interval (95% CI). p-value was determined by Wald test, bold if p< 0.05.

Characteristic	G3BP1 low		G3BP1 high		p
	N	%	N	%	
<b>Age</b>					
<50	16	34.0	17	35.5	0.769
>50	31	66.0	29	34.5	
<b>Grade</b>					
1	5	10.6	3	6.5	0.332
2	15	31.9	13	28.3	
3	23	48.9	20	43.5	
N/A	4	8.5	10	21.7	
<b>Nodes</b>					
0	27	54.4	18	39.1	0.141
1-3	11	23.4	19	41.3	
>4	9	19.1	9	19.6	
<b>Stage</b>					
I	10	21.3	7	15.2	0.704
II	27	57.4	27	58.7	
III	10	21.3	12	26.1	
<b>Histology</b>					
Ductal	41	87.2	38	82.6	0.813
Lobular	4	8.5	5	10.9	
Others	2	4.3	3	6.5	
<b>Hormonal R.</b>					
Negative	10	21.3	8	17.4	0.635
Positive	37	78.7	38	82.6	

**Table A4: G3BP1 expression and clinicopathological characteristics of breast tumors.** Low and high expression of G3BP1 is referred to the dichotomization by median. N and % indicate the number and percentage of breast cancer biopsies in each group. p is the p-value of Pearson's chi-square test. p<0.05 was considered as significant. There are no significant differences.

Parameter	N	(%)	Events	DFS 5 year (prop.)	SEM	95% CI	p
<b>Nodes</b>							
0	50	50	8	0.85	0.05	0.74-0.95	<b>0.001</b>
1 to 3	32	32	12	0.65	0.09	0.48-0.82	
>3	19	19	11	0.51	0.12	0.28-0.74	
<b>Stage</b>							
I	21	21	2	0.95	0.05	0.85-1.05	<b>0.001</b>
II	57	56	16	0.72	0.06	0.60-0.84	
III	23	23	13	0.51	0.11	0.31-0.72	
<b>Grade</b>							
1/2	38	10	7	0.86	0.6		<b>0.012</b>
3	48	56	20	0.62	0.07	0.47-0.76	
<b>GAPDH</b>							
Low	72	71	18	0.77	0.05	0.67-0.87	0.056
High	29	29	13	0.62	0.09	0.44-0.81	
<b><math>\beta</math>-cluster</b>							
C1	81	83	21	0.77	0.05	0.67-0.86	<b>0.003</b>
C2	17	17	10	0.46	0.12	0.22-0.70	
<b>HuR</b>							
Low	37	42	14	0.65	0.08	0.49-0.81	0.053
High	52	58	10	0.82	0.05	0.72-0.93	
<b>G3BP1</b>							
Low	47	50	11	0.78	0.06	0.66-0.90	0.052
High	46	50	19	0.63	0.07	0.49-0.77	

**Table A5: Univariate disease-free survival analysis of breast cancer patients.** Kaplan-Meier disease-free survival analysis was performed with all breast cancer patients using clinicopathological (number of nodes, clinical stage and histological grade) and molecular parameters (GAPDH,  $\beta$ -cluster, HuR and G3BP1), whose expression has been analyzed (Isidoro et al., 2005; Ortega et al., 2008). The low and high tumor expression level is referred to the dichotomization cut point. G3BP1 was dichotomized by median, for HuR see Ortega et al., 2008, for expression of  $\beta$ -F1-ATPase ( $\beta$ -cluster) and GAPDH see Isidoro et al., 2005. N and % indicate the number and percentage of breast cancer patients in each group. Events, number of patients with recurrence of disease in each group. DFS 5 years, cumulated proportion of patients with 5 years distant disease-free survival (DFS) with the standard error of the mean (SEM) and the 95% confidence interval (CI). P-value as determined by log-rank test, in bold if  $p < 0.05$ .



# **PUBLICATIONS**







## Review

# Post-transcriptional regulation of the mitochondrial H<sup>+</sup>-ATP synthase: A key regulator of the metabolic phenotype in cancer<sup>☆</sup>

Imke M. Willers, José M. Cuezva<sup>\*</sup>

Departamento de Biología Molecular, Centro de Biología Molecular Severo Ochoa, CSIC-UAM, Centro de Investigación Biomédica en Red de Enfermedades Raras (CIBERER), ISCIII, Universidad Autónoma de Madrid, 28049 Madrid, Spain

## ARTICLE INFO

## Article history:

Received 20 July 2010

Received in revised form 19 October 2010

Accepted 20 October 2010

Available online 27 October 2010

## Keywords:

Mitochondria

Cancer

H<sup>+</sup>-ATP synthase

Aerobic glycolysis

ATPase Inhibitory Factor 1 (IF1)

Ras-GAP SH3 binding protein 1 (G3BP1)

## ABSTRACT

A distinctive metabolic trait of tumors is their enforced aerobic glycolysis. This phenotype was first reported by Otto Warburg, who suggested that the increased glucose consumption of cancer cells under aerobic conditions might result from an impaired bioenergetic activity of their mitochondria. A central player in defining the bioenergetic activity of the cell is the mitochondrial H<sup>+</sup>-ATP synthase. The expression of its catalytic subunit  $\beta$ -F1-ATPase is tightly regulated at post-transcriptional levels during mammalian development and in the cell cycle. Moreover, the down-regulation of  $\beta$ -F1-ATPase is a hallmark of most human carcinomas. In this review we summarize our present understanding of the molecular mechanisms that participate in promoting the “abnormal” aerobic glycolysis of prevalent human carcinomas. The role of the ATPase Inhibitor Factor 1 (IF1) and of Ras-GAP SH3 binding protein 1 (G3BP1), controlling the activity of the H<sup>+</sup>-ATP synthase and the translation of  $\beta$ -F1-ATPase mRNA respectively in cancer cells is emphasized. Furthermore, we underline the role of mitochondrial dysfunction as a pivotal player of tumorigenesis. This article is part of a Special Issue entitled: Bioenergetics of Cancer.

© 2010 Elsevier B.V. All rights reserved.

## 1. Introduction

The term cancer is used to define a set of heterogeneous diseases in which abnormal cells divide without control and are able to invade other tissues. The primary cause of cancer development was initially attributed to genetic mutations [1]. However, some properties of cancer cells cannot be explained only by mutations and it has been accepted that the tumor microenvironment [2] and other epigenetic events [3] contribute to cancer development and its behavior. A phenotypic trait of tumors is its peculiar aerobic glycolytic metabolism [4–7], a hallmark that has been recently added to other alterations acquired by cancer cells in their progression to malignancy [8]. The enforced aerobic glycolytic metabolism of tumors and cancer cells was first discovered by Otto Warburg many years ago [9,10]. Because the availability of oxygen was known to repress the cellular rates of glucose consumption (Pasteur effect) [11], Warburg suggested that the increased aerobic glycolysis observed in carcinomas should result from an impaired bioenergetic activity of mitochondria [9,10]. His hypothesis was heatedly debated [12–14] and mostly abandoned until the last decade of the previous century

when radiation oncologists put back into stage Warburg's postulates [15–17].

Nowadays, the increased aerobic glycolysis of tumors is out of question and has been underlined by the widespread clinical application of tumor imaging by <sup>18</sup>F-2-deoxyglucose (FDG) positron emission tomography (PET), for the diagnosis, staging and follow-up of cancer patients [15,16]. The boost in aerobic glycolysis is a requirement for tumorigenesis because it ensures the provision of the building blocks and reducing power required for the biosynthesis of the macromolecules that are needed for proliferation [6,18,19]. It has been argued that some cancer cells growing *in vitro* depend on oxidative phosphorylation as the main energy provision pathway [20–22]. However, transcriptomic, proteomic and functional studies in prevalent human carcinomas indicate that an enhanced glycolysis and a repressed bioenergetic activity of mitochondria are required for tumor progression [23–29]. Moreover, other studies have demonstrated and summarized the metabolic, molecular and functional alterations of mitochondria in cancer cells [30–35].

Several mechanisms directly promoting glycolysis, the inhibition of mitochondrial function or both have been proposed aimed at explaining the Warburg phenotype of cancer cells and tumors [4,6,17,19,36–41]. Some authors suggest that the shift to a glycolytic phenotype results from adaptation to the hypoxic environment where the tumor grows. Others support that the aforementioned change is the result of mutations in oncogenes, tumor suppressors and proteins related to signal transduction pathways (myc, Akt, p53, HIF1- $\alpha$ , and

<sup>☆</sup> This article is part of a Special Issue entitled: Bioenergetics of Cancer.

<sup>\*</sup> Corresponding author. Centro de Biología Molecular Severo Ochoa, Universidad Autónoma de Madrid, 28049 Madrid, Spain. Tel.: +34 91 196 4618; fax: +34 91 196 4420.

E-mail address: [jmcuezva@cbm.uam.es](mailto:jmcuezva@cbm.uam.es) (J.M. Cuezva).

# Human G3BP1 interacts with $\beta$ -F1-ATPase mRNA and inhibits its translation

Álvaro D. Ortega\*, Imke M. Willers\*, Sandra Sala and José M. Cuezva<sup>†</sup>

Departamento de Biología Molecular, Centro de Biología Molecular Severo Ochoa (CBMSO), CSIC-UAM, Centro de Investigación Biomédica en Red de Enfermedades Raras (CIBERER), ISCIII, Universidad Autónoma de Madrid, 28049 Madrid, Spain

\*These authors contributed equally to this work

<sup>†</sup>Author for correspondence ([jmcuezva@cbm.uam.es](mailto:jmcuezva@cbm.uam.es))

Accepted 1 May 2010

Journal of Cell Science 123, 2685–2696

© 2010. Published by The Company of Biologists Ltd

doi:10.1242/jcs.065920

## Summary

The post-transcriptional regulation of nuclear mRNAs that encode core components of mitochondria has relevant implications in cell physiology. The mRNA that encodes the catalytic subunit of the mitochondrial H<sup>+</sup>-ATP synthase subunit  $\beta$  (*ATP5B*,  $\beta$ -F1-ATPase) is localized in a large ribonucleoprotein (RNP) complex ( $\beta$ -F1-RNP), which is subjected to stringent translational control during development and the cell cycle, and in carcinogenesis. Because downregulation of  $\beta$ -F1-ATPase is a conserved feature of most prevalent human carcinomas, we have investigated the molecular composition of the human  $\beta$ -F1-RNP. By means of an improved affinity-chromatography procedure and protein sequencing we have identified nine RNA-binding proteins (RNABPs) of the  $\beta$ -F1-RNP. Immunoprecipitation assays of Ras-GAP SH3 binding protein 1 (G3BP1) and fluorescent in-situ hybridization of mRNA indicate a direct interaction of the endogenous G3BP1 with mRNA of  $\beta$ -F1-ATPase ( $\beta$ -F1 mRNA). RNA-bridged trimolecular fluorescence complementation (TriFC) assays confirm the interaction of G3BP1 with the 3'-UTR of  $\beta$ -F1 mRNA in cytoplasmic RNA-granules. Confocal and high-resolution immunoelectron-microscopy experiments suggest that the  $\beta$ -F1-RNP is sorted to the periphery of mitochondria. Molecular and functional studies indicate that the interaction of G3BP1 with  $\beta$ -F1 mRNA inhibits its translation at the initiation level, supporting a role for G3BP1 in the glycolytic switch that occurs in cancer.

**Key words:** RNA-binding proteins, RNABP, RNABP affinity purification, Cancer, H<sup>+</sup>-ATP synthase, Mitochondria, In-vivo RNA-protein interactions

## Introduction

The bio-energetic phenotype of eukaryotic cells is adjusted upon changes in environmental and/or physiological conditions by regulating the activity of its mitochondria (Rossignol et al., 2004). Changes in the molecular composition of mitochondria require the concerted expression of nuclear and mitochondrial genes (Scarpulla, 2008). Regulation of mitochondrial biogenesis is mainly exerted at the level of transcription in the nucleus and by replication and/or transcription in the mitochondrial genome (Scarpulla, 2008). The localization of mRNAs also exerts a fundamental role in the regulation of gene expression (Martin and Ephrussi, 2009). Mechanisms that control the localization (Lithgow et al., 1997; Marc et al., 2002) and translation (de Heredia et al., 2000; Izquierdo and Cuezva, 1997; Martinez-Diez et al., 2006) of nucleus-encoded mRNAs of mitochondria have been shown to define the bioenergetic phenotype of the cell. The sorting of mRNAs to the vicinity of mitochondria is a conserved feature in both yeast and mammalian cells (Lithgow et al., 1997; Sylvestre et al., 2003b) affecting those mRNAs that encode core components of mitochondrial complexes (Egea et al., 1997; Garcia et al., 2007; Marc et al., 2002). The targeting of mRNAs involves multiple steps and *cis*-acting elements placed in the 3'-untranslated region (3'UTR) of the mRNAs can confer mitochondrial targeting (Marc et al., 2002; Martin and Ephrussi, 2009).

Genetic screening and affinity purification methods have allowed the identification of several *trans*-acting factors involved in mRNA transport, anchoring, stability and translation (Martin and Ephrussi, 2009; Rodriguez et al., 2008). The Pumilio (PUF) family of RNA-binding proteins (RNABPs) binds 3'UTRs and modulates mRNA expression in a wide variety of eukaryotic species (Wickens et al.,

2002). Studies aimed at identifying Puf-associated mRNAs in yeast, flies and human cells have shown that Puf targets display conserved binding sites and usually fall into the same functionally annotated pathway (Galgano et al., 2008; Gerber et al., 2004; Gerber et al., 2006). In this regard, Puf3p specifically associates with 256 mRNAs in *Saccharomyces cerevisiae*, 90% of which are nucleus-encoded mitochondrial proteins that are highly enriched in mitochondria-bound polysomes (Gerber et al., 2004; Saint-Georges et al., 2008). Consistently, yeast strains overexpressing Puf3p exhibit respiratory dysfunction, and abnormal mitochondrial morphology and motility (Garcia-Rodriguez et al., 2007; Gerber et al., 2004). A second class of 224 mitochondria-associated transcripts that lack Puf-binding sites, and whose expression and localization is not affected by PUF3 deletion, has been described (Saint-Georges et al., 2008), suggesting the existence of at least two pathways for mRNA sorting to mitochondria.

The subcellular localization and translation of mRNA of the catalytic subunit of the mitochondrial H<sup>+</sup>-ATP synthase subunit  $\beta$  (*ATP5B*, hereafter referred to  $\beta$ -F1-ATPase) has been studied both in yeast and in rat liver cells (Egea et al., 1997; Izquierdo and Cuezva, 1997; Lithgow et al., 1997; Margeot et al., 2002; Margeot et al., 2005). In yeast,  $\beta$ -F1-ATPase (*ATP2*) mRNA is preferentially sorted to the vicinity of mitochondria by the 3'UTR (Margeot et al., 2002; Margeot et al., 2005). Deletion of the 3'UTR in the *ATP2* gene leads to deficient protein import, reduced ATP synthesis, depletion of mitochondrial DNA and respiratory dysfunction (Margeot et al., 2002; Margeot et al., 2005). Interestingly, *ATP2* mRNA was not found as a Puf3p target and belongs to the above mentioned class of Puf3-independent mitochondrion-localized mRNAs for which the *trans*-acting

## Selective inhibition of $\beta$ -F1-ATPase mRNA translation in human tumours

Imke M. WILLERS\*<sup>1</sup>, Antonio ISIDORO\*<sup>1</sup>, Álvaro D. ORTEGA\*, Pedro L. FERNÁNDEZ† and José M. CUEZVA\*<sup>2</sup>

\*Departamento de Biología Molecular, Centro de Biología Molecular Severo Ochoa, CSIC-UAM, Centro de Investigación Biomédica en Red de Enfermedades Raras (CIBERER), ISCIII, Universidad Autónoma de Madrid, 28049 Madrid, Spain, and †Departamento de Anatomía Patológica, IDIBAPS, Hospital Clínic y Universidad de Barcelona, 08036 Barcelona, Spain

Down-regulation of  $\beta$ -F1-ATPase (the catalytic subunit of the mitochondrial  $H^+$ -ATP synthase) is a hallmark of many human tumours. The expression level of  $\beta$ -F1-ATPase provides a marker of the prognosis of cancer patients, as well as of the tumour response to chemotherapy. However, the mechanisms that participate in down-regulating its expression in human tumours remain unknown. In the present study, we have investigated the expression of  $\beta$ -F1-ATPase mRNA (termed  $\beta$ -mRNA) in breast, colon and lung adenocarcinomas and squamous carcinomas of the lung. Despite the down-regulation of the protein, tumour  $\beta$ -mRNA levels remained either unchanged (breast and lung adenocarcinomas) or significantly increased (colon and squamous lung carcinomas) when compared with paired normal tissues, suggesting a specific translation-masking event for  $\beta$ -mRNA in human cancer. Consistently, we show using cell-free translation

assays that a large fraction ( $\sim 70\%$ ) of protein extracts derived from breast and lung adenocarcinomas specifically repress the translation of  $\beta$ -mRNA. We show that the 3'UTR (3' untranslated region) of human  $\beta$ -mRNA is a relevant *cis*-acting element required for efficient translation of the transcript. However, an RNA chimaera bearing the 3'UTR of human  $\beta$ -mRNA does not recapitulate the inhibitory effect of tumour extracts on  $\beta$ -mRNA translation. Overall, the findings of the present study support the hypothesis that down-regulation of the bioenergetic activity of mitochondria in human tumours is exerted by translation silencing of  $\beta$ -mRNA.

Key words: cancer,  $H^+$ -ATP synthase, mitochondrion, oxidative phosphorylation, regulation of gene expression, translation.

### INTRODUCTION

Mitochondria play a central role in the physiology of eukaryotic cells. The biogenesis of mitochondria is a complex genetic programme that requires the concerted transcriptional response of nuclear and mitochondrial genes [1]. However, mechanisms that control the localization, stability and translation of mRNAs also contribute to defining the mitochondrial phenotype of the cell [2]. In oxidative phosphorylation, ATP is synthesized by the  $H^+$ -ATP synthase, a rotatory engine of the inner mitochondrial membrane that utilizes as a driving force the proton electrochemical gradient generated by the respiratory chain.  $\beta$ -F1-ATPase (the  $\beta$ -subunit of the mitochondrial  $H^+$ -ATP synthase) is the catalytic subunit of the complex and rate-limiting component for the production of ATP [3]. The expression of  $\beta$ -F1-ATPase in the liver [4–6], in brown adipose tissue [7] and during progression through the cell cycle [8] indicates that the mitochondrial localization and translation of  $\beta$ -F1-ATPase mRNA (termed  $\beta$ -mRNA) are primary sites for regulating the spatial and temporal expression of the protein. Similar findings have been obtained in yeast, where the sorting of  $\beta$ -mRNA to the vicinity of mitochondria is mediated by its 3'UTR (3' untranslated region), and deletion of this element leads to deficient protein import, reduced ATP synthesis, mtDNA (mitochondrial DNA) depletion and respiratory dysfunction [9,10]. In rat liver, the 3'UTR of  $\beta$ -mRNA has a functional internal ribosome entry sequence [11,12] which controls the synthesis of the protein at the  $G_2/M$ -phase of the cell cycle [8]. The binding of developmentally regulated RNA-binding proteins to the 3'UTR of  $\beta$ -mRNA has been shown to inhibit its translation during foetal stages of liver development [4]. The re-installment of the same mechanism of

translational repression seems to control the expression of  $\beta$ -F1-ATPase in rat hepatomas [13].

Mitochondrial malfunctioning is implicated in the pathogenesis of various human disorders including cancer [14,15]. Cancer cells are characterized by a predominant glycolytic metabolism even under aerobic conditions [16,17]. The distinctive glycolytic shift of cancer cells is accompanied by silencing of the bioenergetic activity of mitochondria [3]. In this regard, we and others have reported that the expression level of  $\beta$ -F1-ATPase is consistently down-regulated in different human tumours when compared with normal tissue [3,14,18–24]. Moreover, the relative cellular expression level of the protein [ $\beta$ -F1-ATPase/GAPDH (glyceraldehyde-3-phosphate dehydrogenase) ratio] provides a bioenergetic signature of the tumour with potential clinical utility [16]. In fact, a diminished bioenergetic signature of the tumour is associated with poor prognosis as assessed in large cohorts of colon [14,25], lung [3,19] and breast [20] cancer patients. Interestingly, the bioenergetic signature of cancer cells and tumours also affords a promising predictive marker of the response to therapy [25–28]. Even though the expression of  $\beta$ -F1-ATPase is compromised in cancer and its down-regulation involved in progression of the disease, our knowledge of the mechanisms that control  $\beta$ -F1-ATPase expression in human tumours is virtually nil. In the present study we show that post-transcriptional expression of  $\beta$ -mRNA plays a key role in defining the bioenergetic phenotype of colon, lung and breast carcinomas. Consistently, we illustrate in cell-free translation assays that a large fraction of breast and lung carcinoma extracts trigger the specific repression of  $\beta$ -mRNA translation when compared with extracts derived from normal tissue of the same patients. In agreement with previous findings in the rat [4,12], we document

Abbreviations used: ARF, ADP-ribosylation factor; DTT, dithiothreitol;  $\beta$ -F1-ATPase, the catalytic subunit of the mitochondrial  $H^+$ -ATP synthase; GAPDH, glyceraldehyde-3-phosphate dehydrogenase; GFP, green fluorescent protein; miRNA, microRNA;  $\beta$ -mRNA,  $\beta$ -F1-ATPase mRNA; p $\beta$ F1, precursor of  $\beta$ -subunit; qPCR, quantitative PCR; RT, reverse transcription; 3'UTR, 3' untranslated region.

<sup>1</sup> These authors equally contributed to the present study.

<sup>2</sup> To whom correspondence should be addressed (email jmcuezva@cbm.uam.es).

## SUPPLEMENTARY ONLINE DATA

# Selective inhibition of $\beta$ -F1-ATPase mRNA translation in human tumours

Imke M. WILLERS\*<sup>1</sup>, Antonio ISIDORO\*<sup>1</sup>, Álvaro D. ORTEGA\*, Pedro L. FERNÁNDEZ† and José M. CUEZVA\*<sup>2</sup>

\*Departamento de Biología Molecular, Centro de Biología Molecular Severo Ochoa, CSIC-UAM, Centro de Investigación Biomédica en Red de Enfermedades Raras (CIBERER), ISCIII, Universidad Autónoma de Madrid, 28049 Madrid, Spain, and †Departamento de Anatomía Patológica, IDIBAPS, Hospital Clínico y Universidad de Barcelona, 08036 Barcelona, Spain

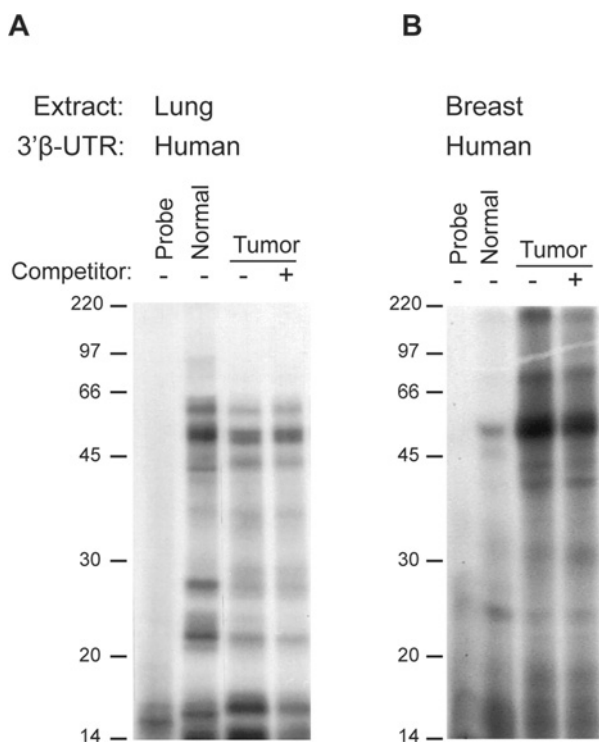


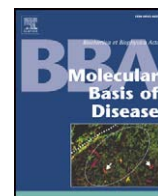
**Figure S1** The human 3'UTR of  $\beta$ -mRNA does not interact specifically with proteins of breast and lung tumour extracts

The radiolabelled 3'UTR of human  $\beta$ -F1-ATPase mRNA (3'β-UTR) was incubated with 10  $\mu$ g of protein of normal and tumour lung (**A**) or breast (**B**) extracts and subjected to UV cross-linking. Addition of an excess of unlabelled human 3'β-UTR (+) was used as a competitor to assess the specificity of the binding. The RNA–protein complexes were resolved by SDS/PAGE. Representative examples of lung and breast cancer patients are shown. The migration of protein standards of 220, 97, 66, 45, 30, 20 and 14 kDa are indicated on the left-hand side.

Received 9 October 2009/18 December 2009; accepted 23 December 2009  
Published as BJ Immediate Publication 23 December 2009, doi:10.1042/BJ20091570

<sup>1</sup> These authors equally contributed to the present study.

<sup>2</sup> To whom correspondence should be addressed (email jmcuezva@cbm.uam.es).



## Review

## The tumor suppressor function of mitochondria: Translation into the clinics

José M. Cuezva\*, Álvaro D. Ortega, Imke Willers, Laura Sánchez-Cenizo, Marcos Aldea, María Sánchez-Aragó

Departamento de Biología Molecular, Centro de Biología Molecular Severo Ochoa, CSIC-UAM and CIBER de Enfermedades Raras (CIBERER), Universidad Autónoma de Madrid, 28049 Madrid, Spain

## ARTICLE INFO

## Article history:

Received 23 September 2008

Received in revised form 15 December 2008

Accepted 16 January 2009

Available online 23 January 2009

## Keywords:

Cancer

Cell cycle

Cell death

Glycolysis

H<sup>+</sup>-ATP synthase

Markers of prognosis

Metabolic inhibitor

Oxidative phosphorylation

ROS

## ABSTRACT

Recently, the inevitable metabolic reprogramming experienced by cancer cells as a result of the onset of cellular proliferation has been added to the list of hallmarks of the cancer cell phenotype. Proliferation is bound to the synchronous fluctuation of cycles of an increased glycolysis concurrent with a restrained oxidative phosphorylation. Mitochondria are key players in the metabolic cycling experienced during proliferation because of their essential roles in the transduction of biological energy and in defining the life–death fate of the cell. These two activities are molecularly and functionally integrated and are both targets of commonly altered cancer genes. Moreover, energetic metabolism of the cancer cell also affords a target to develop new therapies because the activity of mitochondria has an unquestionable tumor suppressor function. In this review, we summarize most of these findings paying special attention to the opportunity that translation of energetic metabolism into the clinics could afford for the management of cancer patients. More specifically, we emphasize the role that mitochondrial  $\beta$ -F1-ATPase has as a marker for the prognosis of different cancer patients as well as in predicting the tumor response to therapy.

© 2009 Elsevier B.V. All rights reserved.

## 1. Introduction

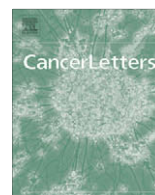
Cancer is considered a highly heterogeneous and complex genetic disease that drives the progressive transformation of normal cells into malignancy by a multistep and sequential ordered process. However, and in addition to the contribution of genetic mutations in the well established cancer genes (oncogenes and tumor suppressors), the onset and progression of cancer is also bound to the cancer cell's microenvironment and to other epigenetic events that contribute to funnel the cell into malignancy. In this regard, large projects aimed at deciphering the genetic changes occurring in tumors are being questioned due to their limited applicability for the development of effective therapies [1]. These arguments [1,2] suggest that the development of an effective therapy against cancer will require the targeting of the biological pathways commonly altered in the cancer cell [1–5]. A starting point for this change of gear was the admirable summary of the phenotype of the cancer cell in the following six traits: an unlimited replicative potential, sustained angiogenesis, evasion of apoptosis, self-sufficiency in growth signals, insensitivity to anti-growth signals and tissue invasion and metastasis [2]. Quite recently, the so-called “metabolic reprogramming” of the cancer cell has been added as a seventh hallmark of the cancer phenotype [3,5].

Indeed, the incidence of malignant disorders increases with age while the activity of mitochondrial oxidative metabolism diminishes in

most tissues during the ageing process. The apparent inverse correlation that exists between mitochondrial activity and cellular transformation was first suggested by Otto Warburg back in the early days of the previous century (for review see [6]). He made the seminal observation that tumors have an abnormal high aerobic glycolysis and therefore proposed that the bioenergetic activity of mitochondria was impaired in the cancer cell [7,8]. However, with the advancement of molecular biology, Warburg's hypothesis was largely neglected [9–11] or considered an epiphenomenon of cell transformation [12] until the early days of the present century when it has been formally contrasted for a relevant part of it [13,14] (for review see [5]). Indeed, many biochemical, molecular, functional and clinical studies have confirmed that most human tumors and cancer cells display, even in the presence of oxygen, increased rates of glucose consumption and of lactate release when compared to normal tissues, extending the original Warburg observation to many different neoplasias [5]. However, the strongest backing to the so-called Warburg phenotype of the tumors came from the development and clinical application of tumor imaging by positron emission tomography (PET) using 2-deoxy-2-[<sup>18</sup>F]fluoro-D-glucose (FDG) as a probe [15]. This technique, that actually measures the glucose analogue captured by the tumor relative to its surrounding non-tumor tissue, has proven to be one of the most effective techniques to detect tumors and its metastasis as well as for the staging, follow-up and prognosis of cancer patients [14,15]. In this regard, both FDG-PET and expression data of markers of mitochondrial bioenergetic function in tumors of lung cancer patients, as well as findings on the rates of glycolysis of cancer cells, have strongly supported that an altered

\* Corresponding author. Tel.: +34 911 964 618; fax: +34 911 964 420.

E-mail address: [jmcuezva@cbm.uam.es](mailto:jmcuezva@cbm.uam.es) (J.M. Cuezva).



## Mini-review

## Glucose avidity of carcinomas

Álvaro D. Ortega, María Sánchez-Aragó, Daniel Giner-Sánchez, Laura Sánchez-Cenizo, Imke Willers, José M. Cuezva \*

Departamento de Biología Molecular, Centro de Biología Molecular Severo Ochoa, CSIC-UAM, Universidad Autónoma de Madrid and Centro de Investigación Biomédica en Red de Enfermedades Raras (CIBERER), ISCIII, 28049 Madrid, Spain

## ARTICLE INFO

## Article history:

Received 8 May 2008

Received in revised form 21 July 2008

Accepted 4 August 2008

## Keywords:

Glycolysis

Mitochondria

H<sup>+</sup>-ATP synthase

Warburg hypothesis

## ABSTRACT

The cancer cell phenotype has been summarized in six hallmarks [D. Hanahan, R.A. Weinberg, The hallmarks of cancer, *Cell* 100 (1) (2000) 57–70]. Following the conceptual trait established in that review towards the comprehension of cancer, herein we summarize the basis of an underlying principle that is fulfilled by cancer cells and tumors: its avidity for glucose. Our purpose is to push forward that the metabolic reprogramming that operates in the cancer cell represents a seventh hallmark of the phenotype that offers a vast array of possibilities for the future treatment of the disease. We summarize the metabolic pathways that extract matter and energy from glucose, paying special attention to the concerted regulation of these pathways by the ATP mass-action ratio. The molecular and functional evidences that support the high glucose uptake and the “abnormal” aerobic glycolysis of the carcinomas are detailed discussing also the role that some oncogenes and tumor suppressors have in these pathways. We overview past and present evidences that sustain that mitochondria of the cancer cell are impaired, supporting the original Warburg’s formulation that ascribed the high glucose uptake of cancer cells to a defective mitochondria. A simple proteomic approach designed to assess the metabolic phenotype of cancer, i.e., its bioenergetic signature, molecularly and functionally supports Warburg’s hypothesis. Furthermore, we discuss the clinical utility that the bioenergetic signature might provide. Glycolysis is presented as the “selfish” pathway used for cellular proliferation, providing both the metabolic precursors and the energy required for biosynthetic purposes, in the context of a plethora of substrates. The glucose avidity of carcinomas is thus presented as the result of both the installment of glycolysis for cellular proliferation and of the impairment of mitochondrial activity in the cancer cell. At the end, the repression of mitochondrial activity affords the cancer cell with a cell-death resistant phenotype making them prone to malignant growth.

© 2008 Elsevier Ireland Ltd. All rights reserved.

## 1. Introduction

Cancer is nowadays considered a multi-step complex genetic disease orchestrated by the acquisition of gain-of-function mutations in oncogenes and loss-of-function mutations in tumor suppressor genes. Because of the genetic background of the disease, the study of cancer has traditionally been focused in the identification and func-

tional characterization of many of these cancer genes that, when modeled in different experimental systems, reproduce the phenotype of the disease. Following with this line of thinking the International Cancer Genome Consortium has been recently launched with the purpose of generating the catalogue of mutations present in the human genome of a large collection of different types of cancer. However, with the birth of the new century a breath of fresh air stepped into the field of cancer as a result of the seminal work of Douglas Hanahan and Robert A. Weinberg in the January issue of *Cell* 2000 [1]. These authors anticipated

\* Corresponding author. Tel.: +34 911 964 618; fax: +34 911 964 420.  
E-mail address: [jmcuezva@cbm.uam.es](mailto:jmcuezva@cbm.uam.es) (J.M. Cuezva).